Non-Archimedean and Non-Local Physics

Ziming Ji

a dissertation
presented to the faculty
of princeton university
in candidacy for the degree
of Doctor of Philosophy

recommended for acceptance
by the Department of
Physics

Adviser: Steve Gubser, Simone Giombi

September 2021

Abstract

Physics defined on real manifolds and equipped with locality has achieved many successes theoretically as well as in describing our universe. Nevertheless, from a mathematical point of view, it is not as privileged. This thesis explores the possibility of non-Archimedean and non-local physics by studying a range of discrete and continuous models. We begin by discussing how continuous dimensions with different topologies emerge from a sparse coupling lattice model inspired by a recent cold atom experiment proposal. A field theory with both non-Archimedean and Archimedean dimensions is then studied. The propagator of the theory possesses oscillatory behavior. We work out the renormalization and compare the theory with the quantum Dyson's hierarchical model at the criticality. We then proceed to study two non-local field theories: the non-local non-linear sigma model and the non-local quantum electrodynamics. Non-locality altered the behavior of NLSM profoundly by eliminating the Ricci flow and demanding higher-order covariant corrections in the target space. At the same time, the interplay between non-locality and gauge symmetry generates unique RG flows in the non-local QED and makes the theory more controllable. We conclude by introducing a monodromy defect defined in $O(N)$ symmetric conformal theories, which by definition, supports a non-local CFT on the defect. Throughout the journey, we want to convey the idea that non-Archimedean physics and non-local physics exhibits rich and unique phenomena yet are not disconnected from the more ordinary physics.

The following authors contributed to Chapter 1: Steve Gubser, Christian Jepsen, and Brian Trundy[54].
The following authors contributed to Chapter 2: Steve Gubser, Christian Jepsen, and Brian Trundy[56].
The following authors contributed to Chapter 3: Steve Gubser, Christian Jepsen, Brian Trundy, and Amos Yarom[60].
The following authors contributed to Chapter 4: Matthew Heydeman, Christian Jepsen, and Amos Yarom[68].
The following authors contributed to Chapter 5: Simone Giombi, Elizabeth Helfenberger, and Himanshu Khanchandani[47].

Contents

In memory of Steve Gubser and Yinghai Ji.

Acknowledgments

I feel strongly like expressing my gratitude to the fantastic people at Princeton who have shown me the gorgeous scenery of theoretical physics. Without your endless inspiration and generous help, this thesis would not have come into existence at all. I want to thank Herman Verlinde for my first quantum field theory class at Princeton. I want to thank Igor Klebanov for all the great theoretical courses and for your incredibly high tolerance of my naive questions. I am very grateful to Silviu Pufu for reading my thesis. Thanks to Andrew Leifer and Bob Austin for your guidance in my first year and on my experimental project. I am hugely indebted to Simone Giombi. Thank you for reaching out to me so kindly in that difficult time, and thank you for advising me in the last two years. Thank you, Christian Baadsgaard Jepsen, for your inspiration in life and physics since day one. I want to thank Brian Trundy for all the discussion we had on mathematics. I do not dare to forget my wonderful collaborators: Amos Yarom, Matthew Heydeman, Himanshu Khanchandani, and Elizabeth Helfenberger. You are the best, and I must be so lucky to have you all along the way. I want to thank Ho Tat Lam, Akash Goel, Fedor Popov, Wentao Fan, Wenli Zhao, Yiming Chen, Zhenbin Yang, Sarthak Parikh, Jiaqi Jiang, Wayne Zhao, Henry Lin, Brad Bachu, Yale Fan, for all the discussions, confusions, and laughter we had together in seminars, in Friday beers, and in the incredible high-energy journal clubs you hold. Thanks to Shai Chester, William Coulton, Akshay Yelleshpur, Matthew Moschella, Preethi Pallegar, and Siddharth Sharma for constantly keeping office 422 in Jadwin Hall a lovely place. Thanks to my roommates Zhelun Wu, Po-Shen Hsin, Yichen Fu, and Xinwei Yu, who have significantly contributed to the quality of my life. I want to thank Eve Xu, Junyi Zhang, Ilya Belopolski, Seth Olsen, Samuel Higginbotham, Javier Roulet, Diana Valverde Mendez, Fang Xie, Xiaowen Chen, Yunqin Zheng, Jie Wang, Tong Gao, Huan He, Jingyu Luo, Brandon Bonham, Zijia Cheng, Peter Czajka, James Loy, Nick Haubrich, Nicholas Quirk, Xue Song, Average Phan, Suerfu, Bowen Zhao, Muni Zhou, Shaorui Li, Heqiu Li, Ji Jiang, Angkun Wu, Wei Gu, Kasey Wagoner, and many others for your company along this journey and all the memories we share. I want to thank Katsushi Arisaka, Aravinthan Samuel, and Vivek Venkatachalam for your mentorship for my undergraduate research. I also want to thank Catherine Brosowsky and all the Princeton Physics staff members. Special thanks to mom for being absolutely supportive and everything.

To Steven Scott Gubser: My words are not enough to express even a tiny bit of my indebtedness and deepest gratitude to you. I miss your humorous teaching, your piano playing, and your witty comments. You were my favorite science book writer and a great talented physicist. You were an amazing advisor. The memory and the legacy of you will always be the bright star that guides me in the adventure into this uncertain world.

0

Introduction

0.1 An invitation

Developments in modern physics have deepened our comprehension of space-time and matter. The usual concept of the space-time continuum is based on the real number field and its extensions, like the complex number field. Physics theories defined with real or complex manifolds have been studied extensively. Among them are the Standard Model and

String Theory, representing our most advanced knowledge of the four fundamental interactions and all the fundamental particles in nature to date. Rich topological and analytical structures of the Pseudo-Riemannian or Riemannian manifold have been enlightening us in our understanding of nature and serving our pure theoretical interests in some other time.

Continuum is not always given. Sometimes continuous physics emerges from physics on the discrete, lattice models. From the famous Ising model to lattice gauge theories to topological matters in modern condensed matter theory, lattice models have taught us so much that would be difficult to grab merely from the angle of the continuum. Although often well-motivated by itself, like in cold atom physics or condensed matter physics, lattice models are also important because of their connection with the continuous theory. We can look at scalar quantum field theories, for instance. A fundamental field can usually be understood as a map from the base space to a value space, which is always built upon real numbers. Because of the continuous base space, we can move fields to arbitrarily short distances or arbitrarily high energy. In many theories, this operation causes arbitrarily large quantum fluctuation. The shorter the distance, the more significant the fluctuation, hence the term ultra-violet divergences. Renormalization and regularization are needed to deal with divergences properly while allowing that arbitrariness or absolute continuum, or equivalently, without requiring the UV details, by studying the change of fields in response to the change

of scales. High energy details, or a UV completion of the theory, can be a lattice theory. More generally speaking, a lattice theory does not need to be the UV completion to share the same IR physics with a continuous theory. The connection between critical Ising models and critical ϕ^4 theories is a good example. One important motivation of this thesis is to explore the possibility of non-Archimedean and non-local continuous theories as primarily inspired by the lattice way of thinking. We will explain the main ideas and the relevant definitions in the rest of this introduction.

0.2 Coupling pattern topology

When we take a discrete set of points as the base space, some usual concepts about spacetime are altered. For example, the number of dimensions is determined by the number of neighbors in nearest-neighbor models. Moreover, the metric is necessarily discrete and is less important if the coupling pattern is not specified. In short, because infinite countable (discrete uncountable sets are not considered here) sets can be one-to-one mapped to each other, it does not matter how the lattices look geometrically. What defines the theory is how the physics fields on every site interact with each other. Put in other words, we seem to have more freedom when defining a theory on the lattice. In this thesis, the coupling pattern that we restrict ourselves to is defined by the quadratic coupling term in the statistical

Figure 1: A 1D Ising spin chain.

Hamiltonian:

$$H_0 \equiv \sum_{i,j} J_{ij}\phi_i\phi_j \ , \tag{1}$$

where J_{ij} is real and represents the coupling between site i and j, and ϕ_i is the field living on the site i. A familiar example is the Ising model, where J_{ij} is constant if i and j are the nearest neighbors and $J_{ij} = 0$ if they are not. Figure 1 shows the one-dimensional Ising spin chain, where all couplings are illustrated by black arcs, and we highlight the nearest-neighbor coupling of one site.

A clear one-dimensional topology is derived from the number of nearest neighbors being two and the lattice translational invariance. In higher dimensions, the number of nearest neighbors and the number of discrete symmetries increase. Lattice models with locally defined site-to-site couplings represent a variety of discrete counterparts of various usual field theories with local quadratic kinetic terms. Let us abstract the metric-like coupling J_{ij} to a rule for the neighborhood for now. We define sites that directly couple to each other to be in the same neighborhood. We can generate the neighborhood topology for the one-dimensional Ising model, as in figure 2 (only drawing neighborhoods defined by the coupling while others are added according to the axioms of the neighborhood).

Translational $i \to i \pm 1$ invariance is a stringent constraint, and we can find interest-

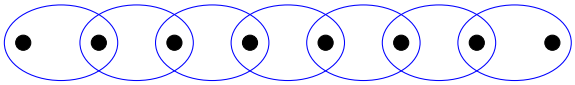

Figure 2: Topology from neighborhoods: Ising model

ing generalizations by rearranging neighborhoods. We first remove some neighborhoods. Of course, breaking all of them would generate a set of independent sites decoupled with each other, and that is boring. We can try to keep only "half" of them, as depicted by blue ellipses in figure 3. That alone merely gives decoupled pairs of sites that are not interesting. Now the original translational invariance is downgraded to an $i \to i \pm 2$ invariance. We then add back couplings to pairs of pairs, and then pairs of pairs of pairs (black and gray ellipses in figure 3), which breaks translational invariance more and more (to $i \to i \pm 4$ and to $i \to i \pm 8$). For an infinite lattice, we keep doing this so a hierarchical structure is formed and no translational invariance is left in the end. One obvious difference with the Ising is that this is an all-to-all coupling pattern. This hierarchical coupling is also less "connected", as the intersection of two neighborhoods at the same level is always empty. This means that we can easily break the space into infinitely many disjoint sets by ignoring couplings higher than a certain level. This is Dyson's hierarchical model[36]. Freeman Dyson introduced this model in 1968 and showed that this "one-dimensional" model could have phase transitions. Lattice models with this topology are known to have rich physics.[14,104]

Now that we obtain an all-to-all coupling, it is tempting to go back to the metric form J_{ij}. The question is how to express the coupling as $J(i-j)$ because the translational invari-

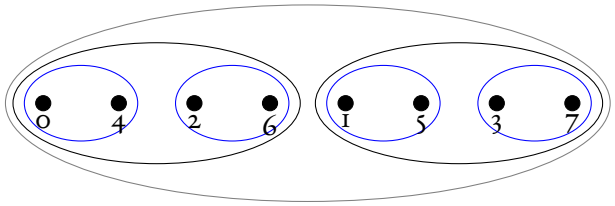

Figure 3: Topology from neighborhoods: Dyson's hierarchical model

ance is totally broken in the infinite lattice. Nonetheless, for a finite lattice, equivalently for a finite set of integers, one can always assign it a distance function such that $J_{ij} = J(i - j)$. If we want J to be a function of the absolute value $|i - j|$, then the form of the function must be increasingly complicated as the lattice size increases. If we want a simple form of J, we need a distance function that describes the hierarchy. We have relabeled the sites in figure 3, which is free because of the finite lattice (note that for a lattice of different size, the relabeling is also different). In such a label, $i - j$ has the same power of 2 for any i and j having the same hierarchical distance, which is the size of the smallest neighbor that contains both i and j. This is a primary version of the p-adic norm $|i - j|_p$ with p, a prime number, being 2. The p-adic norm is one of the main topics in the next chapter. We will see that p-adic norm is non-Archimedean, as opposed to the Archimedean real norm.

All-to-all non-local couplings that have real translational symmetry are more familiar. One famous example is the long-range Ising model[40] where $J_{ij} \propto |i - j|^{\alpha}$. We are used to the fact that the continuum limits of these real translational invariant lattices are described by field theories defined on the real number field. If we naively take the infinite size limit

and zero spacing limit of a lattice, then we get the rational numbers $\mathbb{Q}$ which can be one-to-one mapped to the integers. Rational numbers are often not good enough to support a field theory. One needs the completion of the rationals to enjoy better analytic properties. Real numbers are the completion of the rationals with respect to the real norm. The completion of the rational number field with respect to the p-adic norm is called the p-adic number field, which is to be introduced more carefully in the next sections. Thus, it is also natural to consider field theories defined over the p-adic numbers. Note that the real numbers are also algebraically closed. The completion of the algebraic closure of p-adic numbers is, instead, very complicated and will not be discussed in this thesis.

Note that the translational invariance is restored in the continuum limit of the hierarchical model with the p-adic norm. This is not a contradiction, as the continuum limit, the p-adic numbers, is a very different number field from the real numbers. We could phrase it as the real translational symmetry versus the p-adic translational symmetry. We have discussed various possibilities of the continuum as inspired by the lattice. In chapter 2, we compute the Green's functions of a one-parameter family of lattice models to study the base space topology in the continuous limit.* We compute the Green's function and its Hölder continuity to study a transition from the "real smoothness" to the "p-adic smoothness".

*Similar philosophy is also seen in the continuum. For example, the authors [81] consider a (non-Riemannian) metric on space-time that arises from the two-point function of a scalar field theory.

Ordinary integers $\mathbb{Z}$ is a natural extension to the concept of natural numbers. The ring of ordinary integers is an algebraic structure on the set $\mathbb{Z}$ equipped with addition, subtraction, and multiplication. If one also demands division, then we have the field of $\mathbb{Q}$, rational numbers. Any rational number can be expressed as $\frac{p}{q}$, where $p, q \in \mathbb{Z}, q \neq 0$. As sets, both are countable and have cardinality $\aleph_0$, but as topological spaces, they have very different topologies. As a metric space, rational numbers $\mathbb{Q}$ are not complete, meaning that not every converging sequence in $\mathbb{Q}$ converges to an element that belongs to $\mathbb{Q}$ itself. Adding these missing limits to the field is called completion. For example, the construction of real numbers $\mathbb{R}$ is the completion of $\mathbb{Q}$ with the metric as the absolute value of the difference. A different metric could give a different completion of $\mathbb{Q}$.

For any positive integer z, picking a prime number p, we can easily write down the following expansion

$$z = p^v \sum_{n=0}^{N} a_n p^n = p^v (a_0 + a_1 p + a_2 p^2 + ... + a_N p^N), \tag{2}$$

and we know this expansion is unique. It is called a "p-adic expansion"[85]. Any finite ordinary integer will be a finite sequence under this expansion, and we can see higher power terms are bigger in the sense of absolute value. In such a case, extending N to infinity is

meaningless, and all that will become just a formal notion of infinity ∞. A sensible infinite expansion in real numbers extends the sequence to $-\infty$ power, and that resembles our familiar decimal or binary representation. However, are there other notions of norms where higher power terms in (2) contribute less to the norm? The answer is yes, and such a norm is called the p-adic norm. It is defined for a positive integer $p^v a$, where $a \in \mathbb{Z}$ is co-prime to p, and hence $v \in \mathbb{Z}$ is the largest power that p^v divide this number, as

$$|p^v a|_p = p^{-v}, \tag{3}$$

and $|0|_p = 0$. If p is not a prime number, then the axiom $|x|_p|y|_p = |xy|_p$ can not be guaranteed. p-adic norm satisfies the norm axioms, but in fact, it satisfies a stronger version of the triangle inequality

$$|x + y|_p \leq \max\{|x|_p, |y|_p\}. \tag{4}$$

which is called the ultra-metric property. This breaks the Archimedean property (if $0 < |a|_\infty < |b|_\infty$, then for some $n \in \mathbb{Z}$ we have $|na|_\infty > |b|_\infty$) and such norms are called non-Archimedean or ultra-metric norms: when you add up quantities, you only obtain quantities with equal or smaller norms. It can be proved that the non-Archimedean property is, in fact, equivalent to the ultra-metric property for a norm, so that we will use these two notions interchangeably from now on. We also want to point out Ostrowski's theo-

rem: every non-trivial norm on the rational numbers $\mathbb{Q}$ is equivalent to either the usual real norm or a p-adic norm.

Now we can formally extend N in (2) to infinity and because higher terms is smaller in this p-adic norm, we could obtain a converging sequence in such manner(and p-adic metric is defined as the p-adic norm of the difference). Then we can figure out p-adic expansions for every rational number through algebraic equations. We give some examples for $p = 17$[†],

- -1 as the root of $x + 1 = 0$, then

$$-1 = \sum_{n=0}^{\infty} 16 \times 17^n = 16 + 16 \times 17 + 16 \times 17^2 + 16 \times 17^3 + ... \tag{5}$$

- $\frac{1}{2}$ as the root of $2x = 1$, then

$$\frac{1}{2} = 9 + \sum_{n=0}^{\infty} 8 \times 17^n = 9 + 8 \times 17 + 8 \times 17^2 + 8 \times 17^3 + ... \tag{6}$$

- v can be extended to negative integers, for example

$$\frac{23}{17} = 17^{-1}(6 + 1 \times 17) \tag{7}$$

  and $|\frac{23}{17}|_{17} = (17)^{-(-1)} = 17$.

Rational numbers are not complete under the p-adic metric as partially shown by the infinite series. The completion of $\mathbb{Q}$ under p-adic metric gives p-adic numbers $\mathbb{Q}_p$. Unfortu-

[†]Year 2021 happens to be the emerging year of the 17-year periodical cicadas. This kind of cicadas follow the period of a large prime number to avoid cycles of natural predators.

nately, $\mathbb{Q}_p$ is not algebraically closed. Not like in real numbers, to get a complete algebraic closure, one should deal with infinite extensions of $\mathbb{Q}_p$, and the final object is called Ω or $\mathbb{C}_p$. Most of the p-adic physics literature only deals with $\mathbb{Q}_p$ and its finite extension.

p-adic number $\mathbb{Q}_p$ has the same cardinality $2^{\aleph_0}$ as real numbers, but they have very different topologies. In fact, as a topological space, $\mathbb{Q}_p$ is totally disconnected, like $\mathbb{Q}$. This is saying that for any two numbers $x, y \in \mathbb{Q}_p$, there exists open sets S_1 and S_2 such that $x \in S_1, y \in S_2, S_1 \cap S_2 = \emptyset$ and $S_1 \cup S_2 = \mathbb{Q}_p$. This is not true in real numbers. This difference can be roughly represented as following: in $\mathbb{R}$, one can typically approach a number using sequences converging from above or below, for example representing 1 as $0.99999...$ and $1.00000...$; while for $\mathbb{Q}_p$, this is not possible as the converging sequences all have the same p-adic norm. This difference in topology is an important reason why p-adic physics usually have different features from "real physics".

Now we can think about the hierarchical model or the 2-adic lattice in the last section. We can take the infinite limit by keeping doubling the number of sites and relabeling the sites such that the coupling can always be described by a power of $|i-j|_2$. The same process can be realized for any prime number p. The infinite set we obtain is called $\mathbb{Z}_p$, the ring of integer of $\mathbb{Q}_p$. $\mathbb{Z}_p$ is an infinite subset of $\mathbb{Q}_p$ consisting of all the p-adic numbers that have p-adic norm equal or smaller than one. The ordinary fine graining process, where one just adds numbers to the ends, gives us the integer(or $\mathbb{Q}$ as for a continuous topology) line.

Both $\mathbb{Z}$ and $\mathbb{Z}_p$ enjoy ring structures, but from this, we could see that $\mathbb{Z}_p$ has the special tree-like topology while $\mathbb{Z}$ has the ordinary discrete topology(or $\mathbb{Q}$ has an ordinary continuous topology). This difference in topology almost guarantees different physical properties when we consider lattice models on a "p-adic" lattice rather than a regular lattice. In fact, not like $\mathbb{Z}$ or $\mathbb{Q}$, $\mathbb{Z}_p$ has cardinality $2^{\aleph_0}$ and is uncountable. Even more differently, $\mathbb{Z}_p$ is itself dense and complete.

Arithmetics is defined as usual on p-adic numbers. Integrals can be defined with a similar change of variable rule as real integrals.

$$\int_{\mathbb{Z}_p} dx = 1, \quad \int_{\mathbb{U}} dx = \int_{c^{-1}\mathbb{U}} d(cx) = \int_{c^{-1}\mathbb{U}} dx \ |c|_p \tag{8}$$

Fourier transforms can be defined when introducing character function $\chi(x) = e^{2\pi i\{x\}}$, where $\{x\}$ is the fractional part of x. And the integral of the character function is

$$\int_{p^v\mathbb{U}_p} dy\, \chi(y) = \begin{cases} p^{-v}(1-p^{-1}) & \text{if} \quad v \geq 0 \\ -1 & \text{if} \quad v = -1 \\ 0 & \text{if} \quad v < -1 \end{cases} \tag{9}$$

In particular, the integral of χ over $\mathbb{Q}_p$ is zero and thus we can define the Fourier transform

of the character itself to be the distribution in analogue of Dirac Delta in the reals:

$$\int_{\mathbb{Q}_p} dx\ \chi(k_1 x)\chi(k_2 x) = \delta(k_1 + k_2) \tag{10}$$

Similarly, Mellin transform can be defined. Gelfan-Graev gamma functions can be defined as the Mellin transform of the character functions:

$$\Gamma_p(s) \equiv \int_{\mathbb{Q}_p} \frac{du}{|u|_p} \chi(u)|u|_p^s. \tag{11}$$

With local zeta functions defined as

$$\zeta_p(s) \equiv \frac{1}{1 - p^{-s}}\,, \tag{12}$$

it is not hard to check that

$$\Gamma_p(s) = \frac{\zeta_p(s)}{\zeta_p(1-s)}. \tag{13}$$

Adelic product relation can be constructed, relating real special functions with p-adic special functions. Moreover, as an analog of Cauchy's integral formula, Vladimirov derivatives

can be defined over p-adic numbers:

$$D_y^s f(y) \equiv \frac{1}{\Gamma_p(-s)} \int_{\mathbb{Q}_p} dx \frac{f(x)}{|x-y|_p^{1+s}}. \tag{14}$$

In particular, we can see that

$$D_y^s \chi(ky) = |k|_p^s \chi(ky). \tag{15}$$

As one can observe, the techniques needed to study p-adic field theories are of a similar form with the real bi-local field theories, essentially due to the similar definition of fractional derivatives. We will discuss some of these analytic tools in the next section.

In fact, field theories over the p-adic numbers have been studied extensively, starting with Dyson's hierarchical model[36] and continuing with the rigorous results of[14], with the field theory perspective emerging clearly in[92]. In particular, the point that p-adic field theories can be obtained as continuum limits of hierarchical models was first made in[92]. The reviews[15,101,103,124] provide useful points of entry into the large literature on p-adic field theory and related topics.

0.4 Non-local field theories

0.4.1 Fourier transforms

In loop calculations we will often need to go back and forth between momentum space expressions and their real space counterparts, using the Fourier transforms

$$\phi(x) = \int_V d^n k \, e^{2\pi i k \cdot x} \hat{\phi}(k) \qquad\qquad \hat{\phi}(k) = \int_V d^n x \, e^{-2\pi i k \cdot x} \phi(x) \, . \tag{16}$$

The relevant results are fairly similar between real and p-adic cases, so we present them together. When $V = \mathbb{R}^n$, the definitions (16) are entirely standard, and $k \cdot x$ can be understood as the ordinary dot product. Likewise, in this case, $|x|$ is understood as the standard L^2 norm on $\mathbb{R}^n$. We will use real and Archimedean interchangeably from now on.

The simplest n-dimensional p-adic construction is based on letting $V = \mathbb{Q}_{p^n}$ be the (unique) unramified n-dimensional extension of $\mathbb{Q}_p$. Let N and Tr be the field norm and field trace with respect to the extension $\mathbb{Q}_{p^n}/\mathbb{Q}_p$. Then we define $|x| = |\,\mathrm{N}(x)|_p^{1/n}$ where $|\cdot|_p$ is the usual p-adic norm. We will refer to the p-adic case as ultrametric or non-Archimedean. Next we define $k \cdot x = \frac{1}{n}\,\mathrm{Tr}(kx)$. Note that $k \cdot x \in \mathbb{Q}_p$, so to give meaning to $e^{2\pi i k \cdot x}$ we now only need to define $e^{2\pi i \xi}$ for $\xi \in \mathbb{Q}_p$. To this end we find the unique p-adic integer $\lfloor \xi \rfloor$ such that $\xi - \lfloor \xi \rfloor \in [0, 1) \cap \mathbb{Q}$, and we understand that by $e^{2\pi i \xi}$ we really mean $e^{2\pi i (\xi - \lfloor \xi \rfloor)}$.

We are particularly interested in the Fourier transform of powers of $|k|$:

$$\int_V d^n k\, e^{2\pi i k\cdot x} |k|^s = \frac{\Gamma_V(n+s)}{|x|^{n+s}} + (\text{contact terms})\,. \tag{17}$$

Here $\Gamma_V(s)$ is a meromorphic function of s which can be evaluated as

$$\Gamma_V(s) = \frac{\zeta_v(s)}{\zeta_v(n-s)} \tag{18}$$

where we set $v = \infty$ in the Archimedean case and $v = p$ in the ultrametric case, with

$$\zeta_\infty(s) \equiv \pi^{-s/2}\Gamma_{\text{Euler}}(s/2) \qquad\qquad \zeta_p(s) \equiv \frac{1}{1-p^{-s}}\,. \tag{19}$$

Intuitively, Γ_V is a variant of the Euler gamma, specific to the choice of V, and constructed so as to be the coefficient of the $1/|x|^{n+s}$ term in (17). In the remainder of our discussion, integrals are over V unless otherwise indicated.

The contact terms in (17) are somewhat delicate and dependent on detail. When $-n < s < 0$, the integral in (17) is convergent, and no contact terms are needed. One can easily check that $\Gamma_V(n+s) \to 0$ as $s \to 0$, so when $s = 0$ the power law term goes away and we recover the obvious result

$$\int d^n k\, e^{2\pi i k\cdot x} = \delta^n(x)\,. \tag{20}$$

For $s > 0$, the integral in (17) diverges, and we need a more careful approach. A good first step is to understand (17) in terms of its action on a test function $\phi\colon V \to \mathbb{R}$:

$$\int d^n k\, e^{2\pi i k\cdot x} |k|^s \hat{\phi}(k) = D^s \phi(x)\,, \tag{21}$$

where D^s is some linear map on functions $\phi(x)$. A suitable class of test functions is the so-called Schwartz-Bruhat functions. When $\phi\colon \mathbb{Q}_{p^n} \to \mathbb{R}$, we require that ϕ is locally constant with compact support. For example, the characteristic function of the p-adic integers is a Schwartz-Bruhat function on $\mathbb{Q}_p$. When $\phi\colon \mathbb{R}^n \to \mathbb{R}$, the test functions are more appropriately called Schwartz functions, and their defining property is that they go to 0 faster than any power of $|x|$, as do all their derivatives. An example is a Gaussian. Both in the real and ultrametric cases, the Fourier transform $\hat{\phi}(k)$ of a Schwartz-Bruhat function is again a Schwartz-Bruhat function.

0.4.2 Fractional derivatives in position space

With (21) taken as the definition of D^s, our task is to find a representation of D^s entirely in position space. In the ultrametric case for arbitrarily positive s, one finds

$$D^s \phi(x) = \Gamma_V(n+s) \int d^n y \frac{\phi(y) - \phi(x)}{|x-y|^{n+s}}\,. \tag{22}$$

This is the Vladimirov derivative. In the Archimedean case, the same expression (22) is valid for $0 < s < 2$. There is one more easy case to dispose of: even positive integer s for Archimedean V. Then $\Gamma_V(n+s) = 0$, which makes sense in (17) because the right hand should be purely distributional, on account of $|k|^s = (k^2)^{s/2}$ being analytic in k^2. Explicitly,

$$D^s\phi(x) = \frac{1}{(2\pi)^s}(-\Box)^{s/2}\phi(x) \qquad \text{for positive even } s\,, \tag{23}$$

where $\Box = \sum_{i=1}^n \partial^2_{x^i}$.

We are left with the task of defining D^s for Archimedean V and for $s > 2$ but not an even integer. Heuristically, the contact terms in (17) are a sum of terms of the form $\Box^r\delta^n(x)$, where $0 \le r < s/2$, with divergent coefficients. To state this more precisely, we write

$$D^s\phi(x) = \Gamma_V(n+s)\int' d^n y \frac{\phi(y)-\phi(x)}{|x-y|^{n+s}}\,, \tag{24}$$

where a regulated integral

$$\int' d^n y \frac{G(x,y)}{|x-y|^{n+s}} \tag{25}$$

is rendered finite (if possible) by allowing the subtraction from $G(x,y)$ of a finite sum of smooth functions of either of the following types:

I. Pure powers: more precisely, any function whose y dependence comes solely through a factor $|x-y|^\alpha$ where α is a real number. This is meant to include, through the case $\alpha = 0$, functions which have no y dependence.

II. Higher partial waves: more precisely, any function of the form $Y(\widehat{y-x})g(|x-y|)$ where $Y(\hat{z})$ is a spherical harmonic on S^{n-1} other than the s-wave.

Type I functions are never integrable, whereas type II functions may or may not be; so at best there is a unique choice of type I functions that will work, whereas many choices of type II functions are possible. An alternative approach, generalizing the principle value prescription, is to eschew modifications of the integrand and instead carry out y integration in polar coordinates centered around x, as follows. One first performs the angular integrals. Then the radial integral is restricted to run from l to L. One next allows the subtraction of an arbitrary finite sum of negative powers of l and/or positive powers of L, chosen (if possible) so that the limits $l \to 0$ and $L \to \infty$, taken independently, lead to a finite result. Doing the angular integration first obviates the need for type II functions, while the ultraviolet and infrared cutoffs, l and L, obviate the need for type I.[‡]

While the subtractions described can in principle cure either ultraviolet (UV) or infrared (IR) divergences, we will be interested only in applications where UV divergences matter: that is, divergences arising when $|x-y| \to 0$ (with x held fixed). Type II subtractions are relatively innocuous because they follow automatically from performing angular integrations first; therefore we will use the notation $\int d^n y \ldots$ to indicate a y integration with type

[‡]The alert reader may notice that the alternative approach using cutoffs is not quite equivalent to adjusting $G(x,y)$ by pure powers of $|x-y|$: For example, if s is a positive even integer and $G(x,y) = |x-y|^s$, then we get a logarithmic divergence that would obviously be canceled using an appropriate type I function but cannot be cured using powers of l and/or L after a cutoff integration. Because we avoid even integer s as well as functions $G(x,y)$ which grow as positive powers of large separation $|x-y|$, we do not need to specify a resolution to this inequivalence.

II subtractions which we usually omit to write explicitly.

Although we have stated our integration prescriptions in the abstract, it is easy to see how to apply them to (24) when ϕ is a Schwartz function. Consider the case $2 < s < 3$, and set $x = 0$ for simplicity. Then (24) becomes

$$\int' \frac{d^n y}{|y|^{n+s}} \left[\phi(y) - \phi(0)\right] = \int \frac{d^n y}{|y|^{n+s}} \left[\phi(y) - \phi(0) - y_i \partial_i \phi(0) - \frac{1}{2} y_{i_1} y_{i_2} \partial_{i_1} \partial_{i_2} \phi(0)\right] . \tag{26}$$

The extra terms in square brackets on the right hand side of (26) evidently render the integral convergent near $y = 0$ for $2 < s < 3$. The term linear in y is clearly a type II function, and the term quadratic in y is a sum of a type II function proportional to $y_{i_1} y_{i_2} - \frac{y^2}{n} \delta_{i_1 i_2}$ (a d-wave term) and a type I function proportional to y^2. If $3 \leq s < 4$, then we would need one additional term in the Taylor series expansion of ϕ around $y = 0$, and this additional term is a type II function. In summary, for $2 < s < 4$, and omitting type II subtractions,

$$D^s \phi(0) = \int \frac{d^n y}{|y|^{n+s}} \left[\phi(y) - \phi(0) - \frac{y^2}{2n} \Box \phi(0)\right] . \tag{27}$$

Evidently, if $0 < s < 2$, a simpler subtraction scheme would work, resulting in (27) with the laplacian term omitted, in agreement with (22).

For general $s > 0$ (other than positive even integers) and Archimedean V,

$$D^s\phi(0) = \Gamma_V(n+s)\int \frac{d^n y}{|y|^{n+s}}\left[\phi(y) - \sum_{r=0}^{\lfloor s/2\rfloor} y^{2r} b_r \Box^r \phi(0)\right] \tag{28}$$

where

$$b_r = \frac{\Gamma_{\text{Euler}}(\frac{n}{2})}{2^{2r}\Gamma_{\text{Euler}}(r+\frac{n}{2})\Gamma_{\text{Euler}}(r+1)}\,. \tag{29}$$

In principle, one may derive (28) by subtracting an appropriate number of terms in the Taylor series expansion of $\phi(y)$ and then finding appropriate type II subtractions to bring the result into the form (28).

A more efficient way to determine the coefficients b_r is to start from (28) and Fourier transform:

$$\begin{aligned}
&\int d^n x\, e^{-2\pi i k\cdot x} D^s\phi(x) \\
&\quad = \Gamma_V(n+s)\int d^n x\, e^{-2\pi i k\cdot x}\int \frac{d^n y}{|x-y|^{n+s}}\left[\phi(y) - \sum_{r=0}^{\lfloor s/2\rfloor}(x-y)^{2r} b_r \Box^r\phi(x)\right] \\
&\quad = \frac{2\Gamma_V(n+s)}{\zeta_\infty(n-1)}\int_0^\infty \frac{d\tilde{y}}{\tilde{y}^{s+1}}\int_0^\pi d\theta\,(\sin\theta)^{n-2}\hat{\phi}(k)\left[e^{2\pi i|k|\tilde{y}\cos\theta} - \sum_{r=0}^{\lfloor s/2\rfloor} b_r (2\pi i)^{2r} k^{2r}\tilde{y}^{2r}\right] \\
&\quad = \Gamma_V(n+s)(2\pi)^{\frac{n}{2}+s}|k|^s\hat{\phi}(k)\int_0^\infty d\rho\,\left[\rho^{-\frac{n}{2}-s} J_{\frac{n}{2}-1}(\rho) - \sum_{r=0}^{\lfloor s/2\rfloor} a_r \rho^{2r-s-1}\right]
\end{aligned} \tag{30}$$

In the second equality of (30), we have partially carried out the y integral in polar coordi-

nates around the point $y = x$, introducing a radial variable $\tilde{y} = |x - y|$. In the third equality, we have carried out the angular θ integral and introduced a new radial variable, $\rho = 2\pi|k|\tilde{y}$. The ρ integral in the last line of (30) converges, provided s is positive but not an even integer, and provided the coefficients a_r are coefficients in the Taylor series expansion of the Bessel function around $\rho = 0$. These coefficients a_r are well known, and from them one can recover the expression (29) for the b_r.

0.4.3 Bi-local integrals

We are particularly interested in double integrals of the form

$$\int_{V\times V} \frac{d^n x d^n y}{|x-y|^{n+s}} G(x,y) \tag{31}$$

where $s > 0$ and $G(x,y)$ is piecewise constant if V is ultrametric and smooth if V is Archimedean. Unless otherwise noted, all double integrals over x and y will by taken over all of $V \times V$. In the ultrametric case, for any $s > 0$, following (22) we define

$$\int' \frac{d^n x d^n y}{|x-y|^{n+s}} G(x,y) \equiv \int \frac{d^n x d^n y}{|x-y|^{n+s}} \left[G(x,y) - G(x,x)\right] . \tag{32}$$

In the Archimedean case, we define

$$\int' \frac{d^n x d^n y}{|x-y|^{n+s}} G(x,y) \tag{33}$$

by performing the y integration first and allowing the subtraction of type I and type II functions to $G(x,y)$ in order to achieve a finite result (if possible). As in the previous section, type II subtractions are deemed relatively inconsequential, so even unprimed integration over x and y means to perform the y integration first, allowing the subtraction of type II functions in order to achieve a finite result (if possible). Explicitly, for s not a positive even integer,

$$\int' \frac{d^n x d^n y}{|x-y|^{n+s}} G(x,y) = \int \frac{d^n x d^n y}{|x-y|^{n+s}} \left[G(x,y) - \sum_{r=0}^{\lfloor s/2 \rfloor} b_r \Box_y^r G(x,y) \Big|_{y=x} (y-x)^{2r} \right], \tag{34}$$

where the coefficients b_r are as given in (29). We avoid positive even integer s when V is Archimedean because in this case we expect that our constructions will lead instead to purely local theories; also, precisely in this case, the subtleties pointed out in footnote ‡ regarding logarithmic divergences come into play.

Our computational strategy will turn on converting bi-local position space integrals into Fourier space integrals. Let's start with the simplest example of that calculation, valid for ultrametric V and any $s > 0$, and also for Archimedean V and $0 < s < 2$. Let $\phi \colon V \to \mathbb{R}$

be a Schwartz-Bruhat function. Then

$$\begin{aligned}\int \frac{d^n x d^n y}{|x-y|^{n+s}} \left[\phi(x)-\phi(y)\right]^2 &= \int \frac{d^n x d^n y}{|x-y|^{n+s}} \left(\left[\phi(x)-\phi(y)\right]^2 + \phi(x)^2 - \phi(y)^2\right) \\ &= -2\int d^n x\, \phi(x) \int \frac{d^n y}{|x-y|^{n+s}} \left[\phi(y)-\phi(x)\right] \\ &= -\frac{2}{\Gamma_V(n+s)} \int d^n x\, \phi(x) D^s \phi(x) = -\frac{2}{\Gamma_V(n+s)} \int d^n k\, \hat{\phi}(-k)|k|^s \hat{\phi}(k)\,. \end{aligned} \tag{35}$$

The first step is actually the trickiest, because it is not clear from the rules of integration set forth following (33) that we are allowed to add a function like $\phi(x)^2 - \phi(y)^2$ to the integrand. To justify this step, we denote $f(x) = \phi(x)^2$, and we argue that

$$\int \frac{d^n x d^n y}{|x-y|^{n+s}} \left[\phi(y)^2 - \phi(x)^2\right] = \frac{1}{\Gamma_V(n+s)} \int d^n x\, D^s f(x) = 0\,. \tag{36}$$

The second integral in (36) is the $k = 0$ component of the Fourier transform of $D^s f(x)$. But this Fourier transform is $|k|^s \hat{f}(k)$, and since $s > 0$ the $k = 0$ component indeed vanishes.

Let's now pursue the same computation for the Archimedean case with $2 < s < 4$. On

one hand, using (34),

$$\int' \frac{d^n x d^n y}{|x-y|^{n+s}} \left[\phi(x)-\phi(y)\right]^2 = \int \frac{d^n x d^n y}{|x-y|^{n+s}} \left(\left[\phi(x)-\phi(y)\right]^2 - \frac{(y-x)^2}{n} (\partial\phi(x))^2 \right)$$
$$= \int \frac{d^n x d^n y}{|x-y|^{n+s}} \left(\left[\phi(x)-\phi(y)\right]^2 - \frac{(y-x)^2}{2n} \left[-2\phi(x)\Box\phi(x) + \Box\phi(x)^2\right] \right) . \tag{37}$$

On the other hand, using (27),

$$-\frac{2}{\Gamma_V(n+s)} \int d^n k\, \hat{\phi}(-k)|k|^s \hat{\phi}(k) = -2 \int d^n x\, \phi(x) \int' \frac{d^n z}{|z|^{n+s}} \left[\phi(x+z)-\phi(x)\right]$$
$$= \int \frac{d^n x d^n y}{|x-y|^{n+s}} \left(2\phi(x)\left[\phi(x)-\phi(y)\right] + \frac{(y-x)^2}{n} \phi(x)\Box\phi(x) \right) . \tag{38}$$

In order to conclude

$$\int' \frac{d^n x d^n y}{|x-y|^{n+s}} \left[\phi(x)-\phi(y)\right]^2 = -\frac{2}{\Gamma_V(n+s)} \int d^n k\, \hat{\phi}(-k)|k|^s \hat{\phi}(k) \,, \tag{39}$$

we must therefore argue that the final integrals in (37) and (38) agree. Subtracting (38) from (37) and simplifying slightly with the definition $f(x) = \phi(x)^2$, we arrive at

$$\int \frac{d^n x d^n y}{|x-y|^{n+s}} \left[f(y) - f(x) - \frac{(y-x)^2}{2n} \Box f(x) \right] = \frac{1}{\Gamma_V(n+s)} \int d^n x\, D^s f(x) = 0 \,. \tag{40}$$

The first equality in (40) follows from (27), and the second is by the same argument used

following (36). To summarize, for Archimedean V and for $2 < s < 4$,

$$\begin{aligned}\int \frac{d^n x d^n y}{|x-y|^{n+s}} \left(\frac{(y-x)^2}{n} (\partial\phi(x))^2 - [\phi(x)-\phi(y)]^2 \right) \\ = \frac{2}{\Gamma_V(n+s)} \int d^n k \, \phi(-k) |k|^s \phi(k) \, .\end{aligned} \tag{41}$$

$\Gamma_V(n+s) > 0$ for $2 < s < 4$, and so without the $(\partial\phi)^2$ on the left hand side of (41) we would have a sign problem. The equality (39) can be checked in a similar manner for $s > 4$. A key relation is

$$\Box_y^m \left(\phi(x) - \phi(y)\right)^2 \Big|_{x=y} = -2\phi(x)\Box^m\phi(x) + \Box^m\phi(x)^2 \, . \tag{42}$$

Two take-away lessons are:

- When we write simple $|k|^s$ kinetic terms in momentum space, in position space we are combining non-local position space terms and local terms involving derivatives in a precisely tuned ratio.
- There is some freedom in the precise structure of the position space form, as exemplified by the equality of the last integrals in (37) and (38) due to a manipulation which is the non-local version of integration by parts.

0.4.4 Non-renormalization theorem

$$S = \frac{1}{2} \int_V d^n k \, \hat{\phi}(-k) |k|^s \hat{\phi}(k) + \int_V d^n x \, U(\phi(x)) \, , \tag{43}$$

We exhibit the simplest manifestation of the non-renormalization theorem of the non-local quadratic kinetic term in the action (3.2), where $V = \mathbb{R}^n$ or $\mathbb{Q}_{p^n}$, with

$$U(\phi) = \frac{g}{3!}\phi^3 \,. \tag{44}$$

The purely cubic theory is unstable, but it serves our purpose because we are only interested in analyzing the behavior of the one-loop correction to the propagator. We obtain the one-loop contribution to the quadratic part of the one-particle irreducible (1PI) effective action:

$$\delta\Gamma_2(k) = -\frac{g^2}{2} I \qquad \text{where} \qquad I = \int \frac{d^n\ell}{|\ell|^s |k-\ell|^s} \,. \tag{45}$$

We continue the convention of integrating over all of V except as otherwise indicated. Let's assume $n > 2s$, so I is UV divergent (and IR convergent). To regulate the divergence, we introduce a hard cutoff: $|\ell| \leq \Lambda$. If $V = \mathbb{R}^n$, then Λ can be any positive real number. If $V = \mathbb{Q}_{p^n}$, then we will require that Λ is an integer power of p.

The ultrametric case is easy to analyze, because when $|\ell| > |k|$ we have $|\ell| = |k-\ell|$ exactly. So, except in the compact region where $|\ell| \leq |k|$, the integrand has no k dependence at all. Therefore, any UV divergences are entirely independent of k, and to evaluate them

we can set $k = 0$:

$$\begin{aligned} I(\Lambda) &= \int_{|\ell|\leq\Lambda} \frac{d^n\ell}{|\ell|^s|k-\ell|^s} = \int_{|\ell|\leq\Lambda} \frac{d^n\ell}{|\ell|^{2s}} + (\text{UV finite}) \\ &= \frac{\zeta_p(n-2s)}{\zeta_p(n)}\Lambda^{n-2s} + (\text{UV finite})\,. \end{aligned} \tag{46}$$

The last equality comes from splitting the integration region into shells with fixed $|\ell|$; then the integral becomes a geometric sum. Because the divergent part of $I(\Lambda)$ has no k-dependence, the counterterm required to cancel it is proportional to $\int d^n k\, \hat{\phi}(-k)\hat{\phi}(k) = \int d^n x\, \phi(x)^2$. In other words, it is a mass term. This argument is easy to generalize to the statement that only purely local terms (powers of $\phi(x)$) can be radiatively generated starting from the action (3.2) over $V = \mathbb{Q}_{p^n}$. An essentially equivalent argument was made in a Wilsonian picture in [92].

The Archimedean case is more subtle because of the possibility of subleading divergences. A straightforward approach is to expand

$$I(\Lambda) = \int_{|\ell|\leq\Lambda} \frac{d^n\ell}{|\ell|^s|k-\ell|^s} = \int_{|\ell|\leq\Lambda} \frac{d^n\ell}{|\ell|^{2s}} \left(1 - \frac{2k\cdot\hat{\ell}}{|\ell|} + \frac{k^2}{\ell^2}\right)^{-s/2} \tag{47}$$

in powers of k. Terms with an odd number of powers of k vanish by parity, leaving only terms analytic in k^2. Of these, only terms proportional to k^{2r} with $r \leq \frac{n}{2} - s$ are UV divergent. In short, the divergent part of $I(\Lambda)$ is a polynomial in k^2 whose order is $\left\lfloor \frac{n}{2} - s \right\rfloor$. A

divergent term proportional to k^{2r} requires a counterterm proportional to $\int d^n x\, \phi(x) \Box^r \phi(x)$. These again are local terms and leave the non-local kinetic term unchanged.

We should note a troublesome feature of the hard momentum cutoff for Archimedean theories: The coefficients one finds for sub-leading divergences depend on how one implements the cutoff. For example, it is easy to check that the coefficient of the k^2 term in $I(\Lambda)$ changes if instead of requiring $|\ell| \leq \Lambda$ we impose the more democratic condition $\left|\ell - \frac{k}{2}\right| \leq \Lambda$. However, the feature that we care about, namely the fact that the divergent terms have only polynomial dependence on k^2, doesn't depend on the details of the cutoff. It is perhaps instructive to consider one other alternative, namely dimensional regularization, in which one first computes

$$I = \frac{\Gamma_\infty(2s-n)}{\Gamma_\infty(s)^2}(k^2)^{\frac{n-2s}{2}} \tag{48}$$

by continuing to a domain of n in which the integral is convergent. (In the current example, $s < n < 2s$ is such a domain.) The only divergences one then tracks are poles of the right hand side of (48) as a function of n. These occur precisely when $\frac{n-2s}{2}$ is a non-negative integer. It is characteristic of dimensional regularization that there is (at most) one divergent term for a given n, corresponding to a logarithmic divergence in the original integral.

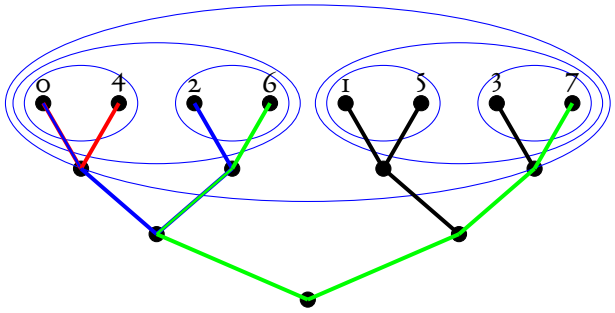

Figure 4: The boundary of a tree graph.

0.5 On the boundary

In figure 1, where we draw all the couplings of the Ising model, a clear real one dimension emerges and represents the topology as depicted by neighborhoods in figure 2. One may worry that illustrating all coupling links in a graph for an all-to-all coupling pattern is not informative. It turns out for a hierarchical model like in figure 3, the coupling strength can be conveniently described by a not-so-complicated graph, a tree graph (see figure 4). The red path represents the only non-backtracking path connecting two sites belonging to the smallest neighborhood. The blue one connects the next nearest, and the green connects the next next nearest in the hierarchical sense. Note that for any two sites on the boundary of the tree, there is a unique non-backtracking path connecting them. And given the number of links connecting i and j being n, then $2^{n/2}/8 = |i - j|_2$. The tree graph perfectly captures the p-adic metric on this finite lattice on the boundary. For a general prime number p, the coordination number of the tree is $p + 1$.

If we take the above tree structure and extend the bulk tree infinitely in both directions, we will obtain the $\mathbb{Q}_p$ line (more rigorously, a projective space $\mathbb{P}^1(\mathbb{Q}_p)$) on the boundary. Interestingly, this limiting process also uniquely generates the p-adic number field. After taking the infinite limit on the tree, the boundary is automatically completed by the p-adic norm. This is not true for real numbers as there is no obvious lattice to the knowledge of the author that uniquely generates the real number field when taken the infinite limit. One always has to complete the field by hand. This is a subtle difference between real type lattice models and p-adic type lattice models. Since the p-adic numbers are inevitably the boundary of a tree, theories on the p-adics must be related to theories on the tree graph. This particular infinite tree, called the Bruhat-Tits tree, has negative constant graph curvature and is a graph analog of the AdS space. In recent years there are works on p-adic AdS/CFT[62,69], where by considering nearest-neighbor scalar models on the tree graph and p-adic scalar field theories on the boundary, these authors study the bulk boundary correspondence and find results that can be compared to the real Ads/CFT through adelic formulas. Fermions in the bulk, however, need the line graph of a Bruhat-Tits tree[59].

The boundary of a lattice model that shows real topology is not as restrained and is less clear as there are infinitely many paths that connect two sites on the boundary. For example, we picture a nearest-neighbor square lattice model and all its coupling links in figure 5. It is free to conclude that the boundary theory becomes an all-to-all coupling model as for

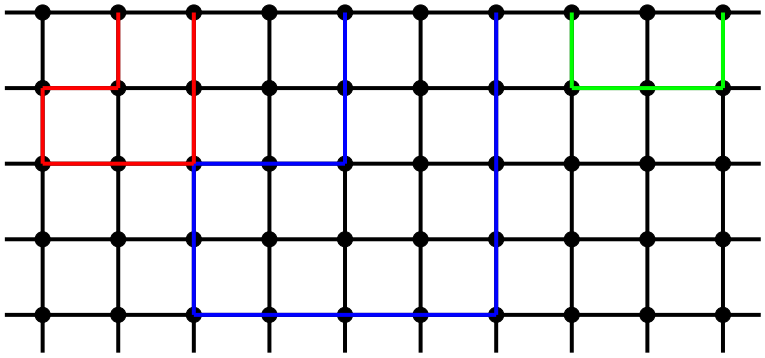

Figure 5: The boundary of a square lattice.

any given two sites on the boundary, there are always paths connecting them through the bulk. What really remains unclear is the coupling J_{ij} as a function of real distance $|i-j|$. We are only able to make a reasonable guess. Suppose we are away from the criticality, then each link contributes a damping factor λ. The contribution to $J(1)$ of the red path is then λ^7 while the contribution to $J(2)$ of the blue path is λ^{14}. However, J should decrease less than the exponential law because there are certain paths that do not have a shorter distance counterpart when the distance is large, like the green path. A naive guess then is the power law. We think that to determine $J(|i-j|)$ completely, one needs to sum all the self-avoiding random walks that begin and end on the boundary. In fact, in the continuum limit, the counterpart of this problem is rather easy to address: dimension reduction of $\mathbb{R}\times\mathbb{R}^+$ to $\mathbb{R}$ generates non-local power-law propagators of the free fields, as will be treated in details in later chapters. In chapter 4, we study a non-local version of QED, which is equivalent to coupling bulk photons to boundary fermions. In chapter 5, we briefly discuss

a codimension two monodromy defect defined in $O(N)$ symmetric theories where interaction will be turned on throughout the bulk and the boundary.

1

Sparse coupling pattern

The sparse coupling pattern that we want to study eliminates couplings between spins i and j unless $|i-j|$ or $2^N - |i-j|$ is a power of 2. It can be written as

$$J_h^{\text{sparse}} = J_* \sum_{n=0}^{N-1} 2^{ns} (\delta_{h-2^n} + \delta_{h+2^n} - 2\delta_h) \,. \tag{1.1}$$

So for the case $N = 3$ shown in figure 4, we drop the coupling between spins 0 and 3, and between 0 and 5, and between all translated copies of these pairs, for example, the pairs $(1, 4)$ and $(1, 6)$. For this small value of N, the "sparse" coupling pattern is still nearly all-to-all. But for large N, the number of spins coupling to one spin increases linearly with N instead of as 2^N. This sparseness reduces the decoherence cost by site-to-site couplings, making it more experimentally accessible while still keeps important features of quantum many-body systems, like chaos and fast scrambling. Similar ideas have been considered by cold atom physicists. In this paper[10], the authors proposed the cold atom realization of this sparse coupling pattern and studied the system from a quantum many-body point of view by simulation.

If the spectral exponent s is large and negative, intuitively, we expect to recover the nearest-neighbor coupling as only the first term ($n = 0$) matters in that limit. Meanwhile, as we will see, when the spectral parameter s is made large and positive, there is strong evidence that we recover 2-adic couplings. In the former case, the two-point Green's function of the nearest neighbor model with 2^N spins is then well-approximated at large N by a continuum Green's function that we can extract from field theory over $\mathbb{R}$. This Green's function is smooth in an Archimedean sense, except at zero separation. In fact, if we are considering the model with pure nearest-neighbor interactions, the Green's function away from zero separation is C^∞. The smoothness of the continuum limit of Green's function is

a good way to understand how continuous quantities emerge from a discrete lattice description, as we have mentioned in the introduction.

The smoothness of p-adic functions may be less familiar to the reader. For a function that maps $\mathbb{Q}_p$ to $\mathbb{R}$, the derivative is neither real nor p-adic and hence tricky to define. We have demonstrated that Green's function realizes that map through the p-adic norm function, which is to say, $G(x)$ is only a function of $|x|_p$. Because the values of p-adic norm belong to a countable set, the norm function is locally constant (given x, there exists $\delta > 0$ such that every y with $|x - y|_p < \delta$ has $f(x) = f(y)$), so is the p-adic Green's function. Green's functions in models with perfectly p-adic coupling are also locally constant (piecewise constant for a discrete base space) except at zero separation, as we will see in examples soon. In fact, the accepted analog of a C^∞ condition is to require that a map G from $\mathbb{Q}_p$ to $\mathbb{R}$ is locally constant. Note that a function from $\mathbb{Q}_p$ to $\mathbb{R}$ which is everywhere locally constant need not be globally constant (as it would for a function from $\mathbb{R}$ to $\mathbb{R}$). A more complete introduction to smooth test functions over the p-adic numbers than we will provide can be found, for example, in[116]. When we turn to sparse coupling patterns, we will recognize that we are recovering 2-adic continuity precisely when the two-point Green's function is well approximated by a locally constant function. This is exactly what happens in the limit of large positive s for the 2-adic statistical mechanical models that we will study explicitly.

In short, as the spectral exponent s ranges from large negative to large positive values, the Green's functions we study the transition from showing emergent Archimedean continuity to showing emergent p-adic continuity. How this transition occurs is slightly subtle, but we will combine some numerical results with analytical reasoning to characterize it both in momentum space and position space.

1.1 Lattice Green's functions

Consider therefore the following Hamiltonian for a lattice with L sites:

$$H \equiv -\frac{1}{2}\sum_{i,j} J_{ij}\phi_i\phi_j - \sum_j h_j\phi_j\,, \tag{1.2}$$

where the ϕ_i are commuting real numbers. We assume J_{ij} only depends on $|i-j|$, where arithmetic operations like $i-j$ are carried out modulo L. Field h is useful in computing two-point Green's functions later. Define L-dimensional vectors $\vec{v}_\kappa$ by

$$v_{\kappa,j} \equiv \frac{1}{\sqrt{L}} e^{2\pi i\kappa j/L} \qquad \text{for} \qquad \kappa = 0, 1, 2, \ldots, L-1\,. \tag{1.3}$$

The discrete Fourier transform is defined as

$$X_j = \sum_{\kappa=0}^{L-1} \tilde{X}_\kappa v_{\kappa,j}\,. \tag{1.4}$$

An easy calculation shows that

$$\mathbf{J}\vec{v}_\kappa = \sqrt{L}\tilde{J}_\kappa \vec{v}_\kappa \,, \tag{1.5}$$

where $\mathbf{J}$ without indices means the symmetric matrix J_{ij}, and $\tilde{J}_\kappa$ is the Fourier transform of the coupling strengths J_h. Using (1.4)-(1.5), we have immediately

$$H = -\frac{\sqrt{L}}{2}\sum_{\kappa=0}^{L-1}\tilde{J}_\kappa\tilde{\phi}_{-\kappa}\tilde{\phi}_\kappa - \sum_{\kappa=0}^{L-1}\tilde{h}_{-\kappa}\tilde{\phi}_\kappa \,. \tag{1.6}$$

We now make two assumptions:

- $\tilde{J}_0 = 0$. This is saying $\sum_i J_{ij} = 0$. We understand this as a consequence of assuming the existence of a symmetry where all the ϕ_i are shifted by a common value.
- $\tilde{J}_\kappa < 0$ for all $\kappa \neq 0$. This amounts to saying that the interactions among the ϕ_i are ferromagnetic.

It is useful to note that the second assumption follows from the first together with the requirement that all $J_h \geq 0$ for $h \neq 0$, with not all of them equal to zero.

It is slightly tricky to extract the Green's function from the naively defined partition function because $1/\tilde{J}_0$ diverges. In order to make the statistical mechanics well-defined, we insert a factor of $\delta(\tilde{\phi}_0)$ into the partition function:

$$Z[h] \equiv \left(\prod_{j=0}^{L-1}\int_{-\infty}^{\infty} d\phi_j\right)\delta(\tilde{\phi}_0)e^{-\beta H} = Z[0]\exp\left\{-\frac{\beta}{2\sqrt{L}}\sum_{\kappa=1}^{L-1}\frac{1}{\tilde{J}_\kappa}\tilde{h}_{-\kappa}\tilde{h}_\kappa\right\} . \tag{1.7}$$

We are interested in the two-point function

$$G_{ij} = \langle \phi_i \phi_j \rangle = \frac{1}{\beta^2 Z[0]} \left. \frac{\partial^2 Z[h]}{\partial h_i \partial h_j} \right|_{h=0} . \tag{1.8}$$

From $J_{ij} = J_{i-j}$ it follows that $G_{ij} = G_{i-j}$. A short calculation starting with (1.8) leads to

$$G_h = -\frac{1}{\beta L^{3/2}} \sum_{\kappa=1}^{L-1} \frac{1}{\tilde{J}_\kappa} e^{2\pi i \kappa h / L} . \tag{1.9}$$

The factor of $\delta(\tilde{\phi}_0)$ in the partition function is to say $\sum_i \phi_i = 0$. This corresponds to something more familiar in field theory techniques: regularization of independent infinities by discarding global integrals or discarding boundary terms. It may seem undesirable, though, from the point of view of constructing Hamiltonians with only sparse couplings among the spins, because $\delta(\tilde{\phi}_0)$ can be viewed as the $K \to \infty$ limit of $e^{-K\tilde{\phi}_0^2}$, and this amounts to a strong all-to-all coupling among spins (though of a very particular form). In fact, we could achieve essentially the same results by omitting the factor of $\delta(\tilde{\phi}_0)$ while sending $J_0 \to J_0 - \mu$ where μ is small and positive. Then $\tilde{J}_0 \propto -\mu$, while the other $\tilde{J}_\kappa$ would scarcely be affected since they are finite and negative already at $\mathcal{O}(\mu^0)$. Use of (1.8) would then lead to the same G_h as in (1.9), up to an overall constant proportional to $1/\mu$. Discarding this uninteresting constant and then taking the limit $\mu \to 0$ would lead to precisely the result given in (1.9). In other words, we can recover (1.9) by starting with a massive

theory with truly sparse couplings and taking the massless limit.

Even with (1.9), exact analytic treatment of the sparse coupling model is too difficult. We will first apply the analysis leading to (1.9) to the Archimedean and p-adic statistical models as best as we can and then numerically study the sparse coupling model letting it interpolates between the two as the spectral parameter ranges from negative to positive values.

1.1.1 Archimedean coupling

As an extremal case of an Archimedean statistical model, we consider the model with nearest-neighbor coupling specified by

$$J_h^{\mathrm{NN}} = J_*(\delta_{h+1} + \delta_{h-1} - 2\delta_h)\,, \tag{1.10}$$

which leads to

$$G_h^{\mathrm{NN}} = \frac{1}{4\beta J_* L} \sum_{\kappa=1}^{L-1} \frac{e^{2\pi i \kappa h/L}}{\sin^2 \frac{\pi\kappa}{L}}\,. \tag{1.11}$$

If L is large, then we can approximate $\sin \frac{\pi\kappa}{L} \approx \frac{\pi\kappa}{L}$ and extend the sum to infinity:

$$G_h^{\mathrm{NN}} \approx \frac{L}{\beta J_*} \sum_{\kappa=-\infty,\ \kappa\neq 0}^{\infty} \frac{e^{2\pi i \kappa h/L}}{4\pi^2\kappa^2} = \frac{L}{\beta J_*} G(h/L)\,, \tag{1.12}$$

where the continuum two-point function $G(x)$ takes the form

$$G(x) = \frac{1}{2}\left(x - \frac{1}{2}\right)^2 - \frac{1}{24} \qquad \text{for} \qquad x \in [0,1]\,. \tag{1.13}$$

Properly speaking, $G(x)$ is defined on a circle with $x \sim x+1$, with periodic boundary conditions, and it satisfies

$$\frac{d^2G}{dx^2} = -\delta(x) + 1 \qquad \text{and} \qquad \int_0^1 dx\, G(x) = 0\,. \tag{1.14}$$

If instead of nearest neighbor coupling we have some generic finite-range J_h satisfying $J_h = J_{-h} > 0$ for $h \neq 0$ and $\tilde{J}_0 = 0$, then we get essentially the same result:

$$\tilde{J}_\kappa \approx -\frac{4\pi^2\kappa^2}{L^{5/2}} J_* \qquad \text{for} \qquad \left|\frac{\kappa}{L}\right|_\infty \ll 1 \tag{1.15}$$

for some positive constant J_*, and so for large L,

$$G_h \approx \frac{L}{\beta J_*} G(h/L) \tag{1.16}$$

with the same continuum function $G(x)$ given in (1.13). This suggests it has the same continuum limit as the nearest neighbor coupling, which makes sense due to the finite range being negligible compared to L sent to infinity.

It is worth noting that if we focus on small $|h/L|_\infty$, then we are mostly insensitive to the fact that the system is at finite volume, and we find $G(x) \approx G(0) - |x|_\infty/2$, which is the right power-law behavior for a local scalar in one dimension.

To compare to the sparse coupling, we want to generalize the nearest neighbor model to include a spectral parameter. As described in the introduction, we can also define non-local power law models. The exact Green's would be difficult to compute that way. We can reverse engineer it by first defining

$$\tilde{J}_\kappa^{\text{power}} \equiv -\frac{J_*}{2^s\sqrt{L}}\left[\sin\left(\frac{\pi\kappa}{L}\right)\right]^{-s} \tag{1.17}$$

so that

$$\tilde{G}_\kappa^{\text{power}} = \frac{2^s}{\beta J_*\sqrt{L}}\left[\sin\left(\frac{\pi\kappa}{L}\right)\right]^{s}. \tag{1.18}$$

For $s = -2$, this model reduces to the nearest neighbor coupling model. In general for $s < 1$, one can approximate the Fourier series of (1.17) with an integral in the limit $h/L \to 0$ to find that

$$J_h^{\text{power}} \sim -\frac{J_*}{\pi}\frac{\Gamma(1-s)\sin(\pi s/2)\Gamma(h+s/2)}{\Gamma(1+h-s/2)}. \tag{1.19}$$

By additionally invoking Sterling's formula, it becomes apparent that in the regime $1 \ll h \ll L$, the model we are considering does indeed couple the spins according to a power

law:

$$J_h^{\text{power}} \sim -\frac{J_*}{\pi}\,\Gamma(1-s)\sin(\pi s/2)\,h^{s-1}. \tag{1.20}$$

For $s < -1$, the large L limit of the position space Green's function asymptotes to

$$G_h^{\text{power}} = \frac{2^s\pi^s}{\beta J_* L^{1+s}}\left[\text{Li}_{-s}(e^{2\pi i h/L}) + \text{Li}_{-s}(e^{-2\pi i h/L})\right], \tag{1.21}$$

where $\text{Li}_n(x)$ denotes the polylogarithm function.

1.1.2 p-ADIC COUPLING

Choose a prime number p and a positive integer N, and assume

$$L = p^N\,. \tag{1.22}$$

Then an all-to-all coupling of spins can be defined based on the p-adic norm:

$$J_h^{p-\text{adic}} = \begin{cases} J_*|h|_p^{-s-1} & \text{if } h \neq 0 \\ -J_* L\dfrac{\zeta_p(-s)}{\zeta_p(1)\zeta_p(-Ns)} & \text{if } h = 0\,. \end{cases} \tag{1.23}$$

Here we have used the local zeta function

$$\zeta_p(s) \equiv \frac{1}{1-p^{-s}}\,, \tag{1.24}$$

so named because the usual Riemann zeta function is $\zeta(s) = \prod_p \zeta_p(s)$ where the product is over all prime numbers.

To analyze (1.23), it is useful first to work out the Fourier transform of the following function:

$$f_h = A|h|_p^{-s-1}(1-\delta_h) + B + C\delta_h\,. \tag{1.25}$$

A tedious but straightforward calculation suffices to show that

$$\tilde{f}_\kappa = \tilde{A}|\kappa|_p^{s}(1-\delta_\kappa) + \tilde{B} + \tilde{C}\delta_\kappa \tag{1.26}$$

where

$$\tilde{A} = L^{s+\frac{1}{2}}\frac{\zeta_p(-s)}{\zeta_p(1+s)}A \qquad \tilde{B} = \frac{C}{\sqrt{L}} - L^{s+\frac{1}{2}}\frac{\zeta_p(-s)}{\zeta_p(1)}A \qquad \tilde{C} = \sqrt{L}\left(B + \frac{\zeta_p(-s)}{\zeta_p(1)}A\right)\,. \tag{1.27}$$

With the help of (1.27) one can see immediately that $J_0^{p-\text{adic}}$ was chosen in (1.23) precisely so

as to have $\tilde{J}_0^{p-\text{adic}} = 0$. Indeed,

$$\tilde{J}_\kappa^{p-\text{adic}} = J_* \sqrt{L} \left[\frac{\zeta_p(-s)}{\zeta_p(1+s)} \left| \frac{\kappa}{L} \right|_p^s - \frac{\zeta_p(-s)}{\zeta_p(1)} \right] (1 - \delta_\kappa) \,. \tag{1.28}$$

While $\tilde{J}_\kappa^{p-\text{adic}} < 0$ for $\kappa \neq 0$ for any $s \in \mathbb{R}$, we are mostly interested in the regime $s > 0$, in which case the absolute value of the first term in square brackets in (1.28) is larger than the absolute value of the second. Thus we may expand

$$\tilde{G}_\kappa^{p-\text{adic}} = -\frac{1}{\beta L \tilde{J}_\kappa} (1 - \delta_\kappa) = -\frac{\zeta_p(1)/\zeta_p(-s)}{\beta L^{3/2} J_*} \sum_{n=1}^{\infty} \left(\frac{\zeta_p(1+s)}{\zeta_p(1)} L^{-s} \right)^n |\kappa|_p^{-ns} (1 - \delta_\kappa) \,. \tag{1.29}$$

The expansion is useful because it allows us to apply the Fourier transform (1.25)-(1.27) and obtain

$$\begin{aligned} G_h^{p-\text{adic}} = -\frac{\zeta_p(1)/\zeta_p(-s)}{\beta L^2 J_*} \sum_{n=1}^{\infty} \frac{\zeta_p(1+s)^n}{\zeta_p(1)^n} \Bigg[\left(\frac{\zeta_p(-ns+1)}{\zeta_p(ns)} |h|_p^{ns-1} - \frac{\zeta_p(-ns+1)}{\zeta_p(1)} \right) (1 - \delta_h) \\ - \frac{\zeta_p(-ns+1)}{\zeta_p(1)\zeta_p(N(ns-1))} \delta_h \Bigg] \,. \end{aligned} \tag{1.30}$$

The result (1.30) may seem complicated, but note that its leading term is $G_h^{p-\text{adic}} = A|h|_p^{s-1} + B + C\delta_h$ for some constants A, B, and C depending on s and proportional to $\frac{1}{\beta L^2 J_*}$. This is perhaps not too surprising when compared with power-law interactions in real field theories. Indeed, a power law $1/|x|_\infty^\alpha$ in the action leads to a power law $1/|x|_\infty^{\tilde{\alpha}}$ in the Green's

functions, where $\tilde{\alpha} + \alpha = 2d$ and d is the dimension of the field theory. The current setup is essentially the same, except that the ordinary absolute value has been replaced by the p-adic norm. Also, if we hold $L^2 J_*$ fixed, then except at $h = 0$ there is no L dependence at all in $G_h^{p-\text{adic}}$; the only thing that changes is the range of allowed h. Taking L large means that the range of h becomes p-adically dense in the p-adic integers $\mathbb{Z}_p$, defined as the subset of $\mathbb{Q}_p$ consisting of elements whose norm is no greater than 1. $\mathbb{Z}_p$ can be understood as the p-adic analog of the interval $[-1, 1] \subset \mathbb{R}$. Because $G_h^{p-\text{adic}}$ is a function of h only through its p-adic norm $|h|_p$, we see that its continuum limit is locally constant everywhere on $\mathbb{Z}_p$, except at $h = 0$.

1.1.3 The sparse coupling

Now let

$$L = 2^N \tag{1.31}$$

for some positive integer N. Then we can consider a sparse coupling of the form

$$J_h^{\text{sparse}} = J_* \sum_{n=0}^{N-1} 2^{ns} (\delta_{h-2^n} + \delta_{h+2^n} - 2\delta_h) \,. \tag{1.32}$$

By sparse, we mean that out of L independent values of J_h, only $\mathcal{O}(\log L)$ are non-vanishing. Of course, we could generalize from $p = 2$ to other values of p, but some unobvious com-

plications arise in doing so, which we prefer to postpone.

The main qualitative features of G_h^{sparse} are:

- For sufficiently negative s, G_h^{sparse} closely approximates G_h^{NN}. This makes sense because when s is large and negative, only the first few terms in the sum matter.
- For sufficiently positive s, G_h^{sparse} closely approximates $G_h^{2-\mathrm{adic}}$. This is less obvious and will be investigated further in the next section.
- As s crosses from negative to positive values, G_h^{sparse} undergoes a transition from being closer to a smooth function in an Archimedean sense to being closer to a smooth function in a 2-adic sense.

To visualize the behavior of G_h^{sparse}, we have found it helpful to mention again the discrete version of the Monna map, introduced for $p = 2$ already in the introduction. For completeness, we record here its definition for any p. Let any $h \in \{0, 1, 2, \ldots, L-1\}$ be expressed as

$$h = \sum_{n=0}^{N-1} h_n p^n \qquad \text{where each } h_n \in \{0, 1, 2, \ldots, p-1\} \ . \tag{1.33}$$

Then the image of h under the Monna map is

$$\mathfrak{M}(h) \equiv \sum_{n=0}^{N-1} h_{N-1-n} p^n \ . \tag{1.34}$$

In figure 1.1 we show G_h^{sparse} and $G_h^{2-\mathrm{adic}}$, the former as a function of both h and $\log_2 \mathfrak{M}(h)$, for various values of s, to confirm the qualitative features listed above.

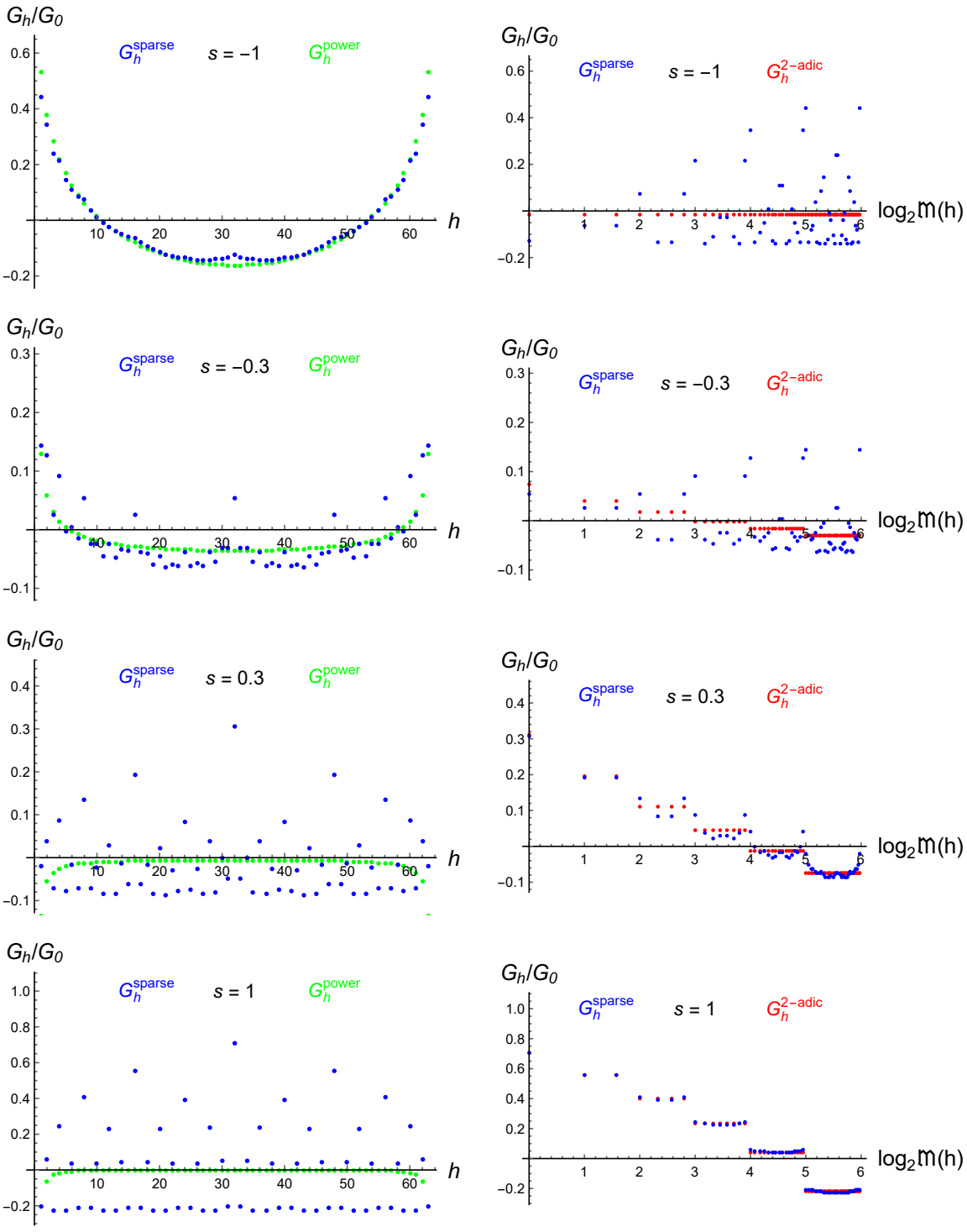

Figure 1.1: Left: G_h^{sparse} and G_h^{power} versus h. Right: G_h^{sparse} and $G_h^{2-\text{adic}}$ versus $\log_2 \mathfrak{M}(h)$.

1.2 Hölder Continuity bounds

Having observed an apparent change from Archimedean to 2-adic continuity in the discrete models of section 1.1.3, we are now ready to discuss the continuum limit. In general, smoothness based on derivatives is hard to define for p-adic like theories. The best we can hope for is some kind of continuity bound, in our case, the Hölder continuity bound or the Hölder conditions. Before getting into the main field theory calculations, let's review what Hölder conditions are in general. Let F be either $\mathbb{Q}_p$ or $\mathbb{R}$, and denote the norm on F as $|\cdot|$. Let f be a map from some subset $D \subset F$ to $\mathbb{R}$. Usually, if $F = \mathbb{R}$, then for us D will be an open interval, while if $F = \mathbb{Q}_p$, then D will be an affine copy of $\mathbb{Z}_p$. Let O be any subset of D. Then f satisfies a Hölder condition over O with positive real exponent α iff there is some positive real constant K such that

$$|f(x_1) - f(x_2)|_\infty < K|x_1 - x_2|^\alpha \tag{1.35}$$

for all x_1 and x_2 in O. If $O = D$, then we would say that f is globally α-Hölder continuous. We say that f is locally α-Hölder continuous at x iff there exists some open set I containing x such that f is α-Hölder continuous on I. And we describe f as a whole as locally α-Hölder continuous if it is locally α-Hölder continuous at every point in its domain (assumed to be an open set). A Hölder continuous function with any positive exponent α is

continuous in the usual sense. The bigger the α is, the smoother the function is. However, when the base space is real, then α cannot be bigger than 1 generically, unless $df/dx = 0$ in an open region. But if $F = \mathbb{Q}_p$, then it is possible to have non-constant functions with arbitrarily positive Hölder continuity exponent. This is another feature indicating that traditional derivatives of p-adic functions must be absent. *

The distinction between global and local α-Hölder continuity is important to us because the continuum limit of the two-point function G_h^{sparse} is, in some cases, globally Hölder continuous with one exponent (as hinted by the field theory analysis) and locally Hölder continuous away from the origin with a larger exponent (mostly numerical evidence). We will only present numerical evidences in this thesis. For rigorous field theory results with sparse couplings, we suggest readers to the reference[54].

1.2.1 2-adic approximation of sparse coupling results

Ratios between Green's functions derived from the sparse coupling and from the 2-adic coupling should be bounded above and below when s is positive:

$$K_1 < \tilde{G}_\kappa^{\text{sparse}} / \tilde{G}_\kappa^{2-\text{adic}} < K_2 \tag{1.36}$$

*A useful example of an α-Hölder continuous function $f(x)$ is a linear combination of functions $|x - x_i|^\alpha$ where the x_i are constants. $||x_1 - x_0|^\alpha - |x_2 - x_0|^\alpha|_\infty < |x_1 - x_2|^\alpha$ can be derived based on a fun fact that for three points in a space with non-Archimedean metric (which is automatically an ultrametric), two distances must be equal and the third must be less or equal to the other two.

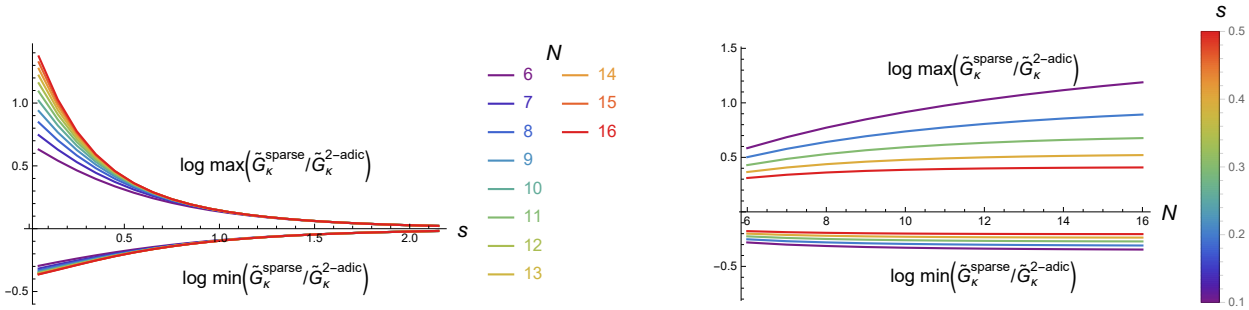

Figure 1.2: Left: Optimal values of the constants K_1 and K_2 appearing in (1.36) as functions of s for fixed N. Right: Optimal values of the constants K_1 and K_2 as function of N for fixed s.

for some positive constants K_1 and K_2 which may depend on s. When the normalization is taken care of (as we did), the ratio should asymptotically approach unity. Numerical support for this conclusion is shown in figure 1.2, where we show optimal values of K_1 and K_2 as functions of s for various N. As $s \to 0$, K_2 seems to diverge as N increases.

Away from small positive s, $\tilde{G}_\kappa^{\text{sparse}} \approx \tilde{G}_\kappa^{2-\text{adic}}$ is evidently an excellent approximation. Based on empirically examining the curves on the left side of figure 1.2, we find $K_i \approx 1 + 2^{-2s}\varkappa_i(s)$ where the functions $\varkappa_i(s)$ vary relatively slowly with s, possibly as a negative power of s, or possibly as a small positive power of 2^{-s}. The right plot shows that K_1 and K_2 goes to constants at sufficiently large N, for a given positive s not too small. In order to obtain K_1 and K_2 numerically as functions of N and s, the actual procedure was as follows:

1. For fixed N and s, compute $\tilde{G}_\kappa^{\text{sparse}}$ numerically using the methods of section 1.1, and adjust the overall coupling strength J_* so that $G_h^{\text{sparse}} = 1$ when $h = 0$. (In other words, the normalization condition is implemented in *position space*.)

2. Likewise compute $\tilde{G}_\kappa^{2-\mathrm{adic}}$ with $G_0^{2-\mathrm{adic}} = 1$.

3. Compute K_1 and K_2 as

$$\begin{aligned} K_1 &= \min\left(\frac{\tilde{G}_\kappa^{\mathrm{sparse}}}{\tilde{G}_\kappa^{2-\mathrm{adic}}}\right) \equiv \min_{\kappa\neq 0} \frac{\tilde{G}_\kappa^{\mathrm{sparse}}}{\tilde{G}_\kappa^{2-\mathrm{adic}}} \\ K_2 &= \max\left(\frac{\tilde{G}_\kappa^{\mathrm{sparse}}}{\tilde{G}_\kappa^{2-\mathrm{adic}}}\right) \equiv \max_{\kappa\neq 0} \frac{\tilde{G}_\kappa^{\mathrm{sparse}}}{\tilde{G}_\kappa^{2-\mathrm{adic}}} \,. \end{aligned} \tag{1.37}$$

We also want to quantify how ragged the Green's functions become in momentum space in regimes where one couldn't derive any continuity bound (by methods developed in the current work). The Hölder bounds, as derived in field theory in section 1.2, are approximately as follows:

- $|\tilde{G}^{\mathrm{sparse}}(k_1) - \tilde{G}^{\mathrm{sparse}}(k_2)|_\infty < K|k_1 - k_2|_2^s$ when $s > 0$. More precisely, $\tilde{G}^{\mathrm{sparse}}(k)$ as a map from $\mathbb{Q}_2$ to $\mathbb{R}$ is locally s-Hölder continuous away from $k = 0$.
- $|\tilde{G}^{\mathrm{sparse}}(k_1) - \tilde{G}^{\mathrm{sparse}}(k_2)|_\infty < K|k_1 - k_2|_\infty^{-s}$ when $-1 < s < 0$. More precisely, $\tilde{G}^{\mathrm{sparse}}(k)$ as a map from $\mathbb{R}$ to $\mathbb{R}$ is locally $-s$-Hölder continuous away from $k = 0$ when $-1 < s < 0$, and locally 1-Hölder continuous away from $k = 0$ when $-2 < s < -1$.

1.2.2 Local Hölder condition in momentum space

Next we would like to understand how well the local Hölder continuity bounds in momentum space are reflected in the numerics. To test the Hölder bound on the p-adic side, we first adjust the overall coupling strength J_* so that $G_0^{\mathrm{sparse}} = 1$, and likewise $G_0^{2-\mathrm{adic}} = 1$.

Then we define

$$\tilde{A}^{2-\text{adic}}(N,s) \equiv \log_2 \max_{\kappa \text{ odd}} \left| \frac{\tilde{G}^{\text{sparse}}_{\kappa}}{\tilde{G}^{2-\text{adic}}_{\kappa}} - \frac{\tilde{G}^{\text{sparse}}_{\kappa+L/2}}{\tilde{G}^{2-\text{adic}}_{\kappa+L/2}} \right|_{\infty} , \tag{1.38}$$

where on the right hand side we understand that $\tilde{G}^{\text{sparse}}_{\kappa}$ and $\tilde{G}^{2-\text{adic}}_{\kappa}$ are computed using the same values of N and s. Two points with the separation $L/2$ has the smallest p-adic distance. We find numerically that $\tilde{A}^{2-\text{adic}}(N,s)$ is linear in N:

$$\tilde{A}^{2-\text{adic}}(N,s) \approx -s(N-1) + \log_2 \tilde{K}^{2-\text{adic}}(s) \,, \tag{1.39}$$

where $\tilde{K}^{2-\text{adic}}(s)$ is N-independent. These linear trajectories persist even at negative s, after 2-adic continuity is lost. See figure 1.3. To make the connection to Hölder continuity bounds more transparent, we note that (1.38)-(1.39) are equivalent to

$$\left| \frac{\tilde{G}^{\text{sparse}}_{\kappa_1}}{\tilde{G}^{2-\text{adic}}_{\kappa_1}} - \frac{\tilde{G}^{\text{sparse}}_{\kappa_2}}{\tilde{G}^{2-\text{adic}}_{\kappa_2}} \right|_{\infty} \leq 2^{\tilde{A}^{2-\text{adic}}(N,s)} \approx \tilde{K}^{2-\text{adic}}(s) \, |\kappa_1 - \kappa_2|_2^s \tag{1.40}$$

for all odd κ_1 and κ_2 with $\kappa_2 - \kappa_1 = L/2$. The inequality (1.40) is clearly a close relative of the local s-Hölder continuity condition on $\tilde{G}(k)$. Numerically including more separations does not affect the final result. So, $\tilde{G}^{\text{sparse}}_{\kappa}$ satisfies a local 2-adic Hölder condition whose most positive exponent is approximately $\tilde{\alpha}^{2-\text{adic}}(N,s) \equiv -\tilde{A}^{2-\text{adic}}(N,s) + \tilde{A}^{2-\text{adic}}(N -$

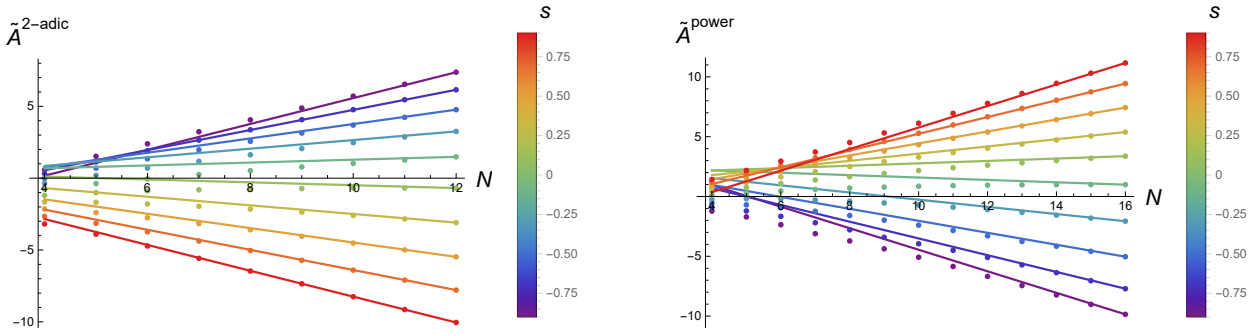

Figure 1.3: Left: 2-adic continuity in momentum space. The dots are evaluations of $\tilde{A}^{2-\text{adic}}(N, s)$ in (1.38), and the lines are plots of the linear trajectories indicated in (1.39), with $K(s)$ chosen so that the line goes through the last data point.
Right: Archimedean continuity in momentum space. The dots are evaluations of $\tilde{A}^{\text{power}}(N, s)$ in (1.41), and the lines are plots of the linear trajectories indicated in (1.42), with $K(s)$ chosen so that the line goes through the last data point.

$1, s) \approx s$.

On the Archimedean side, in order to pursue a similar strategy, we need some standard of comparison analogous to $\tilde{G}_\kappa^{2-\text{adic}}$. We define

$$\tilde{A}^{\text{power}}(N, s) \equiv \log_2 \max_{\frac{L}{4} \le \kappa < \frac{3L}{4}} \left| \frac{\tilde{G}_\kappa^{\text{sparse}}}{\tilde{G}_\kappa^{\text{power}}} - \frac{\tilde{G}_{\kappa+1}^{\text{sparse}}}{\tilde{G}_{\kappa+1}^{\text{power}}} \right|_\infty , \tag{1.41}$$

where $\tilde{G}_\kappa^{\text{power}}$ is given in (1.18) as usual. We can adjust J_* so that $G_h^{\text{power}} = 1$ when $h = 0$ in position space.

Because $\tilde{G}^{\text{power}}$ is C^∞ away from $\kappa = 0$, forming the ratio $\tilde{G}_\kappa^{\text{sparse}}/\tilde{G}_\kappa^{\text{power}}$ doesn't affect the local smoothness properties of $\tilde{G}_\kappa^{\text{power}}$. However, this ratio does cancel out part of the overall trend whereby $\tilde{G}_\kappa^{\text{sparse}}$ gets bigger near $\kappa = 0$ and $\kappa = L$. As a result, studying

$\tilde{G}_\kappa^{\text{sparse}}/\tilde{G}_\kappa^{\text{power}}$ rather than $\tilde{G}_\kappa^{\text{sparse}}$ by itself makes it easier to accurately pick out the local smoothness properties from a finite sampling of points. As on the 2-adic side, the numerical data approximately follow exponential trajectories:

$$\tilde{A}^{\text{power}}(N,s) \approx s(N-1) + \log_2 K^{\text{power}}(s)\,, \tag{1.42}$$

where $K(s)$ is N-independent. These trajectories persist even at positive s, after Archimedean continuity is lost. So we can usefully define

$$\tilde{\alpha}^{\text{power}}(N,s) \equiv -\tilde{A}^{\text{power}}(N,s) + \tilde{A}^{\text{power}}(N-1,s)\,, \tag{1.43}$$

and then $\tilde{\alpha}^{\text{power}}(N,s) \approx -s$ for large N is our numerical estimate of the most positive exponent appearing in a local Archimedean Hölder condition for $\tilde{G}_\kappa^{\text{sparse}}$.

1.2.3 Local Hölder condition in position space

Position space smoothness can be studied using quantities analogous to the ones used in section 1.2.2 for momentum space. Specifically, we define

$$\begin{aligned} A^{2-\text{adic}}(N,s) &\equiv \log_2 \max_{h \text{ odd}} \left| \frac{G_h^{\text{sparse}}}{G_h^{2-\text{adic}}} - \frac{G_{h+L/2}^{\text{sparse}}}{G_{h+L/2}^{2-\text{adic}}} \right|_\infty \\ \alpha^{2-\text{adic}}(N,s) &\equiv -A^{2-\text{adic}}(N,s) + A^{2-\text{adic}}(N-1,s)\,, \end{aligned} \tag{1.44}$$

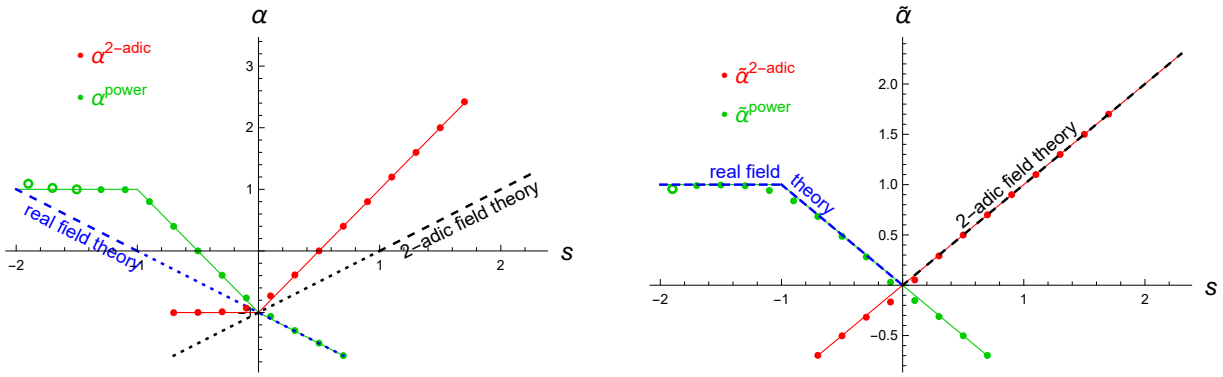

Figure 1.4: α versus s and $\tilde{\alpha}$ versus s in the 2-adic and Archimedean settings. Field theory bounds derived in [54] are shown in dashed black and dashed blue. Dotted black and dotted blue show the naive extrapolations of these bounds to negative α and $\tilde{\alpha}$. Red and green dots are numerical evaluations of α and $\tilde{\alpha}$ as defined in sections 1.2.3 and 1.2.2, respectively, with $N = 20$. Solid red and green lines show the obvious piecewise linear trends which approximately match the numerical evaluations. Open circles denote evaluations in which we restricted $\frac{7L}{16} \leq h < \frac{9L}{16}$; otherwise we use half the available points as explained in the main text. For $s \leq -2$, convergence of the sparse model to the nearest neighbor model implies that $\alpha = \tilde{\alpha} = 1$, but our numerical scheme for picking out α and $\tilde{\alpha}$ becomes less reliable in this region due to difficulty normalizing G^{sparse} and G^{power} in a mutually consistent way.

and then, assuming $\alpha^{2-\text{adic}}(N, s)$ is nearly constant for large N, its large N limit is our numerical estimate of the best possible local Hölder exponent for G_h^{sparse} in a 2-adic setting. Likewise, we define

$$\begin{aligned} A^{\text{power}}(N, s) &\equiv \log_2 \max_{\frac{L}{4} \leq h < \frac{3L}{4}} \left| \frac{G_h^{\text{sparse}}}{G_h^{\text{power}}} - \frac{G_{h+1}^{\text{sparse}}}{G_{h+1}^{\text{power}}} \right|_\infty \\ \alpha^{\text{power}}(N, s) &\equiv -A^{\text{power}}(N, s) + A^{\text{power}}(N-1, s)\,. \end{aligned} \tag{1.45}$$

The large N limit of $\alpha^{\text{power}}(N, s)$ (assuming it exists) is our numerical estimate of the most positive local Hölder exponent for G_h^{sparse} in an Archimedean setting.

We find good evidence that $\alpha^{2-\text{adic}}(N, s)$ and $\alpha^{\text{power}}(N, s)$ have finite large N limits.

Our numerical results are well described by piecewise linear dependence of α on s, and in particular by

$$\begin{aligned} \alpha^{\text{power}} &= -2(s+1/2) \qquad \text{for} \quad -1 < s < 0 \\ \alpha^{2-\text{adic}} &= 2(s-1/2) \qquad \text{for} \quad 0 < s < 1\,. \end{aligned} \tag{1.46}$$

See figure 1.4. Note the difference between position space bounds and momentum space bounds in general. When $|s| > 1$, it becomes harder to get good numerical results, particularly on the Archimedean side, because the functions under consideration are quite smooth, and we have to compute very small differences accurately. Even apart from issues of numerical accuracy, it becomes challenging on the Archimedean side to distinguish between rapid but smooth variation and the slightly non-smooth behavior that determines the Hölder exponent.

1.2.4 Transition between Archimedean and non-Archimedean continuity

The most interesting regime in position space is $-1 < s < 1$, where we are losing Archimedean continuity and gaining 2-adic continuity. We focus in this section entirely on this regime, and we present the simplest account of the transition from Archimedean to non-Archimedean continuity, which is consistent with our numerics. Due to finite numerical resolution, we cannot rigorously determine the measure-theoretic behavior of the position space Green's functions in regions where the Green's functions are very ragged. We

attempt to qualify our claims below with the appropriate level of confidence.

In momentum space, our numerics are consistent with there being a single exponent on the 2-adic side, $\tilde{\alpha}^{2-\mathrm{adic}} = s$, which describes both the global Hölder continuity condition over all k and the local continuity at each possible value of k. In other words, as far as we can tell, the function $\tilde{G}(k)$ is equally ragged everywhere. A similarly uniform story applies on the Archimedean side, with $\tilde{\alpha}^{\mathrm{power}} = -s$. Numerical results are fully in accord with expectations from field theory. The upshot is that the transition from Archimedean to non-Archimedean continuity happens rather simply, with ordinary continuity failing just as 2-adic continuity emerges: i.e. $\tilde{\alpha}^{\mathrm{power}}$ becomes negative just as $\tilde{\alpha}^{2-\mathrm{adic}}$ becomes positive, at $s = 0$.

The field theory estimates of the Hölder exponents for the position-space Green's function were $s - 1$ on the 2-adic side and $-s - 1$ on the Archimedean side. We believe this characterizes the behavior of $G(x)$ close to $x = 0$: That is, $G(x) \approx |x|_2^{s-1}$ on the 2-adic side, while $G(x) \approx |x|_\infty^{-s-1}$ on the Archimedean side. The surprise we get from numerics is that away from $x = 0$, a more complicated dependence of Hölder smoothness on s emerges, with local Hölder exponents α somewhat more positive than the field theory bounds: That is, $G(x)$ seems to be somewhat smoother away from the origin than its behavior right near $x = 0$. Our numerical results are consistent with there being a piecewise linear dependence of α on s, as summarized in particular by (1.46). These results (1.46) indi-

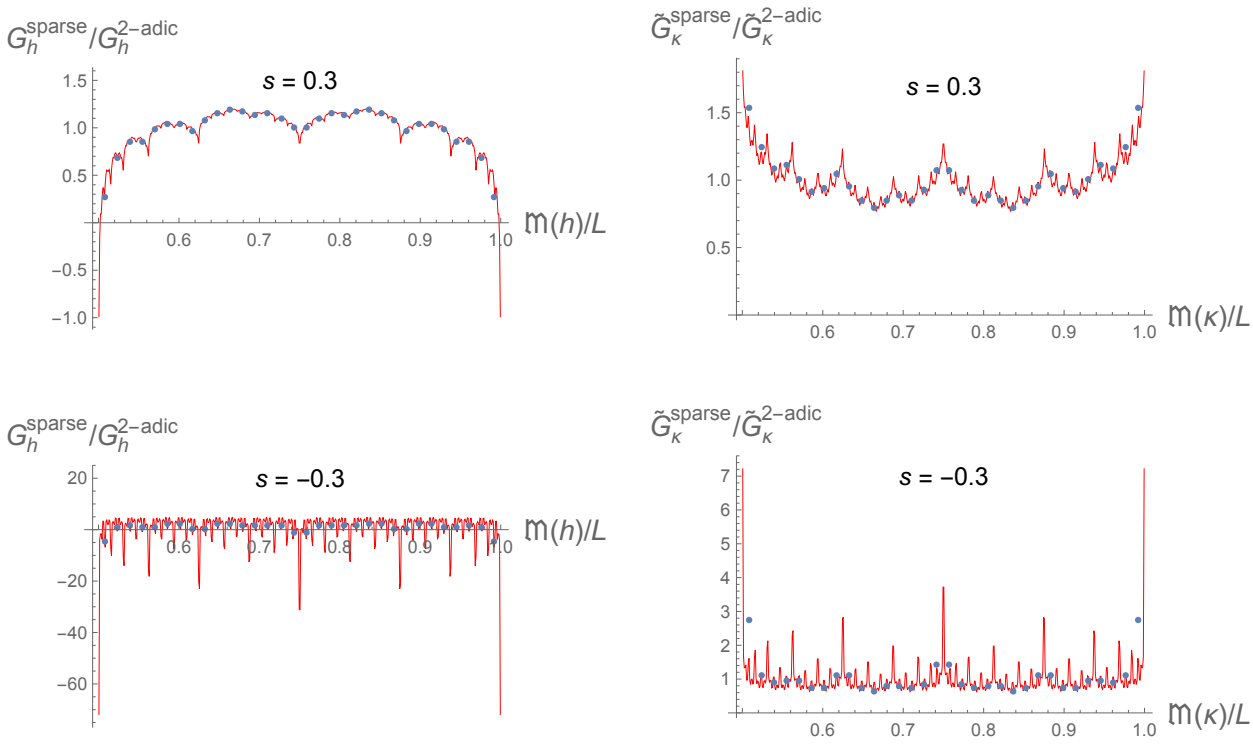

Figure 1.5: Plots of $G_h^{\text{sparse}}/G_h^{2-\text{adic}}$ and $\tilde{G}_\kappa^{\text{sparse}}/\tilde{G}_\kappa^{2-\text{adic}}$ over the Monna map of the odd integers. As s becomes more positive, the numerical data is closer to a 2-adically continuous curve when N is large. Blue points are for $N = 6$, while the red curves are for $N = 10$.

cate that Archimedean Hölder continuity of G_h^{sparse} is lost at $s = -1/2$, but 2-adic Hölder continuity doesn't emerge until $s = 1/2$. So, what happens for $-1/2 < s < 1/2$, when both α^{power} and $\alpha^{2-\text{adic}}$ are negative?

To better understand the region of transition between the Archimedean and 2-adic smoothness, it is instructive to inspect overlaid plots of the Green's function for different system sizes, see figures 1.5 and 1.6. Based on these figures and related studies, the scenario we regard as most likely is that for $-1/2 < s < 0$, the continuum limit of G_h^{power} defines

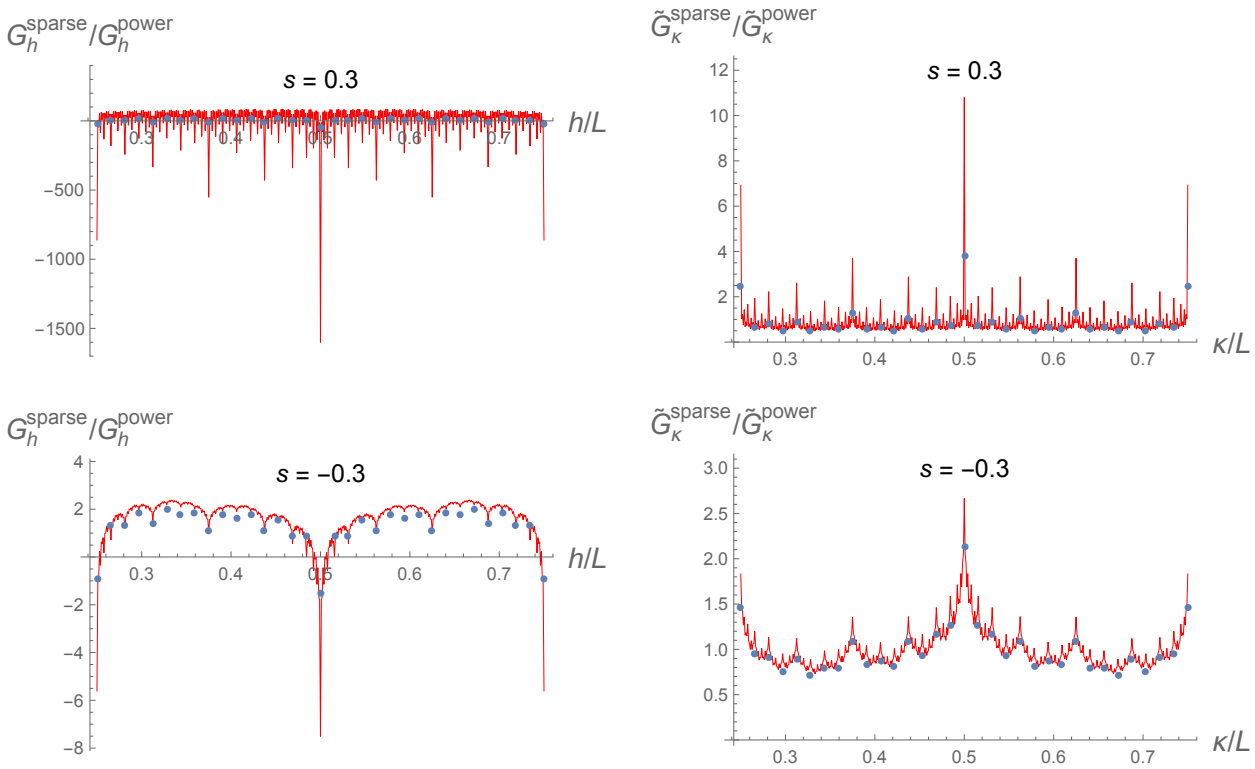

Figure 1.6: Plots of $G_h^{\text{sparse}}/G_h^{\text{power}}$ and $\tilde{G}_\kappa^{\text{sparse}}/\tilde{G}_\kappa^{\text{power}}$ over the middle half of points. As s becomes more negative, the numerical data is closer to a continuous curve when N is large. Blue points are for $N = 6$, while the red curves are for $N = 10$.

an absolutely continuous measure, $G(x)dx$, with respect to ordinary Lebesgue measure dx, but for $s > 0$ any such continuum limit would necessarily have a singular term in its Radon-Nikodym (Lebesgue) decomposition. Similarly, we suggest that for $0 < s < 1/2$, the continuum limit of $G_h^{2-\text{adic}}$ defines an absolutely continuous measure with respect to the standard Haar measure on $\mathbb{Q}_2$ while for $s < 0$ any such continuum limit would have a singular term (with respect to the Haar measure on $\mathbb{Q}_2$) in its Radon-Nikodym decomposition. We find support for the claim of absolutely continuous measures in the above-mentioned regimes when we study the scaling of the height of the spikes in figures 1.5 and 1.6 as a function of N: the weight of each spike (meaning the integral over a small region including the spike) distinctly appears to tend to zero with increasing N. When singular terms in Radon-Nikodym decompositions do exist, we conjecture that they have as their support sets which are dense in position space.

One way in which singular terms in Radon-Nikodym decompositions could arise is for the continuum limit $G(x)$ to include delta functions. Inspection of figure 1.5 is consistent with there being a dense set of delta function spikes in $G(x)$ as a function of 2-adic x when $s = -0.3$, but none when $s = 0.3$. Similarly, figure 1.6 is consistent with there being a dense set of delta function spikes in $G(x)$ as a function of real x when $s = 0.3$, but none with $s = -0.3$. The discerning reader may note, however, that the spikes on the Archimedean side are stronger at $s = 0.3$ than the ones on the 2-adic side at $s = -0.3$.

This asymmetry manifests itself in the scaling of the height of these spikes with N, for the weight of each spike grows with N on the Archimedean side for $s = 0.3$, but may be trending very slowly toward 0 on the 2-adic side at $s = -0.3$. A related effect appears in figure 1.4: $\alpha^{2-\text{adic}} \approx -1$ for $s < 0$, while $\alpha^{\text{power}} \approx -1 - s$ for $s > 0$.

Inspection of figures 1.5 and 1.6 reveals some self-similarity in the Green's functions both before and after the Monna map is applied. We have not investigated this fractal behavior in detail; however, we note that similar behavior has been found independently in band structure calculations in connection with cold atom experiments[10].

1.3 Conjecture about the interacting theory

For decades, p-adic numbers have been considered as an alternative to real numbers as a notion of the continuum which could underlie fundamental physics at a microscopic scale; see for example[124]. The current study shows how the large system size limit of an underlying discrete system naturally interpolates between a one-dimensional Archimedean continuum and a 2-adic continuum as we vary a spectral exponent. By focusing on a free field example, we are able to solve the model through essentially trivial Fourier space manipulations. The correlators of the theories we study are all determined in terms of the two-point function through the application of Wick's theorem. The two-point function is smooth in an Archimedean sense when s is sufficiently negative and in a 2-adic sense when s is suf-

ficiently positive. The transition from these two incompatible notions of continuity can be precisely characterized in terms of Hölder exponents characterizing the smoothness of the two-point function. We have found the dependence of these exponents on s through numerics on finite but large systems.

All the examples above remain within the paradigm of free field theory. Still easy to formulate but obviously much harder to solve are interacting theories with sparse couplings. For example, we could start with any of the models introduced in section 1.1 and add a term $\sum_i V(\phi_i)$ to the Hamiltonian describing arbitrary on-site interactions. To get some first hints of what to expect these interactions to do, recall in 2-adic field theory that $G(x) \approx |x|_2^{s-1}$ at small x. Comparing this to the standard expectation $G(x) \approx |x|_2^{2\Delta_\phi}$, we arrive at $\Delta_\phi = (1-s)/2$ as the ultraviolet dimension of ϕ. When describing perturbations of the Gaussian theory, we can use normal UV power counting: $[\phi^n] = n\Delta_\phi$. Thus ϕ^n is relevant when $s > 1 - 2/n$. If we impose $\mathbb{Z}_2$ symmetry, $\phi \to -\phi$, then in the region $s < 1/2$, the Gaussian theory has no relevant local perturbations, but as s increases from $1/2$ to 1, first ϕ^4 and then higher powers of ϕ^2 become relevant. It is reasonable to expect some analog of Wilson-Fisher fixed points to appear. Possibly as $s \to 1$, these fixed points extrapolate to analogs of minimal models. An analogous story presumably applies on the Archimedean side to power-law field theories controlled by s in the range $(-1, 0)$, with $G(x) \approx |x|_\infty^{-s-1}$ and therefore $\Delta_\phi = (1+s)/2$. See figure 1.7.

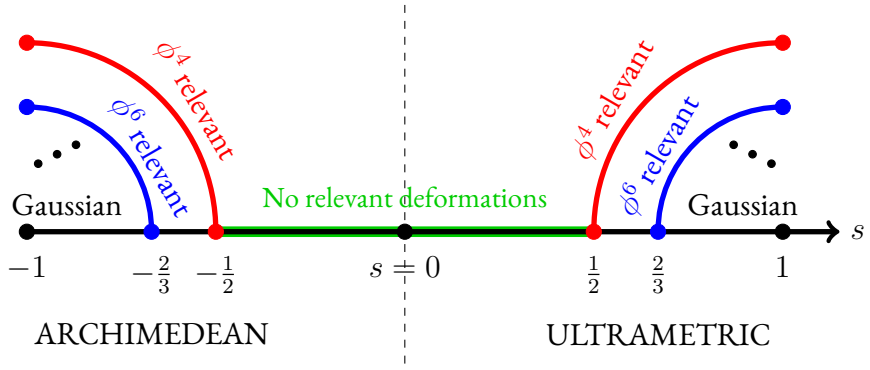

Figure 1.7: Conjectured pattern of fixed points of the renormalization group for interacting field theories of a single bosonic scalar field with $\phi \to -\phi$ symmetry.

The sparse coupling theories are sufficiently similar to 2-adic field theories for $s > 0$ and to power-law field theories for $s < 0$ that it is reasonable to conjecture that the same pattern of renormalization group fixed points arises. This line of reasoning leaves out a lot, though: In particular, we have no deep understanding of how the improved local Hölder smoothness arises, nor how it might affect renormalization group flows. A Monte Carlo study of the phases of the sparsely coupling Ising model might help refine our understanding of the renormalization group flows available to interacting models, particularly in the range $-2/3 < s < 2/3$ where no powers of ϕ higher than ϕ^4 are relevant—according at least to naive power counting as presented here.

2

p-adic, but real-ly mixed

2.1 Mixed field theory

Field theory has been a reliable tool for studying critical phenomena. Various techniques of renormalization group flow make it possible to classify continuous phase transitions in different statistical models. A frequently mentioned example is the ϕ^4 theory, which is a scalar field theory equipped with a quartic interaction term. Below its upper critical

dimension $D = 4$ and above its lower critical dimension $D = 2$, ϕ^4 theory exhibits a Wilson-Fisher fixed point[128]. Values of anomalous dimension and scaling exponent of the two-point function at the fixed point are "critical," and they are universal quantities within the same universality class. For example, Wilson-Fisher fixed point of ϕ^4 theory and the critical Ising model in three dimensions are in the same universality class. The ϵ-expansion in $D = 4 - \epsilon$ of ϕ^4 theory with $\epsilon = 1$ gives critical exponents that agree with results obtained on the lattice with high precision[110].

Having understood that Dyson's hierarchical model corresponds to the pure p-adic field theory[92], we would like to consider a quantum generalization of it: a one-dimensional spin chain with p-adic coupling and transverse magnetic field

$$H = -Jg \sum_m \hat{\sigma}_m^x - J \sum_{m,n} |m-n|_p^{s-1} \hat{\sigma}_m^z \hat{\sigma}_n^z \,, \tag{2.1}$$

where $|\cdot|_p$ is the standard p-adic norm, σ_m is a quantum Ising operator, m and n take values in $\{0, 1, 2, \ldots, p^\ell - 1\}$ and ℓ is some positive integer. There are four motivations for this kind of Hamiltonian. First, we are interested in extending p-adic AdS/CFT beyond the domain of Euclidean statistical mechanical models as studied in[62], to a quantum mechanical setting. The independent work[69] did consider quantum mechanical aspects, but time evolution was left implicit. Second, we are aware of developing experimental setups which can realize an approximation of p-adic couplings in a cold atom system[10]. Third, p-adic

extra-dimensions are interesting to think of and have been considered, for example, in these works[4,124]. Forth, the original classical version of this model, where there is no transverse field, and σ_m is a classical spin variable taking values of $+1$ and -1, has been studied well, and it guarantees some interesting features. This s exponent also serves as an RG variable, and one can get a continuum set of Wilson-Fisher fixed points parametrized by s. Models of this kind show interesting criticalities, which are first solved by Bleher[14]. p-adic field theory computations[103,57] agrees with Bleher's results. s exponent plays essentially the same role in the quantum model, and there are guaranteed criticalities found by Monthus[104].

We want to present a field theory as a candidate for the continuum limit of this quantum model. A rough analog is the map between a d-dimensional quantum Ising and a $d+1$-dimensional classical Ising model, the extra dimension being generated by the transverse field. Field theories describing non-local quantum lattice models are usually inevitably faced with a strong anisotropy, as the "quantum dimension" is always local. We will not provide a rigorous map between the quantum Dyson's model and a field theory. Also, field theories defined on two different number fields are not well studied. Here we propose the ϕ^4 "mixed field theory" with one direction being the usual real number field and the other

direction being the p-adic number field. The action we consider is:

$$S = \frac{1}{2}\int_{\mathbb{R}} d\omega \int_{\mathbb{Q}_p} dk\, \tilde{\phi}(-\omega,-k)\left(\omega^2 + |k|_p^{2z} + r\right)\tilde{\phi}(\omega,k) + \frac{\lambda}{4!}\int_{\mathbb{R}} d\tau \int_{\mathbb{Q}_p} dx\, \phi(\tau,x)^4. \tag{2.2}$$

where r serves as a dial for g in the quantum lattice model. For simplicity, we choose to forbid the ratio between real and p-adic terms to change. With the definition of Vladimirov derivative D_x^{2z}, we could see that the above action is equivalent to the following

$$S = \frac{1}{2}\int_{\mathbb{R}} d\tau \int_{\mathbb{Q}_p} dx\, \phi(\tau,x)\left(\frac{-\partial_t^2}{(2\pi)^2} + D_x^{2z} + r\right)\phi(\tau,x) + \frac{\lambda}{4!}\int_{\mathbb{R}} d\tau \int_{\mathbb{Q}_p} dx\, \phi(\tau,x)^4 \tag{2.3}$$

up to some regulating terms.

Power counting in ultrametric theories is well understood: See for example[s8]. The key point is that when we scale $k \to pk$, the norm and the integration measure scale oppositely: $|k|_p \to \frac{1}{p}|k|_p$ and $dk \to \frac{1}{p}dk$. We regard this scaling as a step toward the infrared. We see from the kinetic term of (2.2) that we must accompany $k \to pk$ with $\omega \to \frac{1}{p^z}\omega$ and $r \to \frac{1}{p^{2z}}r$. In general, we associate to a quantity X an engineering dimension $[X]$ if upon a scaling $k \to pk$ we have $X \to p^{-[X]}X$. Then the natural assignments that make S

dimensionless consistent with (2.2) are

X	k	$\lvert k\rvert_p$	dk	x	$\lvert x\rvert_p$	dx	ω	$d\omega$	S	ϕ	$\tilde{\phi}$	r	λ
$[X]$	-1	1	1	1	-1	-1	z	z	0	$\frac{1-z}{2}$	$-\frac{3z+1}{2}$	$2z$	$3z-1$

(2.4)

We refer to these assignments as engineering dimensions because they describe scalings of the classical action without reference to loop corrections. We see in particular that λ has a positive dimension, meaning that ϕ^4 is a relevant perturbation of the Gaussian fixed point theory, precisely when $z > 1/3$—whereas r is always relevant in the same sense since we require $z > 0$.

As compared to ordinary ϕ^4 theory on $\mathbb{R}^d$, we see from the assignments (2.4) that increasing z is like decreasing d; that $z = 1/3$ is like the upper critical dimension $d = 4$, where ϕ^4 becomes marginal; and that $z = 1$ is like the lower critical dimension, where the dimension of ϕ goes to 0. Thus, at least naively, we are expecting critical points as indicated in figure 2.1. We added in a conjectured branch of multi-critical points based on the fact that for $z > 1/2$, both ϕ^4 and ϕ^6 are relevant deformations of the Gaussian fixed point. For $0 < z < 1/3$, our expectation based on power counting is that the Gaussian critical point is the only one available.

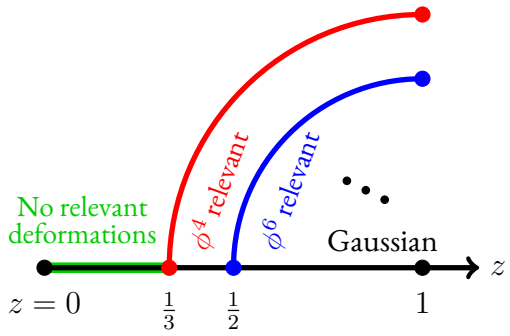

Figure 2.1: Conjectured pattern of critical points of (2.2).

2.2 Tree-level results

In a free massless($r = 0, \lambda = 0$) theory, the mixed field theory is diagonalized in momentum space, and the Green's function is just

$$\widetilde{G}(\omega, k) = \frac{1}{\omega^2 + |k|_p^{2z}} \,. \tag{2.5}$$

Now we want to study the position space Green's function by Fourier transforming the real and p-adic components(we here assume that Fubini's theorem still applies) :

$$G(\tau, x) \equiv \langle \phi(\tau, x)\phi(0,0)\rangle = \int_{\mathbb{R}} d\omega \int_{\mathbb{Q}_p} dk \, \frac{e^{-2\pi i\omega\tau}\chi(kx)}{\omega^2 + |k|_p^{2z}} \,. \tag{2.6}$$

In a real theory, we can determine the scaling behavior of Green's function in a conformal theory just by changing variables and make the integral above dimensionless. Here the same is not expected because of a mixing of real and p-adic term in the denominator. In

fact, there are oscillatory corrections to the power-law relation $G(\tau,0) \propto |\tau|^{(z-1)/z}$. One hint comes from the fact that $|k|_p^{2z}$ can only take discrete values p^{-2zv} where $v \in \mathbb{Z}$. It is not hard to see by changing variable that $G(\tau,0) = \text{const}|\tau|^{(z-1)/z}$ only if τ takes value in $p^{z\mathbb{Z}}$. This means our theory only enjoys a discrete scaling symmetry under $\tau \to p^{vz}\tau$ where $v \in \mathbb{Z}$.

We can obtain approximations of the position space Green's function where the oscillatory terms are more explicit. To carry out the ω integral first and then the k integral in (2.6) is a lot easier than the other way around. To perform the k integral, we use the standard result in p-adic Fourier analysis that we introduce in the introduction:

$$\int_{p^v\mathbb{U}_p} dy\, \chi(y) = \begin{cases} p^{-v}/\zeta_p(1) & \text{if} \quad v \geq 0 \\ -1 & \text{if} \quad v = -1 \\ 0 & \text{if} \quad v < -1 \end{cases} \tag{2.7}$$

We consider two special cases $\tau = 0$ and $x = 0$:

- $\tau = 0$

$$G(0,x) = \int_{\mathbb{Q}_p} dk\ \frac{\pi\chi(kx)}{|k|_p^z} = \frac{\pi\Gamma_p(1-z)}{|x|_p^{1-z}} \tag{2.8}$$

  This is the same as a Green's function in a purely p-adic field theory.

- $x = 0$

$$G(\tau,0) = \int_{\mathbb{Q}_p} dk\ \frac{\pi e^{-2|k|_p^z \pi|\tau|}}{|k|_p^z} = (1-p^{-1}) \sum_{v=-\infty}^{\infty} \pi p^{v(z-1)} e^{-2\pi|\tau|p^{-vz}} \tag{2.9}$$
$$= \frac{\pi(2\pi|\tau|)^{1-z^{-1}}}{z\zeta_p(1)\log p} \sum_{\tilde{v}=-\infty}^{\infty} \Gamma\left(\frac{2i\pi\tilde{v}}{z\log p} + \frac{1}{z} - 1\right) e^{-2\pi i \frac{\log(2\pi|\tau|)}{z\log p}\tilde{v}}$$

where Poisson summation formula has been used and the Fourier transform of a double exponential is a Gamma function. We can see that in addition to the $|\tau|^{1-z^{-1}}$ scaling, there are oscillatory terms that are periodic in $\log|\tau|$. Gamma function decays quickly along the imaginary direction, so in most of the cases the non-oscillatory term dominates. Note that we can only carry the calculation in $0 < z < 1$, but then $G(\tau,0)$ in (2.9) can be analytically continued to $z > 1$ as well. No matter what region of z we are considering, for the mixed field theory with large enough p, we would face situations where oscillatory terms dominate. In such case the scaling behaviour of τ in Green's function could be totally ruined, but it will always be positive(because it is a sum of positive numbers) even when the leading oscillatory terms fluctuate around zero.

2.3 Loop diagrams and Renormalization

From now on, we will consider $O(N)$ symmetric mixed vector model in Euclidean signature with a coupling term like $\frac{\lambda}{4!}(\vec{\phi}^2)^2$ because essentially all the computations in a scalar ϕ^4 mixed theory generalize without subtlety. The dimension of coupling is $[\lambda] = 3 - 1/z$. So at $z = 1/3$, the ϕ^4 operator becomes marginal, and the theory is renormalizable. We will perturb the free massless mixed field theory with a mass term $r\vec{\phi}^2$ and $\frac{\lambda}{4!}(\vec{\phi}^2)^2$ interac-

tion term at $z = 1/3$ and follow the MS scheme and renormalize the theory with a ultraviolet cut-off Λ. Then we perturb the exponent. Wilson-Fisher fixed point exists, and we obtained the anomalous mass dimension at the WF fixed point, which can be compared with lattice model results in[104].

In this low dimension theory, ω integrals over the real numbers are always performed exactly without any UV cut-off. So there could be symmetry issues when we put UV cut-off only in the ultrametric dimension. This is usually not a big problem in a theory with highly anisotropic terms, see for example[75,38] where different UV cut-offs are applied to time and space integrals in the renormalization of Lifshitz scalar theory. Note also that from time to time, we will introduce infra-red cut-off λ when performing p-adic momentum integrals. This is one way of regularizing p-adic integrals, and no term depending on Λ will emerge from this treatment. So in an MS scheme, this will not change the behavior of this theory under renormalization.

2.3.1 One-loop renormalization of the mixed field theory

Consider now the bubble diagram,

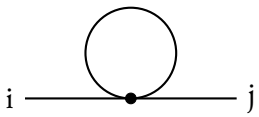

$$= \frac{1}{2}(-\lambda)\frac{2+N}{3}\delta^{ij} I_2^{(1)}\,, \tag{2.10}$$

where the loop integral is given by

$$I_2^{(1)} = \int_{\mathbb{R}} d\omega \int_{\mathbb{Q}_p} dk \frac{1}{\omega^2 + |k|_p^{2/3} + r} = \int_{\mathbb{Q}_p} dk \frac{\pi}{\sqrt{|k|_p^{2/3} + r}} \,. \tag{2.11}$$

This plus a counterterm is the only one-loop correction to the propagator in our theory. At this point, we impose the UV cut-off Λ and an IR cut-off λ(they both have mass dimension $\frac{3}{2}[r]$) and complete the p-adic integral. We are perturbing the massless theory with a mass term so that we can expand the integrand near $r = 0$, and the linear term corresponds to the insertion of a mass operator with no momentum flowing in or out.

$$\text{Linear term} = \quad r\vec{\phi}^2 \tag{2.12}$$

And the result is

$$\begin{aligned} \int_{\lambda \le |k|_p \le \Lambda} dk \frac{\pi}{\sqrt{|k|_p^{2/3} + r}} &= \frac{\pi}{\zeta_p(1)} \sum_{v=-\frac{\log \Lambda}{\log p}}^{-\frac{\log \lambda}{\log p}} \left(p^{-\frac{2v}{3}} - \frac{r}{2} \right) + \text{finite terms} \\ &= \frac{\pi}{\zeta_p(1)} \left(\frac{\Lambda^{2/3} p^{2/3}}{p^{2/3} - 1} - \frac{r \log \Lambda}{2 \log p} \right) + \text{finite terms} \\ &= \frac{\pi}{\zeta_p(1)} \left(\zeta_p(\tfrac{2}{3}) \Lambda^{\frac{2}{3}} - \frac{r}{2} \frac{\log \Lambda}{\log p} \right) + \text{finite terms} \,. \end{aligned} \tag{2.13}$$

There is no external momentum dependence, so the anomalous dimension of the field is zero at one-loop order. Consider this diagram as the one-particle-irreducible diagram at the

one-loop level. Then the insertion will shift the mass parameter r in the propagator. The mass acquires an anomalous dimension γ_r during the RG, and by dimensional analysis, we know that this must cancel the shift by the $r \log \Lambda$ term. The net effect is changing r to $r^{1+\frac{1}{2}\gamma_r}$ where γ_r is the anomalous mass dimension. We expand it in γ_r and identify the $r \log r^{\frac{1}{2z}}$ term with minus the $r \log \Lambda$ piece of the bubble diagram, and we find that the anomalous mass dimension is given by

$$\gamma_r = \frac{2+N}{12z} \frac{\pi}{\zeta_p(1)} \frac{\lambda}{\log p} \,. \tag{2.14}$$

We comment that this $\log \Lambda$ term here comes from the term $-\frac{r}{2}$ in (2.13) where the p dependence cancels. By power counting, we could see that this happens exactly at $z = 1/3$. This story is very similar to the real scalar theory case, while the connection seems somehow miraculous because, in real and mixed cases, the integrals are carried out very differently.

In order to see a Wilson-Fisher fixed point, we should compute the one-loop correction

to the vertex. We need to consider the sum of three Feynman diagrams:

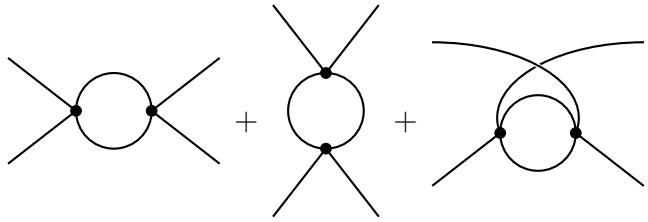

$$
\begin{aligned}
= \frac{1}{2}(-\lambda)^2 \frac{1}{9} \Big\{ & I_4(\omega_1+\omega_2, k_1+k_2)\Big[(N+4)\delta_{i_1 i_2}\delta_{i_3 i_4} + 2\delta_{i_1 i_3}\delta_{i_2 i_4} + 2\delta_{i_1 i_4}\delta_{i_2 i_3}\Big] \\
& + I_4(\omega_1+\omega_3, k_1+k_3)\Big[(N+4)\delta_{i_1 i_3}\delta_{i_2 i_4} + 2\delta_{i_1 i_2}\delta_{i_3 i_4} + 2\delta_{i_1 i_4}\delta_{i_2 i_3}\Big] \\
& + I_4(\omega_1+\omega_4, k_1+k_4)\Big[(N+4)\delta_{i_1 i_4}\delta_{i_1 i_2} + 2\delta_{i_1 i_2}\delta_{i_3 i_4} + 2\delta_{i_1 i_3}\delta_{i_2 i_4}\Big]\Big\}
\end{aligned}
\tag{2.15}
$$

where the loop integral is given by

$$
I_4(\omega, k) = \int_{\mathbb{R}} d\omega_0 \int_{\mathbb{Q}_p} dk_0 \frac{1}{\omega_0^2 + |k_0|_p^{2/3} + r} \frac{1}{(\omega_0-\omega)^2 + |k_0-k|_p^{2/3} + r} \,. \tag{2.16}
$$

We can set them to zero to simplify the computation because the leading piece that we are interested in is independent of ω and r. We perform the real integral first and then complete the p-adic integral:

$$
I_4(\omega, k) = \frac{3\pi}{4\zeta_p(1)} \frac{\log \Lambda^{2/3}}{\log p} + \text{ finite terms} \,. \tag{2.17}
$$

Similar $\log \Lambda$ term appears as in the real ϕ^4 theory, for the reason that we comment before.

The Callan-Symanzik equation of the four-point function is

$$0 = \left[\frac{\partial}{\partial\Lambda} + \frac{d\lambda}{d\Lambda}\frac{\partial}{\partial\lambda} + \frac{dr}{d\Lambda}\frac{\partial}{\partial r}\right]\left(-\lambda + \frac{\lambda^2}{2}\frac{N+8}{9}\,3\,\frac{\pi}{2\zeta_p(1)}\frac{\log\Lambda}{\log p}\right). \tag{2.18}$$

The leading order beta function is solved to be

$$\beta(\lambda) = \Lambda\frac{d\lambda}{d\Lambda} = \lambda^2\frac{\pi}{\zeta_p(1)}\frac{N+8}{12\log p}\,. \tag{2.19}$$

We now consider the beta function slightly above the critical z. Then the beta-function picks up a contribution due to the mass dimension of the coupling, $[\lambda] = 3z - 1$, as by redefining the coupling $\tilde{\lambda}$ as $\lambda\Lambda^{-[\lambda]}$, we can make the coupling constant dimensionless again. Now we will abuse the notation and use λ for the new dimensionless coupling, but still use $[\lambda]$ as the dimension before the redefinition.

$$\beta(\lambda) = -[\lambda]\lambda + \lambda^2\frac{\pi}{\zeta_p(1)}\frac{N+8}{12\log p} + \mathrm{O}([\lambda]^2)\,. \tag{2.20}$$

We see that the beta function admits a Wilson-Fisher fixed point at

$$\lambda_* = \frac{\zeta_p(1)}{\pi}\frac{12\log p}{N+8}[\lambda]\,. \tag{2.21}$$

Here the exponent $s = 2z$ serves as a dial of the dimension. In contrast to real scalar ϕ^4 the-

ory, here we can maintain integer dimensions while probing the WF fixed point. Plugging (2.21) into (2.14), we find the anomalous mass dimension at the Wilson-Fisher fixed point:

$$\gamma_r = \frac{N+2}{N+8}\frac{[\lambda]}{z}\,. \tag{2.22}$$

This is the same as the anomalous mass dimension of a real $O(N)$ symmetric vector model equipped with a $(\vec{\phi}^2)^2$ term. At a conformal (here just scale invariance) fixed point, the correlation length diverges. We can compute the p-adic correlation length exponent ν near a fixed point of the $N = 1$ scalar theory in this long-ranged regime (where $2z < 2$) as a rescale of the real correlation length exponent:

$$\nu = \frac{1}{(2-\gamma_r)z}\,. \tag{2.23}$$

For $z = 1/2$, $[\lambda]/z = 1$, and we compute the correlation length exponent ν to be $6/5 = 1.2$, which is quite different from Monthus's result $\nu = 1.482$[104], where they consider the quantum Dyson's hierarchical model which we think should be the lattice version of a mixed field theory. Equivalently, they were looking at each time slice of the theory(a quantum mechanic model), so in our theory, the scaling behavior along the $\mathbb{Q}_p$ line can be compared with their result. This discrepancy cannot be fully explained now. Note that in the supposed mean-field regime($0 < z < 1/3$ or $0 < \sigma < 2/3$ in[104]), the exponents Mon-

thus got is not perfectly $1/\sigma$ or equivalently $1/(2z)$, the long-ranged mean-field value(note that $\nu - 1/\sigma$ is roughly constant for the values they computed). This could be related to the approximation they use in the real space RG process, or the lattice quantum Dyson model and the mixed field theory are not in the same universality class at all. This should be studied further in future work.

2.3.2 Two-loop renormalization of the propagator

The first momentum-dependent correction to the propagator is from a two-loop diagram called the melon(or sunrise, or underground) diagram. So, normally one expects to have the leading field renormalization at this order. In order to investigate this, it is enough for us to consider the melon diagram at $z = 1/3$ in a massless theory:

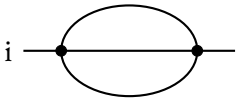

$$= \frac{1}{6}(-\lambda)^2 \frac{3N+6}{9} \delta_{ij} I_2^{(2)}(\omega, k)\,. \tag{2.24}$$

where the loop integral is given by

$$I_2^{(2)}(\omega, k) = \int_{\mathbb{R}} d\omega_1\, d\omega_2\, d\omega_3 \int_{\mathbb{Q}_p} dk_1\, dk_2\, dk_3\, \frac{\delta(\omega + \sum_{i=1}^3 \omega_i)\, \delta_p(k + \sum_{i=1}^3 k_i)}{\left(\omega_1^2 + |k_1|_p^{2/3}\right)\left(\omega_2^2 + |k_2|_p^{2/3}\right)\left(\omega_3^2 + |k_3|_p^{2/3}\right)}\,. \tag{2.25}$$

Before proceeding to compute this diagram, let us first look at an old argument: field strength in a p-adic field theory does not get renormalized[92]. This is explained by Lerner

and Missarov in[92] that the self-similar Hamiltonian contains a counterterm that has the form of a single-particle Hamiltonian and a single particle in a box is always finite. To briefly illustrate this, we adapt the Wilson exact RG equation and imagine defining our theory within a ball in the $\mathbb{Q}_p$ or its finite extension. In a normal scalar theory in real space-time, self-similar conditions in the ball usually introduce higher momentum dependence outside the ball. Thus to achieve a self-similar theory over the whole momentum space(the fixed point), one has to "re-normalize" the theory as it can not be normalized in the ball properly. While for the p-adic case, because of the ultrametricity, the momentum terms inside the ball can not generate higher momentum terms outside the ball, and this term could be properly normalized, or say, it is in any case, finite. In the end, this "breakdown" of Wilsonian RG comes from the totally disconnected topology of $\mathbb{Q}_p$. In our mixed field theory, however, the real momentum term gets renormalized while the p-adic momentum term receives no renormalization. The net effect is a shift of the exponent z. It is tempting to say that we are renormalizing the dimension!

In the ultra-violet region—a momentum space computation

Now we are going to manipulate the integral of (2.25) to find the divergent pieces that we want. Integrals over p-adic momentums are always split into regions where the norm is constant, and the remaining task is to complete the summations of powers of p. Only rational functions of the momentum can be summed easily. Also, the sum of series of rational

functions is usually another rational function, so we can complete the integrals sequentially for each momentum. Thus our task now is to manipulate the integral till we have rational functions. First, using Schwinger parametrization and the ω_i integrals are over the Gaussian functions and can be done straightforwardly. Then we change the variable to Feynman parameters(or symmetric dimensionless parameters):

$$I_2^{(2)}(\omega,k)=\pi\int_{\mathbb{Q}_p^3}dk_1dk_2dk_3\int_0^1 dx_1dx_2dx_3\,\frac{\delta\left(1-\sum_i x_i\right)}{\sqrt{x_1x_2x_3\sum_i 1/x_i}}\,\frac{\delta_p\left(k-\sum_i k_i\right)}{\left(\frac{\omega^2}{\sum_i 1/x_i}+\sum_i x_i|k_i|_p^{2/3}\right)^2}\,. \tag{2.26}$$

This integral has mass dimension 2 and so its superficial UV divergences is of $\Lambda^{2/3}$. So we anticipate following terms in the integral:

$$I_2^{(2)}(\omega,k)=c_2\Lambda^{2/3}+c_0\omega^2\log\frac{\Lambda^{2/3}}{\omega^2}+b_0\omega^2+(\text{other finite terms})\,, \tag{2.27}$$

for some dimensionless constants c_2, c_0, and b_0. We do not include the divergent term with p-adic momentum dependence like $|k|_p^{2/3}\log\Lambda^{2/3}$ because the ultra-metric momentum does not get renormalized (an explicit computation confirms its absence). To fully track the $|k|_p$ term in the integral is difficult and in general one has to consider special quadrilateral structure of momentum conservation, where each triangle in it is either tall isosceles or

equilateral:

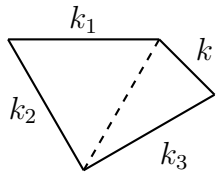

(2.28)

Loosely we can say in the ultra-violet limit where $|k_i|_p$ becomes large, we have $|k - k_1 - k_2|_p = |k_1 + k_2|_p$ due to the ultrametricity and the integral is independent of $|k|_p$ in the UV region. Then the delicate cancellation $k_1+k_2+k_3 = k$ can be split into hard and soft(as soft as k) parts: $k_{1h} + k_{2h} + k_{3h} = k_a$ and $k_{1s} + k_{2s} + k_{3s} = k_b$ where $|k_{ih}|_p > |k_{is}|_p$ and $k_a + k_b = k$. Due to ultrametricity, k_b has to be soft and then consequently k_a is soft. Now in the ultra-violet region where one only deal with hard momentums k_{ih}, we can really forget about k and change the momentum conservation to a loose constrain that $k_{1h} + k_{2h} + k_{3h}$ has to be soft. In such regime we definitely expect no $|k|_p^{2/3} \log \Lambda^{2/3}$ like term.

Now let's focus on the real momentum dependent divergence. In order to investigate the $c_0\omega^2 \log \frac{\Lambda}{|\omega|^3}$ term, we consider the derivative

$$\begin{aligned}
&\frac{\partial I_2^{(2)}(\omega,k)}{\partial \omega^2} = c_0 \log \frac{\Lambda^{2/3}}{\omega^2} - c_0 + b_0 + (\text{other finite terms}) \\
&= -2\pi \int_{|k_i|_p \le \Lambda} dk_1 dk_2 dk_3 \int_0^1 dx_1 dx_2 dx_3 \, \frac{\delta\left(1 - \sum_i x_i\right)}{\sqrt{x_1 x_2 x_3 \left(\sum_i 1/x_i\right)^3}} \, \frac{\delta_p\left(k - \sum_i k_i\right)}{\left(\frac{\omega^2}{\sum_i 1/x_i} + \sum_i x_i |k_i|_p^{2/3}\right)^3} .
\end{aligned} \tag{2.29}$$

As argued above, there is no k dependence in any divergent term, so we can safely focus

on the $k = 0$ case while preserving the RG behaviour. Also, we know c_0 is a constant independent of ω, so we can set $\omega = 0$, as well. And as always, we have to introduce a IR cut-off $\sup |k_i|_p > 1$ by hand to regularize this p-adic integral from below. This is believed to have no effect on c_0. Using the identity

$$\int_0^1 dx_1 dx_2 dx_3 \, \frac{\delta\left(1-\sum_i x_i\right)}{\sqrt{x_1 x_2 x_3 \left(\sum_i 1/x_i\right)^3}} \frac{1}{\left(\sum_i a_i x_i\right)^3} = \frac{\pi/2}{\sqrt{a_1 a_2 a_3}(\sqrt{a_1}+\sqrt{a_2}+\sqrt{a_3})^3} \,, \tag{2.30}$$

for positive a_1, a_2, and a_3, we simplify (2.29) to

$$\frac{\partial I_2^{(2)}(\omega,k)}{\partial \omega^2} = -\pi^2 \int_{1<\sup|k_i|_p\leq\Lambda} dk_1 dk_2 dk_3 \, \frac{\delta_p\left(\sum_i k_i\right)}{|k_1 k_2 k_3|^{1/3}\left(\sum_i |k_i|_p^{1/3}\right)^3} + (\text{finite terms}) \,. \tag{2.31}$$

Momentum conservation now possesses a simple triangle structure. Due to ultrametricity, this triangle is either tall isosceles or equilateral. And thanks to this totally disconnected topology, we can perform the integrals in disjoint regions and then add them up. For the equilateral contribution, we have

$$\int_{1<|k_1|_p=|k_2|_p=|k_3|_p\leq\Lambda} dk_1 dk_2 dk_3 \, \frac{\delta_p\left(\sum_i k_i\right)}{|k_1 k_2 k_3|^{1/3}\left(\sum_i |k_i|_p^{1/3}\right)^3} = \frac{\log \Lambda^{2/3}}{18\zeta_p(1)\log p}\left(1-\frac{2}{p}\right) \,. \tag{2.32}$$

For the tall isosceles contribution, we have

$$\int_{\substack{1<|k_2|_p\leq\Lambda \\ |k_1|_p<|k_2|_p=|k_3|_p}} dk_1 dk_2 dk_3 \, \frac{\delta_p\left(\sum_i k_i\right)}{|k_1 k_2 k_3|^{1/3}\left(\sum_i |k_i|_p^{1/3}\right)^3} = \frac{3\log\Lambda^{2/3}}{16\zeta_p(1)^2\log p}\sum_{v=1}^{\infty}\frac{p^{-2v/3}}{\left(1+\frac{1}{2}p^{-v/3}\right)^3}\,. \tag{2.33}$$

There is no one-loop contribution, so we want the coefficient of $\omega^2\log\omega^2$ term in the counterterm to be the inverse of the coefficient of $\omega^2\log\Lambda^{2/3}$ term from the melon diagram. This is the correction that ω^2 receives in the effective action. Expanding $\omega^{2(1-\gamma_{\omega^2})}$, identifying the coefficient, and we have the final result

$$\gamma_{\omega^2} = -\lambda^2\frac{N+2}{36}\frac{\pi^2}{\log p}\left[\frac{p-2}{9\,p\,\zeta_p(1)}+\frac{9}{8\,\zeta_p(1)^2}\sum_{v=1}^{\infty}\frac{p^{-2v/3}}{(1+\frac{1}{2}p^{-v/3})^3}\right]. \tag{2.34}$$

The same result is obtained in[55] by a position space computation. There we Fourier transform the integral, manipulate the integral in position space, and then Fourier transform back to momentum space. No UV cut-off needs to be introduced, but we use the differential regularization instead, where we drop all the divergent terms when transforming back to momentum space.

Plugging (2.21) into (2.34) we find

$$\gamma_{\omega^2} = -\frac{[\lambda]^2}{z^2}\frac{4\log p}{9}\frac{N+2}{(N+8)^2}\left[\frac{p-2}{9\,p}\zeta_p(1) + \frac{9}{8}\sum_{v=1}^{\infty}\frac{p^{-2v/3}}{(1+\frac{1}{2}p^{-v/3})^3}\right]. \tag{2.35}$$

Now we really see that for different prime numbers p, this mixed field theory falls into different universality classes. Respectively we have

$$\gamma_k = 0\,. \tag{2.36}$$

The net effect of this anisotropic renormalization is a rescaling of z to $z(1-\gamma_{\omega^2})$.

We find no known result in the literature to compare with (2.35) as usually, people study the criticality of a quantum Dyson's hierarchical model via real-space RG where the time direction is equivalently unscaled. γ_{ω^2} is of order coupling square, so the correction to, for example, anomalous mass dimension is not significant and cannot be used as a check, either. The equation $\gamma_k = 0$, or the non-renormalization property, though, agrees with[104], where they find the correlation exponent η to be the long-ranged mean-field value $2-\sigma$ even in a non-mean-field region. Actually, in condense matter literature, it is known for long-ranged isotropic models that their correlation exponent remains the long-ranged mean-field value

during RG flow[39,120,95]. From a field theory perspective, we say that field strength in a purely p-adic theory is not renormalized[92]. Here, however, the connection lies between mixed field theories and long-ranged quantum models.

2.4 Discussion and future directions

With the help of p-adic number, we can construct non-local field theories with diagonalized Lagrangian in momentum space and do perturbative loop calculations just like in a local quantum field theory with a normal kinetic term. In this work, we perturb the free mixed theory by a $(\vec{\phi}^2)^2$ term and find a Wilson Fisher fixed point of the RG flow when spectral exponent z is above the critical value $1/3$. Because of symmetries, we expect that this theory at the WF fixed point should be in the same universality class of a quantum Dyson's hierarchical model. The correlation length exponent ν we compute is slightly smaller than the result in[104] but still close. Note that quantum Dyson's hierarchical model can be partially realized in a cold atom setup[10]. In the future, we hope to see works that could carry the RG to higher loop orders, where we expect an anomalous mass dimension close to what will be found in these cold atom experiments. Note that extra care should be taken of this scaling of z in higher loops.

Understanding this non-renormalization or "mixed renormalization" in the mixed field theory remains to be improved. As mentioned at the end of the last section, z tends to be-

come bigger at the fixed point. We hope to see future works that explore this interesting feature.

Historically, p-adic and fundamental physics get connected by the p-adic string theory, where the world sheet is taken to be p-adic, and the target space is kept real[25,41,125,42]. From a different philosophy, the mixed field theory applications to fundamental physics could be possible as with a compact dimension, the awkward ultrametricity is hidden, and theories are then consistent with our normal space-time, which is Archimedean. Interesting constructions of field theories could be made by considering a p-adic internal space. In the future, we want to further study mixed field theories with compact ultra-metric dimensions. We expect to find a consistent truncation story here due to the ultrametricity: soft modes only multiply to give soft modes. For example, one can consider Fourier expanding the field by momentum along the compact dimension and plugging it in the equation of motion with any non-linear term. A consistent truncation sets all hard momentum modes to zero and gets equations of motion consistent with the original equation of motion. For soft mode equations of motion, setting hard modes to be zero will give us a finite set of equations with only soft modes. For hard mode equations of motion in a real scalar theory, there are terms made of only soft modes, so setting hard modes to be zero will give us an infinite set of equations of the soft modes. There is no guarantee that this infinite set of equations will give solutions that are consistent. While in the p-adic case, thank to the

ultrametricity, there is no term in the hard equations of motion that are made only of soft modes. So setting hard modes to be zero gives us no new equation of the soft, and we get a finite set of soft equations in the end. This is really a detailed way of saying the fact that, at tree level, in a p-adic momentum preserving particle production process, a hard mode cannot decay to or be generated from pure soft modes because a sum of soft momentums will always be soft. We hope to see an exact dimensional reduction that can generate this consistent truncation in the future. With a reduced action, we can study loop effects of the consistent truncation relatively easily in the p-adic setting, which is regarded as a difficult subject in the consistent truncation of Archimedean theories, like supergravity.

3

Non-local field theory I: non-local non-linear sigma model

Scalar field theories over the reals with bi-local kinetic terms were introduced in [40], and the recent work [109] provides a useful point of entry into the extensive literature. Similar field theories over the p-adic numbers were considered in [92] as a continuum description of

Dyson's hierarchical model[36]. A unifying point of view on the bi-local $O(N)$ vector model was provided in[58], showing that the standard large N development can be framed in terms that are largely independent of whether the theory is formulated over the reals or the p-adics. The present work extends the study of bi-local theories to bi-local non-linear sigma models, starting with the action

$$S = \frac{\mu^{n-s}}{2\gamma} \int_{V\times V} \frac{d^n x d^n y}{|x-y|^{n+s}} d(\phi(x), \phi(y))^2 \,, \tag{3.1}$$

where $|x-y|$ is the distance function on the n-dimensional base space V and $d(\phi(x), \phi(y))$ is the distance function on the target manifold. In the limit $s \to n$, where the theory (3.1) becomes classically scale-invariant, we find logarithmic divergences in one-loop diagrams, which can be canceled by counterterms that can be expressed in terms of the target space laplacian of the square of the distance function, together with field redefinitions.*

Ricci flatness suppresses the one-loop divergences that we encounter, so in a sense (and with significant caveats), we may claim that we are deriving the vacuum Einstein equations from conformal invariance, as in[43]. Our work was partly motivated by the more recent results of[72], which were derived for the nearest neighbor arc length model on the Bruhat-Tits tree—in other words, on the other side of the p-adic AdS/CFT duality[62,69] from our results

*An exception, as we will see, is when s is an even integer and the base space $V = \mathbb{R}^n$. Through a procedure we will omit here, one recovers, in this case, a local non-linear sigma model, and at least for $s = 2$, we can use our results to check the standard analysis[43] of the one-loop beta function.

for field theories over the p-adic numbers. However, the particular structure of counterterm we find suggests that renormalization of our theories have less to do with renormalization of the local metric as normally understood (i.e. Ricci flow) than with an augmentation of the action (3.1) to include the target space laplacian of $d(\phi(x), \phi(y))^2$.

A conservative expectation is that once non-local terms are allowed in a field theory, they proliferate, and the theory becomes non-renormalizable. Theories with purely quadratic bi-local kinetic terms, as studied in [40,92] (as well as many subsequent works) avoid such problems through a non-renormalization theorem: If we write

$$S = \frac{1}{2}\int_V d^n k\, \hat{\phi}(-k)|k|^s \hat{\phi}(k) + \int_V d^n x\, U(\phi(x))\,, \tag{3.2}$$

then the claim is that the quadratic bi-local term is never renormalized (at least perturbatively), though the purely local term $U(\phi(x))$ certainly is—and depending on details, derivative terms might be radiatively generated. Non-local interaction terms vitiate this non-renormalization theorem, and one's suspicions could be renewed that there is no sensible theory. We will not be able in this work entirely to allay such concerns because we do not give a demonstration parallel to the one in [43] that Ward identities based on diffeomorphism invariance guarantee that loop divergences can only modify the original form of the action. Indeed, the counterterms we generate at one loop do modify the bi-local action in an unexpected way, but one which appears to be controlled in a derivative expansion so

that higher derivative terms can be radiatively generated at each new order without spoiling results from lower orders.

The organization of the rest of this chapter is as follows. In section 0.4.1 we present the main results in Fourier analysis that we need, both over the reals and the p-adics. In section 0.4.3 we explain how double integrals such as the one in (3.1) can be regulated if divergences arise as $|x-y| \to 0$. In section 3.1 we introduce the classical action for the bi-local non-linear sigma model. In section 0.4.4 we discuss loop divergences in general terms, including an introductory account of the non-renormalization property of the kinetic term in (3.2). In sections 3.2.1-3.2.4 we investigate the simplest one-loop divergences of the bi-local non-linear sigma model, and then in section 3.2.5 we argue that all these divergences can be canceled by a laplacian counterterm in place of renormalization of the local metric, together with field redefinitions.

3.1 The bi-local non-linear sigma model

Let M be a smooth D-dimensional manifold with a Riemannian metric g_{ab}, whose Riemann and Ricci tensors are

$$R_{ab}{}^{c}{}_{d} = \partial_a \Gamma^c_{bd} - \partial_b \Gamma^c_{ad} + \Gamma^c_{ae}\Gamma^e_{bd} - \Gamma^c_{be}\Gamma^e_{ad} \qquad\qquad R_{ac} = g^{bd} R_{abcd}\,. \tag{3.3}$$

Given any two points X and Y on M, let

$$Q(X,Y) = d(X,Y)^2 \tag{3.4}$$

be the square of the shortest distance between X and Y. Clearly, $Q(X,Y)$ is a smooth function of X and Y, provided X and Y are not too far apart. For smooth functions $\phi\colon V \to M$ whose range is sufficiently localized, we consider the action functional

$$S = \frac{\mu^{n-s}}{2\gamma} \int'_{\mathbb{R}^n} \frac{d^n x d^n y}{|x-y|^{n+s}} Q(\phi(x),\phi(y))\,, \tag{3.5}$$

where $\int'$ indicates a regulated double integral of the type discussed around (32)-(34).[†] Note that this discussion requires us to avoid positive even integer s. When $s > 2$, there are derivative terms like $(\partial\phi)^2$ implicitly built into (3.5), with coefficients tuned so as to ensure convergence of the integral. The parameter μ has dimensions of energy so that we can regard ϕ and $Q(\phi(x),\phi(y))$ as dimensionless. The factor γ is a loop-counting parameter: Classical effects are $O(\gamma^{-1})$, one-loop amplitudes are $O(\gamma^0)$, two-loop amplitudes are $O(\gamma)$, and so forth. In other words, γ plays the role of $\hbar$.

[†]One may wonder whether the primed integral, as defined following (33), spoils coordinate invariance of the integrand. For instance, if s is sufficiently large we may, in light of (34), be required to include a $\Box_y Q$ term to the integrand, which if written only in terms of partial derivatives does not appear to be coordinate invariant. In fact, it is easy to convince oneself that, e.g., $\Box_y Q$ can be constructed from covariant quantities: $\partial_{y^a}\partial_{y^b} Q = \frac{\partial^2 Q}{\partial\phi^i\partial\phi^j}\frac{\partial\phi^i}{\partial y^a}\frac{\partial\phi^j}{\partial y^b} + \frac{\partial Q}{\partial\phi^i}\frac{\partial^2\phi^i}{\partial y^a\partial y^b} = \left(\nabla_{\phi^i}\frac{\partial Q}{\partial\phi^j}\right)\frac{\partial\phi^i}{\partial y^a}\frac{\partial\phi^j}{\partial y^b} + \frac{\partial Q}{\partial\phi^i}\frac{\partial\phi^j}{\partial y^a}\nabla_{\phi^j}\frac{\partial\phi^i}{\partial y^b}$.

A close cousin of the action (3.5) was considered in[72]:

$$S = \sum_{\langle xy \rangle} d(\phi(x), \phi(y))^2 \tag{3.6}$$

where now x and y are vertices of a graph, and the sum is over undirected edges. The formula actually appears earlier in[43], though it was intended there to be considered on a square lattice, as a regulator for the local non-linear sigma model, rather than on the Bruhat-Tits tree as in[72].

We require the range of the maps ϕ to be sufficiently localized in order to ensure that we do not encounter any failures of smoothness in $Q(X, Y)$, and in order to ensure that we can use a single system of Riemann normal coordinates for ϕ throughout. One can now solve the geodesic equation perturbatively in the curvature and use that to expand $Q(X, Y)$. We observe that the action (3.5) consists of a non-local kinetic term (quadratic term in the expansion of Q) and non-local interaction terms (higher-order terms in that expansion) where the combination of Riemann tensors play the role of coupling constants. Once the loop integrals are studied systematically and independent of the metric tensor, the task becomes to study the contractions of Riemann tensors according to the rules defined by those loop integrals.

Before presenting the result of expanding Q, we find it convenient to introduce some

abbreviated notation, based on the following equivalences:

standard	$a_1 a_2$	$\nabla_{(a_1}\nabla_{a_2)}$	$X^{a_1}X^{a_2}$
abbreviated	a_{12}	$\nabla_{a_{12}}$	$X^{a_{12}}$

(3.7)

Here $(ab) = \frac{1}{2}(ab + ba)$. We employ obvious extensions of (3.7) to larger index sets, e.g. $X^{a_{123}}$ means $X^{a_1}X^{a_2}X^{a_3}$.

We will often need to simplify expressions involving the curvature tensor and its covariant derivatives. A primary tool is the Bianchi identities, which we may write using our abbreviated notation as

$$\begin{aligned} R_{a_{1234}} + R_{a_{1423}} + R_{a_{1342}} &= 0 \\ \nabla_{a_5} R_{a_{1234}} + \nabla_{a_1} R_{a_{2534}} + \nabla_{a_2} R_{a_{5134}} &= 0\,. \end{aligned} \tag{3.8}$$

A contracted form of the second Bianchi identity,

$$\nabla_b R^b{}_{a_{123}} = \nabla_{a_2} R_{a_{13}} - \nabla_{a_3} R_{a_{12}} \tag{3.9}$$

shows that any three-index contraction of $\nabla_{a_5} R_{a_{1234}}$ (meaning any contraction leaving three indices free) can be expressed as linear combinations of re-indexed versions of the tensor $\nabla_{a_1} R_{a_{23}}$; in this sense $\nabla_{a_1} R_{a_{23}}$ by itself is a basis for all the three-index contractions

of $\nabla_{a_1} R_{a_{2345}}$. This observation will be useful to us when we consider the possible Wick contractions of the five-point interaction vertex in the bi-local non-linear sigma model.

Acting on the contracted second Bianchi identity (3.9) with ∇_{b_1} gives

$$\nabla_{b_1 b_2} R^{b_2}{}_{a_{123}} = \nabla_{b_1 a_2} R_{a_{13}} - \nabla_{b_1 a_3} R_{a_{12}} + \frac{1}{2}[\nabla_{b_1}, \nabla_{a_2}] R_{a_{13}} - \frac{1}{2}[\nabla_{b_1}, \nabla_{a_3}] R_{a_{12}} - \frac{1}{2}[\nabla_{b_1}, \nabla_{b_2}] R^{b_2}{}_{a_{123}} \,. \tag{3.10}$$

We describe the terms in the second line of (3.10) as commutator terms. Evidently, they can be written as curvature bilinears, meaning contractions of two factors of the Riemann and/or Ricci tensors, with no covariant derivatives. Acting on the uncontracted second Bianchi identity (the second line of (3.8)) with ∇^{a_5} gives

$$\nabla^2 R_{a_{1234}} = \nabla_{a_{13}} R_{a_{24}} + \nabla_{a_{24}} R_{a_{13}} - \nabla_{a_{14}} R_{a_{23}} - \nabla_{a_{23}} R_{a_{14}} + (\text{commutators}) \,, \tag{3.11}$$

where $\nabla^2 = \nabla^b \nabla_b$, and the commutator terms are similar to the ones occurring in (3.10): In particular, they are curvature bilinears. The results (3.10) and (3.11) show that all four-index contractions of $\nabla_{a_{56}} R_{a_{1234}}$ can be expressed in terms of linear combinations of re-indexed versions of the tensor $\nabla_{a_{12}} R_{a_{34}}$, together with curvature bilinears.

So far, all formulas in this section have been entirely independent of the choice of coordinate system. We now pass to Riemann normal coordinates in order to study the square of

the arc length, $Q(X,Y) = d(X,Y)^2$ between two points X and Y. We have from[17]‡

$$\begin{aligned}
Q(X,Y) &= g_{a_{12}}(X^{a_1} - Y^{a_1})(X^{a_2} - Y^{a_2}) + \sum_{r>3} Q_r(X,Y) \\
Q_4(X,Y) &= -\frac{1}{3} R_{a_{1234}} X^{a_{13}} Y^{a_{24}} \\
Q_5(X,Y) &= -\frac{1}{12} \nabla_{a_5} R_{a_{1234}} X^{a_{13}} Y^{a_{24}} (X^{a_5} + Y^{a_5}) \\
Q_6(X,Y) &= Q_6^{\nabla\nabla R}(X,Y) + Q_6^{RR}(X,Y) \\
Q_6^{\nabla\nabla R}(X,Y) &= -\frac{1}{60} \nabla_{a_{56}} R_{a_{1234}} (X^{a_{1356}} Y^{a_{24}} + X^{a_{13}} Y^{a_{2456}} + X^{a_{135}} Y^{a_{246}}) \\
Q_6^{RR}(X,Y) &= \frac{1}{45} R^b{}_{a_{123}} R_{ba_{456}} (4X^{a_{125}} Y^{a_{346}} - X^{a_{1245}} Y^{a_{36}} - X^{a_{25}} Y^{a_{1346}})
\end{aligned} \tag{3.12}$$

Here $g_{a_{12}}$, $R_{a_{1234}}$, and its derivatives are all evaluated at the origin of Riemann normal coordinates, which is the origin in terms of the coordinates X^a and Y^a used in (3.12).

3.1.1 Loop integrals in momentum space

The loop is a single propagator starting and ending at the same vertex. This matters because there is then only one internal momentum ℓ, and imposing the hard cutoff $|\ell| \leq \Lambda$ is a privileged choice because it corresponds to integrating ℓ over an $O(n)$-invariant region. An

‡Note however that the results leading to Q_6^{RR} in [17] contain errors. In particular, 44 should have been 4 in the first line of (11.24). We believe the error appears earlier in equation (11.18), among the Riemann-Riemann terms. The correct expression has many equivalent forms, one of them is $24R^a{}_{egb}R_{gcfd} - 24R^a{}_{bge}R_{gcfd} - 8R^a{}_{bgc}R_{gefd}$.

example is the diagram proportional to

$$I_0 = \int \frac{d^n \ell}{|\ell|^s}\,, \tag{3.13}$$

assuming that whatever vertex factor is needed to fully evaluate the diagram doesn't depend on ℓ. We also assume $n > s$ so that I_0 is UV divergent but IR convergent. We straightforwardly find

$$I_0 = \frac{2}{\zeta_\infty(n)} \frac{\Lambda^{n-s}}{n-s}. \tag{3.14}$$

There are obviously no subleading divergences in I_0.

For convenience we introduce $\epsilon = n - s$. We are interested in divergences proportional to $\log \Lambda$ that arise when $\epsilon = n - s = 0$. As a technical trick to isolate these divergences, we make ϵ small and positive, and we look for divergences of the form $\Lambda^\epsilon/\epsilon$, which in the $\epsilon \to 0^+$ limit give rise to $\log \Lambda$ terms. To characterize this limit precisely, given $n_0 > 0$ and $\lambda \in \mathbb{R}$, we set $n = n_0 + \lambda\epsilon$ and $s = n_0 + (\lambda - 1)\epsilon$ and then take the $\epsilon \to 0^+$ limit with n_0 and λ held fixed. (Clearly then we are allowing non-integer n, in the spirit of[43].) For the most part, our final results are independent of λ. When ϵ is sufficiently small, we may replace (3.14) with

$$I_0 = i_0 \frac{\Lambda^\epsilon}{\epsilon} \qquad \text{where} \qquad i_0 = \frac{2}{\zeta_\infty(n_0)} + O(\epsilon). \tag{3.15}$$

The important point is that in the limit $\epsilon \to 0^+$, I_0 includes a logarithmic term $i_0 \log \Lambda$, and isolating this term is our stated objective.

We will encounter one other loop integral:

$$I_2(k) = \int d^n \ell \, \frac{|k-\ell|^s}{|\ell|^s} \, . \tag{3.16}$$

It comes from graphs similar to the one in (3.13), but with a vertex prefactor $|k-\ell|^s$. Using the same reasoning that led to (46), we see that when a hard cutoff $|\ell| \leq \Lambda$ is imposed, one obtains, if n is positive but not an even integer,

$$I_2(k) = \sum_{r=0}^{\lfloor n/2 \rfloor} c_r k^{2r} \frac{\Lambda^{n-2r}}{n-2r} + (\text{UV finite}) \tag{3.17}$$

for some coefficients c_r. If we choose n_0 positive but not an even integer and fix any finite value of λ, then for sufficiently small ϵ, (3.17) applies, and the least singular power of Λ appearing in it is $\Lambda^{n-2\lfloor n/2 \rfloor}$. As $\epsilon \to 0^+$, this power remains positive and finite, tending to $\Lambda^{n_0 - 2\lfloor n_0/2 \rfloor}$. So there is no $\log \Lambda$ behavior, even in the $\epsilon \to 0^+$ limit. If instead we make n_0 a positive even integer, then by choosing the very particular value $\lambda = 1$, so that $s = n_0$ exactly, we find (for sufficiently small $\epsilon > 0$) that the least singular term in (3.17) is $c_{\lfloor n/2 \rfloor} |k|^s \frac{\Lambda^\epsilon}{\epsilon}$, which does contribute a $c_{\lfloor n/2 \rfloor} |k|^s \log \Lambda$ divergence in the $\epsilon \to 0^+$ limit;

moreover, in this case, by calculation, $c_{\lfloor n/2 \rfloor} = i_0 + O(\epsilon)$.[§]

We can summarize the situation by stating that for $\epsilon = n - s$ positive but sufficiently small, then subject to the restriction that n cannot be a positive even integer,

$$I_2(k) = (\text{higher powers of } \Lambda) + i_2 |k|^s \frac{\Lambda^\epsilon}{\epsilon} + (\text{UV finite}) \,, \tag{3.18}$$

where

$$i_2 = \begin{cases} i_0 + O(\epsilon) & s \text{ is a positive even integer} \\ \\ 0 & \text{otherwise} \,. \end{cases} \tag{3.19}$$

The higher powers of Λ in (3.18) are accompanied by non-negative integer powers of k^2, and they correspond to operators which remain relevant in the $\epsilon \to 0^+$ limit. The only $\log \Lambda$ behavior arising from $I_2(k)$, in the $\epsilon \to 0^+$ limits described above, is the $i_2 |k|^s \log \Lambda$ term coming from the $i_2 |k|^s \frac{\Lambda^\epsilon}{\epsilon}$ term shown in (3.18). We are not concerned about $O(\epsilon)$ terms to i_0 and i_2 because they drop out of the $\log \Lambda$ behavior in the $\epsilon \to 0^+$ limit. In the following sections, therefore, we will drop $O(\epsilon)$ terms from (3.15) and (3.19), and we will evaluate i_0 and i_2 in terms of n rather than n_0.

[§]Although we have argued that the hard cutoff prescription $|\ell| \leq \Lambda$ is the natural one to use, it is interesting to note that if instead we impose $|k - \ell| \leq \Lambda$, then still $c_{\lfloor n/2 \rfloor} = i_0 + O(\epsilon)$ when $s = 2\lfloor n/2 \rfloor$ and ϵ is sufficiently small.

3.2 Renormalization at one-loop

As we have said, computing loop diagrams amounts to setting rules for vertices contractions. Now we are ready to approach the main body of this chapter: having fun with Riemann tensors. The way we present these results will not be altered significantly from the original paper[60], especially the part where we use color-coding. Readers may also find it helpful when deriving or checking these results on Riemann tensors using tensor computation packages, like Cadabra (python) or xAct (Wolfram).

3.2.1 The propagator

To derive the tree-level propagator, we use an obvious generalization of (39) to multi-component scalar fields to rewrite the free action in momentum space:

$$S_2 = \frac{\mu^\epsilon}{2\hat{\gamma}} g_{ab} \int d^n k \, \hat{\phi}^a(-k)|k|^s \hat{\phi}^b(k) \,, \tag{3.20}$$

where we recall that $\epsilon = n - s$, and for notational convenience we have introduced[¶]

$$\hat{\gamma} = -\frac{\Gamma_\infty(n+s)}{2}\gamma\,. \tag{3.21}$$

We immediately extract from (3.20) the propagator

$$\begin{aligned}\hat{G}^{ab}(k) &= \frac{\hat{\gamma} g^{ab}}{\mu^\epsilon |k|^s} \\ G^{ab}(x) &= \Gamma_\infty(\epsilon)\frac{\hat{\gamma} g^{ab}}{(\mu|x|)^\epsilon} + (\text{contact terms})\,.\end{aligned} \tag{3.22}$$

We are primarily interested in ϵ small so that $G^{ab}(x)$ is nearly logarithmic.

We can understand the one-loop correction to the propagator as a contribution to the 1PI effective action coming from all possible Wick contractions of the two of the four factors of ϕ in S_{int}. The calculation is done most straightforwardly in momentum space, where we can express

$$\begin{aligned}S_4 &= \frac{\mu^\epsilon}{12\hat{\gamma}} R_{abcd}\int d^n k\, (\widehat{\phi^a\phi^c})(-k)|k|^s(\widehat{\phi^b\phi^d})(k) \\ &= \frac{\mu^\epsilon}{12\hat{\gamma}} R_{abcd}\int d^{4n}k\, \delta^n\left(\textstyle\sum_{i=1}^4 k_i\right)\hat{\phi}^a(k_1)\hat{\phi}^b(k_2)\hat{\phi}^c(k_3)\hat{\phi}^d(k_4)|k_2+k_4|^s\,,\end{aligned} \tag{3.23}$$

[¶]A point worthy of remark is that while $\hat{\gamma}$ and γ have the same sign for $0 < s < 2$, for $2 < s < 4$ they have the opposite sign. The integral in (3.20) is well-defined and positive, so to make our theory sensible we should always choose $\hat{\gamma} > 0$. This means that $\gamma < 0$ for $2 < s < 4$. As explained in (41) for a single real scalar, the regulated position space integral used to define the action (3.5) includes a $(\partial\phi)^2$ term that enters with the opposite sign of the non-local $[\phi(x)-\phi(y)]^2$ term, so positivity conditions are difficult to judge in position space.

where $d^{4n}k = \prod_{i=1}^{4} d^n k_i$. Symbolically, the Wick-contracted quartic action is

$$S_4^{\text{Wick}} = \frac{\mu^\epsilon}{12\hat{\gamma}} R_{abcd} \int d^{4n}k\, \delta^n\left(\textstyle\sum_{i=1}^4 k_i\right) \hat{\phi}^a(k_1)\overbrace{\hat{\phi}^b(k_2)\hat{\phi}^c}(k_3)\hat{\phi}^d(k_4)|k_2+k_4|^s \\ + (\hat{\phi}^a\hat{\phi}^d \text{ contraction})\,. \tag{3.24}$$

We understand $\overbrace{\hat{\phi}^b(k_2)\hat{\phi}^c}(k_3)$ to mean a replacement of $\hat{\phi}^b(k_2)\hat{\phi}^c(k_3)$ by $\hat{G}^{bc}(k_2)\delta^n(k_2 + k_3)$. We omit the $\hat{\phi}^a\hat{\phi}^b$ and $\hat{\phi}^c\hat{\phi}^d$ contractions from (3.24) because of the antisymmetry of R_{abcd} in ab and cd. We omit the $\hat{\phi}^a\hat{\phi}^c$ and $\hat{\phi}^b\hat{\phi}^d$ contractions because they include a factor $|k_1 + k_3|^s\delta^n(k_1 + k_3)$, which vanishes when $s > 0$. After some straightforward algebra, we obtain from (3.24) the form

$$S_4^{\text{Wick}} = -\frac{1}{6} R_{ab} \int d^n k\, \hat{\phi}^a(-k) I_2(k) \hat{\phi}^b(k)\,, \tag{3.25}$$

where $I_2(k)$ is given in (3.16).

As discussed below (3.16), for suitably small positive $\epsilon = n - s$, $I_2(k)$ includes a term $i_2|k|^s\frac{\Lambda^\epsilon}{\epsilon}$ iff s is a positive even integer. This is the case which leads to local non-linear sigma models. Otherwise the divergent terms in $I_2(k)$ are proportional to $|k|^{2r}\Lambda^{n-2r}$ for non-negative powers $n - 2r$ which remain finite as $\epsilon \to 0^+$. Therefore, apart from the case of local non-linear sigma models, the effects of the ultraviolet divergences in (3.25) are limited to generating relevant, local interactions. We assume that relevant terms of this type can be

(a) (b)

Figure 3.1: (a) The one-loop contribution to the propagator. (b) The one-loop contribution to the 1PI three-point vertex.

tuned away.

It would be tempting at this point to conclude that the non-local action (3.5) is non-renormalized, as in the case (3.2). The reality is more subtle: We will see in section 3.2.4 that higher point diagrams generate one-loop divergences that require non-local counterterms; however, they are not quite of the form (3.5), involving the target space laplacian of $Q(X, Y)$ instead.

3.2.2 Three-point vertices

There are no three-point vertices at tree-level provided we employ Riemann normal coordinates. As we will explain in this section, three-point vertices appear to be generated at the one-loop level, by the diagram in figure 3.1b; however, they can be absorbed through non-linear field redefinition.

As for our discussion in section 3.2.1 of the one-loop corrections to the propagator, the one-loop contribution to the three-point function can be obtained efficiently through

Wick contractions in the momentum space of the quintic term in the action:

$$\begin{aligned} S_5 &= \frac{1}{2\gamma}\int' \frac{d^n x d^n y}{|x-y|^{n+s}} Q_5(\phi(x),\phi(y)) \\ &= \frac{\mu^\epsilon}{24\hat{\gamma}} \nabla_{a_5} R_{a_{1234}} \int \left[\prod_{i=1}^{5} d^n k_i\, \hat{\phi}^{a_i}(k_i)\right] \delta^n\left(\textstyle\sum_{i=1}^5 k_i\right) |k_{24}|^s \,. \end{aligned} \tag{3.26}$$

High-dimensional Fourier integrals of the type seen in the second line of (3.26) are common in our calculations, so we have found it useful to introduce some shorthand notation:

standard	$d^n k_1 d^n k_2$	$\delta^n(k_1+k_2)$	$\lvert k_1+k_2\rvert$	$\hat{\phi}^{a_1}(k_1)\hat{\phi}^{a_2}(k_2)$
abbreviated	$d^{2n}k_{12}$	$\delta^n(k_{12})$	$\lvert k_{12}\rvert$	$\hat{\phi}^{a_{12}}(k_{12})$

(3.27)

with obvious extensions to larger index sets. If A is any ordered set of indices, like 123, and $|A|$ is the number of indices in the set, then the integrals we see most often are of the form

$$\begin{aligned} \mathcal{J}^{a_A}_{\phi,k_A}\left[q(k_A)\right] &\equiv \int \left[\prod_{i\in A} d^n k_i\, \hat{\phi}^{a_i}(k_i)\right] \delta^n\left(\textstyle\sum_{i\in A} k_i\right) q(k_A) \\ &= \int d^{|A|n} k_A\, \delta^n(k_A)\hat{\phi}^{a_A}(k_A) q(k_A)\,, \end{aligned} \tag{3.28}$$

where $q(k_A)$ is any function of the k_i, and the third expression is just a rewriting of the second using the shorthand notation introduced in (3.27). Evidently, the $\mathcal{J}_\phi$ integrals are convergent for reasonable integrands q, like powers of norms of sums of momenta, provided the ϕ^a are Schwartz-Bruhat functions. When there is no risk of confusion, we will omit the

subscripted k_A and just write $\mathcal{J}_\phi^{a_A}$. We can now rewrite (3.26) as

$$S_5 = \frac{\mu^\epsilon}{24\hat{\gamma}} \nabla_{a_5} R_{a_{1234}} \mathcal{J}_\phi^{a_{12345}}[|k_{24}|^s] \,. \tag{3.29}$$

As in section 3.2.1, a Wick contraction amounts to a replacement

$$\hat{\phi}^{\overbracket{a_i}}(k_i)\hat{\phi}^{a_j}(k_j) \to \hat{G}^{a_{ij}}(k_j)\delta^n(k_{ij}) = \frac{\hat{\gamma}}{\mu^\epsilon} g^{a_{ij}} \delta^n(k_{ij})|k_j|^{-s} \,. \tag{3.30}$$

It is helpful to note the following examples of Wick contraction:

$$\begin{aligned}
\mathcal{J}_{\phi,k_{12A}}^{\overbracket{a_1 a_2} a_A}[|k_{12}|^s] &= \int d^{(|A|+2)n} k_{12A}\, \delta^n(k_{12A}) \hat{\phi}^{\overbracket{a_1}}(k_1)\hat{\phi}^{a_2}(k_2)\hat{\phi}^{a_A}(k_A)|k_{12}|^s \\
&= \frac{\hat{\gamma}}{\mu^\epsilon} g^{a_{12}} \int d^{|A|n} k_A\, \delta^n(k_A)\hat{\phi}^{a_A}(k_A) \int d^{2n}k_{12}\, \delta^n(k_{12})|k_2|^{-s}|k_{12}|^s = 0 \\
\mathcal{J}_{\phi,k_{12A}}^{\overbracket{a_1 a_2} a_A}[|k_C|^s] &= \frac{\hat{\gamma}}{\mu^\epsilon} g^{a_{12}} \int d^{|A|n} k_A\, \delta^n(k_A)\hat{\phi}^{a_A}(k_A)|k_C|^s \int d^{2n}k_{12}\, \delta^n(k_{12})|k_2|^{-s} \\
&= \frac{\hat{\gamma}}{\mu^\epsilon} g^{a_{12}} \mathcal{J}_{\phi,k_A}^{a_A}[|k_C|^s] I_0 = \mathcal{J}_{\phi,k_A}^{\overbracket{a_1 a_2} a_A}[|k_{12C}|^s] \\
\mathcal{J}_{\phi,k_{12A}}^{\overbracket{a_1 a_2} a_A}[|k_{1C}|^s] &= \frac{\hat{\gamma}}{\mu^\epsilon} g^{a_{12}} \int d^{|A|n} k_A\, \delta^n(k_A)\hat{\phi}^{a_A}(k_A) \int d^{2n}k_{12}\, \delta^n(k_{12})|k_2|^{-s}|k_{1C}|^s \\
&= \frac{\hat{\gamma}}{\mu^\epsilon} g^{a_{12}} \mathcal{J}_{\phi,k_A}^{a_A}[I_2(k_C)] \,.
\end{aligned} \tag{3.31}$$

Here A and C are collections of indices, neither including 1 or 2, with $C \subset A$, and we assume $s > 0$ in order to obtain the vanishing of the first integral. Recall from section 0.4.4 that I_0 diverges as $\Lambda^\epsilon/\epsilon$ when $\epsilon = n - s$ is sufficiently small and positive, giving rise to $\log \Lambda$

behavior in the limit $\epsilon \to 0^+$.

There are $\binom{5}{2} = 10$ possible single Wick contractions of S_5, but the (12) contraction (meaning the contraction of a_1 and a_2) vanishes because $g^{a_{12}} \nabla_{a_5} R_{a_{1234}} = 0$; likewise the (34) contraction vanishes. Meanwhile the (14) and (23) contractions are equal because both $\nabla_{a_5} R_{a_{1234}}$ and $|k_{24}|^s$ are symmetrical under the simultaneous exchange of $1 \leftrightarrow 3$ and $2 \leftrightarrow 4$. For the same reason, the (15) and (35) contractions are equal, and so are the (25) and (45) contractions. Finally, the (24) contraction vanishes because of the first line of (3.31). We are left with

$$S_5^{\text{Wick}} = S_{5,(13)}^{\text{Wick}} + 2S_{5,(14)}^{\text{Wick}} + 2S_{5,(15)}^{\text{Wick}} + 2S_{5,(25)}^{\text{Wick}} \tag{3.32}$$

where

$$
\begin{aligned}
S^{\text{Wick}}_{5,(13)} &= \frac{\mu^\epsilon/\hat{\gamma}}{24}\nabla_{a_5}R_{a_{1234}}\mathcal{J}_\phi^{\overbrace{a_1a_2a_3}a_{45}}[|k_{24}|^s] = \frac{1}{24}\nabla_{a_5}R_{a_{24}}\mathcal{J}_\phi^{a_{245}}[|k_{24}|^s] \\
&= \frac{1}{24}\nabla_{a_3}R_{a_{12}}\mathcal{J}_\phi^{a_{123}}[|k_3|^s]I_0 \\
S^{\text{Wick}}_{5,(14)} &= \frac{\mu^\epsilon/\hat{\gamma}}{24}\nabla_{a_5}R_{a_{1234}}\mathcal{J}_\phi^{\overbrace{a_1a_{23}a_4}a_5}[|k_{24}|^s] = -\frac{1}{24}\nabla_{a_5}R_{a_{23}}\mathcal{J}_\phi^{a_{235}}[I_2(k_2)] \\
&= -\frac{1}{24}\nabla_{a_1}R_{a_{23}}\mathcal{J}_\phi^{a_{123}}[I_2(k_3)] \\
S^{\text{Wick}}_{5,(15)} &= \frac{\mu^\epsilon/\hat{\gamma}}{24}\nabla_{a_5}R_{a_{1234}}\mathcal{J}_\phi^{\overbrace{a_1a_{234}a_5}}[|k_{24}|^s] = \frac{1}{24}(\nabla_{a_3}R_{a_{24}} - \nabla_{a_4}R_{a_{23}})\mathcal{J}_\phi^{a_{234}}[|k_{24}|^s]I_0 \\
&= \frac{1}{24}(\nabla_{a_3}R_{a_{12}} - \nabla_{a_1}R_{a_{23}})\mathcal{J}_\phi^{a_{123}}[|k_3|^s]I_0 \\
S^{\text{Wick}}_{5,(25)} &= \frac{\mu^\epsilon/\hat{\gamma}}{24}\nabla_{a_5}R_{a_{1234}}\mathcal{J}_\phi^{a_1\overbrace{a_2a_{34}a_5}}[|k_{24}|^s] = -\frac{1}{24}(\nabla_{a_3}R_{a_{14}} - \nabla_{a_4}R_{a_{13}})\mathcal{J}_\phi^{a_{134}}[I_2(k_4)] \\
&= \frac{1}{24}(\nabla_{a_3}R_{a_{12}} - \nabla_{a_1}R_{a_{23}})\mathcal{J}_\phi^{a_{123}}[I_2(k_3)]\,.
\end{aligned}
\tag{3.33}
$$

A few comments are in order:

- Because $S^{\text{Wick}}_{5,(14)}$ and $S^{\text{Wick}}_{5,(25)}$ are proportional to the I_2 loop integral, they do not contribute logarithmic divergences in the $\epsilon \to 0^+$ limits described in section 0.4.4, except when s is a positive even integer. In a position space account, these non-logarithmic terms correspond to contractions of $\phi(x)$ with $\phi(y)$.

- We are mostly interested in $S^{\text{Wick}}_{5,(13)}$ and $S^{\text{Wick}}_{5,(15)}$ because I_0 does produce a logarithmic divergence in the $\epsilon \to 0^+$ limit. Note that in these terms, the vertex factor $|k_{13}|^s$ involves only external momenta. This is the crucial feature, which allows non-local counterterms to arise. In position space, the logarithmic terms correspond to contractions of $\phi(y)$ with itself.

In summary,

$$S_5^{\text{Wick}} = \frac{1}{24}\int d^{3n}k_{123}\,\delta^n(k_{123})\hat{\phi}^{a_{123}}(k_{123})\Big[I_2(k_3)(2\nabla_{a_3}R_{a_{12}} - 4\nabla_{a_1}R_{a_{23}}) + I_0|k_3|^s(3\nabla_{a_3}R_{a_{12}} - 2\nabla_{a_1}R_{a_{23}})\Big]\,. \tag{3.34}$$

The minimal counterterm needed to cancel the $\Lambda^\epsilon/\epsilon$ divergences in (3.34) is

$$S_3^{\text{ct}} = \frac{\Lambda^\epsilon}{2\epsilon}\int d^{3n}k_{123}\,\delta^n(k_{123})\hat{\phi}^{a_{123}}(k_{123})|k_3|^s\left[K_1\nabla_{a_3}R_{a_{12}} + K_2\nabla_{(a_1}R_{a_2)a_3}\right] \tag{3.35}$$

where

$$K_1 = -\frac{3i_0 + 2i_2}{12} \qquad\qquad K_2 = \frac{i_0 + 2i_2}{6}\,, \tag{3.36}$$

and i_0 and i_2 are as defined in (3.15) and (3.19). We use the notation S_3^{ct} to denote a counterterm that is cubic in the fields. Our primary interest is in cases where $i_2 = 0$—namely, cases in which s is not a positive even integer. However, tracking I_0, $I_2(k)$, i_0, and i_2 throughout our computations is useful as a bookkeeping device in order to simultaneously treat the local and bi-local theories, in the $\epsilon \to 0^+$ limit, with i_2 entering in only to describe the local theories.

3.2.3 Renormalization through cubic order in the fields

Before entering into the more complicated story of quartic terms in the action, let's preview the endgame of our analysis. We produce a bare action that incorporates the renormalized action plus the counterterms in a form we can express entirely in terms of arc length.

First, let's rephrase the Wick-contracted quartic action (3.25) as

$$S_4^{\text{Wick}} = -\frac{1}{6}\int d^{2n}k_{12}\,\delta^n(k_{12})\hat{\phi}^{a_{12}}(k_{12})I_2(k_2)R_{a_{12}}\,, \tag{3.37}$$

from which we conclude that we need a counterterm quadratic in the fields of the form

$$S_2^{\text{ct}} = \frac{\Lambda^\epsilon}{2\epsilon}\int d^{2n}k_{12}\,\delta^n(k_{12})\hat{\phi}^{a_{12}}(k_{12})|k_2|^s K_0 R_{a_{12}}\,, \tag{3.38}$$

where

$$K_0 = \frac{i_2}{3}\,. \tag{3.39}$$

The results (3.38) and (3.35) together put some constraints on the renormalization procedure, but as we will see they do not completely determine it.

The question of renormalizability is whether we can reorganize the renormalized action

plus counterterms into a bare action whose form is the same that we started with:

$$S[\phi] + S^{\text{ct}}[\phi] = S^{\text{B}}[\phi_{\text{B}}]\,. \tag{3.40}$$

where

$$S^{\text{ct}}[\phi] = \sum_{r>1} S^{\text{ct}}_r \tag{3.41}$$

is the sum of all counterterms, $S[\phi]$ is as given in (3.5), and

$$S^{\text{B}}[\phi_{\text{B}}] = \frac{\Lambda^{n-s}}{2\gamma} \int'_{V\times V} \frac{d^n x d^n y}{|x-y|^{n+s}} Q^{\text{B}}(\phi_{\text{B}}(x), \phi_{\text{B}}(y))\,, \tag{3.42}$$

where $Q^{\text{B}}(X_{\text{B}}, Y_{\text{B}}) = d^{\text{B}}(X_{\text{B}}, Y_{\text{B}})^2$. The bare arc length d^{B}, derived from a bare metric tensor g^{B}_{ab}, may differ from the renormalized arc length d, and the bare coordinates ϕ^a_{B} may likewise differ from the renormalized coordinates ϕ^a. We require however that the points $\phi_{\text{B}} = 0$ and $\phi = 0$ coincide. At tree level, where we ignore all counterterms, we have the relations

$$\left(\frac{\Lambda}{\mu}\right)^{\epsilon} g^{\text{B}}_{ab}(\phi_{\text{B}}) = g_{ab}(\phi) \qquad\qquad \phi^a_{\text{B}} = \phi^a\,, \tag{3.43}$$

and our key task is to find perturbative corrections to these relations that render (3.40) correct.

To begin, let's examine the quadratic terms in (3.40), using the counterterm S^{ct}_2 from

(3.38):

$$\begin{aligned}\int d^{2n}k_{12}\,\delta^n(k_{12})\hat{\phi}^{a_{12}}(k_{12})|k_2|^s\left[g_{a_{12}}+\frac{\hat{\gamma}}{\epsilon}\left(\frac{\Lambda}{\mu}\right)^\epsilon K_0 R_{a_{12}}\right]+O(\phi^3)+O(\hat{\gamma}^2)\\ =\left(\frac{\Lambda}{\mu}\right)^\epsilon\int d^{2n}k_{12}\,\delta^n(k_{12})\hat{\phi}_{\mathtt{B}}^{a_{12}}(k_{12})|k_2|^s g_{a_{12}}^{\mathtt{B}}\,,\end{aligned}\tag{3.44}$$

where for simplicity we multiplied through by $2\hat{\gamma}/\mu^\epsilon$. We surmise from (3.44) that corrections to (3.43) can be expressed as a power series in the dimensionless quantity

$$\tilde{\gamma}=\frac{\hat{\gamma}}{\epsilon}\left(\frac{\Lambda}{\mu}\right)^\epsilon\,.\tag{3.45}$$

That is,

$$\phi_{\mathtt{B}}^a(x)=\phi^a(x)+\tilde{\gamma}\left[U^a{}_b\phi^b(x)+V^a{}_{b_{12}}\phi^{b_{12}}(x)+W^a{}_{b_{123}}\phi^{b_{123}}(x)\right]+O(\phi^4)+O(\tilde{\gamma}^2)\,,\tag{3.46}$$

where $V^a{}_{b_{12}}$ and $W^a{}_{b_{123}}$ are fully symmetric in their lower indices, and U, V, and W are all independent of ϕ (and $\phi_{\mathtt{B}}$). In other words, (3.46) is a Taylor expansion of $\phi_{\mathtt{B}}^a$ in the coordinates ϕ^a. Also,

$$\left(\frac{\Lambda}{\mu}\right)^\epsilon g_{ab}^{\mathtt{B}}(\phi_{\mathtt{B}})=g_{ab}(\phi)+\tilde{\gamma}T_{ab}(\phi)+O(\tilde{\gamma}^2)\tag{3.47}$$

for some tensor $T_{ab}(\phi)$. As our notation indicates, $T_{ab}(\phi)$ does depend on ϕ. As with other tensors, if we omit the argument, we mean that T_{ab} is evaluated at $\phi=0$. Using (3.46) and

(3.47), we see that (3.44) is satisfied provided

$$g_{a_{12}} + \tilde{\gamma} K_0 R_{a_{12}} = (\delta^{b_1}_{a_1} + \tilde{\gamma} U^{b_1}{}_{a_1})(\delta^{b_2}_{a_2} + \tilde{\gamma} U^{b_2}{}_{a_2})(g_{b_{12}} + \tilde{\gamma} T_{b_{12}}) + O(\hat{\gamma}^2)\,, \tag{3.48}$$

or in other words, provided

$$T_{a_{12}} + 2U_{a_{(12)}} = K_0 R_{a_{12}}\,, \tag{3.49}$$

where

$$U_{a_{12}} = U^b{}_{a_2} g_{a_1 b} \qquad\qquad U_{a_{(12)}} = \frac{1}{2}(U_{a_{12}} + U_{a_{21}})\,. \tag{3.50}$$

It should be kept in mind that $T_{a_{12}}$ is the $\phi = 0$ value of a tensor field $T_{a_{12}}(\phi)$ defined over the whole of M, whereas $U_{a_{(12)}}$ is defined only at $\phi = 0$. Let's assume that

$$T_{a_{12}}(\phi) = t_0 R_{a_{12}}(\phi) \qquad\qquad U_{a_{(12)}} = u_0 R_{a_{12}}\,. \tag{3.51}$$

(A term in $T_{a_{12}}(\phi)$ proportional to $R(\phi) g_{a_{12}}(\phi)$ is also possible, but the divergences we will encounter do not require it.) Then (3.49) reduces to

$$t_0 + 2u_0 = K_0\,. \tag{3.52}$$

As previously noted, based on the treatment of quadratic terms alone, we cannot distinguish between metric renormalization (related to the coefficient t_0) and field redefinition (related to the coefficient u_0).

In order to proceed to higher orders, we require the squared arc length formula for bare quantities:

$$Q^{\mathtt{B}}(X_{\mathtt{B}}, Y_{\mathtt{B}}) = g^{\mathtt{B}}_{a_{12}}(X^{a_1}_{\mathtt{B}} - Y^{a_1}_{\mathtt{B}})(X^{a_2}_{\mathtt{B}} - Y^{a_2}_{\mathtt{B}}) + \sum_{r>2} Q^{\mathtt{B}}_r(X_{\mathtt{B}}, Y_{\mathtt{B}})\,. \tag{3.53}$$

We do not require $\phi_{\mathtt{B}}$ to be Riemann normal coordinates for $d^{\mathtt{B}}$, so there are contributions to $Q^{\mathtt{B}}$ at cubic order:

$$Q^{\mathtt{B}}_3(X_{\mathtt{B}}, Y_{\mathtt{B}}) = \Gamma^{\mathtt{B}}_{a_{123}}(X^{a_1}_{\mathtt{B}} - Y^{a_1}_{\mathtt{B}})(X^{a_2}_{\mathtt{B}} - Y^{a_2}_{\mathtt{B}})(X^{a_3}_{\mathtt{B}} + Y^{a_3}_{\mathtt{B}})\,, \tag{3.54}$$

where $\Gamma^{\mathtt{B}}_{abc} = g^{\mathtt{B}}_{ad}\Gamma^{\mathtt{B}d}_{bc}$ and $\Gamma^{\mathtt{B}a}_{bc}$ is the Christoffel connection for $g^{\mathtt{B}}_{ab}$. From (3.47) we have immediately

$$\left(\frac{\Lambda}{\mu}\right)^{\epsilon} \Gamma^{\mathtt{B}}_{a_{312}} = \tilde{\gamma}\left[\nabla_{(a_1}T_{a_2)a_3} - \frac{1}{2}\nabla_{a_3}T_{a_{12}}\right] + O(\tilde{\gamma}^2)\,, \tag{3.55}$$

From $Q_3^{\mathtt{B}}$ we obtain a cubic term in the bare action:

$$\begin{aligned} S_3^{\mathtt{B}} &= \frac{\Lambda^\epsilon}{2\gamma}\int' \frac{d^n x d^n y}{|x-y|^{n+s}} Q_3^{\mathtt{B}}(\phi_{\mathtt{B}}(x),\phi_{\mathtt{B}}(y)) = \frac{\Lambda^\epsilon}{2\hat{\gamma}}\mathcal{J}_{\phi_{\mathtt{B}}}^{a_{123}}[|k_3|^s]\Gamma^{\mathtt{B}}_{a_{312}} \\ &= \frac{\Lambda^\epsilon}{2\epsilon}\mathcal{J}_{\phi}^{a_{123}}[|k_3|^s]\left[\nabla_{(a_1}T_{a_2)a_3} - \frac{1}{2}\nabla_{a_3}T_{a_{12}}\right] + O(\tilde{\gamma})\,. \end{aligned} \tag{3.56}$$

Another term cubic in ϕ arises in the bare action from plugging the non-linear field redefinition (3.46) into the quadratic term $S_2^{\mathtt{B}}$. To work this out, it helps first to note that passing (3.46) through a Fourier transform yields

$$\hat{\phi}^a_{\mathtt{B}}(k) = \hat{\phi}^a(k) + \tilde{\gamma}\delta\hat{\phi}^a(k) + O(\tilde{\gamma}^2) \tag{3.57}$$

where

$$\delta\hat{\phi}^a(k) = U^a{}_b\hat{\phi}^b(k) + V^a{}_{b_{12}}(\hat{\phi}^{b_1} * \hat{\phi}^{b_2})(k) + W^a{}_{b_{123}}(\hat{\phi}^{b_1} * \hat{\phi}^{b_2} * \hat{\phi}^{b_3})(k) + O(\phi^4) \tag{3.58}$$

and $*$ denotes convolution. It follows immediately that

$$\begin{aligned} \mathcal{J}_{\phi_{\mathtt{B}}}^{a_{12}}[|k_2|^s] &= \mathcal{J}_{\phi}^{a_{12}}[|k_2|^s] + 2\tilde{\gamma}\int d^{2n}k_{12}\,\delta^n(k_{12})\delta\hat{\phi}^{(a_1}(k_1)\hat{\phi}^{a_2)}(k_2)|k_2|^s + O(\phi^5) + O(\tilde{\gamma}^2) \\ &= \mathcal{J}_{\phi}^{a_{12}}[|k_2|^s] + 2\tilde{\gamma}\Big[U^{(a_1}{}_b\mathcal{J}_{\phi,k_2\ell}^{a_2)b}[|k_2|^s] + V^{(a_1}{}_{b_{12}}\mathcal{J}_{\phi,k_2\ell_{12}}^{a_2)b_{12}}[|k_2|^s] \\ &\qquad + W^{(a_1}{}_{b_{123}}\mathcal{J}_{\phi,k_2\ell_{123}}^{a_2)b_{123}}[|k_2|^s]\Big] + O(\phi^5) + O(\tilde{\gamma}^2)\,, \end{aligned} \tag{3.59}$$

and so

$$S_2^{\mathsf{B}} = \frac{\Lambda^\epsilon}{2\hat{\gamma}}\mathcal{J}_{\phi_{\mathsf{B}}}^{a_{12}}[|k_2|^s]g_{a_{12}}^{\mathsf{B}} = S_2 + \frac{\Lambda^\epsilon}{2\epsilon}\mathcal{J}_{\phi}^{a_{12}}[|k_2|^s]\left[T_{a_{12}} + 2U_{a_{12}}\right] + \frac{\Lambda^\epsilon}{\epsilon}\mathcal{J}_{\phi}^{a_{123}}[|k_3|^s]V_{a_{312}} + \frac{\Lambda^\epsilon}{\epsilon}\mathcal{J}_{\phi}^{a_{1234}}[|k_4|^s]W_{a_{4123}} + O(\phi^5) + O(\tilde{\gamma})\,, \tag{3.60}$$

where we are lowering indices on V and W with the renormalized metric g_{ab}. The $T_{a_{12}} + 2U_{a_{12}}$ term in (3.60) is the same combination we saw in (3.49), with the symmetrization $U_{a_{12}} \to U_{a_{(12)}}$ implied because we multiply by $\mathcal{J}_{\phi}^{a_{12}}[|k_2|^s]$, which is symmetric. The next term in (3.60) is the interesting one for us. The only constraint on $V_{a_{312}}$ is symmetry in the 12 indices. This is the same symmetry that $\mathcal{J}_{\phi}^{a_{123}}[|k_3|^s]$ possesses. Therefore $\mathcal{J}_{\phi}^{a_{123}}[|k_3|^s]V_{a_{312}}$ is the most general linear combination of terms coming from $\mathcal{J}_{\phi}^{a_{123}}[|k_3|^s]$ integrals. Likewise, the only constraint on $W_{a_{4123}}$ is symmetry in 123, so the last term shown explicitly in (3.60) is the most general linear combination of terms coming from $\mathcal{J}_{\phi}^{a_{1234}}[|k_4|^s]$ integrals.

We now have all the ingredients needed to calculate the $O(\phi^3)$ correction to (3.44). Specifically, we expand (3.40) to cubic order in the renormalized fields, using the expression (3.35) for S_3^{ct}, as well as S_3^{B} from (3.56) and the $O(\phi^3)$ term from (3.60). The result is

$$\mathcal{J}_{\phi}^{a_{123}}[|k_3|^s]\left[K_1\nabla_{a_3}R_{a_{12}} + K_2\nabla_{(a_1}R_{a_2)a_3}\right] = \mathcal{J}_{\phi}^{a_{123}}[|k_3|^s]\left[\nabla_{(a_1}T_{a_2)a_3} - \frac{1}{2}\nabla_{a_3}T_{a_{12}} + 2V_{a_{312}}\right]\,. \tag{3.61}$$

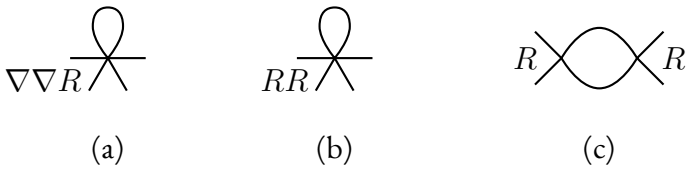

(a) (b) (c)

Figure 3.2: One-loop contributions to the 1PI four-point vertex: (a) Single Wick contractions of the $\nabla\nabla R$ six-point vertices; (b) Single Wick contractions of RR six-point vertices; (c) Diagrams involving only four-point vertices.

Evidently, we may set

$$V_{a_{312}} = v_1 \nabla_{a_3} R_{a_{12}} + v_2 \nabla_{(a_1} R_{a_2)a_3} \,, \tag{3.62}$$

where

$$-\frac{1}{2} t_0 + 2v_1 = K_1 \qquad\qquad t_0 + 2v_2 = K_2 \,. \tag{3.63}$$

The larger message is that $V_{a_{312}}$ is sufficiently unconstrained that we could use it to absorb any counterterm proportional to $\mathcal{J}_\phi^{a_{123}}[|k_3|^s]$. By the same token, when we get to quartic order, the field redefinition coefficients $W_{a_{4123}}$ can be used to absorb any terms proportional to $\mathcal{J}_\phi^{a_{1234}}[|k_4|^s]$. Therefore, when we do proceed to quartic order, we may simplify our work by systematically dropping all such terms. We will see in section 3.2.4 that other terms emerge, proportional to $\mathcal{J}_\phi^{a_{1234}}[|k_{24}|^s]$. These are the ones that cannot be absorbed into field redefinitions.

3.2.4 Quartic counterterms

Four-point vertices are present at tree-level, and they are also generated by three different types of one-loop diagrams, as shown in figure 3.2. Our goal in this section is to evaluate one-loop divergences proportional to $\nabla_{a_{12}} R_{a_{34}}$ (and re-indexings of it). The claim is that only the diagram in figure 3.2a can contribute. Tracking only target space indices, the vertex factor in this diagram is $\nabla_{a_{56}} R_{a_{1234}}$, and the internal propagator can tie any two of the six indices together. So the diagram as a whole must be proportional to four-index contractions of $\nabla_{a_{56}} R_{a_{1234}}$. As explained in section 3.1, re-indexed versions of $\nabla_{a_{12}} R_{a_{34}}$, together with curvature bilinears, provide a basis for such contractions. The diagrams in figure 3.2b and 3.2c are manifestly proportional to curvature bilinears, so they cannot contribute terms proportional to $\nabla_{a_{12}} R_{a_{34}}$. (One immediate way to see this is that the Riemann tensor could vanish at $\phi = 0$ without its derivatives vanishing.) In the explicit calculations below, we will encounter and discard many curvature bilinear terms, which we generically write as $O(RR)$, meaning some contraction of $R_{a_{1234}} R_{a_{5678}}$.

We claim that the counterterms needed to cancel the divergences from the diagram in figure 3.2a proportional to $\nabla_{a_{12}} R_{a_{34}}$ (and re-indexings of it) are

$$S^{\text{ct}}_{6,\nabla\nabla R} = \frac{\Lambda^\epsilon}{2\epsilon}\Big[\mathcal{J}_\phi^{a_{1234}}[|k_{24}|^s]\,(K_3 \nabla_{a_{12}} R_{a_{34}} + K_4 \nabla_{a_{13}} R_{a_{24}}) + \mathcal{J}_\phi^{a_{1234}}[|k_4|^s]\,(K_5 \nabla_{a_{12}} R_{a_{34}} + K_6 \nabla_{a_{34}} R_{a_{12}})\Big]\,, \tag{3.64}$$

where

$$\begin{aligned} K_3 &= \frac{3i_0+2i_2}{30} & K_4 &= -\frac{7i_0+3i_2}{60} \\ K_5 &= \frac{i_0+3i_2}{30} & K_6 &= -\frac{3i_0+4i_2}{60}\,. \end{aligned} \tag{3.65}$$

Color-coding in (3.64) is to help track to which term in (3.64) each of the many terms in later equations contribute. The remainder of this section is devoted to deriving (3.65).

To derive the sixth-order vertex used in figure 3.2a, we start from the $Q_6^{\nabla\nabla R}$ term in (3.12) and extract the following six-order terms in the action:

$$S_{6,\nabla\nabla R} = \frac{\mu^\epsilon}{2\gamma}\int' \frac{d^n x d^n y}{|x-y|^{n+s}} Q_6^{\nabla\nabla R}(\phi(x),\phi(y)) = S^{4+2}_{6,\nabla\nabla R} + S^{3+3}_{6,\nabla\nabla R} \tag{3.66}$$

where

$$\begin{aligned} S^{4+2}_{6,\nabla\nabla R} &= \frac{\mu^\epsilon}{120\hat{\gamma}} \nabla_{a_{56}} R_{a_{1234}} \mathcal{J}_\phi^{a_{123456}}[|k_{24}|^s] \\ S^{3+3}_{6,\nabla\nabla R} &= \frac{\mu^\epsilon}{240\hat{\gamma}} \nabla_{a_{56}} R_{a_{1234}} \mathcal{J}_\phi^{a_{123456}}[|k_{246}|^s]\,. \end{aligned} \tag{3.67}$$

Our task is to compute the counterterms for all the single Wick contractions of $S^{4+2}_{6,\nabla\nabla R}$ and $S^{3+3}_{6,\nabla\nabla R}$.

For $S^{4+2}_{6,\nabla\nabla R}$, relations among Wick contractions that are obvious from symmetries plus the first line of (3.31) are as follows:

$$\begin{gathered} (12)=0 \qquad (34)=0 \qquad (24)=0 \\ (14)=(23) \qquad (15)=(35)=(16)=(36) \qquad (25)=(45)=(26)=(46)\,. \end{gathered} \tag{3.68}$$

Thus, of fifteen single Wick contractions of $S^{4+2}_{6,\nabla\nabla R}$, there are actually only five that determine the full answer:

$$S^{4+2,\text{Wick}}_{6,\nabla\nabla R} = S^{4+2,\text{Wick}}_{6,\nabla\nabla R,(13)} + 2S^{4+2,\text{Wick}}_{6,\nabla\nabla R,(14)} + 4S^{4+2,\text{Wick}}_{6,\nabla\nabla R,(15)} + 4S^{4+2,\text{Wick}}_{6,\nabla\nabla R,(25)} + S^{4+2,\text{Wick}}_{6,\nabla\nabla R,(56)} \,. \tag{3.69}$$

If we write the counterterm for an expression Q as $\{Q\}_{\text{ct}}$, then the rules of computation we need are a trivial adaptation of (3.31):

$$\begin{aligned} \left\{ \mathcal{J}_\phi^{\overbrace{a_1 a_2} a_A}[|k_C|^s] \right\}_{\text{ct}} &= \left\{ \mathcal{J}_\phi^{\overbrace{a_1 a_2} a_A}[|k_{12C}|^s] \right\}_{\text{ct}} = -\tilde{\gamma} g^{a_{12}} \mathcal{J}_\phi^{a_A}[|k_C|^s] i_0 \\ \left\{ \mathcal{J}_\phi^{\overbrace{a_1 a_2} a_A}[|k_{1C}|^s] \right\}_{\text{ct}} &= -\tilde{\gamma} g^{a_{12}} \mathcal{J}_\phi^{a_A}[|k_C|^s] i_2 \,. \end{aligned} \tag{3.70}$$

The counterterms that we need to cancel divergences coming from the single Wick contractions of $S^{4+2}_{6,\nabla\nabla R}$, as shown in (3.69), are

$$S^{4+2,\text{ct}}_{6,\nabla\nabla R} = \frac{\Lambda^\epsilon}{120\epsilon} \left[I^{4+2,\text{ct}}_{6,\nabla\nabla R,(13)} + 2I^{4+2,\text{ct}}_{6,\nabla\nabla R,(14)} + 4I^{4+2,\text{ct}}_{6,\nabla\nabla R,(15)} + 4I^{4+2,\text{ct}}_{6,\nabla\nabla R,(25)} + I^{4+2,\text{ct}}_{6,\nabla\nabla R,(56)} \right] \tag{3.71}$$

where

$$
\begin{aligned}
I^{4+2,\text{ct}}_{6,\nabla\nabla R,(13)} &= \frac{1}{\tilde{\gamma}}\nabla_{a_{56}}R_{a_{1234}}\left\{\mathcal{J}_\phi^{a_1\overbrace{a_2a_3}a_{456}}[|k_{24}|^s]\right\}_{\text{ct}} = -\nabla_{a_{56}}R_{a_{24}}\mathcal{J}_\phi^{a_2456}[|k_{24}|^s]i_0 \\
&= -\nabla_{a_{13}}R_{a_{24}}\mathcal{J}_\phi^{a_1234}[|k_{24}|^s]i_0 \\
I^{4+2,\text{ct}}_{6,\nabla\nabla R,(14)} &= \frac{1}{\tilde{\gamma}}\nabla_{a_{56}}R_{a_{1234}}\left\{\mathcal{J}_\phi^{a_1\overbrace{a_{23}a_4}a_{56}}[|k_{24}|^s]\right\}_{\text{ct}} = \nabla_{a_{56}}R_{a_{23}}\mathcal{J}_\phi^{a_2356}[|k_2|^s]i_2 \\
&= \nabla_{a_{12}}R_{a_{34}}\mathcal{J}_\phi^{a_1234}[|k_4|^s]i_2 \\
I^{4+2,\text{ct}}_{6,\nabla\nabla R,(15)} &= \frac{1}{\tilde{\gamma}}\nabla_{a_{56}}R_{a_{1234}}\left\{\mathcal{J}_\phi^{a_1\overbrace{a_{234}a_5}a_6}[|k_{24}|^s]\right\}_{\text{ct}} = -\nabla_{ba_6}R^b{}_{a_{234}}\mathcal{J}_\phi^{a_2346}[|k_{24}|^s]i_0 \\
&= (-\nabla_{a_{63}}R_{a_{24}} + \nabla_{a_{64}}R_{a_{23}})\mathcal{J}_\phi^{a_2346}[|k_{24}|^s]i_0 + O(RR) \\
&= (\nabla_{a_{12}}R_{a_{34}} - \nabla_{a_{13}}R_{a_{24}})\mathcal{J}_\phi^{a_1234}[|k_{24}|^s]i_0 + O(RR) \\
I^{4+2,\text{ct}}_{6,\nabla\nabla R,(25)} &= \frac{1}{\tilde{\gamma}}\nabla_{a_{56}}R_{a_{1234}}\left\{\mathcal{J}_\phi^{a_1\overbrace{a_2a_{34}a_5}a_6}[|k_{24}|^s]\right\}_{\text{ct}} = -\nabla_{ba_6}R_{a_1}{}^b{}_{a_{34}}\mathcal{J}_\phi^{a_1346}[|k_4|^s]i_2 \\
&= (\nabla_{a_{63}}R_{a_{14}} - \nabla_{a_{64}}R_{a_{13}})\mathcal{J}_\phi^{a_1346}[|k_4|^s]i_2 + O(RR) \\
&= (\nabla_{a_{12}}R_{a_{34}} - \nabla_{a_{34}}R_{a_{12}})\mathcal{J}_\phi^{a_1234}[|k_4|^s]i_2 + O(RR) \\
I^{4+2,\text{ct}}_{6,\nabla\nabla R,(56)} &= \frac{1}{\tilde{\gamma}}\nabla_{a_{56}}R_{a_{1234}}\left\{\mathcal{J}_\phi^{a_{1234}\overbrace{a_5a_6}}[|k_{24}|^s]\right\}_{\text{ct}} = -\nabla^2 R_{a_{1234}}\mathcal{J}_\phi^{a_1234}[|k_{24}|^s]i_0 \\
&= (-2\nabla_{a_{13}}R_{a_{24}} + 2\nabla_{a_{12}}R_{a_{34}})\mathcal{J}_\phi^{a_1234}[|k_{24}|^s]i_0 + O(RR)\,,
\end{aligned}
\tag{3.72}
$$

where the color coding is to show which terms in (3.72) contribute to which terms of (3.64).

Let us briefly summarize the analogous steps for $S^{3+3}_{6,\nabla\nabla R}$. Obvious relations are

$$(12) = 0 \qquad (34) = 0 \qquad (13) = (24)$$
$$(14) = (23) \qquad (15) = (35) = (26) = (46) \qquad (16) = (36) = (25) = (45)\,, \tag{3.73}$$

from which it follows that the desired counterterms are

$$S^{3+3,\text{ct}}_{6,\nabla\nabla R} = \frac{\Lambda^\epsilon}{240\epsilon}\left[2I^{3+3,\text{ct}}_{6,\nabla\nabla R,(13)} + 2I^{3+3,\text{ct}}_{6,\nabla\nabla R,(14)} + 4I^{3+3,\text{ct}}_{6,\nabla\nabla R,(15)} + 4I^{3+3,\text{ct}}_{6,\nabla\nabla R,(25)} + I^{3+3,\text{ct}}_{6,\nabla\nabla R,(56)}\right]\,. \tag{3.74}$$

By direct computation using the rules (3.70),

$$
\begin{aligned}
I^{3+3,\mathrm{ct}}_{6,\nabla\nabla R,(13)} &= \frac{1}{\tilde{\gamma}}\nabla_{a_{56}}R_{a_{1234}}\left\{\mathcal{J}_\phi^{a_1\overbrace{a_2a_3}a_{456}}[|k_{246}|^s]\right\}_{\mathrm{ct}} = -\nabla_{a_{56}}R_{a_{24}}\mathcal{J}_\phi^{a_{2456}}[|k_{246}|^s]i_0 \\
&= -\nabla_{a_{34}}R_{a_{12}}\mathcal{J}_\phi^{a_{1234}}[|k_4|^s]i_0 \\
I^{3+3,\mathrm{ct}}_{6,\nabla\nabla R,(14)} &= \frac{1}{\tilde{\gamma}}\nabla_{a_{56}}R_{a_{1234}}\left\{\mathcal{J}_\phi^{a_1\overbrace{a_{23}a_4}a_{56}}[|k_{246}|^s]\right\}_{\mathrm{ct}} = \nabla_{a_{56}}R_{a_{23}}\mathcal{J}_\phi^{a_{2356}}[|k_{26}|^s]i_2 \\
&= \nabla_{a_{12}}R_{a_{34}}\mathcal{J}_\phi^{a_{1234}}[|k_{24}|^s]i_2 \\
I^{3+3,\mathrm{ct}}_{6,\nabla\nabla R,(15)} &= \frac{1}{\tilde{\gamma}}\nabla_{a_{56}}R_{a_{1234}}\left\{\mathcal{J}_\phi^{a_1\overbrace{a_{234}a_5}a_6}[|k_{246}|^s]\right\}_{\mathrm{ct}} = -\nabla_{ba_6}R^{b}{}_{a_{234}}\mathcal{J}_\phi^{a_{2346}}[|k_{246}|^s]i_0 \\
&= (\nabla_{a_{12}}R_{a_{34}} - \nabla_{a_{34}}R_{a_{12}})\mathcal{J}_\phi^{a_{1234}}[|k_4|^s]i_0 + O(RR) \\
I^{3+3,\mathrm{ct}}_{6,\nabla\nabla R,(25)} &= \frac{1}{\tilde{\gamma}}\nabla_{a_{56}}R_{a_{1234}}\left\{\mathcal{J}_\phi^{a_1a_2\overbrace{a_{34}a_5}a_6}[|k_{246}|^s]\right\}_{\mathrm{ct}} = -\nabla_{ba_6}R_{a_1}{}^{b}{}_{a_{34}}\mathcal{J}_\phi^{a_{1346}}[|k_{46}|^s]i_2 \\
&= (\nabla_{a_{12}}R_{a_{34}} - \nabla_{a_{13}}R_{a_{24}})\mathcal{J}_\phi^{a_{1234}}[|k_{24}|^s]i_2 + O(RR) \\
I^{3+3,\mathrm{ct}}_{6,\nabla\nabla R,(56)} &= \frac{1}{\tilde{\gamma}}\nabla_{a_{56}}R_{a_{1234}}\left\{\mathcal{J}_\phi^{a_{1234}\overbrace{a_5a_6}}[|k_{246}|^s]\right\}_{\mathrm{ct}} = -\nabla^2 R_{a_{1234}}\mathcal{J}_\phi^{a_{1234}}[|k_{24}|^s]i_2 \\
&= (-2\nabla_{a_{13}}R_{a_{24}} + 2\nabla_{a_{12}}R_{a_{34}})\mathcal{J}_\phi^{a_{1234}}[|k_{24}|^s]i_2 + O(RR)\,.
\end{aligned}
\tag{3.75}
$$

Putting (3.71)-(3.72) and (3.74)-(3.75) together and comparing with (3.64), we arrive at

$$\begin{aligned} K_3 &= \frac{4}{60} i_0 + \frac{2}{60} i_0 + \frac{2}{120} i_2 + \frac{4}{120} i_2 + \frac{2}{120} i_2 \\ K_4 &= -\frac{1}{60} i_0 - \frac{4}{60} i_0 - \frac{2}{60} i_0 - \frac{4}{120} i_2 - \frac{2}{120} i_2 \\ K_5 &= \frac{2}{60} i_2 + \frac{4}{60} i_2 + \frac{4}{120} i_0 \\ K_6 &= -\frac{4}{60} i_2 - \frac{2}{120} i_0 - \frac{4}{120} i_0 \,, \end{aligned} \tag{3.76}$$

which agrees with (3.65).

3.2.5 Renormalization through quartic order in the fields

To renormalize at quartic order, we first inquire whether the counterterms (3.64) can be organized into the bare arc length action (3.42), using the field redefinition (3.46) and the relationship (3.47) between the bare and renormalized metric. For the non-local model, we will find that this is impossible! So we will turn to a generalized form of the bare action that includes a term proportional to the target space laplacian of the square of the arc length.

To get started, we need the bare arc length formula to quartic order in the bare fields: That is, we need one more term in the series (3.53) than we computed in section 3.2.3. The computation of arc length is less simple than for the renormalized metric because the ϕ^a_{B} are not Riemann normal coordinates for g^{B}_{ab}—due to effects at $O(\tilde{\gamma})$, in particular a connection $\Gamma^{\mathrm{B}a}_{b_{12}} \sim O(\tilde{\gamma})$. As a technical device, we therefore introduce a third set of coordinates,

$\overline{\phi}^a$, which are Riemann normal coordinates for the bare metric, which in barred coordinates takes the form $\overline{g}_{ab}(\overline{\phi})$. We can express $\overline{\phi}^a$ in terms of $\phi^a_{\mathtt{B}}$ as

$$\overline{\phi}^a = \phi^a_{\mathtt{B}} + \tilde{\gamma}\left[L^a{}_{b_{12}}\phi^{b_{12}}_{\mathtt{B}} + M^a{}_{b_{123}}\phi^{b_{123}}_{\mathtt{B}}\right] + O(\phi^4_{\mathtt{B}}) + O(\tilde{\gamma}^2)\,, \tag{3.77}$$

and we can write $g^{\mathtt{B}}_{ab}(\phi_{\mathtt{B}})$ in terms of $\overline{g}_{ab}(\overline{\phi})$ as

$$g^{\mathtt{B}}_{b_{12}}(\phi_{\mathtt{B}}) = \overline{g}_{a_{12}}(\overline{\phi})\frac{\partial\overline{\phi}^{a_1}}{\partial\phi^{b_1}_{\mathtt{B}}}\frac{\partial\overline{\phi}^{a_2}}{\partial\phi^{b_2}_{\mathtt{B}}}\,. \tag{3.78}$$

Note that, by assumption, $g^{\mathtt{B}}_{a_{12}} = \overline{g}_{a_{12}}$ at $\phi_{\mathtt{B}} = \overline{\phi} = 0$. The condition that $\overline{\phi}^a$ are Riemann normal coordinates allows us to conclude

$$\tilde{\gamma}L^a{}_{b_{12}} = \frac{1}{2}\Gamma^{\mathtt{B}a}_{b_{12}} \qquad\qquad \tilde{\gamma}M^a{}_{b_{123}} = \frac{1}{6}\left(\frac{\partial}{\partial\phi^{(b_1}_{\mathtt{B}}}\Gamma^{\mathtt{B}a}_{b_{23})} + \Gamma^{\mathtt{B}a}_{b(b_1}\Gamma^{\mathtt{B}b}_{b_{23})}\right)\,; \tag{3.79}$$

see for example[Brewin] for a derivation. The $\Gamma^{\mathtt{B}}\Gamma^{\mathtt{B}}$ term in the expression (3.79) for $M^a{}_{b_{123}}$ is optional because it is $O(\tilde{\gamma}^2)$, but it arises naturally in the derivation of[Brewin], so we include it.

The bare arc length coincides between $\overline{\phi}$ and $\phi_{\mathtt{B}}$ coordinate systems because these are just

different coordinate systems for the same metric, as per (3.78). Explicitly,

$$Q^{\mathtt{B}}(X_{\mathtt{B}}, Y_{\mathtt{B}}) = \overline{Q}(\overline{X}, \overline{Y}) = \overline{g}_{a_{12}}(\overline{X}^{a_1} - \overline{Y}^{a_1})(\overline{X}^{a_2} - \overline{Y}^{a_2}) - \frac{1}{3}\overline{R}_{a_{1234}}\overline{X}^{a_{13}}\overline{Y}^{a_{24}} + O(\overline{\phi}^5)\,, \tag{3.80}$$

where in the second equality we used the fact that $\overline{\phi}^a$ are Riemann normal coordinates. The notation $O(\bar{\phi}^5)$ in (3.80) is short for all terms involving five or more powers of $\overline{X}$ and $\overline{Y}$ combined; similar notation is used below. Using the first equation in (3.77) to eliminate $\overline{X}$ and $\overline{Y}$ in favor of $X_{\mathtt{B}}$ and $Y_{\mathtt{B}}$, we arrive at

$$\begin{aligned} Q^{\mathtt{B}}(X_{\mathtt{B}},Y_{\mathtt{B}}) = {} & g^{\mathtt{B}}_{a_{12}}(X^{a_1}_{\mathtt{B}} - Y^{a_1}_{\mathtt{B}})(X^{a_2}_{\mathtt{B}} - Y^{a_2}_{\mathtt{B}}) \\ & + 2\tilde{\gamma}\left[L_{a_{312}}(X^{a_{12}}_{\mathtt{B}} - Y^{a_{12}}_{\mathtt{B}})(X^{a_3}_{\mathtt{B}} - Y^{a_3}_{\mathtt{B}}) + M_{a_{4123}}(X^{a_{123}}_{\mathtt{B}} - Y^{a_{123}}_{\mathtt{B}})(X^{a_4}_{\mathtt{B}} - Y^{a_4}_{\mathtt{B}})\right] \\ & - \frac{1}{3}R^{\mathtt{B}}_{a_{1234}}X^{a_{13}}_{\mathtt{B}}Y^{a_{24}}_{\mathtt{B}} + O(\phi^5_{\mathtt{B}}) + O(\tilde{\gamma}^2)\,, \end{aligned} \tag{3.81}$$

where $L_{a_{312}} = g^{\mathtt{B}}_{a_3 b}L^{b}{}_{a_{12}}$ and $M_{a_{4123}} = g^{\mathtt{B}}_{a_4 b}M^{b}{}_{a_{123}}$. Note that the cubic terms in (3.81) agree with (3.54), and recall from the subsequent analysis that the corresponding cubic term $S^{\mathtt{B}}_3$ does *not* need to match $S_3 + S^{\mathtt{ct}}_3$, because of the additional term cubic in ϕ in (3.60) arising from the $O(\tilde{\gamma})$ difference between $\phi_{\mathtt{B}}$ and ϕ. Likewise, the term in (3.81) proportional to $M_{a_{4123}}$ gives rise to a term proportional to $\mathcal{J}_{\phi_{\mathtt{B}}}[|k_4|^s]$ in the action, but we do not need to track it explicitly because the quartic term in (3.60) shows that it is precisely the sort of

term that we can absorb into the field redefinition coefficient $W^{a}{}_{b_{123}}$. Thus we may write

$$S_4^{\mathtt{B}} = \frac{\Lambda^\epsilon}{2\gamma}\int' \frac{d^n x d^n y}{|x-y|^{n+s}} Q_4^{\mathtt{B}}(\phi_{\mathtt{B}}(x),\phi_{\mathtt{B}}(y)) = \frac{\Lambda^\epsilon}{12\hat{\gamma}}\mathcal{J}_{\phi_{\mathtt{B}}}^{a_{1234}}[|k_{24}|^s]R^{\mathtt{B}}_{a_{1234}} + (\text{field redef})\,, \tag{3.82}$$

where (field redef) indicates field redefinition terms as discussed above.

Next we express $S_4^{\mathtt{B}}$ in terms of renormalized quantities in order to compare to (3.64). Starting from (3.47), we obtain

$$\begin{aligned}\left(\frac{\Lambda}{\mu}\right)^\epsilon R^{\mathtt{B}}_{a_{1234}} = R_{a_{1234}} + \frac{\tilde{\gamma}}{2}(\nabla_{a_{14}}T_{a_{23}} - \nabla_{a_{24}}T_{a_{13}} - \nabla_{a_{13}}T_{a_{24}} + \nabla_{a_{23}}T_{a_{14}}) \\ + O(RR) + O(\tilde{\gamma}^2)\,.\end{aligned} \tag{3.83}$$

Thus we find

$$\begin{aligned}S_4^{\mathtt{B}} = S_4 + \frac{\Lambda^\epsilon}{12\epsilon}\mathcal{J}_{\phi}^{a_{1234}}[|k_{24}|^s]\,[t_0\nabla_{a_{12}}R_{a_{34}} - t_0\nabla_{a_{13}}R_{a_{24}}] \\ + (\text{field redef}) + O(RR) + O(\tilde{\gamma})\,.\end{aligned} \tag{3.84}$$

$O(RR)$ terms arise in (3.84) not just from those in (3.83), but also from expressing $\mathcal{J}_{\phi_{\mathtt{B}}}^{a_{1234}}[|k_{24}|^s]$ in terms of the renormalized field ϕ.[‖] We have color-coded terms in (3.84) to match the way we did in (3.64). Comparing the two equations, we can see that $S_4^{\mathtt{B}}$ accommodates the counterterms $S^{\mathtt{ct}}_{6,\nabla\nabla R}$ iff $K_3 = -K_4$. Based on (3.65), this happens iff $i_0 = i_2$, which means iff s

[‖] $S_3^{\mathtt{B}}$ does not contribute terms quartic in ϕ that we need to track because it starts at $O(\tilde{\gamma}^0)$, so quartic terms coming from expressing $\mathcal{J}_{\phi_{\mathtt{B}}}^{a_{123}}[|k_3|^s]$ in terms of the renormalized ϕ enter at $O(\tilde{\gamma})$.

is a positive even integer. This corresponds to the case of local non-linear sigma models.

Let us pursue further here what happens for the non-local case. Because $i_2 = 0$, we have $K_1/K_2 = -6/7$, there is no hope of rendering the theory renormalizable with just the arc length action we have been using so far. Some generalization of the arc length action is needed. Whatever modification we make should involve two target space derivatives relative to the original action, so as to absorb counterterms that appear with two extra derivatives—like the $\nabla_{a_{12}} R_{a_{34}}$ structure in $S^{\text{ct}}_{6,\nabla\nabla R}$ as compared to $R_{a_{1234}}$ in S_4. Luckily, there is a new term with the right properties which we can add to S^{B}:

$$\delta S^{\text{B}} = \kappa_{\text{B}} \frac{\Lambda^\epsilon}{2\gamma} \int' \frac{d^n x d^n y}{|x-y|^{n+s}} Q^{\text{B}\prime\prime}(\phi_{\text{B}}(x), \phi_{\text{B}}(y)) \tag{3.85}$$

where we define

$$Q^{\text{B}\prime\prime}(X_{\text{B}}, Y_{\text{B}}) \equiv (\nabla^2_{X_{\text{B}}} + \nabla^2_{Y_{\text{B}}}) Q^{\text{B}}(X_{\text{B}}, Y_{\text{B}})\,. \tag{3.86}$$

By explicit calculation (as sketched below (3.94)),

$$\begin{aligned} \delta S^{\text{B}} = \kappa_{\text{B}} \frac{\Lambda^\epsilon}{60\gamma} &(-6\nabla^{\text{B}}_{a_{12}} R^{\text{B}}_{a_{34}} + 7\nabla^{\text{B}}_{a_{13}} R^{\text{B}}_{a_{24}}) \\ &\times \int' \frac{d^n x d^n y}{|x-y|^{n+s}} \left[\phi^{a_{13}}_{\text{B}}(x) - \phi^{a_{13}}_{\text{B}}(y)\right] \left[\phi^{a_{24}}_{\text{B}}(x) - \phi^{a_{24}}_{\text{B}}(y)\right] \\ &+ (\text{field redef}) + O(\phi^5_{\text{B}}) + O(RR)\,, \end{aligned} \tag{3.87}$$

Passing to momentum space, we find

$$\begin{aligned}\delta S^{\mathtt{B}} = \kappa_{\mathtt{B}} \frac{\Lambda^\epsilon}{60\hat{\gamma}} (-6\nabla^{\mathtt{B}}_{a_{12}} R^{\mathtt{B}}_{a_{34}} + 7\nabla^{\mathtt{B}}_{a_{13}} R^{\mathtt{B}}_{a_{24}}) \mathcal{J}^{a_{1234}}_{\phi_{\mathtt{B}}}[|k_{24}|^s] \\ + (\text{field redef}) + O(\phi_{\mathtt{B}}^5) + O(RR)\,.\end{aligned} \tag{3.88}$$

Note that $-6/7$ ratio! Combining (3.84) and (3.88) and comparing with (3.64), we see that $\kappa_{\mathtt{B}} = -\frac{\hat{\gamma}}{\epsilon}\frac{i_0}{2}$. Strikingly, we are forced also to choose $t_0 = 0$: That is, the metric is not renormalized!

Having allowed the two-derivative term (3.85) in $S^{\mathtt{B}}$, we should allow addition of a similar term to the renormalized action:

$$\delta S = \kappa \frac{\mu^\epsilon}{2\gamma} \int' \frac{d^n x d^n y}{|x-y|^{n+s}} Q''(\phi(x), \phi(y))\,. \tag{3.89}$$

We restrict κ to be an $O(\gamma)$ quantity, which makes sense because then the overall scaling with γ of (3.89) is $O(\gamma^0)$, and this aligns with the invariance of $Q''(X,Y)$ under overall rescaling of the target manifold. The additional term (3.89) changes all the one-loop amplitudes, but only by $O(\gamma)$ quantities, relative to the $O(\gamma^0)$ scaling of one-loop amplitudes and counterterms that we obtained in previous sections. In short, the only effect of allowing non-zero κ in our counterterm analysis is to lead to a direct tree-level contribution to

κ_{B}, so that in total,

$$\left(\frac{\Lambda}{\mu}\right)^{\epsilon} \kappa_{\text{B}} = \kappa - \tilde{\gamma}\frac{i_0}{2}\,. \tag{3.90}$$

To rephrase this result in terms of the renormalization group, we can rewrite (3.90) as

$$\Lambda^{\epsilon}\left(\kappa_{\text{B}} + \frac{\hat{\gamma}}{\epsilon}\frac{i_0}{2}\right) = \mu^{\epsilon}\kappa\,, \tag{3.91}$$

and then since the right hand side is independent of Λ, we arrive at

$$\Lambda\frac{d\kappa_{\text{B}}}{d\Lambda} = -\epsilon\kappa_{\text{B}} - \hat{\gamma}\frac{i_0}{2}\,. \tag{3.92}$$

The first term on the right hand side of (3.92) is the tree-level term coming from the engineering dimension factor of $(\Lambda/\mu)^{\epsilon}$ in (3.90). The one-loop effects are responsible for the second term in (3.92). If we now take $\epsilon \to 0$ in (3.92), we see that κ_{B} runs logarithmically:

$$\kappa_{\text{B}} = -\hat{\gamma}\frac{i_0}{2}\log\frac{\Lambda}{\Lambda_0}\,, \tag{3.93}$$

where Λ_0 is a dynamically generated scale. Note that $\hat{\gamma}$ and i_0 are positive, so κ_{B} is positive at scales Λ below Λ_0 and negative above Λ_0.

To see that (3.87) is correct, let's work on the renormalized side and note that

$$\begin{aligned} g^{b_{12}}\frac{\partial^2}{\partial X^{b_1}\partial X^{b_2}}Q_6^{\nabla\nabla R} &= -\frac{1}{60}\nabla_{a_{56}}R_{a_{1234}}Y^{a_{24}}g^{b_{12}}\frac{\partial^2 X^{a_{1356}}}{\partial X^{b_1}\partial X^{b_2}}+\dots \\ &= -\frac{1}{30}(\nabla_{a_{13}}R_{a_{24}}+4\nabla_{a_1 b}R^{b}{}_{a_{234}}+\nabla^2 R_{a_{1234}})X^{a_{13}}Y^{a_{24}}+\dots \\ &= -\frac{1}{30}(6\nabla_{a_{13}}R_{a_{24}}-6\nabla_{a_{12}}R_{a_{34}}+\nabla_{a_{24}}R_{a_{13}})X^{a_{13}}Y^{a_{24}}+\dots . \end{aligned} \tag{3.94}$$

The expression (3.94) is part of $\nabla_X^2 Q(X,Y)$, and it is easy to see that it is the only part contributing terms of the form $(\nabla\nabla R)XXYY$. Therefore

$$\begin{aligned} Q''(X,Y) = -\frac{1}{30}&(-6\nabla_{a_{12}}R_{a_{34}}+7\nabla_{a_{13}}R_{a_{24}})(X^{a_{13}}Y^{a_{24}}+X^{a_{24}}Y^{a_{13}}) \\ &+O(\phi^5)+O(RR)+\dots . \end{aligned} \tag{3.95}$$

The ellipses in (3.94) and (3.95) indicate terms that are not quadratic in both X and Y, for example terms schematically of the form $(\nabla\nabla R)XYYY$ or $(\nabla\nabla R)YYYY$, as well as lower order terms which are either independent of X or Y, or linear in X or Y. Plugging

(3.95) into (3.89), we find

$$\begin{aligned}\delta S = &-\kappa\frac{\mu^\epsilon}{60\gamma}(-6\nabla_{a_{12}}R_{a_{34}} + 7\nabla_{a_{13}}R_{a_{24}}) \\ &\qquad \times \int' \frac{d^n x d^n y}{|x-y|^{n+s}} \left[\phi^{a_{13}}(x)\phi^{a_{24}}(y) + \phi^{a_{24}}(x)\phi^{a_{13}}(y)\right] \\ &\quad + (\text{field redef}) + O(\phi^5) + O(RR) \\ = &\,\kappa\frac{\mu^\epsilon}{60\gamma}(-6\nabla_{a_{12}}R_{a_{34}} + 7\nabla_{a_{13}}R_{a_{24}}) \\ &\qquad \times \int' \frac{d^n x d^n y}{|x-y|^{n+s}} \left[\phi^{a_{13}}(x) - \phi^{a_{13}}(y)\right]\left[\phi^{a_{24}}(x) - \phi^{a_{24}}(y)\right] \\ &\quad + (\text{field redef}) + O(\phi^5) + O(RR)\,.\end{aligned} \tag{3.96}$$

The contributions labeled (field redef) in (3.96) are linear in $\phi(x)$ or $\phi(y)$. To see that (3.96) is correct, we have only to understand why we can freely add or drop from the integrand smooth functions which depend only on x or only on y, such as the direct terms $\phi^{a_{1234}}(x) + \phi^{a_{1234}}(y)$ which are present in the last expression in (3.96) but not the middle expression. As in section 0.4.3, this follows from careful use of the regulated integral prescription:

$$\begin{aligned}\int' \frac{d^n x d^n y}{|x-y|^{n+s}} f(y) &= \int \frac{d^n x d^n y}{|x-y|^{n+s}} \left[f(y) - \sum_{r=0}^{\lfloor s/2 \rfloor} b_r \Box^r f(x)(y-x)^{2r}\right] \\ &= \frac{1}{\Gamma_V(n+s)} \int d^n x\, D^s f(x) = 0\end{aligned} \tag{3.97}$$

for smooth functions $f(x)$ with suitable falloff conditions at large x. The integral $\int' \frac{d^n x d^n y}{|x-y|^{n+s}} f(x)$ vanishes more trivially by subtraction of the $r = 0$ term in the sum appearing in square brackets in (3.97).

3.3 Large N

Let's start with a recapitulation of the main points of our analysis. The starting point action is

$$S = \frac{\mu^\epsilon}{2\gamma} \int'_{xy} Q(\phi(x), \phi(y)) \,, \tag{3.98}$$

where $Q(X, Y) = d(X, Y)^2$ is the square of the shortest distance between points X and Y on the target manifold, and we understand that

$$\int'_{xy} G(x, y) = \int' \frac{d^n x d^n y}{|x - y|^{n+s}} G(x, y) \tag{3.99}$$

is defined with a suitable regulation prescription, as in section 0.4.3. Recall that $\epsilon = n - s$. Focusing on the limit $\epsilon \to 0^+$, with n and s converging to some positive n_0 which is not an even integer, we find that we are obliged to generalize the action (3.98) to

$$S_{\text{improved}} = \frac{\mu^\epsilon}{2\gamma} \int'_{xy} \left[Q(\phi(x), \phi(y)) + \kappa Q''(\phi(x), \phi(y)) \right] \,, \tag{3.100}$$

where $Q''(X,Y) = (\nabla_X^2 + \nabla_Y^2)Q(X,Y)$, and $\kappa \sim O(\gamma)$. With this improved action, one-loop amplitudes at $O(\gamma^0)$ have a divergence structure which, as far as we have taken the computations, can be absorbed entirely through field redefinitions and additive renormalization of κ, as given in the form of a renormalization group equation for the bare version of κ in (3.92). No metric renormalization arises in the non-local model (at one loop). This is in contrast with the local non-linear sigma model, where no improvement terms are needed, and we cancel one-loop divergences instead through field redefinitions and renormalization of the metric. We know that the $O(N)$ symmetric local non-linear sigma model has the same large N limit like the $O(N)$ $(\phi^2)^2$ theory at the IR fixed point. One could hope that the large target space dimension N limit of the non-local non-linear sigma model recover its renormalizability, but we will later see that this is not the case, at least in the spherical target spaces. We will comment on the reason for this robust non-renormalizability of the unimproved Q^2 action.

The general covariance of our arc length action makes it possible to study the theory with any given metric conveniently. We can just plug in the tensor values at the very end in loops and counterterms. (Otherwise, if no covariance, the loops or counterterms may not be universal, and one has to work from the beginning for each different metric.) In odd critical dimensions, our theory has the property that the metric is not renormalized, with the covariance as constraints. We can quickly check this using a sphere metric. Plugging in

$R_{abcd} = k(g_{ac}g_{bd} - g_{ad}g_{bc})$ for a sphere, the counterterms (in N target space dimensions) are

$$(\frac{26}{45}k^2 - \frac{16}{45}Nk^2)X^aX^bY_aY_b + (-\frac{4}{15}k^2 + \frac{2}{45}Nk^2)X_aX^aY_bY^b \tag{3.101}$$

In the original arc length action, we have simply

$$\frac{1}{3}k\, X^aX^bY_aY_b - \frac{1}{3}k\, X_aX^aY_bY^b \tag{3.102}$$

To make it renormalizable, we want the coefficients in the counter-terms to have the same ratio as in the action, because we only have one RG parameter k. Solving it we find that only in $N = 1$ (one dimension) is the theory renormalizable, which is the free theory. Tracking all the quartic terms in the $\nabla^2 d^2$ counter-terms gives

$$\begin{aligned}
&-\frac{8}{45}k^2X_aX^aX^bY_b + \frac{8}{45}Nk^2X_aX^aX^bY_b + \frac{26}{45}k^2X^aX^bY_aY_b - \frac{16}{45}Nk^2X^aX^bY_aY_b \\
&-\frac{4}{15}k^2X_aX^aY_bY^b + \frac{2}{45}Nk^2X_aX^aY_bY^b - \frac{8}{45}k^2X^aY_aY_bY^b + \frac{8}{45}Nk^2X^aY_aY_bY^b \\
&\qquad + \frac{2}{45}k^2Y_aY^aY_bY^b - \frac{2}{45}Nk^2Y_aY^aY_bY^b
\end{aligned} \tag{3.103}$$

Solving the over-constrained equations (XXYY terms having the correct ratio and all other terms vanishing) also gives $N = 1$.

We could also ask what happens exactly in the large N limit. The numerator of the regu-

lated d^2 Lagrangian in Riemann normal coordinates up to sixth order is

$$-2X^aY_a+\frac{1}{3}g\,X^aX^bY_aY_b-\frac{1}{3}g\,X_aX^aY_bY^b+\frac{1}{45}g^2X_aX^aX^bX^cY_bY_c-\frac{4}{45}g^2X^aX^bX^cY_aY_bY_c$$
$$-\frac{1}{45}g^2X_aX^aX_bX^bY_cY^c+\frac{4}{45}g^2X_aX^aX^bY_bY_cY^c+\frac{1}{45}g^2X^aX^bY_aY_bY_cY^c-\frac{1}{45}g^2X_aX^aY_bY^bY_cY^c \tag{3.104}$$

where g is the scalar metric. We want to see whether the large N limit renders this ϕ^4 plus ϕ^6 theory renormalizable. We will now first reproduce the 1-loop computation as a counterpart of the covariant case. The propagator of the theory is

$$G^{ab}(k)=C\frac{\delta^{ab}}{|k|^s} \tag{3.105}$$

In odd dimension there is no one loop correction to the propagator due to the fact that there is usually no sub-leading divergency and thus many diagrams do not contribute to the log divergency. One loop correction to the four point vertex comes from the fish diagram and the jellyfish digram with four legs. The fish digram consists of two four point vertices and is of order g^2, while the jellyfish diagram consists of one six point vertices and is also of order g^2. The fish diagram can be represented by the following contraction:

$$\begin{aligned}\frac{1}{3}g(g_{ac}g_{bd}-g_{ab}g_{cd})X^aX^bY^cY^d\frac{1}{3}g(g_{ac}g_{bd}-g_{ab}g_{cd})X^aX^bY^cY^d\to\\ \frac{4}{9}g^2(1-N)X^aX^bX_aY_b+\frac{4}{9}g^2(1-N)Y^aY^bY_aX_b\end{aligned} \tag{3.106}$$

The jellyfish diagram can be represented by the following contraction:

$$\frac{1}{45}g^2X_aX^aX^bX^cY_bY_c-\frac{4}{45}g^2X^aX^bX^cY_aY_bY_c-\frac{1}{45}g^2X_aX^aX_bX^bY_cY^c+\frac{4}{45}g^2X_aX^aX^bY_bY_cY^c$$
$$+\frac{1}{45}g^2X^aX^bY_aY_bY_cY^c-\frac{1}{45}g^2X_aX^aY_bY^bY_cY^c\rightarrow$$
$$\frac{2}{45}g^2[(2N-2)X^aX^bX_aY_b+(2N-2)Y^aY^bY_aX_b+(-2N-3)X^aX_aY^bY_b+(N+4)X^aX^bY_aY_b] \tag{3.107}$$

The total contribution to the vertex is then (note that the integral part is universal for all these terms and we omit it for now)

$$\frac{2}{45}g^2[(-8N+8)X^aX^bX_aY_b+(-8N+8)Y^aY^bY_aX_b+(-2N-3)X^aX_aY^bY_b+(N+4)X^aX^bY_aY_b] \tag{3.108}$$

Compare it to the original four point vertex:

$$\frac{1}{3}g\,X^aX^bY_aY_b-\frac{1}{3}g\,X_aX^aY_bY^b \tag{3.109}$$

One has to add counterterms that cannot be realized by rescaling the coupling g or shifting the field, thus the theory is not renormalizable in odd dimensions. The extra counterterms

needed are

$$\frac{E}{45}g^2[(8N-8)X^aX^bX_aY_b+(8N-8)Y^aY^bY_aX_b+(2N-12)X^aX_aY^bY_b+(-16N+26)X^aX^bY_aY_b] \tag{3.110}$$

where E is a constant. Under this, the "renormalization" of the theory is

$$X^a \to X^a + A^a{}_b X^b + B^a{}_{bc} X^b X^c + C^a{}_{bcd} X^b X^c X^d \tag{3.111}$$

$$g \to g + Dg \tag{3.112}$$

where

$$\begin{aligned} A^a{}_b &= 0 \\ B^a_{bc} &= 0 \end{aligned} \tag{3.113}$$

and then we have a set of equations for C, D and E:

$$\begin{aligned} \frac{1}{3}gD + \frac{E}{45}g^2(-16N+26) + \frac{2I_2}{45}g^2(N+4) &= 0 \\ -\frac{1}{3}gD + \frac{E}{45}g^2(2N-12) + \frac{2I_2}{45}g^2(-2N-3) &= 0 \\ -2C + \frac{E}{45}g^2(8N-8) + \frac{2I_2}{45}g^2(-8N+8) &= 0 \end{aligned} \tag{3.114}$$

Solving the equations we have

$$\begin{aligned} C^{a}{}_{bcd} &= -\frac{4N-4}{21} g^2 I_2 \delta^{a}{}_{b} \delta_{cd} \\ D &= -\frac{2N+2}{7} g I_2 \\ E &= \frac{-I_2}{7} \end{aligned} \tag{3.115}$$

As expected, we need E the extra counterterm to make the constraints solvable. A remarkable feature is that E is independent of the target space dimension N. This is consistent with the covariant picture. So naively speaking, large N is not rendering the theory renormalizable. This non-renormalizability is closely related to the fact that non-local actions allow more possible tensor structures. For example, $X_a X_b Y^a Y^b$ and $X_a X^a Y_b Y^b$ would be indistinguishable for its local counterpart $X_a X_b X^a X^b$. Note that the conclusion is only for the order studied in this work now. It is thrilling to look for higher improvement terms and to discover what they lead us to. Here RG flow leads the target space geometric flow, but not in the usual way of Ricci flow. We would like to know what the geodesic arc length flows to and why.

4

Non-local field theory II: non-local quantum electrodynamics

We have seen the non-renormalization of the non-local kinetic terms. While the anomalous dimension of these fields is zero, classically marginal coupling constants of these theories are not necessarily protected and may or may not run under renormalization group (RG)

flow. In some cases, a combination of the non-renormalization property described above together with additional constraints of the action may protect the dimension of a classically marginal coupling so that it becomes exactly marginal. In other instances, renormalization group flow may generate local kinetic terms, which, if relevant, may dominate the infrared physics. In this chapter, we present an example where both can happen, depending on the non-local spectral exponent and the dimensions.

The Euclidean action of a non-local version of quantum electrodynamics (QED), where the kinetic term for the photons is non-local, and the fermions are local, is given by

$$S = \int d^d x \left(\frac{1}{4} F_{\mu\nu} D^{s-2} F^{\mu\nu} + \frac{1}{2\xi} (\partial_\mu A^\mu) D^{s-2} (\partial_\nu A^\nu) + \sum_{i=1}^{N_f} \bar{\psi}^i \left(i\partial\!\!\!/ - e A\!\!\!/ \right) \psi^i \right) \tag{4.1}$$

where the non-local derivative D^s is defined through

$$\int d^d x D^s \phi(x) e^{ikx} = |k|^s \hat{\phi}(k) \qquad \int d^d x \phi(x) e^{ikx} = \hat{\phi}(k) \,. \tag{4.2}$$

Our conventions for the Gamma matrices are

$$\{\gamma_\mu, \, \gamma_\nu\} = -2\delta_{\mu\nu} \tag{4.3}$$

which coincide with those of[77]. We have derived in the introduction the real space expres-

sion for the kinetic term (and gauge fixing term) of the photon in (4.1):

$$D^s\phi(0) = (2\pi)^s \frac{\pi^{-\frac{d}{2}-s}\Gamma\left(\frac{d+s}{2}\right)}{\Gamma\left(-\frac{s}{2}\right)} \int \frac{d^d y}{|y|^{d+s}} \left(\phi(y) - \sum_{r=0}^{\lfloor s/2 \rfloor} b_r y^{2r} \left(\Box^r \phi\right)(0) \right) \tag{4.4}$$

with

$$b_r = \frac{\Gamma\left(\frac{d}{2}\right)}{2^{2r}\Gamma\left(r+\frac{d}{2}\right)\Gamma\left(r+1\right)} \tag{4.5}$$

with Γ the Euler Gamma function, and s a real number greater than $-d$ which is not a non-negative even integer. Here we adapt a slightly different convention for the Fourier transform from some previous chapters to simplify the notation, and hence the factor of $(2\pi)^s$. Note that when s is not too negative, the summation in (4.4) is set to zero; that is to say, there is no subtraction on the right-hand side. We choose N_f in (4.1) such that there is no parity anomaly.

As mentioned earlier, actions of the type (4.1) appear throughout the literature. When s is an odd integer these actions are identical to the effective action obtained by considering free photons coupled to fermions on lower-dimensional branes[97,121] (see also[48]). The case of $d = 3$ and $s = 1$ has recently received special attention[64,82,32,29] partly due to its relation to the physics of graphene[118,122] and its possible connection to the infrared fixed point of three-dimensional QED[3,2,130,51,26,52]. In[88] the authors attempt to relate non-local Abelian gauge theories to strange metals. A study of the unitary and causal properties of (4.1) has been car-

ried out in[31,98]. More recently, the authors of[86,5] studied entanglement entropy properties of non-local theories of the type described in this work. In the context of AdS/CFT[96,61,129], the works of[123,83,130,53,50] provided holographic descriptions of large N $\underbrace{\text{QED}_3}$ and related vector models, where the infinite N boundary theory has an effective non-local propagator.

The classical scaling dimensions of the photon, fermion and electric charge in (4.1) are given by

$$[A_\mu] = \frac{1}{2}(d-s) \qquad [\psi] = \frac{1}{2}(d-1) \qquad [e] = \frac{1}{2}(2+s-d) \tag{4.6}$$

implying that the electric charge is classically marginal for $d = s+2$, and that a canonical kinetic term for the photon is classically relevant whenever $s > 2$. We study the beta function for the electric charge associated with (4.1). Some of our findings are as follows:

- We find that the $d = s+2$ theory is exactly marginal as long as d is not an even integer. As mentioned in[97,121] and explained in appendix B the $d = s+2$ theory with $d \geq 3$ odd is the effective boundary theory for

$$S = \int d^{d+1}x \frac{1}{4} F_{\mu\nu} \left(\nabla^2\right)^{d-4} F^{\mu\nu} + \sum_{i=1}^{N_f} \int d^d x \bar{\psi}^i \left(i\partial\!\!\!/ - eA\!\!\!/\right) \psi^i \tag{4.7}$$

  with Neumann boundary conditions for the gauge field. Marginality of the $d = 3$ theory was discussed in[64,82,32] and a check of marginality of the $d = 5$ theory at one loop was carried out in[48] (see also[51]).

- Working in an ϵ expansion around $d = 4$ we find that, as opposed to classical expectations, a canonical kinetic term for the photon becomes relevant for $s > d-2$.

In other words, when $2 \leq d \leq 4$ and the electric charge is relevant, non-local QED flows to the same infrared fixed point as local QED. When the electric charge is irrelevant non-local QED flows to a Gaussian theory. See figure 4.1. This infrared behavior is reminiscent of that of the long-range Ising model, though there, apart from the Gaussian theory, there are two possible infrared fixed points. See [40,115,71,70,109,9,8] for details.

- For even values of d, the electric charge is no longer exactly marginal. We argue that for $d = 4$ and s bigger than 2, the theory is asymptotically free but will generate canonical kinetic terms in the infrared, serving as a UV completion of local four-dimensional QED.
- Treating the non-local kinetic term as the deformation of a local theory, we find that local three-dimensional QED possesses an exactly marginal non-local deformation $F_{\mu\nu} D^{-1} F^{\mu\nu}$.

We argue that the scale invariant $d = s + 2$ theory is also conformally invariant. In doing so, we provide a method for coupling the metric to a non-local derivative. Unitarity of these non-local theories are discussed in section 4.4.

4.1 Non-renormalization of the non-local photon

Action (4.1) falls in the category of non-local quadratic (photon kinetic term) theories perturbed by local interactions (gauge coupling term), so a non-renormalization theorem should apply. We will carefully examine the non-renormalization of the photon wave function to all orders in perturbation theory in this section as a warm-up for the RG analysis of the full theory.

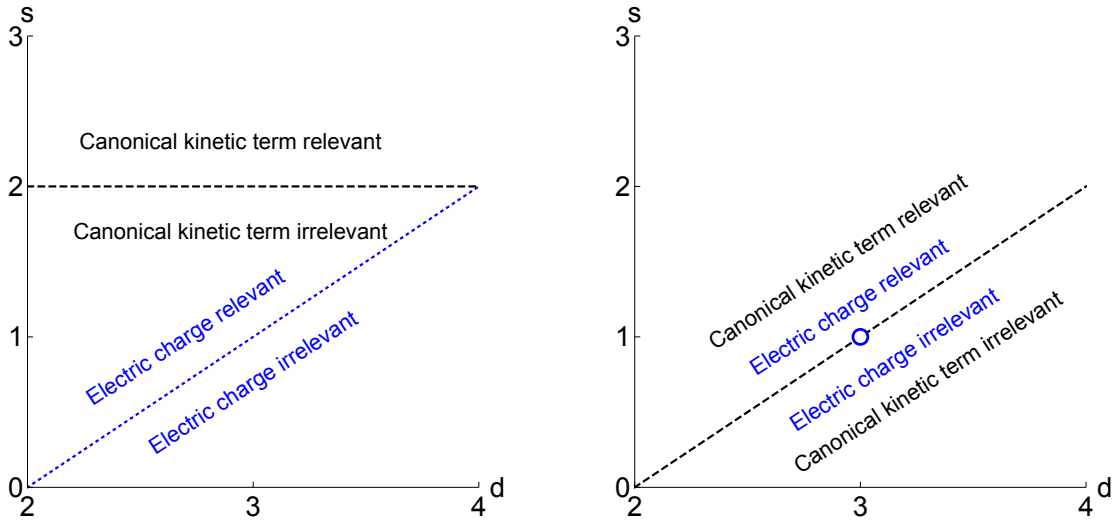

Figure 4.1: Classical (left) and quantum corrected (right) scaling properties of the canonical kinetic term and electric charge for various values of s and d as computed in the main text using an epsilon expansion and extrapolated to large ϵ. The white circle signifies that the $d = 3, s = 1$ theory is exactly marginal, as are all theories with $d = s - 2$ when d is not an even integer.

Let us denote the bare action associated with (4.1) by

$$S_B = \int d^d x \left(\frac{1}{4} Z_3 F_{\mu\nu} D^{s-2} F^{\mu\nu} + \frac{Z_4}{2\xi} \left(\partial_\mu A^\mu\right) D^{s-2} \left(\partial_\mu A^\mu\right) \right.$$
$$\left. + i Z_2 \sum_j \bar{\psi}^j \partial\!\!\!/ \psi^j - Z_1 e_0 \mu^{\frac{1}{2}(2+s-d)} \sum_j \bar{\psi}^j A\!\!\!/ \psi^j \right) \quad (4.8)$$

where bare fields are given by

$$\psi^B = Z_\psi^{\frac{1}{2}} \psi \qquad A^B = Z_A^{\frac{1}{2}} A \qquad e_B = Z_\alpha^{\frac{1}{2}} e_0 \mu^{\frac{1}{2}(2+s-d)} \qquad \xi_B = Z_\xi \xi \quad (4.9)$$

and

$$Z_1 = Z_\alpha^{\frac{1}{2}} Z_\psi Z_A^{\frac{1}{2}} , \qquad Z_2 = Z_\psi , \qquad Z_3 = Z_A , \qquad Z_4 = Z_A Z_\xi^{-1} . \tag{4.10}$$

Gauge invariance dictates that

$$Z_1 = Z_2 . \tag{4.11}$$

The beta function for the normalized square of the electric charge,

$$\frac{\alpha}{(4\pi)} = \frac{e_0^2}{(4\pi)^{d/2}} \tag{4.12}$$

is given by

$$\beta_\alpha = \mu \left(\frac{\partial \alpha}{\partial \mu} \right)_B = -\epsilon\alpha + 2\alpha\gamma_A , \tag{4.13}$$

where the subscript B implies that we keep bare quantities fixed while taking the derivative, and we have defined

$$\epsilon = s + 2 - d , \tag{4.14}$$

and

$$\gamma_A = \frac{1}{2}\mu \frac{\partial}{\partial \mu} \ln Z_A , \tag{4.15}$$

and used (4.11). Now we will argue for the non-renormalization of the photon wave func-

tion based on the work of[71].Alternate derivations of finiteness of the photon propagator for $d = 3$ and $s = 1$ can be found in[32,64].

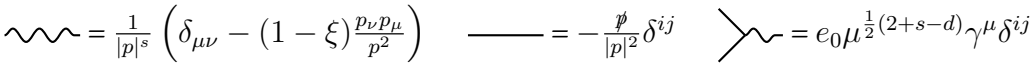

Figure 4.2: Feynman rules for the action (4.1).

First, it is straightforward to compute loop corrections to the photon propagator at one-loop, given the Feynman rules as shown in figure 4.2. The one-loop result is from a fermion loop and is insensitive to the non-local nature of the photon:

$$\begin{aligned}\Pi^{\mu\nu}_{(1)}(k) &= -e_0^2\mu^\epsilon N_f \mathrm{Tr}\int \frac{d^dp}{(2\pi)^d}\frac{\gamma^\mu \not{p}\gamma^\nu\left(\not{p}-\not{k}\right)}{p^2(p-k)^2} \\ &= -\frac{2\alpha}{4\pi}\mu^\epsilon f(d) N_f \frac{\Gamma\left(2-\frac{d}{2}\right)\Gamma\left(\frac{d}{2}\right)^2}{\Gamma(d)}k^{d-4}\left(k^2\delta^{\mu\nu}-k^\mu k^\nu\right)\end{aligned} \tag{4.16}$$

where $f(d)$ is the dimension of the γ matrices ($f(4) = 4$). Thus, if d is odd the one-loop correction to the photon propagator is finite and we find $Z_A = 1 + \mathcal{O}(\alpha^2)$. One can also compute the two-loop diagrams to explicitly show their finiteness for odd d but we skip them as we will soon prove the non-renomalization to all loop orders. For details of the two-loop results, one may consult the original paper[68] and the textbook[77].

We claim that non-local QED diagrams for the photon propagator are finite by arguing that diagrams with a negative degree of divergence and whose subdivergences have been regulated are finite. A similar statement regarding the renormalizability of local QED can be

found in[13]. Indeed, our argument is a special case of a more general theorem due to Weinberg[126] which states that if a Feynman diagram has negative superficial degree of divergence and its subdivergences have been subtracted, then it is finite. While Weinberg's theorem was proven for local theories, a careful analysis of the proof shows that it only relies on the propagator being proportional to a negative power of the momentum. Therefore, it immediately generalizes to non-local theories of the type studied in this work.

Given Weinberg's theorem, and that taking derivatives and adding counterterms commute in a minimal subtraction prescription (see, e.g., [28]), we can argue for finiteness of the photon correlator at any loop order. The superficial degree of divergence of a diagram with e_p external photon lines, no external fermions, and ℓ loops is

$$D = 2 + s - e_p + (d - 2 - s)\ell\,, \tag{4.17}$$

So, the superficial degree of divergence for the photon two-point function for $\epsilon = 0$ is $D = s$. We can now take $D + 1$ derivative of any given diagram $\Pi^{\mu}_{(\ell)\mu}$ together with its associated counterterms with respect to the external momenta k^μ to obtain an expression whose superficial degree of divergence is negative. Thus, any divergences of $\Pi^{\mu}_{(\ell)\mu}$ must be associated with integration constants which vanish when taking sufficiently many $\partial/\partial k^\mu$ derivatives of it. Since $\Pi^{\mu}_{(\ell)\mu}$ is a scalar, all these divergences must be analytic in k^2. So it has to have an even power of k. If s (and therefore d) is odd we conclude that $\Pi^{\mu}_{(\ell)\mu}$ together

with its associated counterterms is finite. Gauge invariance, $k_\mu \Pi^{\mu\nu}_{(\ell)} = 0$, then implies that $\Pi^{\mu\nu}_{(\ell)}$ will be finite as well whenever d is odd. This proves the non-renormalization property of non-local QED for $\epsilon = 0$ and d odd advocated at the beginning of this section.

We note that an argument similar to the one presented above has been used to show that there is no wavefunction renormalization in the continuum limit of the long-range Ising model[71]. Indeed, for generic values of s and d, the superficial degree of divergence of the photon two-point function, D, will not be an even integer, which implies that there is no wavefunction renormalization of the photon in such cases as well. More precisely, at ℓ loops, we have

$$D = (d-2)\ell - s(\ell - 1)\,. \tag{4.18}$$

In order for the diagram to be divergent, it must be the case that $D = 2n$ with $n > 0$ an integer. Thus, whenever

$$s = \frac{\ell}{\ell - 1}(d-2) - \frac{2n}{\ell - 1}\,, \tag{4.19}$$

with $\ell > 1$ the photon two-point function will have a logarithmically divergent contribution. For all other values of s there won't be any wave function renormalization of the photon.

We have seen that for $d = s + 2$ and d odd, the electric charge is exactly marginal. When $d - (s + 2) < 0$, the electric charge is relevant, and the theory may flow to a non-trivial fixed point in the infrared. For example, three-dimensional QED ($d = 3$ and $s = 2$) seems to behave in such a way, at least when N_f is large[2]. If $d = 3$ and $1 < s < 2$ (so that a local kinetic term is classically irrelevant), one might expect the infrared fixed point to be a non-local version of the fixed point of three-dimensional local QED, much like the relation between the fixed point of the long-range Ising model and the short-range Ising model studied in [40,115,71]. When $s > 2$, a local kinetic term becomes a relevant operator, and the expectation is that the theory will flow to a local one in the infrared. However, in what follows, we will find that the interplay between the generation of local kinetic terms and the non-renormalization of the non-local kinetic term is subtle, and the naive classical expectation breaks down, leading to interesting physical effects.

In four dimensions, renormalization of the one-loop correction to the photon propagator (given in (4.16)) requires us to introduce a local kinetic term for the photon. In order to understand whether such a term is relevant in an RG sense, we follow the standard practice of adding it to the action and studying the resulting beta function associated with it.

Working in $d = 4 - \epsilon'$ dimensions, our action takes the form

$$S = \int d^d x \left(\frac{1}{4} b Z_b \mu^{2-s} F_{\mu\nu} D^{s-2} F^{\mu\nu} + \frac{Z_3}{4} F_{\mu\nu} F^{\mu\nu} + (\text{gauge fixing terms}) \right.$$
$$\left. + i Z_2 \sum_j \bar{\psi}^j \not{\partial} \psi^j + Z_1 e_0 \mu^{\frac{\epsilon'}{2}} \sum_j \bar{\psi}^j \not{A} \psi^j \right) . \quad (4.20)$$

With some prescience (and similar to what was done in [115,71]) we have rescaled the gauge field (and electric charge) so that the local kinetic term is canonically normalized at tree level. Rescaling the gauge field (and electric charge) back so that the tree level non-local kinetic term is canonically normalized is a simple algebraic exercise which we will carry out towards the end of this subsection. The bare coupling associated with (4.20) are given by

$$b_B = b Z_b Z_3^{-1} \mu^{2-s} , \qquad e_B^2 = e_0^2 \mu^{\epsilon'} Z_3^{-1} . \quad (4.21)$$

Slightly generalizing the arguments that lead to the non-renormalization theorem of the previous section suggests that for generic values of s,* $Z_b = 1$ leading to

$$\begin{aligned} \beta_\alpha(\alpha, b) &= \alpha \left(-\epsilon' + 2\gamma_A(\alpha, b) \right) \\ \beta_b(\alpha, b) &= b \left((s-2) + 2\gamma_A(\alpha, b) \right) \end{aligned} \quad (4.22)$$

*Non-generic values of s are determined by (4.19) and either satisfy $s = d - 2$ with d even or $s < d - 2$ in which case the electric charge is irrelevant and the theory flows to the Gaussian one in the infrared.

where β_α and γ_A were defined in (4.13) and (4.15) respectively, and $\beta_b = \mu\,(\partial b/\partial\mu)_B$. Unless $s-2=-\epsilon'$ (a special case we will discuss shortly), a non-trivial fixed point will exist only if $b=0$ and $2\gamma_A(\alpha_*,0)=\epsilon'$. This fixed point is IR-stable whenever

$$B(\alpha,b)=\left.\begin{pmatrix}\partial_b\beta_b & \partial_\alpha\beta_b\\ \partial_b\beta_\alpha & \partial_\alpha\beta_\alpha\end{pmatrix}\right|_{\substack{b=0\\ \alpha=\alpha_*}} \succ 0\,. \tag{4.23}$$

Equation (4.23) reduces to

$$s>d-2\,,\qquad \alpha_*\frac{\partial}{\partial\alpha_*}\gamma_A(\alpha_*,0)>0\,. \tag{4.24}$$

The first inequality implies that we must be in the region where the electric charge is relevant. The second equality needs to be checked explicitly. In perturbation theory we find, using (4.16) and setting $d=4$ and $s=2$ that

$$\gamma_A(\alpha,0)=\frac{N_f\alpha}{3\pi}+\mathcal{O}(\alpha^2)\,, \tag{4.25}$$

for small ϵ'.

Note that the first inequality in (4.24) implies that the $b=0$ fixed point is stable as long as $s>d-2$, as opposed to the classical $s>2$. Put differently, we find that the local kinetic term is relevant whenever $s>d-2$ instead of $s>2$ as implied by a naive power counting

argument, at least as far as the epsilon expansion can be relied on. See figure 4.1.

Going back to (4.22), if $d = 3$ and $s = 1$ ($s-2 = -\epsilon'$), there is a one-dimensional family of solutions to $\beta_\alpha = \beta_b = 0$. This exactly marginal direction contains the $b = 0$, $\alpha = \alpha_*$ theory which is the non-trivial infrared fixed point of $\underbrace{\text{QED}_3}$.[†] In other words, $F_{\alpha\beta} D^{-1} F_{\alpha\beta}$ is an exactly marginal deformation of $\underbrace{\text{QED}_3}$. This is perhaps not surprising. Recall that the $d = 3, s = 1$ theory is equivalent to the theory which captures the boundary dynamics of a four-dimensional bulk photon coupled to N_f boundary fermions. Thus, the non-local deformation of the $\underbrace{\text{QED}_3}$ fixed point is equivalent to coupling $\underbrace{\text{QED}_3}$ to an additional bulk photon in 4 dimensions. Such a coupling is exactly marginal.

Finally, let us rescale the gauge field in (4.20) by $1/\sqrt{b\mu^{2-s}}$. In these variables the action (4.20) may be thought of as a deformation of a non-local theory with charge $\tilde{e}_0 = e_0/\sqrt{b}$ by a local operator $\tilde{b}\mu^{s-2}F^2$ with $\tilde{b} = 1/b$. Now

$$\tilde{b}_B = \tilde{b}\mu^{s-2} Z_3 \,, \qquad \tilde{e}_B^2 = \tilde{e}_0^2 \mu^{\epsilon'+s-2} \,, \tag{4.26}$$

so that

$$\begin{aligned} \beta_{\tilde{\alpha}} &= -\tilde{\alpha}\,(s - 2 + \epsilon') \\ \beta_{\tilde{b}} &= -\tilde{b}\,((s-2) + 2\gamma_A) \ . \end{aligned} \tag{4.27}$$

[†]Based on an ϵ expansion analysis, we are assuming that $\gamma_A(\alpha_*, 0)$ is not a local minimum or maximum of γ_A. If it is then there are no other solutions to (4.22) around $b = 0$.

Thus, if $d = 4$ and $s > 2$, a theory with small $\tilde{b}$ is asymptotically free and can serve as a UV completion of QED, sidestepping the infamous Landau pole of the local theory; in the infrared, a (relevant) local kinetic term will be generated and dominate the dynamics.

The analysis we have carried out so far may be generalized to an epsilon expansion around $d = 2n - \epsilon'$ dimensions. For $n > 2$, the action

$$S = \int d^d x \left(\frac{1}{4} b \mu^{2n-(s+2)} Z_b F_{\mu\nu} D^{s-2} F^{\mu\nu} + \frac{Z_3}{4} F_{\mu\nu} D^{2n-4} F^{\mu\nu} + (\text{gauge fixing terms}) \right.$$
$$\left. + i Z_2 \sum_j \bar{\psi}^j \not{\partial} \psi^j + Z_1 e_0 \mu^{\frac{\epsilon'}{2}} \sum_j \bar{\psi}^j \not{A} \psi^j \right) \quad (4.28)$$

generalizes (4.20), the bare coupling,

$$b_B = b Z_b Z_3^{-1} \mu^{2n-(s+2)} \,, \quad (4.29)$$

generalizes (4.21), and the beta functions (4.22) now read

$$\begin{aligned} \beta_\alpha(\alpha, \tilde{b}) &= \alpha \left(-\epsilon' + 2\gamma_A(\alpha, b) \right) \\ \beta_b(\alpha, \tilde{b}) &= b \left((s + 2 - 2n) + 2\gamma_A(\alpha, b) \right) \,. \end{aligned} \quad (4.30)$$

As was the case for $n = 2$, unless $-\epsilon' = s + 2 - 2n$, the only non-trivial fixed point is $b = 0$

and $\gamma(\alpha_*, 0) = \epsilon'$ whose stability is given by (4.24) except that now

$$\gamma(\alpha, 0) = (-1)^n \frac{N_f \alpha f(d)(n-1)}{4^n \sqrt{\pi} \Gamma\left(n + \frac{1}{2}\right)} + \mathcal{O}(\alpha^2)\,. \tag{4.31}$$

For n even, the fixed point is perturbatively stable but for n odd the fixed point is perturbatively unstable, at least for real values of α. A similar observation was made for the $n = 3$ case in [51].

4.3 Conformal invariance and non-local currents

Theories with $d = s + 2$ and s odd are scale invariant for all values of the electric charge. It is then natural to inquire whether they are also conformally invariant. For local, unitary theories with $d = 2$, it is known that scale invariance implies conformal invariance [132,112], but in higher dimensions it is already possible to find simple counterexamples. One such example is free $d = 3$ Maxwell theory [79,37], in which the two-point function of the field strength $F_{\mu\nu}$ exhibits scale invariance but does not possess the correct tensor structure for full conformal invariance. We can also compute two-point functions in the non-local free Maxwell theory to find necessary conditions of conformal invariance. Using our rules for the Fourier transform, the correlator in position space in our gauge is

$$\langle A_\mu(x) A_\nu(0)\rangle = \frac{1}{(2\pi)^s} \frac{\pi^{s-\frac{d}{2}} \Gamma\left(\frac{d-s}{2}\right)}{\Gamma\left(\frac{s}{2}\right)} \frac{\delta_{\mu\nu}}{|x|^{d-s}} \equiv C_A \frac{\delta_{\mu\nu}}{|x|^{d-s}}\,. \tag{4.32}$$

The correlation function (4.32) is not gauge invariant. The gauge invariant operator we will constrain is $F_{\mu\nu} = \partial_\mu A_\nu - \partial_\nu A_\mu$, which we assume to be a primary. The simplest 2-point function we can write down is:

$$\langle F_{\mu\nu}(x) F_{\rho\sigma}(0)\rangle = \langle \partial_\mu A_\nu(x) \partial_\rho A_\sigma(0)\rangle - \langle \partial_\mu A_\nu(x) \partial_\sigma A_\rho(0)\rangle - (\mu \leftrightarrow \nu)\,. \qquad (4.33)$$

To evaluate this, we use the standard technique of inserting the second operator at a point y^ρ, then differentiating and setting $y = 0$ at the end. Doing this and summing over the terms gives:

$$\langle F_{\mu\nu}(x) F_{\rho\sigma}(0)\rangle = C_A \frac{2(d-s)}{x^{d-s+2}} \left(I_{\mu\rho}(x) - \frac{1}{2}(d-s-2)\frac{x_\mu x_\rho}{x^2} \right) \left(I_{\nu\sigma}(x) - \frac{1}{2}(d-s-2)\frac{x_\nu x_\sigma}{x^2} \right) - (\mu \leftrightarrow \nu)\,. \qquad (4.34)$$

where

$$I_{\mu\nu} = \delta_{\mu\nu} - 2\frac{x_\mu x_\nu}{x^2}\,. \qquad (4.35)$$

By construction, this 2-point function comes from a scale invariant theory and is scale covariant. However, as we discussed in the introduction of this section, conformal covariance is a nontrivial requirement. Since $F_{\mu\nu}$ is primary, conformal covariance dictates that the tensorial dependence of the field strength correlation function should appear only through

$I_{\mu\nu}(x)$ defined in (4.35)[107].We see from (4.34) that correlation functions of F are conformally covariant only for $d = s + 2$, or in other words, the scaling dimension of F is exactly 2. One can also see that in the local limit of $d = 3$, $s = 2$, we match the conclusion of[37] that the theory is scale but not conformally invariant. What is free next is that at odd s, the non-renormalization theorem keeps the scaling dimension fixed, and that is evidence of conformal invariance even in the interacting theory.

Since studies of scale invariance versus conformal invariance often rely on the properties of the trace of a local stress tensor (see, e.g.,[127,20,27,112,34,33,35] and references therein), one may worry that a non-local field theory will not possess such an operator rendering such an analysis mute. While a non-local field theory is not expected to support a local stress tensor, it is possible that it allows for a non-local one. In fact, given a Lagrangian description of the theory, one expects to be able to obtain a stress tensor via a Noether procedure or by coupling the fields to an external metric. Indeed, if it is possible to couple the theory to a background metric such that the resulting action transforms as a scalar under general coordinate transformations, then we are guaranteed that the resulting energy momentum tensor, local or not, will be conserved. Such an energy momentum tensor will generate translations in the usual sense. Furthermore, standard arguments show that this stress tensor will be traceless (up to improvement terms) if and only if the theory is conformally invariant.

To warm up and introduce the notion of non-local current in this chapter, we first dis-

cuss simple $U(1)$ currents in non-local scalar theories. Then we will use the Caffarelli-Silvestre extension theorem[19] to couple the non-local Laplacian D^s to an external metric in a general coordinate covariant way. With such an expression in hand, we can couple the action 4.1 to a metric and, from it, compute a (non-local) energy momentum tensor, $T^{\mu\nu}$. We also show that $T^{\mu}{}_{\mu} = 0$ up to improvement terms. An alternate method for computing the stress tensor in non-local theories can be found in[113,87].

4.3.1 Examples of non-local currents

We present two examples in this subsection. We first derive the $U(1)$ current of the one-dimensional free complex scalar to give the readers a hint of what is a non-local conserved current mathematically. Then we proceed to look at the $U(1)$ current of the non-local dual photon in three dimensions, which is a non-local compact scalar, to explain its physical relevance.

Writing D^s as $\Box^{\frac{s}{2}}$, where $\Box$ is the usual local laplacian, the action is

$$S = \int dx\, \bar{\phi}\Box^{\frac{s}{2}}\phi + \phi\Box^{\frac{s}{2}}\bar{\phi} \tag{4.36}$$

The idea is to express the fractional laplacian as a series of powers of usual laplacians:

$$\Box^{\frac{s}{2}} = \lim_{b\to 0}(\Box + b)^{\frac{s}{2}} = \sum_{n=0}^{\infty}\frac{1}{n!}b^{\frac{s}{2}-n}\Box^n\prod_{i=0}^{n-1}(\frac{s}{2} - i) \tag{4.37}$$

Starting with $\bar{\phi}\Box^{\frac{s}{2}}\phi$ for example, we deform the field by a space-time dependent phase

$$\begin{aligned} e^{-i\alpha(x)}\bar{\phi}\Box^{\frac{s}{2}}(e^{i\alpha(x)}\phi) &= e^{-i\alpha(x)}\bar{\phi}\sum_{n=0}^{\infty}\frac{1}{n!}b^{\frac{s}{2}-n}\prod_{i=0}^{n-1}(\frac{s}{2}-i)\Box^n(e^{i\alpha(x)}\phi) \\ &= e^{-i\alpha(x)}\bar{\phi}\sum_{n=0}^{\infty}\frac{1}{n!}b^{\frac{s}{2}-n}\prod_{i=0}^{n-1}(\frac{s}{2}-i)\sum_{m=0}^{2n}\binom{2n}{m}(\partial^{2n-m}(e^{i\alpha(x)})\partial^m\phi) \end{aligned} \tag{4.38}$$

$m \neq 2n$ and $n \neq 0$ terms are the variation of the Lagrangian. Keeping only linear terms in α, the derivative of the phase becomes $i(\partial^{2n-m}\alpha(x))e^{i\alpha(x)}$. Thus, the variation becomes

$$\begin{aligned} e^{-i\alpha(x)}\bar{\phi}\sum_{n=1}^{\infty}\frac{1}{n!}b^{\frac{s}{2}-n}\prod_{i=0}^{n-1}(\frac{s}{2}-i)\sum_{m=0}^{2n-1}\binom{2n}{m}(i(\partial^{2n-m}\alpha(x))e^{i\alpha(x)}\partial^m\phi) \\ = i\sum_{n=1}^{\infty}\frac{1}{n!}b^{\frac{s}{2}-n}\prod_{i=0}^{n-1}(\frac{s}{2}-i)\sum_{m=0}^{2n-1}\binom{2n}{m}(\bar{\phi}\partial^m\phi)\partial^{2n-m}\alpha(x) \end{aligned} \tag{4.39}$$

Then we do integration by part and regard the factor of $\partial\alpha(x)$ as the current:

$$\begin{aligned} & i\sum_{n=1}^{\infty}\frac{1}{n!}b^{\frac{s}{2}-n}\prod_{i=0}^{n-1}(\frac{s}{2}-i)\sum_{m=0}^{2n-1}\binom{2n}{m}(-1)^{2n-m-1}\partial^{2n-m-1}(\bar{\phi}\partial^m\phi) \\ =& i\sum_{n=1}^{\infty}\frac{1}{n!}b^{\frac{s}{2}-n}\prod_{i=0}^{n-1}(\frac{s}{2}-i)\sum_{m=0}^{2n-1}\binom{2n}{m}(-1)^{-m-1}\sum_{l=0}^{2n-m-1}\binom{2n-m-1}{l}(\partial^l\bar{\phi}\partial^{2n-l-1}\phi) \end{aligned} \tag{4.40}$$

We then need two steps to make progress. First, we notice that the absolute value of the coefficient of $\partial^l\bar{\phi}\partial^{2n-l-1}\phi$ should only depend on n. This inspires us to find such an iden-

tity:

$$\sum_{m=0}^{2n-l-1}(-1)^{-m-1}\binom{2n}{m}\binom{2n-m-1}{l}=(-1)^{l} \tag{4.41}$$

A proof of it makes use of the Gauss's hypergeometric theorem.[‡] One can check instead this equivalent identity:

$$\sum_{m=0}^{N}(-1)^{-m-1}\frac{1}{m!(N-m)!}\frac{1}{N+l+1-m}=(-1)^{N+1}\frac{l!}{(N+l+1)!} \tag{4.43}$$

with $N=2n-l-1$. From the definition we have

$$\sum_{m=0}^{N}(-1)^{-m}\frac{N!}{m!(N-m)!}\frac{N+l-1}{N+l+1-m}={}_2F_1(-N,-N-l+1;-N-l-2;1) \tag{4.44}$$

Then Gauss's hypergeometric theorem says

$${}_2F_1(a,b;c;1)=\frac{\Gamma(c)\Gamma(c-a-b)}{\Gamma(c-a)\Gamma(c-b)} \tag{4.45}$$

Then we notice that there are negative integer poles in the gamma function. We can switch

[‡]While in deriving higher dimensional currents, similar observation lets us conjecture another identity:

$$\sum_{m=2}^{2n}\sum_{l=1}^{[\frac{m}{2}]}\binom{n}{l}\binom{n-l}{m-2l}2^{m-2l}(-1)^{m-1}\sum_{t=r-l+1}^{[\frac{r}{2}]}\binom{l-1}{t}\binom{l-1-t}{r-2t}2^{r-2t}=(r+1)(-1)^{r+n} \tag{4.42}$$

where $[x]$ is the integer part of x. But it is beyond our current scope to prove this equation. Direct numerical tests for n not too large find no counterexample.

m and $N-m$:

$$\sum_{m=0}^{N}(-1)^{-m-1}\frac{1}{m!(N-m)!}\frac{1}{N+l+1-m}=\sum_{m=0}^{N}(-1)^{-N+m-1}\frac{1}{m!(N-m)!}\frac{1}{m+l+1}$$
$$={}_2F_1(-N,l+1;l+2;1)\frac{(-1)^{-N-1}}{l+1}\frac{1}{N!} \tag{4.46}$$

Then the theorem tells us that

$${}_2F_1(-N,l+1;l+2;1)=\frac{\Gamma(l+2)\Gamma(N+1)}{\Gamma(1)\Gamma(N+l+2)}=\frac{(l+1)!(N)!}{(N+l+1)!} \tag{4.47}$$

And then

$$\frac{(l+1)!(N)!}{(N+l+1)!}\frac{(-1)^{-N-1}}{l+1}\frac{1}{N!}=(-1)^{N+1}\frac{l!}{(N+l+1)!} \tag{4.48}$$

The identity is proven.

The next step is to introduce linear differential operators that only acts on ϕ or its conju-

gate, similar to those used in higher spin currents. The current is in good shape now:

$$
\begin{aligned}
& i\sum_{n=1}^{\infty}\frac{1}{n!}b^{\frac{s}{2}-n}\prod_{i=0}^{n-1}(\frac{s}{2}-i)\sum_{m=0}^{2n-1}(-1)^{-m-1}\binom{2n}{m}\sum_{l=0}^{2n-m-1}\binom{2n-m-1}{l}(\partial^l\bar{\phi}\partial^{2n-l-1}\phi) \\
=& i\sum_{n=1}^{\infty}\frac{1}{n!}b^{\frac{s}{2}-n}\prod_{i=0}^{n-1}(\frac{s}{2}-i)\sum_{l=0}^{2n-1}\partial^l\bar{\phi}\partial^{2n-1-l}\phi(-1)^l \\
\equiv& i\sum_{n=1}^{\infty}\frac{1}{n!}b^{\frac{s}{2}-n}\prod_{i=0}^{n-1}(\frac{s}{2}-i)\sum_{l=0}^{2n-1}X^lY^{2n-1-l}(\bar{\phi}\phi)(-1)^l \\
=& -\frac{i\left((b+X^2)^{\frac{s}{2}}-(b+Y^2)^{\frac{s}{2}}\right)}{X+Y}(\bar{\phi}\phi)
\end{aligned}
\tag{4.49}
$$

where X only acts on $\bar{\phi}$ and Y only acts on ϕ. That is to say

$$
X^mY^n(\bar{\phi}\phi)\equiv\partial^m\bar{\phi}\partial^n\phi \tag{4.50}
$$

Then the $b\to 0$ limit can be taken smoothly and we have the current

$$
-2\frac{i\left((X^2)^{\frac{s}{2}}-(Y^2)^{\frac{s}{2}}\right)}{X+Y}(\bar{\phi}\phi) \tag{4.51}
$$

The extra factor of 2 comes from the complex conjugation. Annihilation by $X+Y$ under the equation of motion should be understood as the conservation condition. One can also set s to be even integers to recover local or higher derivative currents.

The second example, a three-dimensional free compact scalar,

$$S = \int dx^3 \phi \Box^{\frac{s}{2}} \phi \tag{4.52}$$

has the $\phi \to \phi + \alpha$ symmetry. The non-local current associated with this symmetry can be derived similarly:

$$\begin{aligned} \Delta\mathcal{L} =& (\phi+\alpha)\Box^{\frac{s}{2}}(\phi+\alpha) - \phi\Box^{\frac{s}{2}}\phi \\ =& \lim_{b\to 0} \sum_{n=1}^{\infty} \frac{1}{n!} b^{\frac{s}{2}-n} \prod_{i=0}^{n-1} (\frac{s}{2} - i)(\alpha\Box^n\phi + \phi\Box^n\alpha) \end{aligned} \tag{4.53}$$

After an integration by parts, the coefficients of the $\partial^\mu\alpha$ term are taken as the current:

$$\begin{aligned} & \lim_{b\to 0} -2 \sum_{n=1}^{\infty} \frac{1}{n!} b^{\frac{s}{2}-n} \prod_{i=0}^{n-1} (\frac{s}{2} - i)\Box^{n-1}\partial_\mu\phi \\ =& \lim_{b\to 0} \frac{2(b^{\frac{s}{2}} - (b+\Box)^{\frac{s}{2}})}{\Box} \partial_\mu\phi \\ =& -2\Box^{\frac{s}{2}-1}\partial_\mu\phi \end{aligned} \tag{4.54}$$

Now we have the current and the charge operator

$$j^\mu \propto \Box^{\frac{s}{2}-1}\partial_\mu\phi \qquad Q \propto \int_\Sigma \Box^{\frac{s}{2}-1}\partial_\mu\phi \, n^\mu dS \tag{4.55}$$

where Σ is a orientable closed two-dimensional surface and n is the normal vector of the

surface. We want to show that the monopole operator $M = e^{iq\phi}$ is charged under this Q operator. That amounts to ask what is $[Q, M]$:

$$[Q, M(0)] \propto [\int_\Sigma \Box^{\frac{s}{2}-1}\partial_\mu\phi(x)\, n^\mu dS, e^{iq\phi(0)}] = \int_\Sigma \Box^{\frac{s}{2}-1}\partial_\mu[\phi(x), e^{iq\phi(0)}]\, n^\mu dS \quad (4.56)$$

With $[\phi(x), \phi(0)] = G_F(x)$, we can obtain

$$\begin{aligned}
[\phi(x), e^{iq\phi(0)}] =& [\phi(x), \sum_{n=0}^{\infty} \frac{1}{n!}(iq\phi(0)^n)] \\
=& \sum_{n=0}^{\infty} \frac{1}{n!}(iq)^n[\phi(x), \phi(0)^n] \\
=& \sum_{n=0}^{\infty} \frac{1}{n!}(iq)^n n G_F(x)\phi(0)^{n-1} \\
=& G_F(x) iq e^{iq\phi(0)}
\end{aligned} \quad (4.57)$$

Thus, the charge operator acts on M as

$$[Q, M(0)] \propto iqM \int_\Sigma \Box^{\frac{s}{2}-1}\partial_\mu G_F(x)\, n^\mu dS \quad (4.58)$$

Using the Stokes theorem and the equation of motion, the integral becomes

$$\begin{aligned}\int_\Sigma \Box^{\frac{s}{2}-1}\partial_\mu G_F(x)\, n^\mu dS &= \int_V \partial^\mu \Box^{\frac{s}{2}-1}\partial_\mu G_F(x) dV \\ &\propto \int_V \delta(\vec{x}) dV = \begin{cases} 1, & \text{if } 0 \in V \\ 0, & \text{otherwise} \end{cases}\end{aligned} \tag{4.59}$$

where V is the volume that is wrapped by the closed surface Σ. Note that the final result becomes

$$[Q, M] \propto \begin{cases} qM, & \text{if } M \text{ is inside } \Sigma \\ 0, & \text{otherwise} \end{cases} \tag{4.60}$$

In this sense, the non-local current we obtained has the same physical meaning as its local counterparts.

4.3.2 Non-local stress energy tensor

If a theory is local and translation invariant, one can couple the theory to a metric in a coordinate invariant way by adding a Christoffel connection to the derivative operator ∂_μ, generating a covariant derivative D_μ which is general coordinate covariant, viz.,

$$\left(D_\mu + \delta_\xi D_\mu\right)\left(f_{\nu_1\ldots\nu_n} + \pounds_\xi f_{\nu_1\ldots\nu_n}\right) = D_\mu f_{\nu_1\ldots\nu_n} + \pounds_\xi\left(D_\mu f_{\nu_1\ldots\nu_n}\right) + \mathcal{O}(\xi^2)\,. \tag{4.61}$$

Here $\pounds_\xi$ represents a Lie derivative associated with an infinitesimal coordinate transformation $x \to x + \xi$ and $\delta_\xi D_\mu$ represents the infinitesimal transformation of the covariant derivative under such a coordinate transformation.

To construct a covariant non-local derivative, D^s, we take a somewhat different route and turn our attention to the Caffarelli-Silvestre extension theorem.[§][19] The CS theorem allows one to relate the fractional derivative to a local operator in a higher dimension; Let $u(x^\mu, y)$ be a solution to

$$\left(\nabla_x^2 + \frac{1-s}{y}\partial_y + \partial_y^2\right) u = 0\,, \tag{4.62a}$$

where ∇_x^2 is the Laplacian on $\mathbb{R}^d$ (spanned by the Cartesian coordinates x^μ), $y \in [0, \infty)$, and $0 < s < 2$, supplemented with the boundary conditions

$$u(x, 0) = f(x) \qquad u(x, \infty) = 0\,. \tag{4.62b}$$

The CS extension theorem states that

$$\lim_{y\to 0} y^{1-s}\partial_y u = C D^s f(x)\,, \tag{4.63}$$

[§]The CS theorem was proven for $0 < s < 2$ but the end result we obtain for the covariant derivative can be analytically extended to other values of s.

where

$$C = -\frac{2^{1-s}\Gamma\left(1-\frac{s}{2}\right)}{\Gamma\left(\frac{s}{2}\right)}\,. \tag{4.64}$$

A detailed proof of the CS extension theorem can be found in[19]. Put briefly, consider the ordinary differential equation

$$-\hat{w}(z) + \frac{1-s}{z}\hat{w}'(z) + \hat{w}''(z) = 0 \tag{4.65}$$

with $z \in [0, \infty)$ and boundary conditions

$$\hat{w}(0) = 1 \qquad \hat{w}(\infty) = 0\,. \tag{4.66}$$

We can construct a solution of the Fourier transform of u, $\hat{u}(k, y)$, from $\hat{w}$ via

$$\hat{u}(k, y) = \widehat{f}(k)\hat{w}(|k|y). \tag{4.67}$$

Then

$$\begin{aligned}\lim_{y\to 0} y^{1-s}\partial_y \hat{u} &= |k|^s \widehat{f}(k) \lim_{y\to 0}(|k|y)^{1-s}\hat{w}'(|k|y) \\ &= C|k|^s \widehat{f}(k)\end{aligned} \tag{4.68}$$

with

$$C = \lim_{z \to 0} z^{1-s} \hat{w}'(z). \tag{4.69}$$

Since (4.65) is a Bessel equation, it is straightforward to compute (4.69) explicitly and obtain (4.64).

Using the CS extension theorem, it is possible to construct a fractional derivative $\widetilde{D}^s$ which transforms covariantly under a general coordinate transformation, and reduces to D^s when the background metric is flat. To start, let us replace (4.62a) with

$$\left(\widetilde{\nabla}_x^2 + \frac{1-s}{y} \partial_y + \partial_y^2 \right) u = 0 \,, \tag{4.70}$$

with the same boundary conditions as in (4.62b) but where now $\widetilde{\nabla}_x^2 = g^{\mu\nu} \nabla_\mu \nabla_\nu$ with $g^{\mu\nu}$ a non-trivial metric associated with the space spanned by the x^μ coordinates and ∇_μ its associated covariant derivative.

By construction, equation (4.70) transforms covariantly under coordinate transformations in the x^μ directions implying that the associated $\widetilde{D}^s$ will transform covariantly under general coordinate transformations. To see this explicitly, let T denote a coordinate transformation, $x \to x'(x) = T(x)$, such that $T(f(x)) = f(T(x)), T(u(x,y)) = u(T(x), y)$

and $T(\widetilde{\nabla}_x^2 u(x,y)) = \widetilde{\nabla}_{T(x)}^2 u(T(x),y))$. Then

$$T\left(\left(\widetilde{\nabla}_x^2 + \frac{1-s}{y}\partial_y + \partial_y^2\right) u(x,y)\right) = \left(\widetilde{\nabla}_{T(x)}^2 + \frac{1-s}{y}\partial_y + \partial_y^2\right) u(T(x),y)\,, \quad (4.71)$$

with

$$u(T(x),0) = f(T(x))\,. \quad (4.72)$$

We denote u as the solution of

$$\left(\widetilde{\nabla}_x^2 + \frac{1-s}{y}\partial_y + \partial_y^2\right) u(x,y) = 0 \quad (4.73)$$

or equivalently

$$\left(\widetilde{\nabla}_{T(x)}^2 + \frac{1-s}{y}\partial_y + \partial_y^2\right) u(T(x),y) = 0 \quad (4.74)$$

At the same time, u' represents the solution of

$$\left(\widetilde{\nabla}_{T(x)}^2 + \frac{1-s}{y}\partial_y + \partial_y^2\right) u'(x,y) = 0 \quad (4.75)$$

If we now define

$$C\widetilde{D}^s f(x) = \lim_{y\to 0} y^{1-s}\partial_y u(x,y) \quad (4.76)$$

then, $T(\widetilde{D}^s)$ is defined as

$$C\,T(\widetilde{D}^s)f(x) = \lim_{y\to 0} y^{1-s}\partial_y u'(x,y)\,, \tag{4.77}$$

In the end, we show

$$C\,T(\widetilde{D}^s f(x)) = T\left(\lim_{y\to 0} y^{1-s}\partial_y u(x,y)\right) = \lim_{y\to 0} y^{1-s}\partial_y u(T(x),y) = C\,T(\widetilde{D}^s)f(T(x)) \tag{4.78}$$

as required.

While it is difficult to obtain an explicit expression for $\widetilde{D}^s$, it is straightforward to do so to linear order in metric perturbations around a flat background. Let us expand the metric $g_{\mu\nu} = \eta_{\mu\nu} + h_{\mu\nu}$. The linearized expression for the covariant derivative $\widetilde{\nabla}^2_x$ acting on a rank two antisymmetric tensor is given by

$$\widetilde{\nabla}^2_x F_{\alpha\beta} = \nabla^2_x F_{\alpha\beta} + \nabla^2_x[h]F_{\alpha\beta} + \mathcal{O}(h^2) \tag{4.79}$$

where

$$\begin{aligned}\nabla_x^2[h]F_{\alpha\beta} = &- h^{\mu\nu}\partial_\nu\partial_\mu F_{\alpha\beta} + \frac{1}{2}\partial_\sigma h\partial^\sigma F_{\alpha\beta} - \partial_\nu F_\alpha{}^\sigma\partial_\beta h^\nu{}_\sigma - \partial_\nu F_{\alpha\sigma}\partial^\nu h_\beta{}^\sigma + \partial_\nu F_\alpha{}^\sigma\partial_\sigma h_\beta{}^\nu \\ &+ \partial_\nu F_{\beta\sigma}\partial_\alpha h^{\nu\sigma} + \partial_\nu F_{\beta\sigma}\partial^\nu h_\alpha{}^\sigma + \frac{1}{2}F_\beta{}^\sigma\partial^\nu\partial_\alpha h_{\nu\sigma} - \frac{1}{2}F_{\alpha\sigma}\partial_\nu\partial_\beta h^{\nu\sigma} + \frac{1}{2}F_\beta{}^\sigma\partial_\nu\partial^\nu h_{\alpha\sigma} \\ &- \frac{1}{2}F_\alpha{}^\sigma\partial_\nu\partial^\nu h_{\beta\sigma} - \frac{1}{2}F_\beta{}^\sigma\partial^\nu\partial_\sigma h_{\alpha\nu} + \frac{1}{2}F_\alpha{}^\sigma\partial^\nu\partial_\sigma h_{\beta\nu} - \partial_\nu h^{\nu\sigma}\partial_\sigma F_{\alpha\beta} - \partial^\nu F_\beta{}^\sigma\partial_\sigma h_{\alpha\nu}\,,\end{aligned} \tag{4.80}$$

with $h = \eta^{\mu\nu}h_{\mu\nu}$ and indices are raised and lowered with the Minkowski metric, e.g., $h^{\mu\nu} = \eta^{\mu\alpha}\eta^{\nu\beta}h_{\alpha\beta}$. To compute the associated linear correction to D^s,

$$\widetilde{D}^s = D^s + D_1^s[h] + \mathcal{O}(h^2), \tag{4.81}$$

we must solve (4.70) perturbatively in $h_{\mu\nu}$. We will do so using Green's functions.

Let us expand the solution to (4.70) in powers of h, replacing u with a rank two antisymmetric tensor $\phi_{\alpha\beta}$,

$$\phi_{\alpha\beta} = \phi^0_{\alpha\beta} + \phi^1_{\alpha\beta}[h] + \mathcal{O}(h^2)\,, \tag{4.82}$$

such that

$$\left(\nabla_x^2 + \frac{1-s}{y}\partial_y + \partial_y^2\right)\phi^0_{\alpha\beta} = 0 \tag{4.83a}$$

$$\left(\nabla_x^2 + \frac{1-s}{y}\partial_y + \partial_y^2\right)\phi^1_{\alpha\beta} = -\nabla_x^2[h]\phi^0_{\alpha\beta} \tag{4.83b}$$

etc. The boundary conditions associated with (4.83) are

$$\phi^0_{\alpha\beta}(x,0) = f_{\alpha\beta}(x)\,, \qquad \phi^1_{\alpha\beta}(x,0) = 0\,, \tag{4.84}$$

and so on.

After Fourier transforming in the x directions, the two linearly independent solutions to the scalar version of (4.83a) are given by

$$L_+ = y^{\frac{s}{2}} K_{\frac{s}{2}}(|k|y) \qquad L_- = y^{\frac{s}{2}} I_{\frac{s}{2}}(|k|y) \tag{4.85}$$

where $K_{\frac{s}{2}}$ and $I_{\frac{s}{2}}$ are modified Bessel functions. Note that

$$L_+(0) = |k|^{-\frac{s}{2}}\Gamma\left(\frac{s}{2}\right)2^{\frac{s}{2}-1} + \mathcal{O}(y^s) \qquad L_-(0) = \mathcal{O}(y^s) \tag{4.86}$$

$$L_+(\infty) = 0 \qquad L_-(\infty) = \infty \tag{4.87}$$

Thus,

$$\hat{\phi}^0_{\alpha\beta} = \frac{2^{1-\frac{s}{2}}|k|^{\frac{s}{2}}y^{\frac{s}{2}}}{\Gamma\left(\frac{s}{2}\right)} K_{\frac{s}{2}}(|k|y)\widehat{f}_{\alpha\beta}(k)\,, \tag{4.88}$$

and

$$\lim_{y\to 0} y^{1-s}\partial_y \hat{\phi}^0_{\alpha\beta} = -\frac{2^{1-s}\Gamma\left(1-\frac{s}{2}\right)}{\Gamma\left(\frac{s}{2}\right)}|k|^s \widehat{f}_{\alpha\beta}(k)\,. \tag{4.89}$$

inline with (4.69).

To solve for $\phi^1_{\alpha\beta}$ we look for the Greens function satisfying

$$\left(-|k|^2 + \frac{1-s}{y}\partial_y + \partial_y^2\right) G(y,y') = \delta(y-y')\,. \tag{4.90}$$

Using standard techniques, $G(y,y')$ can be constructed from the two solutions to the homogeneous equation, $L_\pm$. We find

$$G(y,y') = -y^{\frac{s}{2}}(y')^{1-\frac{s}{2}} \begin{cases} I_{\frac{s}{2}}(|k|y')K_{\frac{s}{2}}(|k|y) & y > y' \\ \\ K_{\frac{s}{2}}(|k|y')I_{\frac{s}{2}}(|k|y) & y < y' \end{cases}. \tag{4.91}$$

Thus,

$$\begin{aligned} \widehat{\phi}^1_{\alpha\beta}(k) = &- y^{\frac{s}{2}}K_{\frac{s}{2}}(|k|y)\int_0^y (y')^{1-\frac{s}{2}} I_{\frac{s}{2}}(|k|y')S_{\alpha\beta}(k,y')dy' \\ &- y^{\frac{s}{2}}I_{\frac{s}{2}}(|k|y)\int_y^\infty (y')^{1-\frac{s}{2}} K_{\frac{s}{2}}(|k|y')S_{\alpha\beta}(k,y')dy' \end{aligned} \tag{4.92}$$

with

$$S_{\alpha\beta}(k,y') = -\widehat{\nabla_x^2[h]\phi^0_{\alpha\beta}(x,y')}\,. \tag{4.93}$$

Thus,

$$\begin{aligned}
\widehat{D_1^s[h]f}_{\alpha\beta}(k_1) &= \frac{1}{C}\lim_{y\to 0} y^{1-s}\partial_y\widehat{\phi}^1_{\alpha\beta}(k_1) \\
&= \frac{2^{\frac{s}{2}}k_1^{\frac{s}{2}}}{\Gamma\left(1-\frac{s}{2}\right)}\int_0^\infty (y')^{1-\frac{s}{2}}K_{\frac{s}{2}}(|k_1|y')S_{\alpha\beta}(k_1,y')dy' \\
= -\int \frac{d^dkd^dk_2}{(2\pi)^d}\delta(k+k_2-k_1)\frac{(k_1^s-k_2^s)}{k_1^2-k_2^2} &\times \left(\frac{1}{2}\widehat{h}_{\beta\rho}\left(\left(k^2+2k_2^\mu k_\mu\right)\widehat{f}_\alpha{}^\rho - k^\lambda\left(k^\rho+2{k_2}^\rho\right)\widehat{f}_{\alpha\lambda}\right)\right. \\
&\left. + \frac{1}{2}\widehat{h}_{\lambda\rho}\left(k_\beta\left(k^\lambda+2{k_2}^\lambda\right)\widehat{f}_\alpha{}^\rho + \left(k^\lambda+{k_2}^\lambda\right)k_2{}^\rho\widehat{f}_{\alpha\beta}\right) - \frac{1}{4}k_2^\mu k_\mu\widehat{h}\widehat{f}_{\alpha\beta} - (\alpha\leftrightarrow\beta)\right),
\end{aligned} \tag{4.94}$$

where we have omitted the explicit dependence of $\widehat{f}_{\alpha\beta}$ on k_2 and of $\widehat{h}_{\alpha\beta}$ on k for brevity,

i.e., one should make the replacements

$$\widehat{f}_{\alpha\beta}\to\widehat{f}_{\alpha\beta}(k_2)\,,\qquad \widehat{h}_{\alpha\beta}\to\widehat{h}_{\alpha\beta}(k)\,, \tag{4.95}$$

in (4.94).

Using this method, we may couple the non-local derivative in

$$S = \int d^dx\phi^\dagger D^s\phi + V(|\phi|^2)\,, \tag{4.96}$$

to an external Abelian connection and use this to compute the associated conserved $U(1)$ current immediately,

$$\widehat{J}^{\mu}(-k) = -\int \frac{d^d q_1 d^d q_2}{(2\pi)^d} \frac{\left(-|q_1|^s + |q_2|^s\right)\left(\phi^*(q_2) q_1^{\mu} \phi(q_1) - q_2^{\mu} \phi^*(q_2)\phi(q_1)\right)}{|q_1|^2 - |q_2|^2} \delta(k+q_1+q_2)\,. \tag{4.97}$$

which matches the one-dimensional example. It clear that this method is more powerful in higher dimensions, as the derivation is much simpler.

We can now linearly couple the action (4.1) to an external metric using the covariant derivative $\widetilde{D}^s = D^s + D_1^s + \mathcal{O}(h^2)$. Varying the Maxwell term,

$$S_{\text{Maxwell}} = \frac{1}{4}\int d^d x\, F_{\alpha\beta} D^{s-2} F^{\alpha\beta}\,, \tag{4.98}$$

with respect to the metric we find

$$\begin{aligned}
\widehat{T}^{\mu\nu}_{\text{Maxwell}}(-k) &= \frac{2(2\pi)^d}{\sqrt{\eta}} \frac{\delta}{\delta \widehat{h}_{\mu\nu}(k)} S_{\text{Maxwell}} \\
&= -\frac{1}{4}\int \frac{d^d k_1 d^d k_2 \delta(k+k_1+k_2)}{(2\pi)^d (k_1^2 - k_2^2)} \Big(F_{\alpha\beta}(k_1) F^{\alpha\beta}(k_2) \tau_0^{\mu\nu}(k_1,k_2) + F^{\alpha\mu}(k_1) F_{\alpha}{}^{\nu}(k_2) \tau(k_1,k_2) \\
&\qquad + F^{\beta\alpha}(k_1) F_{\beta}{}^{\nu}(k_2) \tau^{\mu}{}_{\alpha}(k_1,k_2) - F^{\beta\mu}(k_1) F_{\beta}{}^{\alpha}(k_2) \tau^{\nu}{}_{\alpha}(k_1,k_2) \Big)
\end{aligned} \tag{4.99}$$

with

$$\begin{aligned}\tau_0^{\mu\nu} &= k_2^{s-2}(k_1^\nu k_2^\mu + k_1^\mu k_2^\nu + k\cdot k_1\eta^{\mu\nu}) - (k_1 \leftrightarrow k_2)\\ \tau &= -2k_2^{s-2}\left(k^2 + 2k\cdot k_1\right) - (k_1 \leftrightarrow k_2)\\ \tau^\mu{}_\alpha &= 2k_2^{s-2}k_\alpha\left(k_1^\mu - k_2^\mu\right) + (k_1 \leftrightarrow k_2)\ .\end{aligned} \tag{4.100}$$

It is straightforward to compute

$$k_\mu \hat{T}^{\mu\nu}_{\text{Maxwell}}(-k) = \int \frac{d^dk_1 d^dk_2}{(2\pi)^d} k_1^{s-2}\widehat{F}^{\beta\alpha}(k_1)\widehat{F}_\beta{}^\nu(k_2)k_{1\,\alpha}\delta(k+k_1+k_2) \tag{4.101}$$

which vanishes once the equations of motion are satisfied. In obtaining (4.101) we used the Bianchi identity in the form

$$\widehat{F}^{\beta\alpha}(k_1)\widehat{F}_\beta{}^\nu(k_2)k_{1\,\nu} = \frac{1}{2}\widehat{F}_{\beta\nu}(k_1)\widehat{F}^{\beta\nu}(k_2)k_1^\alpha \tag{4.102}$$

and symmetry properties of $\widehat{F}_{\beta\nu}(k_1)\widehat{F}^{\beta\nu}(k_2)$ and $\widehat{F}^{\beta\alpha}(k_1)\widehat{F}_\beta{}^\nu(k_2)$ under exchange of k_1 and k_2, under the integral.

The trace of the energy momentum tensor is given by

$$\eta_{\mu\nu}\widehat{T}^{\mu\nu}_{\text{Maxwell}}(-k) = \int \frac{d^dk_1 d^dk_2}{(2\pi)^d}\delta(k+k_1+k_2) \left(\frac{|k_1|^{s-2}-|k_2|^{s-2}}{k_1^2-k_2^2}k^\mu \widehat{F}_{\alpha\mu}(k_1)\widehat{F}^\alpha{}_\nu(k_2)k^\nu - \frac{1}{4}\widehat{F}_{\alpha\beta}(k_1)\widehat{F}^{\alpha\beta}(k_2)\widetilde{\tau}(k_1,k_2)\right) \tag{4.103}$$

where

$$\widetilde{\tau}(k_1,k_2) = \frac{(d-4)\left(k_2^{s-2}k\cdot k_1 - k_1^{s-2}k\cdot k_2\right) + 2(k_1^{s-2}-k_2^{s-2})(2k^2-k_1\cdot k_2)}{k_1^2-k_2^2}\,. \tag{4.104}$$

Scale invariance of the Maxwell action will follow if

$$\int \eta_{\mu\nu}T^{\mu\nu}_{\text{Maxwell}}(x)d^dx = 0 \tag{4.105}$$

under the equations of motion. Expanding $\widetilde{\tau}$ at small k and using $k_1^\mu = -k^\mu - k_2^\mu$, we find

$$\tilde{\tau}(-k-k_2,k_2) = (s+2-d)k_2^{s-2} + \frac{1}{2}(s-2)(s+2-d)k_2^{s-4}\,k\cdot k_2 + \mathcal{O}(k^2)\,. \tag{4.106}$$

Thus,

$$\eta_{\mu\nu}\widehat{T}^{\mu\nu}_{\text{Maxwell}}(0) = -\frac{i}{2}\int \frac{d^d k_2}{(2\pi)^d}(s+2-d)k_2^{s-2}k_2^{\alpha}\widehat{A}^{\beta}(-k_2)\widehat{F}_{\alpha\beta}(k_2) = 0 \qquad (4.107)$$

under the equations of motion, implying that the Maxwell action is scale invariant for any value of s, as expected for a free theory.

In the special case of $d = s+2$ the leading terms in (4.106) vanishes. Since $\frac{|k+k_2|^{s-2}-|k_2|^{s-2}}{(k+k_2)^2-k_2^2}$ and $\frac{\widetilde{\tau}}{k^2}$ are finite at small k, we write

$$\eta_{\mu\nu}\widehat{T}^{\mu\nu}_{\text{Maxwell}}(-k) = k^{\mu}k^{\nu}\int \frac{d^d k_1 d^d k_2}{(2\pi)^d}\delta(k+k_1+k_2) \left(\frac{|k_1|^{s-2}-|k_2|^{s-2}}{k_1^2-k_2^2}\widehat{F}_{\alpha\mu}(k_1)\widehat{F}^{\alpha}{}_{\nu}(k_2) - \frac{\eta_{\mu\nu}}{4}\widehat{F}_{\alpha\beta}(k_1)\widehat{F}^{\alpha\beta}(k_2)\frac{\widetilde{\tau}(k_1,k_2)}{k^2}\right) \qquad (4.108)$$

implying that the real space expression for $\eta_{\mu\nu}T^{\mu\nu}_{\text{Maxwell}}$ is a double derivative and that the free Maxwell theory is conformally invariant.

Equation (4.106) establishes that the free Maxwell theory stress tensor is traceless upon adding an appropriate improvement term. Thus, the Gaussian theory described by (4.1) with $e = 0$ is conformally invariant; one can use the traceless stress tensor to construct currents associated with scale invariance and special conformal transformations which will be conserved. In the interacting theory, $e \neq 0$, but the trace of the stress tensor will likely

receive contributions which can be repackaged in terms of a beta of function, $\beta(e)$ (see, e.g., [106,78,6,117]), which we know vanishes. Thus, the interacting theory is also expected to be conformally invariant.

4.4 Unitarity and the non-local optical theorem

It is challenging to determine whether time evolution is unitary in non-local field theories. We've shown that the $d = s + 2$ theories with d odd are conformally invariant. Since the field strength has dimension $\frac{1}{2}(d - s + 2)$, it violates the unitarity bound $\frac{1}{2}(d - s + 2) \geq \max(2, d - 2)$ [100,102] whenever $d > 4$. Thus, at least for $d = s + 2$ and $d \geq 5$, we expect that time evolution is not unitary. For other values of d and s unitarity is more difficult to address.

In what follows, we will study the unitarity of a local photon on $\mathbb{R}^{2,1} \times \mathbb{R}_+$ coupled to charged fermions on the $\mathbb{R}^{2,1}$ boundary. The effective action for obtaining S-matrix elements of boundary states can be obtained from a non-local action of the type given in (4.1) with $d = 3$ and $s = 1$. An earlier exploration of unitarity in non-local field theories using the optical theorem can be found in [98].

The theory defined on $\mathbb{R}^{2,1} \times \mathbb{R}_+$ is clearly unitary, and all S-matrix elements are expected to satisfy the optical theorem. Indeed, as we will show by an explicit example below, the optical theorem is satisfied due to the possibility of boundary to bulk scattering pro-

cesses. A non-local theory that reproduces only boundary to boundary S-matrix elements does not allow for such processes.

Consider the Lorentzian action

$$S = -\frac{1}{4}\int d^4x\, F_{mn}F^{mn} + \int d^3x\, \bar{\psi}\left(i\partial\!\!\!/ - eA\!\!\!/\right)\psi\,, \tag{4.109}$$

where now we use the conventions of[111] for the signature of the metric and for solutions to the Dirac equation (adopted to $2+1$ dimensions). We use lower case roman indices $m,\ n$ to denote bulk quantities and greek indices, $\mu,\ \nu$ to denote boundary ones.

An explicit expression for the photon propagator, $G_{mn}(x^\mu, x^3)$, can be obtained using the method of images. For Neumann boundary conditions, the Greens function will be a sum of Greens functions for photons on $\mathbb{R}^{3,1}$ with equal mirror charges. Near the boundary, we have

$$G_{mn}(x^\mu,\ x^3=0) = \int \frac{d^4k}{(2\pi)^4}\frac{-2i\eta_{mn}}{k_m k^m + i\epsilon}e^{-ik_\mu x^\mu}\,, \tag{4.110}$$

where the factor of 2 is a result of the image charge necessary to generate Neumann boundary conditions. Since all the vertices are on the boundary it is convenient to integrate over the bulk momenta. We find

$$G_{mn}(x^\mu,\ x^3=0) = \int \frac{d^3k}{(2\pi)^3}\frac{i\eta_{mn}e^{-ik_\mu x^\mu}}{\sqrt{-k_\mu k^\mu - i\epsilon}}\,. \tag{4.111}$$

The resulting Feynman rules for computing S-matrix elements for boundary incoming and outgoing particles can be found in figure 4.3.

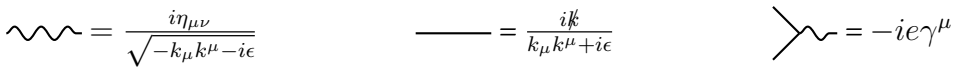

Figure 4.3: Feynman rules for the action (4.109).

The optical theorem in the presence of a boundary is almost identical to the one in its absence. Decomposing the S-matrix into $S = 1 + iT$, unitarity of time evolution implies that $-i(T - T^\dagger) = T^\dagger T$. The Feynman rules (4.3) imply that momentum is conserved in directions parallel to the boundary so that we can write $\langle p_o|iT|p_i\rangle = (2\pi)^3\delta^{(3)}(p_o - p_i)i\mathcal{M}(p_i \to p_o)$ with p_o and p_i the outgoing and incoming momenta. Likewise, we find that $\langle p|iT|p\rangle = (2\pi)^3\delta^{(3)}(p - p_i)i\mathcal{M}(p_i \to p)$ where p_i is the incoming momenta of a particle located at the boundary and p the momentum of an outgoing bulk particle. Note that the momentum-conserving delta function is insensitive to the bulk component of the momenta of the outgoing particles. That is, since the interaction term has support only at the boundary, momentum is not conserved in the direction transverse to it. Thus, we have

$$2\text{Im}\mathcal{M}(p_i \to p_o) = \sum_p \int d\Pi_p \mathcal{M}^* (p_o \to p)\, \mathcal{M}(p_i \to p)\, (2\pi)^3\delta^{(3)}(p_i - p) \quad (4.112)$$

where the sum on the right-hand side is over all appropriately normalized momenta and internal degrees of freedom of intermediate particles.

Let us focus our attention on the tree level electron-positron (Bhabha) t-channel scattering amplitude depicted in the left panel of figure 4.4. The optical theorem (4.112) implies

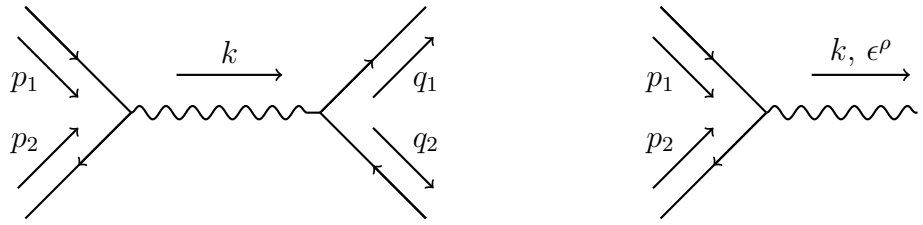

Figure 4.4: Feynman diagrams. (Left) Tree level amplitude for t-channel electron positron scattering. (Right) decay of charged fermions into a (bulk) photon with polarization vector ϵ^ρ.

that

$$2\mathrm{Im}\mathcal{M}_{\rangle\!\!-\!\!\langle}\left(p_1,\, p_2 \to q_1,\, q_2\right) = \sum_{\rho,\,\sigma} \eta_{\rho\sigma} \int \frac{d\vec{k}}{(2\pi)^3} \frac{2}{2E_k} \mathcal{M}^{\sigma\,*}_{\rangle\!\!-\!\!\rangle}\left(q_1,\, q_2 \to k\right) \mathcal{M}^{\rho}_{\rangle\!\!-\!\!\langle}\left(p_1,\, p_2 \to k\right)$$
$$\times\, (2\pi)^3 \delta^{(3)}\left(p_1 + p_2 - k\right)\ , \quad (4.113)$$

where $E_k^2 = |\vec{k}|^2$ and we remind the reader that the momentum conserving delta function has support on the three boundary spacetime directions while the integral is over the three bulk spatial directions. The unusual factor of 2 in the integration measure comes about due to the unconventional factor of 2 in the photon propagator.

Using the Feynman rules from figure 4.3, we find

$$
\begin{aligned}
i\mathcal{M}_{\nearrow\!\!\!\!\!\!\searrow}\left(p_1,\, p_2 \to q_1,\, q_2\right) &= -e^2 u(p_1)\gamma^\mu \bar{v}(p_2) v(q_1)\gamma^\nu \bar{u}(q_2) \frac{i\eta_{\mu\nu}}{\sqrt{-k_\alpha k^\alpha}}\bigg|_{k^\alpha = p_1^\alpha + p_2^\alpha} \\
i\mathcal{M}^\rho_{\nearrow\!\!\!\!\!\!\searrow}\left(p_1,\, p_2 \to k\right) &= -ieu(p_1)\gamma^\mu \bar{v}(p_2)\epsilon^{\rho\,*}_\mu(k)\,.
\end{aligned}
\tag{4.114}
$$

A straightforward computation yields

$$
\begin{aligned}
\sum_{\rho,\,\sigma}\eta_{\rho\sigma}\int \frac{d\vec{k}}{(2\pi)^3}\frac{2}{2E_k}\mathcal{M}^{\sigma\,*}_{\nearrow\!\!\!\!\!\!\searrow}\left(q_1,\, q_2 \to k\right)\mathcal{M}^\rho_{\nearrow\!\!\!\!\!\!\searrow}\left(p_1,\, p_2 \to k\right)(2\pi)^3\delta^{(3)}\left(p_1+p_2-k\right) & \\
= -\Phi\int\frac{d\vec{k}}{E_k}\delta(p_1^0+p_2^0-\sqrt{k_1^2+k_2^2+k_3^2})\delta(p_1^1+p_2^1-k_1)\delta(p_1^2+p_2^2-k_2) & \\
= \begin{cases} -\frac{2\Phi}{\sqrt{k_\alpha k^\alpha}}\Big|_{k^\alpha=p_1^\alpha+p_2^\alpha} & (p_1+p_2)^2 > 0 \\ 0 & (p_1+p_2)^2 < 0 \end{cases}, &
\end{aligned}
\tag{4.115}
$$

where we have defined

$$
\Phi = e^2 u(p_1)\gamma^\mu \bar{v}(p_2) v(q_1)\gamma^\nu \bar{u}(q_2)\eta_{\mu\nu}\,. \tag{4.116}
$$

Equation (4.113) now follows. We get a hint why the optical theorem could hold in a bulk-

boundary picture: at the first glance, it is a bit of tautology

$$\text{If} \qquad 2\text{Im}\mathcal{M} = |\mathcal{M}|^2 \qquad \text{then} \qquad \int \frac{dp^d}{2\pi} 2\text{Im}\mathcal{M} = \int \frac{dp^d}{2\pi} |\mathcal{M}|^2 \tag{4.117}$$

If the optical theorem holds for a bulk theory, it holds for the boundary theory because that amounts to integrating out the perpendicular momentum on both sides. One could have worked with the full propagator and integrate p^d in the very last step as above. If the bulk theory is still unitary with a mass (the mass being $(p^d)^2$) and if this integration and the theorem commute, then we will always get the optical theorem on the boundary. Adding a mass term usually does not ruin the unitarity. The real question is that whether the optical theorems survive the integration of the perpendicular momentum. We can give another example involving loops. But currently, a comprehensive proof is still lacking.

We consider the diagram representing the one-loop correction to the fermion propagator. The inner product of cut diagrams is ($k = (k^0, 0, 0, ...)$) (using p_3 to denote the photon momentum; p_3^d to denote the perpendicular momentum component; p_4 to denote the

fermion momentum) ($\sum_{\text{spins}} \epsilon^* \gamma^\mu u(p_4)\bar{u}(p_4)\gamma^\nu \epsilon = -\gamma^\mu \not{p}_4 \gamma_\mu = (d-2)\not{p}_4$)

$$
\begin{aligned}
&(-i)^*(-i)\int \frac{d^{d+1}p_3}{(2\pi)^{d+1}}\int \frac{d^d p_4}{(2\pi)^d} 2\pi\delta(p_3^2)2\pi\delta(p_4^2)\sum_{\text{spins}}(..)(2\pi)^d\delta^d(p_3+p_4-k)\\
&=\int \frac{d^d\vec{p_3}}{(2\pi)^d}\int \frac{d^{d-1}\vec{p_4}}{(2\pi)^{d-1}}\frac{1}{4E_3E_4}(d-2)\not{p}_4(2\pi)^d\delta^{d-1}(\vec{p_3}'+\vec{p_4})\delta(E_3+E_4-k^0)\\
&=\int \frac{d^d\vec{p_3}}{(2\pi)^d}\frac{1}{4\sqrt{(\vec{p_3}')^2+(p_3^d)^2}\sqrt{(\vec{p_3}')^2}}2\pi\delta\Big(\sqrt{(\vec{p_3}')^2+(p_3^d)^2}+\sqrt{(\vec{p_3}')^2}-k^0\Big)(d-2)\not{p}_4
\end{aligned}
\tag{4.118}
$$

where p_3 is the bulk photon momentum, p_4 is the boundary fermion momentum and $\vec{p_3}'$ is the spatial components of photon momentum that are one the boundary. Now we can see that the integral will be zero if $\sqrt{(\vec{p_3}')^2+(p_3^d)^2}+\sqrt{(\vec{p_3}')^2}-k^0$ cannot be zero for real p_3^d, that is

$$
(\sqrt{(\vec{p_3}')^2}-k^0)^2-\sqrt{(\vec{p_3}')^2}=(k^0)^2-2k^0\sqrt{(\vec{p_3}')^2}<0 \tag{4.119}
$$

So, when the integral is not zero, we have $k^0 > 2\sqrt{(\vec{p_3}')^2}$ and therefore

$$
\begin{aligned}
&\int \frac{d^d\vec{p_3}}{(2\pi)^d}\frac{1}{4\sqrt{(\vec{p_3}')^2+(p_3^d)^2}\sqrt{(\vec{p_3}')^2}}2\pi\frac{\sqrt{(\vec{p_3}')^2+(p_3^d)^2}}{p_3^d}\delta(|p_3^d|-q)(d-2)\not{p}_4\\
&=\int \frac{d^{d-1}\vec{p_3}'}{(2\pi)^{d-1}}\frac{1}{4(k^0-\sqrt{(\vec{p_3}')^2})\sqrt{(\vec{p_3}')^2}}\frac{2(k^0-\sqrt{(\vec{p_3}')^2})}{\sqrt{(k^0-\sqrt{(\vec{p_3}')^2})^2-(\vec{p_3}')^2}}(d-2)\not{p}_4\\
&=\int \frac{d^{d-1}p}{(2\pi)^{d-1}}\frac{1}{2p\sqrt{(k^0)^2-2k^0p}}(d-2)\gamma\cdot(p,-\vec{p})
\end{aligned}
\tag{4.120}
$$

To do this integral, let's restrict to $d=3$ and see that the spatial parts give zero. The time

part is then

$$\frac{\gamma^0}{4\pi}\int_0^\infty dp\frac{p}{\sqrt{(k^0)^2-2k^0p}}=\frac{1}{12\pi}\gamma^0k^0=\frac{\not{k}}{12\pi} \tag{4.121}$$

In order to evaluate this divergent integral, we used the dimensional regularization.

$$\begin{aligned}\frac{1}{4\pi}\int_0^\infty dp\frac{p^{d-2}}{\sqrt{(k^0)^2-2k^0p}}=&\frac{\sqrt{k^2}2^{-d-1}(-k)^{d-3}\Gamma\left(\frac{3}{2}-d\right)\Gamma(d-1)}{\pi^{3/2}}\\ =&\frac{\sqrt{k^2}}{12\pi}\text{ when }d\to 3\end{aligned} \tag{4.122}$$

If the external momentum k is space-like, we can choose $k=(0,k^1,0,...)$ and show that $|\mathcal{M}|^2=0$ because of kinematic reasons.

Computing the imaginary part of the loop: treating $(p^d)^2$ like a mass term and integrating it out later. In such case, we can do Wick rotations.

$$i\mathcal{M}=(-i)^2\int\frac{dp^d}{2\pi}\int\frac{d^dp}{(2\pi)^d}\frac{\gamma^\mu i(\not{p}-\not{k})\gamma^\nu}{(p-k)^2+i\epsilon}\frac{-ig_{\mu\nu}}{p^2-p^{d2}+i\epsilon} \tag{4.123}$$

If doing the dp^d integral first, we would get the non-local photon propagator. Here we will

perform the $d^d p$ integral first and integrate p^d out at an appropriate time.

$$\begin{aligned}\mathcal{M} =& i\int \frac{dp^d}{2\pi}\int \frac{d^d p}{(2\pi)^d}\frac{\gamma^\mu(\not{p}-\not{k})\gamma^\nu}{(p-k)^2+i\epsilon}\frac{g_{\mu\nu}}{p^2-p^{d^2}+i\epsilon}\\ =& i\int \frac{dp^d}{2\pi}\int \frac{d^d p}{(2\pi)^d}\int_0^1 dx\frac{(2-d)(\not{p}-\not{k})}{(p^2-2xkp+xk^2-(1-x)p^{d^2})^2}\\ =& i\int \frac{dp^d}{2\pi}\int_0^1 dx\int \frac{d^d l}{(2\pi)^d}\frac{(2-d)(\not{l}-(1-x)\not{k})}{(l^2+x(1-x)k^2-(1-x)p^{d^2})^2}\end{aligned} \tag{4.124}$$

We have changed the variable $p = l + xk$. Now we can Wick rotate l and obtain this standard integral. Note that $-x(1-x)k^2+(1-x)p^{d^2} > 0$.

$$\begin{aligned}\mathcal{M} =& i\int \frac{dp^d}{2\pi}\int_0^1 dx\int \frac{d^d l}{(2\pi)^d}\frac{(2-d)(\not{l}-(1-x)\not{k})}{(l^2+x(1-x)k^2-(1-x)p^{d^2})^2}\\ =& i\int \frac{dp^d}{2\pi}\int_0^1 dx\frac{-i(1-x)(2-d)\not{k}}{(4\pi)^{d/2}}\frac{\Gamma(2-\frac{d}{2})}{\Gamma(2)}(-x(1-x)k^2+(1-x)p^{d^2})^{\frac{d}{2}-2}\end{aligned} \tag{4.125}$$

We see that this expression is completely real if $k^2 < 0$. So $2\mathrm{Im}\mathcal{M} = 0 = |\mathcal{M}|^2$. What's less non-trivial is the case when k is time-like. Because $k^2 > 0$, $-x(1-x)k^2+(1-x)p^{d^2}$ can be negative. We still say that the $d^d l$ integral in (4.125) gives the same result even when $-x(1-x)k^2+(1-x)p^{d^2} < 0$, as the result of analytic continuation. Now $\mathcal{M}$ has a finite

imaginary part: (using dimreg $d = 3 + \epsilon$)

$$\begin{aligned}\mathcal{M} &= \int_0^1 dx \int \frac{dp^d}{2\pi} \frac{(1-x)(2-d)\not{k}}{(4\pi)^{d/2}} \frac{\Gamma(2-\frac{d}{2})}{\Gamma(2)} (-x(1-x)k^2 + (1-x)p^{d^2})^{\frac{d}{2}-2} \\ &= \int_0^1 dx (1-x)(2-d)\not{k} \frac{2^{-d-1}\pi^{-\frac{d}{2}-\frac{1}{2}} k^{d-3} (1-x)^{\frac{d-4}{2}} x^{\frac{d-3}{2}} \left(-\sec\left(\frac{\pi d}{2}\right) + e^{\frac{i\pi d}{2}}\right) \Gamma\left(2-\frac{d}{2}\right) \Gamma\left(\frac{d}{2}-1\right)}{\Gamma\left(\frac{d-1}{2}\right)} \\ &= \int_0^1 dx (1-x)\not{k} \frac{2^{-\epsilon-4}\pi^{-\frac{\epsilon}{2}-1} k^{\epsilon} (1-x)^{\frac{\epsilon-1}{2}} x^{\epsilon/2} \left(\cot\left(\frac{\pi\epsilon}{2}\right) + i\right)}{\Gamma\left(\frac{\epsilon}{2}+1\right)}\end{aligned} \tag{4.126}$$

The real part is divergent and we drop that. The imaginary part is finite and we can set $\epsilon = 0$ here:

$$\begin{aligned}\text{Im}\mathcal{M} &= \int_0^1 dx (1-x)\not{k} \frac{1}{16\pi\sqrt{1-x}} \\ &= \frac{\not{k}}{24\pi}\end{aligned} \tag{4.127}$$

Now we can see this is exactly a half of (4.121). Therefore, the optical theorem holds and reads:

$$2\text{Im}\mathcal{M} = \begin{cases} \frac{\not{k}}{12\pi}, & k^2 > 0 \\ 0, & k^2 < 0 \end{cases} = |\mathcal{M}|^2 \tag{4.128}$$

We have also checked that this same mechanism applies to the effective description of the long-range Ising model which may be captured by an action describing a free bulk scalar field with a ϕ^4 interaction on the boundary. We have the boundary propagator being

$$\int_{-\infty}^{\infty} \frac{dk^d}{2\pi} \frac{i}{k^2 - k^{d^2} + i\epsilon} = \frac{1}{2\sqrt{k^2 + i\epsilon}} \tag{4.129}$$

For a 3 to 3 tree level scattering, the LHS is

$$2\text{Im}\mathcal{M} = 2\text{Im}\frac{1}{i}(-i)^2\frac{1}{2\sqrt{k^2+i\epsilon}} = \begin{cases} \frac{1}{k}, & k^2 > 0 \\ 0, & k^2 < 0 \end{cases} \tag{4.130}$$

The RHS is

$$\begin{aligned} &(-i)^*(-i)\int \frac{d^{d+1}p}{(2\pi)^{d+1}}2\pi\delta(p^2)(2\pi)^d\delta^d(p-k) \\ &= \begin{cases} \int \frac{dp^d}{(2\pi)}\frac{1}{2|p^d|}(2\pi)\delta(|p^d|-k^0) = \frac{1}{k}, & k^2 > 0 \\ 0, & k^2 < 0 \end{cases} \end{aligned} \tag{4.131}$$

The optical theorem holds.

5

A glimpse of the monodromy defect

We have seen the connection between non-local theories and boundary (codimension one) theories in the introduction chapter and in the previous chapter. In general, one could consider more than one perpendicular momentum, or higher codimensional defects. Conformal defects have gained more attention recently[12,44,89,91,63,76,90,94,67]. A conformal defect of codimension q in a d-dimensional space is a $(d-q)$-dimensional flat or spherical subspace

that preserves a $SO(q) \times SO(d-q+1,1)$ subgroup of the original $SO(d+1,1)$ symmetry group. In this chapter, we provide a quick introduction to the $q = 2$ defect defined by a monodromy

$$\phi(r, \theta + 2\pi, \vec{y}) = \phi^g(r, \theta, \vec{y}) \tag{5.1}$$

where y are the coordinates on the defect, r and θ are the perpendicular coordinates, and g is an element in a global group G acting on the fundamental field ϕ in the theory. For a free scalar field and $3d$ Ising model, $G = Z_2$. Such a monodromy defect in the 3d Ising model (where it is a line defect) was introduced in [11,45], and further studied in [131,94].

A codimension two defect may also be studied by mapping the problem to a hyperbolic cylinder, $S^1 \times H^{d-1}$ (for previous examples of conformal mapping to $H^m \times S^n$ spaces to describe conformal defects, see e.g. [80,73,44,105]). A flat defect in flat space can be related by a Weyl transformation to $S^1 \times H^{d-1}$ as follows

$$ds^2_{\mathbb{R}^d} = r^2 \left(\frac{(d\vec{y})^2 + dr^2}{r^2} + d\theta^2 \right) = r^2 ds^2_{S^1 \times H^{d-1}} \tag{5.2}$$

with $\vec{y}$ and r being the Poincaré coordinates on H^{d-1} and θ being the coordinate on S^1. The monodromy defect is then simply described by imposing twisted periodicity conditions (5.1) along S^1 in the path integral for the theory on $S^1 \times H^{d-1}$ (for instance, in the Z_2 case, this just means taking the scalar to be antiperiodic on S^1). The defect is located at

$r = 0$, which is the boundary of the hyperbolic space. The hyperbolic cylinder setup that we use here is similar to that used in [84,23,24] to study Renyi entropies for a spherical entangling region.* Starting with the theory on $S^1 \times H^{d-1}$, one can then perform a Kaluza-Klein reduction on S^1 to obtain a tower of massive fields on H^{d-1} with the defect theory on its boundary. Standard techniques from the AdS/CFT literature may then be used to obtain results for the defect CFT data. For example, the scaling dimensions of the defect operators can be related to the masses on H^{d-1}. Other examples of defect CFT data may also be extracted conveniently from the hyperbolic space setup, and we will discuss a few explicit such calculations below. Similar ideas have been used in the literature for boundaries in conformal field theory in [108,22,66,65,49] and for higher codimension defects in [105]. Field theory on a hyperbolic cylinder was also studied in [1,114].

A monodromy defect with spherical geometry may be described in the same way by simply using, instead of the Poincaré metric in (5.2), the hyperbolic ball metric for H^{d-1}, so that the boundary is the sphere S^{d-2}. For a spherical defect, it is natural to define its expectation value $\langle \mathcal{D} \rangle$. In the hyperbolic space setup, this expectation value can be obtained in terms of the free energy of the twisted theory on $S^1 \times H^{d-1}$ as

$$-\log\langle \mathcal{D} \rangle = F_{\text{twisted}} - F_{\text{untwisted}} \tag{5.3}$$

*In that case, rather than a twisted periodicity condition, one lets the inverse temperature, i.e., the length of S^1, be $2\pi q$ to describe the qth Renyi entropy. This setup can also be thought of in terms of defect CFT, as discussed in [73].

where F_{twisted} and $F_{\text{untwisted}}$ are the free energies on $S^1 \times H^{d-1}$ in the presence and absence of a monodromy defect respectively. The subtraction of the untwisted theory free energy corresponds to normalizing $\langle \mathcal{D} \rangle$ by the partition function of the theory without defect.

In this chapter, we consider more generally conformal field theories consisting of N scalars that preserve an $O(N)$ symmetry, so $G = O(N)$. We discuss both free and interacting $O(N)$ model, using the large N and ϵ expansions. Already in the free theory, the structure is richer compared to the case of a single free scalar.

5.1 Monodromy defects in free theory

Consider an $O(N)$ symmetric theory of N free scalars in flat space. The most general monodromy defect that we can define imposes that the scalars satisfy[119]

$$\phi^I(r, \theta + 2\pi, \vec{y}) = G^{IJ}\phi^J(r, \theta, \vec{y}), \qquad G^{IJ} \in O(N). \tag{5.4}$$

The most general $O(N)$ matrix G^{IJ}, can always, by a change of basis, be brought to the following form

$$G^{IJ}(\vartheta) = \begin{bmatrix} R(\vartheta_1) & & & & \\ & \ddots & & 0 & \\ & & R(\vartheta_k) & & \\ & & & \pm 1 & \\ & 0 & & & \ddots \\ & & & & & \pm 1 \end{bmatrix}, \qquad R(\vartheta) = \begin{bmatrix} \cos\vartheta & -\sin\vartheta \\ \sin\vartheta & \cos\vartheta \end{bmatrix}. \tag{5.5}$$

So there are k pair of scalars that mix into each other and the rest either remain unchanged or pick up a minus sign as they go around the defect. We can then combine each pair into a complex combination $\Phi = \phi^1 + i\phi^2$ and the monodromy can be represented as

$$\Phi(r, \theta + 2\pi, \vec{y}) = e^{i\vartheta}\Phi(r, \theta, \vec{y}), \qquad \vartheta \sim \vartheta + 2\pi. \tag{5.6}$$

Hence $\vartheta = 0$ describes the trivial defect while $\vartheta = \pi$ describes the special case when the two fields change a sign as they go around the defect. So in the rest of this section, we will consider a single complex scalar with the monodromy defined in (5.6). It has a $U(1) \sim$

$SO(2)$ internal symmetry [†] which is enhanced to $O(2)$ for $\vartheta = 0$ and π ($\Phi \to \bar{\Phi}$, which is a part of $O(2)$ but not $SO(2)$, is also a symmetry for these values of ϑ). One may combine these complex scalars with different ϑ's to obtain results for free $O(N)$ model with a general monodromy defect (for each minus sign in the monodromy matrix (5.5), one can simply set $\vartheta = \pi$ in the result for a complex scalar below, and include an extra factor of $1/2$ to describe a real component instead of a complex one). To make the expressions less cluttered, we define $v = \vartheta/2\pi$ and use either v or ϑ, whichever is convenient. There is a periodicity in v which implies that everything should be invariant under $v \to v + 1$, but for many calculations, we will fix the range of v to be $0 \leq v < 1$. We will write expressions specializing to this range of v, so they may not look periodic in v.

In a conformal field theory with a defect, in addition to the usual short distance OPE in the bulk, a bulk operator can also be expanded in terms of operators living on the defect. For the complex scalar with monodromy given by (5.6), it takes the following form [12,45]

$$\Phi(r,\theta,\vec{y}) = \sum_O C_O^\Phi \frac{e^{is_O\theta}}{r^{\Delta_\Phi - \Delta_O}} \mathcal{B}_{\Delta_O}(r,\vec{\partial}_y) O(\vec{y}), \qquad s_O \in \mathbb{Z} + v. \tag{5.7}$$

As we mentioned in the introduction, $SO(2)$ symmetry of rotations around the defect acts as a global symmetry on the defect. s_O is the charge of the operator O under this global

[†] Not to be confused with the group of rotations around the defect, which is a spacetime symmetry in the bulk and is also $SO(2)$.

symmetry and we will call it transverse spin or just spin. There is also a longitudinal spin l, which is the charge under rotations along the defect, but we will only consider $l = 0$ defect operators in this paper. The remaining conformal invariance fixes the bulk-defect two point function

$$\langle \Phi(x_1)\bar{O}(\vec{y}_2)\rangle = \frac{C_O^{\Phi}\mathcal{C}_{\Delta_O}e^{i\theta s_O}}{r^{\Delta_\Phi-\Delta_O}(r^2+(\vec{y}_{12})^2)^{\Delta_O}} \tag{5.8}$$

where $\bar{O}$ is a defect operator that has spin $-s_O$ and dimension Δ_O. Consistency of (5.7) and (5.8) fixes the form of the function $\mathcal{B}_s(r,\vec{\partial}_y)$

$$\mathcal{B}_{\Delta_O}(r,\vec{\partial}_y) = \sum_{m=0}^{\infty}\frac{(-1)^m r^{2m}(\vec{\partial}_y^2)^m}{m!2^{2m}\left(\Delta_O+2-\frac{d}{2}\right)_m}. \tag{5.9}$$

This is similar to what was done for BCFT in [99]. In general, there could be several defect operators of a given spin. But since Φ is a free field, it satisfies the bulk equation of motion $\nabla^2\Phi = 0$, which implies

$$\begin{aligned}&\left(\frac{\partial^2}{\partial r^2}+\frac{1}{r}\frac{\partial}{\partial r}+\frac{1}{r^2}\frac{\partial^2}{\partial\theta^2}+\frac{\partial^2}{\partial\vec{y}_1^2}\right)\langle\Phi(x_1)\bar{O}(\vec{y}_2)\rangle = 0\\ &\implies \Delta_O = \Delta_\Phi \pm |s_O| = \frac{d}{2}-1\pm|s_O|.\end{aligned} \tag{5.10}$$

The unitarity bound for the CFT on the defect requires the dimensions of the defect operator to satisfy

$$\Delta_O \;\geq\; \max\left(\frac{d}{2}-2,0\right). \tag{5.11}$$

This is always satisfied for the positive sign above (as long as $d > 2$) and we defer the discussion of negative sign until next section. So for every spin, there is a single operator on the defect with dimension $\Delta_s = d/2 - 1 + |s|$. Hence, the bulk-defect OPE of the fundamental fields may be written as a sum over spins

$$\begin{aligned}\Phi(r,\theta,\vec{y}) &= \sum_{s\in\mathbb{Z}+v} C_s^{\Phi} \frac{e^{is\theta}}{r^{\Delta_\Phi-\Delta_s}} \mathcal{B}_s(r,\vec{\partial}_y)\Psi_s(\vec{y}) \\ \bar{\Phi}(r,\theta,\vec{y}) &= \sum_{s\in\mathbb{Z}+v} (C_s^{\Phi})^* \frac{e^{-is\theta}}{r^{\Delta_\Phi-\Delta_s}} \mathcal{B}_s(r,\vec{\partial}_y)\bar{\Psi}_s(\vec{y}).\end{aligned} \tag{5.12}$$

In terms of original real scalar fields, $\Psi_s = \psi_s^1 + i\psi_s^2$ while $\bar{\Psi}_s = \bar{\psi}_s^1 - i\bar{\psi}_s^2 = \psi_{-s}^1 - i\psi_{-s}^2$ where ψ_s^i appear in the bulk-defect OPE of the real scalars ϕ^i.

In the presence of a defect, the two-point function of bulk scalars is fixed up to a function of cross-ratios[12,94]

$$\langle \Phi(x_1)\bar{\Phi}(x_2)\rangle = \frac{\mathcal{F}(\theta_{12},\xi)}{(r_1 r_2)^{\frac{d}{2}-1}}, \qquad \theta_{12} = \theta_1 - \theta_2, \qquad \xi = \frac{(\vec{y}_1-\vec{y}_2)^2 + (r_1-r_2)^2}{4r_1 r_2}. \tag{5.13}$$

Corresponding to the two OPE limits (i.e. the bulk OPE and the bulk-defect OPE), the function $\mathcal{F}$ can be expanded into bulk and defect channel conformal blocks

$$\mathcal{F}(\theta_{12},\xi) = \sum_{\mathcal{O}} C_{\bar{\Phi};\Phi;}{}^{\mathcal{O}} C_1^{\mathcal{O}} g_{\Delta_\mathcal{O},J_\mathcal{O}}(\theta_{12},\xi) = \sum_{O} |C_O^{\Phi}|^2 f_{\Delta_O,s_O}(\theta_{12},\xi) \tag{5.14}$$

where g and f are the bulk channel and defect channel conformal blocks respectively. The sum on the left runs over the bulk operators that get a non-zero one-point function, and the coefficient is the product of the usual bulk OPE coefficient times the one-point function coefficient of the bulk operator. The sum on the right runs over the defect operators that appear in the bulk-defect OPE of Φ.

As we determined above, the operators appearing in the defect channel have spin s and dimension $\Delta_s = d/2 - 1 + |s|$. The defect channel blocks are known in general[12,94]. For the case of a codimension two defect, they simplify and the resulting expression for the two-point function can be written as a sum over defect operators

$$\langle \Phi(x_1)\bar{\Phi}(x_2)\rangle = G_{\bar{\Phi}\Phi}(x_1,x_2) = \sum_{s\in\mathbb{Z}+v} \frac{\Gamma\left(\Delta_s\right) e^{is\theta_{12}}\, {}_2F_1\left(\Delta_s, \Delta_s+\frac{3-d}{2}; 2\Delta_s+3-d; -\frac{1}{\xi}\right)}{2(r_1 r_2)^{\frac{d}{2}-1}\pi^{d/2}\Gamma(\Delta_s+2-\frac{d}{2})(4\xi)^{\Delta_s}}. \tag{5.15}$$

The sum can be explicitly performed in $d=4$ to get

$$\begin{aligned}\langle \Phi(x_1)\bar{\Phi}(x_2)\rangle &= \sum_{s\in\mathbb{Z}+v} \frac{e^{is\theta_{12}}}{8\pi^2 r_1 r_2\sqrt{\xi(1+\xi)}(\sqrt{1+\xi}+\sqrt{\xi})^{2\Delta_s-2}} \\ &= \frac{(\xi(1+\xi))^{-1/2}}{8\pi^2 r_1 r_2}\left(\frac{e^{i\theta_{12}v}\left(\sqrt{\xi}+\sqrt{\xi+1}\right)^{2v}}{-1+e^{i\theta_{12}}\left(2\xi+2\sqrt{\xi(1+\xi)}+1\right)} + \frac{e^{i\theta_{12}v}\left(\sqrt{\xi}+\sqrt{\xi+1}\right)^{2-2v}}{-e^{i\theta_{12}}+2\xi+2\sqrt{\xi(1+\xi)}+1}\right).\end{aligned} \tag{5.16}$$

Note that we are using a normalization, such that in the bulk OPE limit, when $x_1 \to x_2$,

the correlator goes like

$$\langle \Phi(x_1)\bar{\Phi}(x_2)\rangle \sim \frac{\Gamma\left(\frac{d}{2}-1\right)}{2\pi^{d/2}}\frac{1}{|x_1-x_2|^{d-2}}. \tag{5.17}$$

We normalize defect operators such that $C_s^{\Phi} = 1$ in the free theory. The two-point function of the defect operators is then given by

$$\langle \Psi_{s_1}(\vec{y}_1)\bar{\Psi}_{s_2}(\vec{y}_2)\rangle = \frac{\delta_{s_1,s_2}\mathcal{C}_{\Delta_{s_1}}}{(\vec{y}_{12}^2)^{\Delta_{s_1}}}, \qquad \mathcal{C}_{\Delta_{s_1}} = \frac{\Gamma\left(\Delta_{s_1}\right)}{2\pi^{d/2}\Gamma\left(\Delta_{s_1}+2-\frac{d}{2}\right)}. \tag{5.18}$$

In the bulk channel conformal block decomposition, the operators that appear are the bulk scalar $\bar{\Phi}\Phi$ and the conserved currents of all spins, which can be schematically written as $\bar{\Phi}(\partial_\mu)^J\Phi$. To extract the bulk expansion coefficients, one may use the inversion formula of[94]. Here, we restrict to calculating the one-point function of the first few operators of low spin. The one-point function of the operator $\bar{\Phi}\Phi$ can be extracted from the short distance limit of the correlator (5.15)

$$\langle \bar{\Phi}\Phi(x)\rangle = \frac{C_1^{\bar{\Phi}\Phi}}{r^{d-2}}, \qquad C_1^{\bar{\Phi}\Phi} = \frac{(d-1)\Gamma\left(\frac{d}{2}-v\right)\Gamma\left(\frac{d}{2}-1+v\right)\sin\left(v\pi\right)\Gamma\left(\frac{d}{2}\right)}{\pi^{\frac{d}{2}+1}\Gamma(d)(2-d)}. \tag{5.19}$$

The conserved currents, which are spinning operators, also get one-point functions. The

spin one current, which corresponds to the global $U(1)$ symmetry of the theory, is given by

$$J_\mu = i\left(\Phi\partial_\mu\bar{\Phi} - \bar{\Phi}\partial_\mu\Phi\right). \tag{5.20}$$

The one-point function of a parity odd spin one operator in the presence of a defect is fixed by conformal symmetry[12]

$$\langle J_i\rangle = \frac{C_1^J\epsilon_{ij}n^j}{r^d}, \qquad \langle J_a\rangle = 0, \qquad n_i = x_i/r. \tag{5.21}$$

We parametrize the coordinates as $x = (x^i, x^a) =$ with i, j now being Cartesian transverse coordinates, a, b being directions along the defect and ϵ_{ij} is the antisymmetric tensor in transverse directions. We can calculate this one point function by calculating derivatives of (5.15), and then taking the short distance limit. Since it is fixed up to a constant, it is enough to do the calculation just for one component. We do it for the θ component,

$$\begin{aligned}\langle J_\theta\rangle = -\frac{C_1^J}{r^{d-2}} = i\langle\Phi\partial_\theta\bar{\Phi} - \bar{\Phi}\partial_\theta\Phi\rangle &= \frac{2^{2-d}\pi^{-\frac{(d+1)}{2}}\Gamma\left(\frac{3-d}{2}\right)}{r^{d-2}}\sum_{k=-\infty}^{\infty}\frac{(k+v)\Gamma\left(\frac{d}{2}-1+|k+v|\right)}{\Gamma\left(2-\frac{d}{2}+|k+v|\right)} \\ &= \frac{(d-2)(2v-1)}{d-1}\frac{C_1^{\bar{\Phi}\Phi}}{r^{d-2}}.\end{aligned} \tag{5.22}$$

At $v = 1/2$, we expect the internal $U(1)$ symmetry to be enhanced to full $O(2)$ symmetry

which includes $\bar{\Phi} \to \Phi$, under which $J_\mu \to -J_\mu$. So we expect the correlators containing odd powers of J_μ to vanish at $v = 1/2$, and indeed the one-point function vanishes at $v = 1/2$.

Next let's discuss the stress tensor, which is a spin two conserved current. Conformal invariance, tracelessness and conservation fix the form of its one-point function up to a constant[12,74,73]

$$\langle T_{ij} \rangle_{\mathbb{R}^d} = \frac{h}{2\pi} \frac{(d-1)\delta_{ij} - d n_i n_j}{r^d}, \quad \langle T_{ab} \rangle_{\mathbb{R}^d} = -\frac{h}{2\pi} \frac{\delta_{ab}}{r^d}, \quad \langle T_{ai} \rangle_{\mathbb{R}^d} = 0. \tag{5.23}$$

In analogy with the scaling dimensions of local operators, h is referred to as the conformal weight of the defect[80,74,73]. It can be determined by doing an explicit calculation of any component of the stress tensor, and we choose $T_{\theta\theta}$. The canonical stress energy tensor for a free complex scalar in flat space is

$$T_{\mu\nu} = \partial_\mu \bar{\Phi} \partial_\nu \Phi - \frac{1}{2} g_{\mu\nu} \partial \bar{\Phi} \cdot \partial \Phi - \frac{(d-2)}{4(d-1)} \left(\partial_\mu \partial_\nu - g_{\mu\nu} \partial^2 \right) |\Phi|^2. \tag{5.24}$$

This gives

$$\langle T_{\theta\theta} \rangle = \frac{\langle \partial_\theta \bar{\Phi} \partial_\theta \Phi \rangle}{2} - \frac{r^2}{2(d-1)} (\langle \partial_r \bar{\Phi} \partial_r \Phi \rangle + \langle \vec{\partial}_y \bar{\Phi} \vec{\partial}_y \Phi \rangle) - \frac{d-2}{2(d-1)} \langle \bar{\Phi} \partial_\theta^2 \Phi \rangle - \frac{r(d-2)}{2(d-1)} \langle \bar{\Phi} \partial_r \Phi \rangle. \tag{5.25}$$

Using the two-point function in (5.15) and taking appropriate derivatives, we get

$$\langle T_{\theta\theta}\rangle = \frac{\Gamma\left(\frac{3-d}{2}\right)(1-v)v\left(\csc\pi\left(\frac{d}{2}-v\right)-\csc\pi\left(\frac{d}{2}+v\right)\right)}{d(4\pi)^{\frac{d-1}{2}}\Gamma\left(2-\frac{d}{2}-v\right)\Gamma\left(1-\frac{d}{2}+v\right)}\frac{1}{r^{d-2}} = -\frac{(d-2)v(1-v)}{d}\frac{C_1^{\bar{\Phi}\Phi}}{r^{d-2}}. \tag{5.26}$$

Comparing with (5.23), it is easy to see that

$$\langle T_{\theta\theta}\rangle = \frac{(d-1)h}{2\pi\, r^{d-2}} \implies h = -\frac{\pi\Gamma\left(\frac{1-d}{2}\right)(1-v)v\left(\csc\pi\left(\frac{d}{2}-v\right)-\csc\pi\left(\frac{d}{2}+v\right)\right)}{d(4\pi)^{\frac{d-1}{2}}\Gamma\left(2-\frac{d}{2}-v\right)\Gamma\left(1-\frac{d}{2}+v\right)}. \tag{5.27}$$

We checked numerically that this conformal weight h is always positive for $d > 2$. This is consistent with the conjecture proposed in[91] which says that $h \geq 0$ in unitary defect CFTs [‡]. We can follow this logic and calculate the one-point function of any higher spin current. We just do it for one more case here, namely the spin 3 symmetric current. The current is given by (explicit expression in $d = 4$ can be found in, for example,[7])

$$J_{\mu\nu\rho} = 6i\left(\bar{\Phi}\partial_\mu\partial_\nu\partial_\rho\Phi - \frac{3(d+2)}{d-2}\partial_{(\mu}\bar{\Phi}\partial_\nu\partial_{\rho)}\Phi + \frac{6}{d-2}g_{(\mu\nu}\partial^\gamma\bar{\Phi}\partial_\gamma\partial_{\rho)}\Phi\right) + \text{c.c.} \tag{5.28}$$

where $()$ in the subscript means that the indices are symmetrized. Its one-point function is also fixed by conformal symmetry up to a number, so we only look at one of its components with all indices equal to θ. We act with these derivatives on (5.15) and expand them in

[‡] In[91], stress tensor one-point function was written in terms of a_T which is related to h by $h = -2\pi a_T/d$, so they conjectured that $a_T \leq 0$.

the bulk limit $\xi \to 0$ to get

$$\langle J_{\theta\theta\theta} \rangle = \frac{6(1-2v)\left(3d^2 - 2d(2(v-1)v+5) + 4(v-1)v+8\right)}{d-1} \frac{C_1^{\bar{\Phi}\Phi}}{r^{d-2}}. \tag{5.29}$$

5.1.1 Mapping to $S^1 \times H^{d-1}$

As explained in the introduction, the monodromy defect may also be studied on a hyperbolic cylinder by a Weyl transformation as in (5.2). The operators also get rescaled under this Weyl transformation. The scalars, for instance, transform as $O_{S^1 \times \mathbb{H}^{d-1}} = r^{\Delta_O} O_{\mathbb{R}^d}$.

In order to describe a spherical defect, one may use the hyperbolic ball coordinates on H^{d-1}, obtained from the Poincaré coordinates by the following coordinate transformation

$$r = \frac{1}{\cosh\eta - \Omega_1 \sinh\eta}, \qquad y_a = \frac{\Omega_{a+1}\sinh\eta}{\cosh\eta - \Omega_1\sinh\eta} \tag{5.30}$$

where $(\Omega_1, \ldots, \Omega_{d-1})$ are the coordinates on a $d-2$ dimensional sphere with $|\Omega_a|^2 = 1$ and $0 \leq \eta < \infty$. The metric in these coordinates takes the following simple form

$$ds^2_{S^1 \times \mathbb{H}^{d-1}} = d\theta^2 + d\eta^2 + \sinh^2\eta \, ds^2_{S^{d-2}}. \tag{5.31}$$

Note that the defect is compact and is located at the boundary of the hyperbolic ball, $\eta \to \infty$, which is a $d-2$ dimensional sphere, S^{d-2}.

The complex scalar on $S^1 \times H^{d-1}$ is described by the action

$$\begin{aligned} S &= \frac{1}{2}\int d^d x\sqrt{g(x)}\left(g^{\mu\nu}\partial_\mu\Phi\partial_\nu\bar{\Phi} + \left(\frac{(d-2)}{4(d-1)}\mathcal{R} + m^2\right)|\Phi|^2\right) \\ &= \frac{1}{2}\int d^d x\sqrt{g(x)}\left(g^{\mu\nu}\partial_\mu\Phi\partial_\nu\bar{\Phi} - \left(\frac{(d-2)^2}{4} - m^2\right)|\Phi|^2\right) \end{aligned} \tag{5.32}$$

with the field Φ obeying twisted boundary conditions along S^1, $\Phi(r, \vec{y}, \theta+2\pi) = e^{i\vartheta}\Phi(r, \vec{y}, \theta)$. We will be interested in the conformally coupled case with $m^2 = 0$. An equivalent description of the system can be written in terms of untwisted field Ψ defined by $\Phi(x) = e^{iv\theta}\Psi(x)$. Ψ has the usual periodic boundary conditions $\Psi(r, \vec{y}, \theta + 2\pi) = \Psi(r, \vec{y}, \theta)$. The action in terms of Ψ can be written as

$$S = \frac{1}{2}\int d^d x\sqrt{g(x)}\left(\left|\left(\partial_\theta + iv\right)\Psi\right|^2 + g^{\alpha\beta}\partial_\alpha\Psi\partial_\beta\bar{\Psi} - \frac{(d-2)^2}{4}|\Psi|^2\right) \tag{5.33}$$

where α, β are the coordinates on H^{d-1}. This shows that having a monodromy defect is equivalent to having a constant background gauge field in the θ direction. Taking derivatives with v is equivalent to inserting the θ component of the $U(1)$ current

$$-\frac{\delta \log Z}{\delta v} = \frac{i}{2}\int d^d x\sqrt{g(x)}\langle\left(\Phi\partial_\theta\bar{\Phi} - \bar{\Phi}\partial_\theta\Phi\right)\rangle = \frac{1}{2}\int d^d x\sqrt{g(x)}\langle J_\theta\rangle \tag{5.34}$$

where Z is the partition function in presence of the defect.

We then perform a Kaluza-Klein (KK) reduction on S^1 to get a tower of massive scalar fields on H^{d-1}. The bulk field can be expanded into KK modes as $\Phi(r,\vec{y},\theta)=\sum e^{is\theta}\Phi_s(r,\vec{y})$ where $s\in\mathbb{Z}+v$ and modes $\Phi_s(r,\vec{y})$ have mass $s^2-(d-2)^2/4$. Since the defect is located on the boundary of H^{d-1}, we can use the standard AdS/CFT dictionary to calculate the dimensions of the defect operators of spin s induced by Φ

$$\Delta_s(\Delta_s-d+2)=s^2-(d-2)^2/4 \implies \Delta_s=\frac{d}{2}-1\pm|s|. \tag{5.35}$$

As before, we leave the discussion of the $-$ sign until the next section. The two-point function on $S^1\times H^{d-1}$ can then be written as a sum over KK modes with the two-point function of each KK mode being just the usual bulk-bulk propagator on H^{d-1}. This gives

$$\begin{aligned}\langle\Phi(\vec{y}_1,r_1,\theta_1)\bar{\Phi}(\vec{y}_2,r_2,\theta_2)\rangle = G_{\bar{\Phi}\Phi}(x_1,x_2) &= \sum_{s\in\mathbb{Z}+v}\frac{2e^{is\theta_{12}}}{2\pi}G^{bb}_{\Delta_s}\\ &=\sum_{s\in\mathbb{Z}+v}\frac{2\Gamma\left(\Delta_s\right)e^{is\theta_{12}}\,{}_2F_1\left(\Delta_s,\Delta_s+\frac{3-d}{2};2\Delta_s+3-d;-\frac{1}{\xi}\right)}{4\pi^{d/2}\Gamma(\Delta_s+2-\frac{d}{2})(4\xi)^{\Delta_s}}.\end{aligned} \tag{5.36}$$

This is related by a Weyl transformation to the two-point function in flat space (5.15).

A quantity of interest is the free energy on the hyperbolic space since this is related to the expectation value of the spherical monodromy defect. In the free theory, it is given by the

following determinant

$$F_{\text{twisted}}(\vartheta) = \text{tr}\log\left(-\nabla^2 + m^2 - \frac{(d-2)^2}{4}\right). \tag{5.37}$$

The eigenfunctions of the Laplacian on $S^1 \times H^{d-1}$ may be written as $\Phi_{H^{d-1}}(y^i, r)e^{is\theta}$ with $\Phi_{H^{d-1}}$ being the eigenfunction on the $d-1$ dimensional hyperbolic space. The corresponding eigenvalues are $\lambda + (d-2)^2/4 + s^2$ with a degeneracy given by[21,18]

$$D(\lambda)d\lambda = \frac{(\text{Vol}(H^{d-1}))}{(4\pi)^{\frac{d-1}{2}}\Gamma(\frac{d-1}{2})}\frac{|\Gamma(i\sqrt{\lambda}+\frac{d-2}{2})|^2}{|\Gamma(i\sqrt{\lambda})|^2}\frac{d\lambda}{\sqrt{\lambda}}. \tag{5.38}$$

Using this, we can compute the twisted free energy on the hyperbolic space as

$$\begin{aligned} F_{\text{twisted}}(\vartheta) &= \int_0^\infty d\lambda D(\lambda) \sum_{s\in\mathbb{Z}+v} \log\left(\lambda + m^2 + s^2\right) \\ &= \frac{\text{Vol}(H^{d-1})}{(4\pi)^{\frac{d-1}{2}}\Gamma(\frac{d-1}{2})}\int_{-\infty}^\infty d\nu \frac{|\Gamma(i\nu+\frac{d-2}{2})|^2}{|\Gamma(i\nu)|^2} \sum_{s\in\mathbb{Z}+v} \log\left(\nu^2 + s^2 + m^2\right). \end{aligned} \tag{5.39}$$

This can be used to calculate the expectation value of the defect, and it is natural to normalize it by the partition function of the untwisted theory. In the conformally coupled case, it

gives

$$
\begin{aligned}
&-\log\langle\mathcal{D}\rangle = F_{\text{twisted}} - F_{\text{untwisted}} \\
&= \frac{\text{Vol}(\mathbb{H}^{d-1})}{(4\pi)^{\frac{d-1}{2}}\Gamma(\frac{d-1}{2})}\int_{-\infty}^{\infty} d\nu \frac{|\Gamma(i\nu+\frac{d-2}{2})|^2}{|\Gamma(i\nu)|^2}\left(\sum_{n\in\mathbb{Z}+v} - \sum_{n\in\mathbb{Z}}\right)\log\left(\nu^2+n^2\right) \\
&= \frac{\text{Vol}(\mathbb{H}^{d-1})}{(4\pi)^{\frac{d-1}{2}}\Gamma(\frac{d-1}{2})}\int_{-\infty}^{\infty} d\nu \frac{|\Gamma(i\nu+\frac{d-2}{2})|^2}{|\Gamma(i\nu)|^2}\log\left(\frac{1}{2}\text{csch}^2(\pi\nu)\left(\cosh(2\pi\nu)-\cos(2\pi v)\right)\right).
\end{aligned}
\tag{5.40}
$$

To derive the above formula, we had to use the sum[84]

$$
\sum_{k\in\mathbb{Z}}\log\left((k+\alpha)^2+a^2\right) = \log\left(2\cosh(2\pi a)-2\cos(2\pi\alpha)\right). \tag{5.41}
$$

When d is even, the analytic form is easy to obtain by doing the integral over ν first in the second line of (5.40) and regularizing the sum by a Zeta function regularization

$$
\log\langle\mathcal{D}\rangle = \left(\sum_{n\in\mathbb{Z}+v} - \sum_{n\in\mathbb{Z}}\right)\frac{\partial}{\partial\alpha}\left[\frac{\text{Vol}(\mathbb{H}^{d-1})}{(4\pi)^{\frac{d-1}{2}}\Gamma(\frac{d-1}{2})}\int_{-\infty}^{\infty} d\nu \frac{|\Gamma(i\nu+\frac{d-2}{2})|^2}{|\Gamma(i\nu)|^2}\frac{1}{(\nu^2+n^2)^\alpha}\right]_{\alpha\to 0}. \tag{5.42}
$$

It gives

$$
\begin{aligned}
-\log\langle\mathcal{D}\rangle_{d=2} &= \text{Vol}(\mathbb{H}^1)\left(\zeta\left(-1,v\right)+\zeta\left(-1,1-v\right)+\frac{1}{6}\right) = v(1-v)\text{Vol}(\mathbb{H}^1)\\
-\log\langle\mathcal{D}\rangle_{d=4} &= \text{Vol}(\mathbb{H}^3)\left(\frac{-60\zeta\left(-3,v\right)-60\zeta\left(-3,1-v\right)+1}{360\pi}\right) = \frac{v^2(1-v)^2}{12\pi}\text{Vol}(\mathbb{H}^3)\\
-\log\langle\mathcal{D}\rangle_{d=6} &= \text{Vol}(\mathbb{H}^5)\left(\frac{\zeta\left(-5,v\right)+\zeta\left(-5,1-v\right)}{60\pi^2}-\frac{\zeta\left(-3,v\right)+\zeta\left(-3,1-v\right)}{36\pi^2}+\frac{1}{1680\pi^2}\right)\\
&= -\frac{v^2(1-v)^2(-3-v(1-v))}{180\pi^2}\text{Vol}(\mathbb{H}^5).
\end{aligned}
\tag{5.43}
$$

Note that the factors of the hyperbolic space volume here are logarithmically divergent[30,24], see eq. (5.46). The quantity $\tilde{\mathcal{D}}$ defined by

$$
\tilde{\mathcal{D}} \equiv \sin\left(\frac{\pi(d-q)}{2}\right)\log\langle\mathcal{D}\rangle \tag{5.44}
$$

is however finite and it is proportional to the quantities multiplying the volume factors above. Indeed using the above result (5.40), $\tilde{\mathcal{D}}$ can be seen to be a smooth and finite function of d. We plot it for $2 < d < 6$ and in the special case of Z_2 monodromy, $v = 1/2$, in figure 5.1. For future reference, let us also list some explicit values of $\tilde{\mathcal{D}}$ in various d for $v = 1/2$ which can be directly obtained using (5.40)

$$
\begin{aligned}
\tilde{\mathcal{D}}|_{d=3} &= \frac{\log 2}{4}-\frac{7\zeta(3)}{8\pi^2}\,, \qquad \tilde{\mathcal{D}}|_{d=4} = \frac{\pi}{192}\,,\\
\tilde{\mathcal{D}}|_{d=5} &= \frac{\log 2}{64}-\frac{5\zeta(3)}{192\pi^2}-\frac{31\zeta(5)}{128\pi^4}\,, \qquad \tilde{\mathcal{D}}|_{d=6} = \frac{13\pi}{23040}.
\end{aligned}
\tag{5.45}
$$

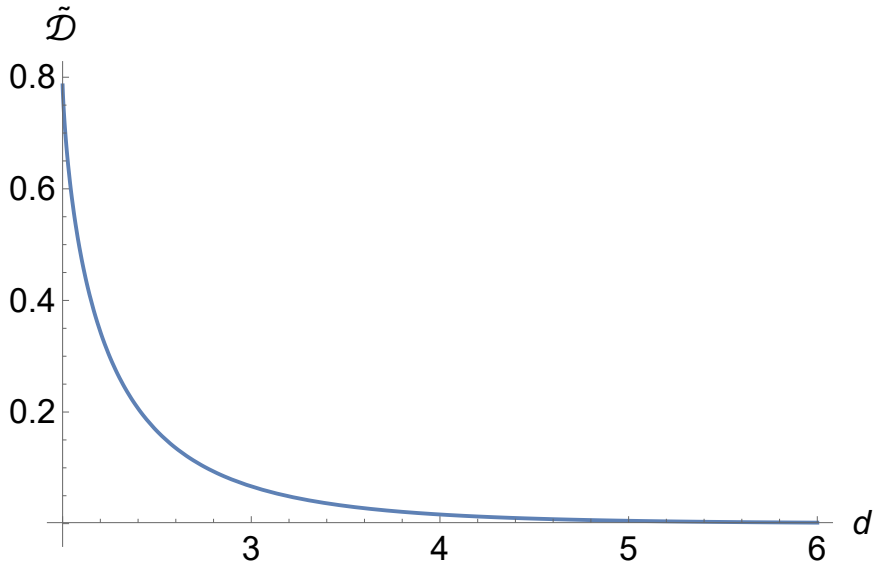

Figure 5.1: A plot of $\tilde{\mathcal{D}}$ for a single free complex scalar between dimensions $2 < d < 6$ when $v = 1/2$.

To do the above calculation and obtain the plot, we had to use the regularized volume of the hyperbolic space[30,24]

$$\text{Vol}(H^{d-1}) = \pi^{\frac{d}{2}-1}\Gamma\left(1-\frac{d}{2}\right). \tag{5.46}$$

5.1.2 One-point functions

One-point functions of bulk operators can also be readily obtained in the hyperbolic space. For the scalar $\bar{\Phi}\Phi$, it is a constant given by

$$C_1^{\bar{\Phi}\Phi} = \frac{1}{\pi \text{Vol}(\mathbb{H}^{d-1})} \frac{\partial F_{\text{twisted}}(\vartheta)}{\partial m^2}\bigg|_{m^2=0} \tag{5.47}$$

The mass derivative of the free energy can be calculated as follows

$$\begin{aligned}\frac{\partial F_{\text{twisted}}(\vartheta)}{\partial m^2} &= \sum_{k=-\infty}^{\infty} \frac{\text{Vol}(H^{d-1})}{(4\pi)^{\frac{d-1}{2}}\Gamma\left(\frac{d-1}{2}\right)} \int_{-\infty}^{\infty} d\nu \frac{|\Gamma(i\nu+\frac{d-2}{2})|^2}{|\Gamma(i\nu)|^2} \left(\frac{1}{\nu^2+(k+v)^2+m^2}\right) \\ &= \frac{\text{Vol}(H^{d-1})\Gamma\left(\frac{3-d}{2}\right)}{(4\pi)^{\frac{d-1}{2}}} \sum_{k=-\infty}^{\infty} \frac{\Gamma\left(\frac{d}{2}-1+\sqrt{m^2+(k+v)^2}\right)}{\Gamma\left(2-\frac{d}{2}+\sqrt{m^2+(k+v)^2}\right)} \\ &= \frac{\text{Vol}(H^{d-1})\Gamma\left(\frac{3-d}{2}\right)}{(4\pi)^{\frac{d-1}{2}}} \sum_{s} \frac{\Gamma\left(\Delta_s\right)}{\Gamma\left(3-d+\Delta_s\right)}.\end{aligned} \tag{5.48}$$

To perform the integral, we had to close the contour in the ν plane and sum over residues[22]. The arc at infinity can only be dropped for $d < 3$, but the final result can be analytically continued in dimensional regularization. One of the Gamma function introduces poles at $\nu = i(d/2 - 1 + 2\kappa)$ for integer κ, which all lie in the upper half plane for $d > 2$ and need to be summed to get the final result. For $m \to 0$, we get

$$\begin{aligned}\left.\frac{\partial F_{\text{twisted}}(\vartheta)}{\partial m^2}\right|_{m^2=0} &= \frac{\text{Vol}(H^{d-1})\Gamma\left(\frac{3-d}{2}\right)}{(4\pi)^{\frac{d-1}{2}}} \sum_{k=-\infty}^{\infty} \frac{\Gamma\left(\frac{d}{2}-1+|k+v|\right)}{\Gamma\left(2-\frac{d}{2}+|k+v|\right)} \\ &= \frac{(d-1)\text{Vol}(H^{d-1})\Gamma\left(\frac{d}{2}-v\right)\Gamma\left(\frac{d}{2}-1+v\right)\sin\left(v\pi\right)}{(4\pi)^{\frac{d-1}{2}}(2-d)\Gamma\left(\frac{d+1}{2}\right)} \\ \implies C_1^{\bar{\Phi}\Phi} &= \frac{(d-1)\Gamma\left(\frac{d}{2}-v\right)\Gamma\left(\frac{d}{2}-1+v\right)\sin\left(v\pi\right)\Gamma\left(\frac{d}{2}\right)}{\pi^{\frac{d}{2}+1}\Gamma(d)(2-d)}.\end{aligned} \tag{5.49}$$

This of course agrees with the flat space result (5.19). For the spin one $U(1)$ current, using its general form in (5.21), it is easy to see that the one-point function of its θ component is a constant on hyperbolic cylinder. It may be calculated as in (5.34), by taking the derivative of free energy with v

$$\begin{aligned}\langle J_\theta \rangle &= \frac{1}{\pi \text{Vol}(\mathbb{H}^{d-1})} \frac{\partial F_{\text{twisted}}(\vartheta)}{\partial v} = \sum_{k=-\infty}^{\infty} \frac{2^{2-d}\pi^{-\frac{(d+1)}{2}}}{\Gamma\left(\frac{d-1}{2}\right)} \int_{-\infty}^{\infty} d\nu \frac{|\Gamma(i\nu + \frac{d-2}{2})|^2}{|\Gamma(i\nu)|^2} \left(\frac{k+v}{\nu^2 + (k+v)^2}\right) \\ &= 2^{2-d}\pi^{-\frac{(d+1)}{2}} \Gamma\left(\frac{3-d}{2}\right) \sum_{k=-\infty}^{\infty} \frac{(k+v)\Gamma\left(\frac{d}{2} - 1 + |k+v|\right)}{\Gamma\left(2 - \frac{d}{2} + |k+v|\right)} \\ &= \frac{(d-2)(2v-1)}{d-1} C_1^{\bar{\Phi}\Phi},\end{aligned} \tag{5.50}$$

which again agrees with the flat space result in (5.22).

Similarly, for the stress tensor, the general form (5.23) tells us that $T_{\theta\theta}$ should have a constant one-point function on the hyperbolic cylinder. There is a simpler way to calculate it on the hyperbolic cylinder[73,93]. We start by keeping the length of S^1 to be a variable β instead of fixing it to 2π. This is equivalent to rescaling the metric component $g_{\theta\theta}$ by $(\beta/2\pi)^2$. So if we compute the free energy for arbitrary β and then take a derivative with respect to β, this is the same as inserting $T_{\theta\theta}$ in the path integral

$$T_{\mu\nu} = \frac{2}{\sqrt{g}} \frac{\delta S}{\delta g^{\mu\nu}} \implies \langle T_{\theta\theta} \rangle_{S^1 \times H^{d-1}} = -\frac{1}{\text{Vol}(H^{d-1})} \frac{\partial F_{\text{twisted}}(\vartheta, \beta)}{\partial \beta}\bigg|_{\beta=2\pi}. \tag{5.51}$$

In practice, we can calculate the free energy for a general β by rescaling n by $2\pi/\beta$

$$F_{\text{twisted}}(\vartheta,\beta)=\frac{\text{Vol}(H^{d-1})}{(4\pi)^{\frac{d-1}{2}}\Gamma(\frac{d-1}{2})}\int_{-\infty}^{\infty}d\nu\frac{|\Gamma(i\nu+\frac{d-2}{2})|^2}{|\Gamma(i\nu)|^2}\sum_{n\in\mathbb{Z}+v}\log\left(\nu^2+\frac{4\pi^2n^2}{\beta^2}\right). \tag{5.52}$$

We can use this to calculate the stress-tensor one-point function

$$\begin{aligned}\langle T_{\theta\theta}\rangle_{S^1\times H^{d-1}}&=\sum_{k=-\infty}^{\infty}\frac{1}{\pi(4\pi)^{\frac{d-1}{2}}\Gamma\left(\frac{d-1}{2}\right)}\int_{-\infty}^{\infty}d\nu\frac{|\Gamma(i\nu+\frac{d-2}{2})|^2}{|\Gamma(i\nu)|^2}\frac{(k+v)^2}{\nu^2+(k+v)^2}\\&=\frac{\Gamma\left(\frac{3-d}{2}\right)}{\pi(4\pi)^{\frac{d-1}{2}}}\sum_{k=-\infty}^{\infty}\frac{\Gamma\left(\frac{d}{2}-1+|k+v|\right)(k+v)^2}{\Gamma\left(2-\frac{d}{2}+|k+v|\right)}\\&=\frac{\Gamma\left(\frac{3-d}{2}\right)(1-v)v\left(\csc\pi\left(\frac{d}{2}-v\right)-\csc\pi\left(\frac{d}{2}+v\right)\right)}{d(4\pi)^{\frac{d-1}{2}}\Gamma\left(2-\frac{d}{2}-v\right)\Gamma\left(1-\frac{d}{2}+v\right)}\end{aligned} \tag{5.53}$$

which is consistent with what we got above by a direct calculation in flat space in (5.26). This hyperbolic space technique will be useful below, when we try to calculate the conformal weight in the interacting theory.

5.2 Monodromy defects at large N

In this section, we study the monodromy defect in the interacting $O(2N)$ model (it will soon be clear why we choose $2N$ instead of N here) at large N. The $S^1\times H^{d-1}$ setup

provides a convenient way to study the problem. The action may be written as [§]

$$S = \int d^d x \sqrt{g(x)} \left(\frac{g^{\mu\nu} \partial_\mu \phi^A \partial_\nu \phi^A}{2} - \frac{(d-2)^2}{8} \phi^A \phi^A + \frac{\lambda}{4} (\phi^A \phi^A)^2 \right) \tag{5.54}$$

where A now goes from 1 to $2N$. We again consider monodromy defect defined as in (5.4). We want to do a large N analysis, and to accomplish that, we want to preserve a large symmetry group. The simplest such case is when we fix the matrix G^{AB} in (5.5) to consist of N identical 2×2 blocks, so that all $\vartheta_i = \vartheta$. This is the only case we consider in this paper. Then, as before, it is convenient to package these $2N$ real scalars into N complex scalars as $\Phi^I = \phi^{2I-1} + i\phi^{2I}$, where I goes from 1 to N and all N complex scalars have the same monodromy as in (5.6). The original theory has $O(2N)$ symmetry, and the defect breaks it down to $U(N)$. However for $\vartheta = 0$ and π which correspond to a trivial defect and Z_2 monodromy defect respectively, the symmetry is enhanced and the defect preserves full $O(2N)$ symmetry. The action in terms of complex variables is

$$S = \int d^d x \sqrt{g(x)} \left(\frac{g^{\mu\nu} \partial_\mu \bar{\Phi}_I \partial_\nu \Phi^I}{2} - \frac{(d-2)^2}{8} \bar{\Phi}_I \Phi^I + \frac{\lambda}{4} (\bar{\Phi}_I \Phi^I)^2 \right). \tag{5.55}$$

[§] We assume that the mass terms have been tuned away so that the bulk is always critical.

At large N, we can use the well-known Hubbard-Stratonovich transformation to write this in terms of auxiliary field $\sigma(x)$

$$S = \int d^d x \sqrt{g(x)} \left(\frac{g^{\mu\nu} \partial_\mu \bar{\Phi}_I \partial_\nu \Phi^I}{2} - \frac{(d-2)^2}{8} \bar{\Phi}_I \Phi^I + \frac{1}{2} \sigma \bar{\Phi}_I \Phi^I \right). \tag{5.56}$$

We dropped a $\sigma^2/4\lambda$ term above, which can be consistently done in the critical limit (see for example[46], for a review). We can then integrate out the fields Φ^I since the action is quadratic in Φ^I to get

$$Z = \exp[-F_{\text{twisted}}] = \int [d\sigma] \exp \left[-N \operatorname{tr} \log \left(-\nabla^2 + \sigma - \frac{(d-2)^2}{4} \right) \right] \tag{5.57}$$

At large N, we can use a saddle point approximation to do the integral over σ and look for a saddle with a constant value for the field $\sigma(x)$. This constant is the one-point function of $\sigma(x)$ which is a constant on the hyperbolic cylinder ¶. So at leading order at large N, the field $\sigma(x)$ only contributes through its one-point function and acts as a mass term for Φ^I. Similar to the case of free theory (5.39), the free energy in the interacting theory at leading order at large N may then be written as

$$F_{\text{twisted}}(\vartheta) = \frac{N \text{Vol}(H^{d-1})}{(4\pi)^{\frac{d-1}{2}} \Gamma(\frac{d-1}{2})} \int_{-\infty}^{\infty} d\nu \frac{|\Gamma(i\nu + \frac{d-2}{2})|^2}{|\Gamma(i\nu)|^2} \sum_{n \in \mathbb{Z}+v} \log \left(\nu^2 + n^2 + \sigma \right). \tag{5.58}$$

¶In the flat space, this one-point function is $\langle \sigma(x) \rangle = \frac{\sigma^*}{r^2}$ with σ^* being the constant one-point function on the hyperbolic cylinder

The value of σ at the large N fixed point, σ^* can be obtained by solving the saddle point equation, which says that the following derivative should vanish

$$\begin{aligned}\left.\frac{\partial F_{\text{twisted}}(\vartheta)}{\partial\sigma}\right|_{\sigma=\sigma^*} &= \frac{N\text{Vol}(H^{d-1})}{(4\pi)^{\frac{d-1}{2}}\Gamma(\frac{d-1}{2})}\int_{-\infty}^{\infty}d\nu\frac{|\Gamma(i\nu+\frac{d-2}{2})|^2}{|\Gamma(i\nu)|^2}\sum_{n\in\mathbb{Z}+v}\frac{1}{\nu^2+n^2+\sigma^*}\\ &= \frac{N\text{Vol}(H^{d-1})\Gamma\left(\frac{3-d}{2}\right)}{(4\pi)^{\frac{d-1}{2}}}\sum_{k=-\infty}^{\infty}\frac{\Gamma\left(\frac{d}{2}-1+\sqrt{\sigma^*+(k+v)^2}\right)}{\Gamma\left(2-\frac{d}{2}+\sqrt{\sigma^*+(k+v)^2}\right)}\\ &= \frac{N\text{Vol}(H^{d-1})\Gamma\left(\frac{3-d}{2}\right)}{(4\pi)^{\frac{d-1}{2}}}\sum_{s\in\mathbb{Z}+v}\frac{\Gamma\left(\Delta_s\right)}{\Gamma\left(3-d+\Delta_s\right)}\end{aligned} \tag{5.59}$$

where the integral over ν is similar to the one in (5.48) and can be performed with similar techniques. In the last line, we used the usual AdS/CFT dictionary to write the expression in terms of the dimensions of defect operators

$$\Delta_s(\Delta_s-d+2)=s^2+\sigma^*-\frac{(d-2)^2}{4}\implies\Delta_s^{\pm}=\frac{d}{2}-1\pm\sqrt{\sigma^*+s^2}. \tag{5.60}$$

Note that we used Δ_s^+ solution to write the above expression of $\partial F/\partial\sigma$ in (5.59). This is because the spectral representation of the free energy is only valid for $\Delta_s > d/2-1$. However, written in terms of Δ_s, the expression in (5.59) can be analytically continued and also used for the case when we impose Δ^- boundary condition on one or more of the

operators. We also want the dimensions of all the defect operators to be real which requires

$$\sigma^* \geq \max\left(-v^2, -(1-v)^2\right). \tag{5.61}$$

Another equivalent way to derive this large N saddle point equation is to look at the two-point function of Φ in the bulk OPE limit. As we discussed above (5.36), the two-point function on the hyperbolic cylinder is given by the sum over bulk-bulk propagators

$$\langle \Phi^I(x_1)\bar{\Phi}_J(x_2)\rangle = \sum_{s\in\mathbb{Z}+v} \delta^I{}_J \frac{\Gamma(\Delta_s)\, e^{is\theta_{12}}\, {}_2F_1\left(\Delta_s, \Delta_s+\frac{3-d}{2}; 2\Delta_s+3-d; -\frac{1}{\xi}\right)}{2\pi^{d/2}\Gamma(\Delta_s+2-\frac{d}{2})(4\xi)^{\Delta_s}} \tag{5.62}$$

and here Δ_s is given by (5.60). In the bulk OPE limit, the two point function behaves as

$$\langle \Phi^I(x_1)\bar{\Phi}_J(x_2)\rangle = \frac{\delta^I{}_J}{\pi(4\pi)^{\frac{d-1}{2}}} \sum_{s\in\mathbb{Z}+v} \left[\frac{\Gamma\left(\frac{d-3}{2}\right)}{\xi^{\frac{d-3}{2}}}(1+O(\xi)) + \frac{\Gamma\left(\frac{3-d}{2}\right)\Gamma(\Delta_s)}{\Gamma(3-d+\Delta_s)}(1+O(\xi))\right]. \tag{5.63}$$

The constant ξ independent piece in the second term represents the presence of operator $\Phi^I\bar{\Phi}_I$ of dimension $d-2$ in the bulk OPE. Recall that in the large N critical $U(N)$ model, this operator is replaced by the operator σ of dimension 2. This should still be true in the presence of the defect, and demanding that this term vanishes is equivalent to the saddle point equation written in (5.59).

When we impose Δ^+ boundary condition on all the operators, σ^* can be determined by

solving the following equation from (5.59)

$$\frac{\text{Vol}(H^{d-1})\Gamma\left(\frac{3-d}{2}\right)}{(4\pi)^{\frac{d-1}{2}}}\sum_{k=-\infty}^{\infty}\frac{\Gamma\left(\frac{d}{2}-1+\sqrt{\sigma^*+(k+v)^2}\right)}{\Gamma\left(2-\frac{d}{2}+\sqrt{\sigma^*+(k+v)^2}\right)}=0. \tag{5.64}$$

It is hard to perform this sum analytically as a function of d. To proceed, we separate out the sum into a divergent piece at large k and a finite piece. The divergent piece of the sum can be performed by dimensional regularization and analytically continued in d. For the finite piece, it is harder to perform the sum as a function of d. However in $d = 4-\epsilon$, we can first do a series expansion in ϵ and then it can be performed up to first two orders in ϵ. Hence, the saddle point equation can be solved order by order in ϵ and it gives

$$\sigma^* = v\,(v-1)\,\epsilon + \frac{3v(v-1)+1}{2}\epsilon^2 + O(\epsilon^3). \tag{5.65}$$

Notice that the order ϵ^2 term does not vanish at $v = 0$ and 1. But the defect becomes trivial at $v = 0$ and 1, so all one-point functions, including the one-point function of σ should vanish at these values of v. This problem arises because we are doing an expansion in ϵ, and we expect this problem to be resolved by higher order terms in ϵ. Indeed when we calculate σ^* numerically in $d = 3.9$ below, we will see that it vanishes at $v = 0$ and 1. One possibility is that the higher order terms in ϵ are singular at $v = 0$ and 1. For example,

consider the ϵ expansion of the following simple function

$$\frac{\epsilon v^{\frac{3}{2}}}{\sqrt{v+\epsilon}} = \epsilon v - \frac{\epsilon^2}{2} + \frac{3\epsilon^2}{2v} + O(\epsilon^4). \tag{5.66}$$

The function vanishes at $v = 0$ for any fixed ϵ, but when we expand at small ϵ, the limit $v \to 0$ becomes problematic. This is similar to what we see here.

Plugging this σ^* into (5.60), we get the dimension of defect operators at large N and leading orders in ϵ

$$\Delta_s^+ = 1 - \frac{\epsilon}{2} + |s| + \frac{v(v-1)}{2|s|}\epsilon + \frac{3v(v-1)+1}{4|s|}\epsilon^2 - \frac{v^2(v-1)^2}{8|s|^3}\epsilon^2 + O(\epsilon^3). \tag{5.67}$$

We can also calculate the twisted free energy at the large N fixed point

$$\begin{aligned} F_{\text{twisted}} &= F_{\text{twisted}}\Big|_{\sigma=0} + \int_0^{\sigma^*} d\sigma \frac{\partial F_{\text{twisted}}}{\partial \sigma} \\ &= F_{\text{twisted}}\Big|_{\sigma=0} + \frac{N\text{Vol}(H^3)}{4\pi}\int_0^{\sigma^*} d\sigma \left(-\frac{\sigma}{\epsilon} + v\,(v-1)\right) \\ &= N F_{\text{twisted}}^{\text{free}} + \frac{N\text{Vol}(H^3) v^2\,(v-1)^2}{8\pi}\epsilon \end{aligned} \tag{5.68}$$

where we used the fact that $F_{\text{twisted}}(\sigma = 0)$ is the same as twisted free energy in the free theory.

Away from $d = 4$, the finite piece of the sum in (5.64) can be performed numerically, for

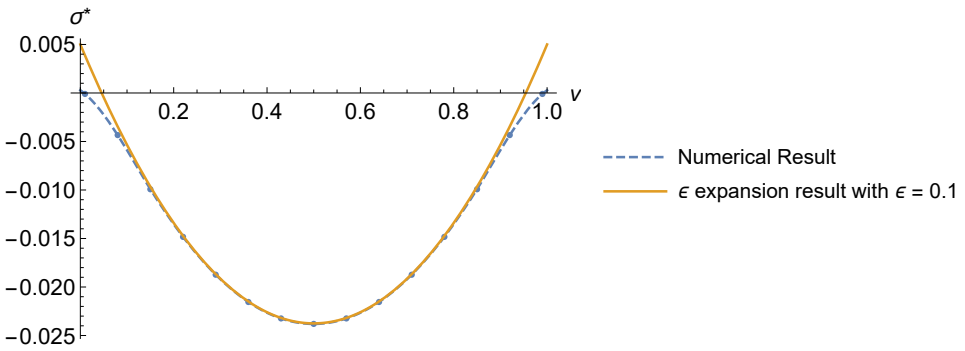

Figure 5.2: Saddle point value of σ^* in $d = 3.9$ critical theory with Δ^+ boundary condition at leading order in large N. Dashed line represents smooth interpolation of the numerical result. For comparison, we also plot the analytic result in $d = 4 - \epsilon$ at $\epsilon = 0.1$.

a given d, σ^* and v. We start with $d = 3.9$, so that we can compare it with the prediction in $d = 4 - \epsilon$. We evaluate the sum for a range of values of σ and v, and then find the root of the equation on the real σ axis for different values of v. We then interpolate in v and plot the value of σ^* in figure 5.2. We also compare the result with the result in $d = 4 - \epsilon$ in (5.65) at $\epsilon = 0.1$.

A similar method also works in $d = 3$ to solve the saddle point equation in (5.64) numerically. We plot the solution in figure 5.3. Once we know σ^*, we can calculate the dimensions of defect operators using (5.60). We also plot the dimensions of three low-lying defect operators in figure 5.3. For $v = 1/2$, corresponding to Z_2 monodromy on all scalars, we get

$$\sigma_* = -0.168, \qquad \Delta_{1/2} = 0.786, \qquad \Delta_{3/2} = 1.943 \tag{5.69}$$

to leading order at large N. We are doing a large N analysis, but it is interesting to compare

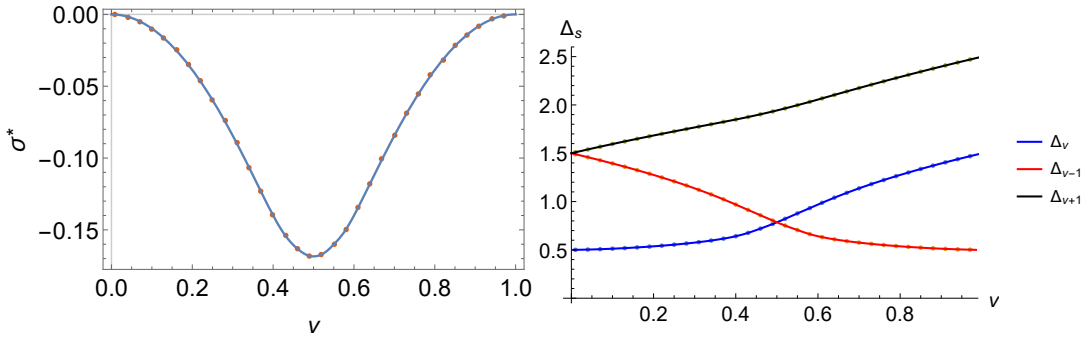

Figure 5.3: Saddle point value of σ^* and the dimensions of defect operators in three dimensional critical theory at large N. The solid lines are smooth interpolation of the numerical results. Note that the defect is one-dimensional, therefore the unitarity bound just requires the defect dimensions to be positive.

the result with the Monte Carlo results for monodromy defect in $d = 3$ Ising model in[11]. They found $\Delta_{1/2} = 0.918$ and $\Delta_{3/2} = 1.99$.

Using σ^*, we can also calculate the expectation value of the defect with spherical geometry. It is defined in the same way as the free theory (5.40), as the negative of the difference between the twisted and the untwisted free energy. However, recall that in the untwisted theory, the one-point functions vanish, so $\sigma^* = 0$. This implies that the corrections due to the interactions for the untwisted free energy start at order $1/N$. So at leading order, we can just use the untwisted free energy of the free theory and the interacting corrections to the defect expectation value are due to the corrections in the twisted free energy

$$-\log\langle\mathcal{D}\rangle = -N\log\langle\mathcal{D}\rangle^{\text{free}} + \int_0^{\sigma^*} d\sigma \frac{\partial F_{\text{twisted}}}{\partial\sigma}. \tag{5.70}$$

The first term above is the free theory result we have from (5.40). We can numerically in-

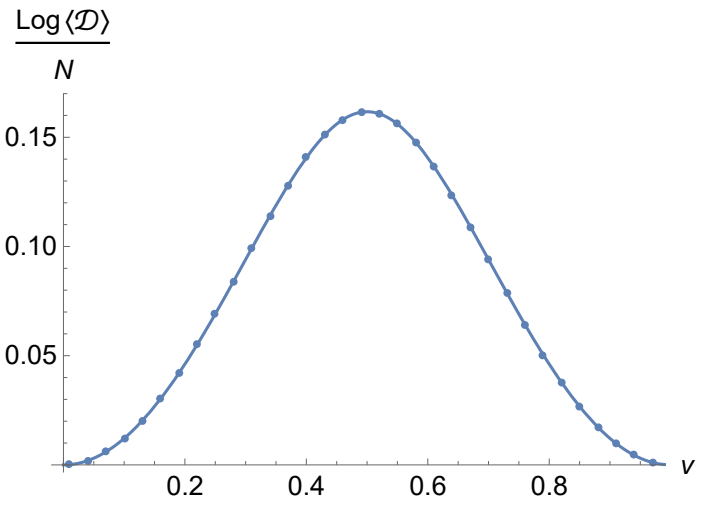

Figure 5.4: Defect expectation value in $d = 3$ critical theory at leading order in large N. Solid line interpolates the numerical results.

tegrate (5.59) using the numerical results for σ^* to evaluate the second term. We plot the result in figure 5.4 for the case of $d = 3$, corresponding to a circular defect. We used the standard regularized volume of H^2, $\mathrm{Vol}(H^2) = -2\pi$, that can be obtained in (5.46).

We can also calculate the conformal weight of the defect in the interacting theory. It is related to $T_{\theta\theta}$ (5.27), which in the hyperbolic cylinder approach is given by (5.51). So we need to know the dependence of the twisted free energy on β. Similar to the case of free theory, when we change the length of S^1 to β, the expression for the free energy changes to

$$F_{\text{twisted}}(\vartheta,\beta) = \frac{N\mathrm{Vol}(H^{d-1})}{(4\pi)^{\frac{d-1}{2}}\Gamma(\frac{d-1}{2})}\int_{-\infty}^{\infty} d\nu \frac{|\Gamma(i\nu+\frac{d-2}{2})|^2}{|\Gamma(i\nu)|^2}\sum_{n\in\mathbb{Z}+v}\log\left(\nu^2+\frac{4\pi^2n^2}{\beta^2}+\sigma\right). \tag{5.71}$$

If we impose Δ^+ boundary condition on all the operators, then the large N saddle point

equation is

$$\left.\frac{\partial F_{\text{twisted}}}{\partial\sigma}\right|_{\sigma=\sigma^*} = \frac{N\text{Vol}(H^{d-1})\Gamma\left(\frac{3-d}{2}\right)}{(4\pi)^{\frac{d-1}{2}}}\sum_{k=-\infty}^{\infty}\frac{\Gamma\left(\frac{d}{2}-1+\sqrt{\frac{4\pi^2}{\beta^2}(k+v)^2+\sigma}\right)}{\Gamma\left(2-\frac{d}{2}+\sqrt{\frac{4\pi^2}{\beta^2}(k+v)^2+\sigma}\right)} = 0 \tag{5.72}$$

Proceeding in the same way as $\beta = 2\pi$, we first expand the sum in general d in large k and isolate the pieces that diverge as $k \to \infty$. The divergent piece of the sum can be performed in dimensional regularization and analytically continued in d. And for the finite piece, we have to either expand in ϵ or turn to numerical methods. In $d = 4 - \epsilon$, the solution to the saddle point equation to leading order in ϵ is

$$\sigma^* = \left(\frac{2\pi^2(6(v-1)v+1)}{3\beta^2} - \frac{1}{6}\right)\epsilon + \mathcal{O}(\epsilon)^2 \tag{5.73}$$

Correction to the twisted free energy, to leading order in ϵ and N is

$$\begin{aligned} F_{\text{twisted}}(\vartheta,\beta) &= F_{\text{twisted}}(\vartheta,\beta)\Big|_{\sigma=0} + N\int_0^{\sigma^*} d\sigma\,\frac{\partial F_{\text{twisted}}}{\partial\sigma} \\ &= F_{\text{twisted}}(\vartheta,\beta)\Big|_{\sigma=0} + \text{Vol}(H^3)N\frac{\left(\beta^2-4\pi^2(6(v-1)v+1)\right)^2}{576\pi^2\beta^3}\epsilon + \mathcal{O}(\epsilon)^2 \end{aligned} \tag{5.74}$$

Using (5.51) and (5.27), we get the conformal weight in terms of the free energy

$$h = -\frac{1}{\text{Vol}(H^{d-1})}\frac{2\pi}{(d-1)}\frac{\partial F_{\text{twisted}}}{\partial \beta}\bigg|_{\beta=2\pi}. \tag{5.75}$$

This gives the conformal weight in the interacting theory to leading order in ϵ

$$\begin{aligned} h &= -\frac{N\pi\Gamma\left(\frac{1-d}{2}\right)(1-v)v\left(\csc\pi\left(\frac{d}{2}-v\right)-\csc\pi\left(\frac{d}{2}+v\right)\right)}{d(4\pi)^{\frac{d-1}{2}}\Gamma\left(2-\frac{d}{2}-v\right)\Gamma\left(1-\frac{d}{2}+v\right)} + \frac{N(1-v)v(9(1-v)v-2)}{72\pi}\epsilon \\ &= \frac{Nv^2(1-v)^2}{12\pi} + \frac{\epsilon N(1-v)^2v^2}{144\pi}\left(-6H^{-v-1} - 6\psi(v-1) + 37 + 6\log(\pi) - \frac{4}{v(1-v)}\right) \end{aligned} \tag{5.76}$$

where ψ is the Polygamma function and H^n is the n^{th} harmonic number. We used the free theory result for conformal weight (5.27) in $d = 4-\epsilon$.

Away from $d = 4$, we can still work numerically. For a given d, we now have three variables in the sum (5.72), namely β, v and σ. We are interested in calculating a derivative with β at $\beta = 2\pi$. So we choose three values of β near 2π as $\beta = \{2\pi - 0.01, 2\pi, 2\pi + 0.01\}$ and then calculate the sum in (5.72) over a range of values of σ and v. We do an interpolation in σ and find the root for several values of v and all three values of β. So we have an analogue of figure 5.3 but for three different values of β. We then use this saddle point solution for σ^* to calculate the integral for free energy in (5.74). We finally calculate the

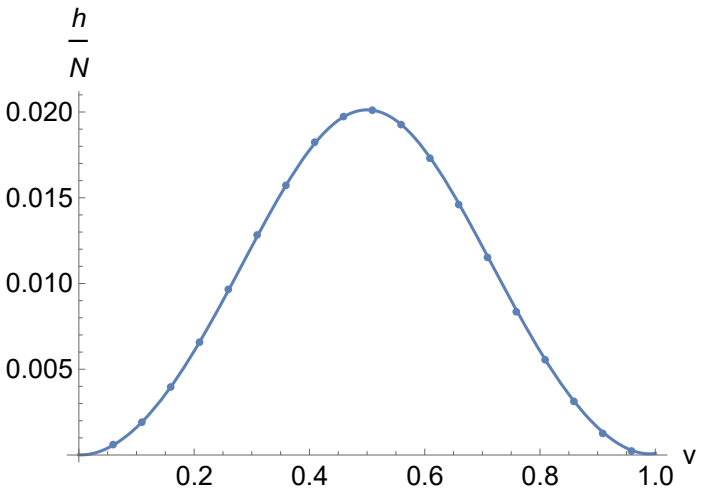

Figure 5.5: Numerical result and a smooth interpolation for conformal weight in $d = 3$.

conformal weight using (5.75) where for the derivative, we use the numerical analogue

$$h = -\frac{1}{\text{Vol}(H^{d-1})}\frac{2\pi}{(d-1)}\frac{F_{\text{twisted}}(2\pi + 0.01) - F_{\text{twisted}}(2\pi - 0.01)}{0.02}. \tag{5.77}$$

We plot the result in $d = 3$ in figure 5.5. It is positive in accordance with the conjecture made in [91].

References

[1] Aharony, O., Berkooz, M., Karasik, A., & Vaknin, T. (2016). Supersymmetric field theories on $AdS_p \times S^q$. *JHEP*, 04, 066.

[2] Appelquist, T., Nash, D., & Wijewardhana, L. C. R. (1988). Critical Behavior in (2+1)-Dimensional QED. *Phys. Rev. Lett.*, 60, 2575.

[3] Appelquist, T. & Pisarski, R. D. (1981). High-Temperature Yang-Mills Theories and Three-Dimensional Quantum Chromodynamics. *Phys. Rev.*, D23, 2305.

[4] Arefeva, I. Y., Dragovich, B., Frampton, P. H., & Volovich, I. V. (1991). Wave function of the universe and p-adic gravity. *Int. J. Mod. Phys. A*, 6, 4341–4358.

[5] Basa, B., La Nave, G., & Phillips, P. W. (2019). Classification of Non-local Actions: Area versus Volume Entanglement Entropy.

[6] Baume, F., Keren-Zur, B., Rattazzi, R., & Vitale, L. (2014). The local Callan-Symanzik equation: structure and applications. *JHEP*, 08, 152.

[7] Beccaria, M. & Tseytlin, A. (2017). On induced action for conformal higher spins in curved background. *Nucl. Phys. B*, 919, 359–383.

[8] Behan, C., Rastelli, L., Rychkov, S., & Zan, B. (2017a). A scaling theory for the long-range to short-range crossover and an infrared duality. *J. Phys.*, A50(35), 354002.

[9] Behan, C., Rastelli, L., Rychkov, S., & Zan, B. (2017b). Long-range critical exponents near the short-range crossover. *Phys. Rev. Lett.*, 118(24), 241601.

[10] Bentsen, G., Hashizume, T., Buyskikh, A. S., Davis, E. J., Daley, A. J., Gubser, S. S., & Schleier-Smith, M. (2019). Treelike interactions and fast scrambling with cold atoms. *Physical review letters*, 123(13), 130601.

[11] Billò, M., Caselle, M., Gaiotto, D., Gliozzi, F., Meineri, M., & Pellegrini, R. (2013). Line defects in the 3d Ising model. *JHEP*, 07, 055.

[12] Billò, M., Gonçalves, V., Lauria, E., & Meineri, M. (2016). Defects in conformal field theory. *JHEP*, 04, 091.

[13] Bjorken, J. D. & Drell, S. D. (1964). *Relativistic quantum mechanics*. International series in pure and applied physics. New York, NY: McGraw-Hill.

[14] Bleher, P. M. & Sinai, J. G. (1973). Investigation of the critical point in models of the type of Dyson's hierarchical models. *Comm. Math. Phys.*, 33(1), 23–42.

[15] Brekke, L. & Freund, P. G. O. (1993). *p*-adic numbers in physics. *Phys. Rept.*, 233, 1–66.

[Brewin] Brewin, L. Riemann normal coordinates. http://users.monash.edu.au/~leo/research/papers/files/lcb96-01.pdf.

[17] Brewin, L. (2009). Riemann Normal Coordinate expansions using Cadabra. *Class. Quant. Grav.*, 26, 175017.

[18] Bytsenko, A. A., Cognola, G., Vanzo, L., & Zerbini, S. (1996). Quantum fields and extended objects in space-times with constant curvature spatial section. *Phys. Rept.*, 266, 1–126.

[19] Caffarelli, L. & Silvestre, L. (2007). An extension problem related to the fractional laplacian. *Communications in partial differential equations*, 32(8), 1245–1260.

[20] Callan, Curtis G., J., Coleman, S., & Jackiw, R. (1970). A new improved energy-momentum tensor. *Annals of Physics*, 59(1), 42–73.

[21] Camporesi, R. & Higuchi, A. (1994). Spectral functions and zeta functions in hyperbolic spaces. *Journal of Mathematical Physics*, 35(8), 4217–4246.

[22] Carmi, D., Di Pietro, L., & Komatsu, S. (2019). A Study of Quantum Field Theories in AdS at Finite Coupling. *JHEP*, 01, 200.

[23] Casini, H. & Huerta, M. (2011). Entanglement entropy for the n-sphere. *Phys. Lett. B*, 694, 167–171.

[24] Casini, H., Huerta, M., & Myers, R. C. (2011). Towards a derivation of holographic entanglement entropy. *JHEP*, 05, 036.

[25] Chekhov, L., Mironov, A., & Zabrodin, A. (1989). Multiloop calculations in p-adic string theory and Bruhat-Tits trees. *Communications in mathematical physics*, 125(4), 675–711.

[26] Chester, S. M. & Pufu, S. S. (2016). Anomalous dimensions of scalar operators in QED$_3$. *JHEP*, 08, 069.

[27] Coleman, S. & Jackiw, R. (1971). Why dilatation generators do not generate dilatations. *Annals of Physics*, 67(2), 552–598.

[28] Collins, J. C. (1986). *Renormalization*, volume 26 of *Cambridge Monographs on Mathematical Physics*. Cambridge: Cambridge University Press.

[29] Di Pietro, L., Gaiotto, D., Lauria, E., & Wu, J. (2019). 3d Abelian Gauge Theories at the Boundary. *JHEP*, 05, 091.

[30] Diaz, D. E. & Dorn, H. (2007). Partition functions and double-trace deformations in AdS/CFT. *JHEP*, 05, 046.

[31] do Amaral, R. L. P. G. & Marino, E. C. (1992). Canonical quantization of theories containing fractional powers of the d'Alembertian operator. *J. Phys.*, A25, 5183–5200.

[32] Dudal, D., Mizher, A. J., & Pais, P. (2019). Exact quantum scale invariance of three-dimensional reduced QED theories. *Phys. Rev.*, D99(4), 045017.

[33] Dymarsky, A., Farnsworth, K., Komargodski, Z., Luty, M. A., & Prilepina, V. (2016). Scale Invariance, Conformality, and Generalized Free Fields. *JHEP*, 02, 099.

[34] Dymarsky, A., Komargodski, Z., Schwimmer, A., & Theisen, S. (2015). On Scale and Conformal Invariance in Four Dimensions. *JHEP*, 10, 171.

[35] Dymarsky, A. & Zhiboedov, A. (2015). Scale-invariant breaking of conformal symmetry. *J. Phys.*, A48(41), 41FT01.

[36] Dyson, F. J. (1969). Existence of a phase transition in a one-dimensional Ising ferromagnet. *Commun. Math. Phys.*, 12, 91–107.

[37] El-Showk, S., Nakayama, Y., & Rychkov, S. (2011). What Maxwell Theory in $D \neq 4$ teaches us about scale and conformal invariance. *Nucl. Phys.*, B848, 578–593.

[38] Eune, M., Kim, W., & Son, E. J. (2011). Effective potentials in the Lifshitz scalar field theory. *Phys. Lett.*, B703, 100–105.

[39] Fisher, M. E., Ma, S.-k., & Nickel, B. (1972a). Critical exponents for long-range interactions. *Physical Review Letters*, 29(14), 917.

[40] Fisher, M. E., Ma, S.-k., & Nickel, B. G. (1972b). Critical Exponents for Long-Range Interactions. *Phys. Rev. Lett.*, 29, 917–920.

[41] Freund, P. G. (2006). p-adic strings and their applications. In *AIP Conference Proceedings*, volume 826 (pp. 65–73).: AIP.

[42] Freund, P. G. & Witten, E. (1987). Adelic string amplitudes. *Physics Letters B*, 199(2), 191–194.

[43] Friedan, D. H. (1985). Nonlinear Models in Two + Epsilon Dimensions. *Annals Phys.*, 163, 318.

[44] Gadde, A. (2020). Conformal constraints on defects. *JHEP*, 01, 038.

[45] Gaiotto, D., Mazac, D., & Paulos, M. F. (2014). Bootstrapping the 3d Ising twist defect. *JHEP*, 03, 100.

[46] Giombi, S. (2017). Higher Spin — CFT Duality. In *Theoretical Advanced Study Institute in Elementary Particle Physics: New Frontiers in Fields and Strings* (pp. 137–214).

[47] Giombi, S., Helfenberger, E., Ji, Z., & Khanchandani, H. (2021). Monodromy Defects from Hyperbolic Space.

[48] Giombi, S. & Khanchandani, H. (2019). $O(N)$ Models with Boundary Interactions and their Long Range Generalizations.

[49] Giombi, S. & Khanchandani, H. (2020). CFT in AdS and boundary RG flows. *JHEP*, 11, 118.

[50] Giombi, S., Klebanov, I. R., Pufu, S. S., Safdi, B. R., & Tarnopolsky, G. (2013). AdS Description of Induced Higher-Spin Gauge Theory. *JHEP*, 10, 016.

[51] Giombi, S., Klebanov, I. R., & Tarnopolsky, G. (2016a). Conformal QED$_d$, F-Theorem and the ϵ Expansion. *J. Phys.*, A49(13), 135403.

[52] Giombi, S., Tarnopolsky, G., & Klebanov, I. R. (2016b). On C_J and C_T in Conformal QED. *JHEP*, 08, 156.

[53] Giombi, S. & Yin, X. (2013). The Higher Spin/Vector Model Duality. *J. Phys.*, A46, 214003.

[54] Gubser, S. S., Jepsen, C., Ji, Z., & Trundy, B. (2018a). Continuum limits of sparse coupling patterns. *Physical Review D*, 98(4), 045009.

[55] Gubser, S. S., Jepsen, C., Ji, Z., & Trundy, B. (2018b). Mixed field theory. *Princeton University preprint PUPT-2574*.

[56] Gubser, S. S., Jepsen, C., Ji, Z., & Trundy, B. (2019a). Mixed field theory. *Journal of High Energy Physics*, 2019(12), 1–23.

[57] Gubser, S. S., Jepsen, C., Parikh, S., & Trundy, B. (2017a). O(N) and O(N) and O(N). *Journal of High Energy Physics*, 2017(11).

[58] Gubser, S. S., Jepsen, C., Parikh, S., & Trundy, B. (2017b). O(N) and O(N) and O(N). *JHEP*, 11, 107.

[59] Gubser, S. S., Jepsen, C., & Trundy, B. (2018c). Spin in p-adic AdS/CFT.

[60] Gubser, S. S., Jepsen, C. B., Ji, Z., Trundy, B., & Yarom, A. (2019b). Non-local non-linear sigma models. *JHEP*, 09, 005.

[61] Gubser, S. S., Klebanov, I. R., & Polyakov, A. M. (1998). Gauge theory correlators from noncritical string theory. *Phys. Lett.*, B428, 105–114.

[62] Gubser, S. S., Knaute, J., Parikh, S., Samberg, A., & Witaszczyk, P. (2016). p-adic AdS/CFT. *Commun. Math. Phys.*, 352(3), 1019–1059.

[63] Guha, S. & Nagaraj, B. (2018). Correlators of Mixed Symmetry Operators in Defect CFTs. *JHEP*, 10, 198.

[64] Herzog, C. P. & Huang, K.-W. (2017). Boundary Conformal Field Theory and a Boundary Central Charge. *JHEP*, 10, 189.

[65] Herzog, C. P. & Kobayashi, N. (2020). The $O(N)$ model with ϕ^6 potential in $\mathbb{R}^2 \times \mathbb{R}^+$.

[66] Herzog, C. P. & Shamir, I. (2019). On Marginal Operators in Boundary Conformal Field Theory. *JHEP*, 10, 088.

[67] Herzog, C. P. & Shrestha, A. (2020). Two Point Functions in Defect CFTs.

[68] Heydeman, M., Jepsen, C. B., Ji, Z., & Yarom, A. (2020). Renormalization and conformal invariance of non-local quantum electrodynamics. *JHEP*, 08, 007.

[69] Heydeman, M., Marcolli, M., Saberi, I., & Stoica, B. (2016). Tensor networks, p-adic fields, and algebraic curves: arithmetic and the $\mathrm{AdS}_3/\mathrm{CFT}_2$ correspondence.

[70] Honkonen, J. (1990). Critical behavior of the long-range $(\phi^2)^2$ model in the short-range limit. *J. Phys.*, A23, 825–831.

[71] Honkonen, J. & Nalimov, M. Yu. (1989). Crossover Between Field Theories With Short-Range And Long-Range Exchange Or Correlations. *J. Phys.*, A22, 751–763.

[72] Huang, A., Stoica, B., & Yau, S.-T. (2019). General relativity from p-adic strings.

[73] Hung, L.-Y., Myers, R. C., & Smolkin, M. (2014). Twist operators in higher dimensions. *JHEP*, 10, 178.

[74] Hung, L.-Y., Myers, R. C., Smolkin, M., & Yale, A. (2011). Holographic Calculations of Renyi Entropy. *JHEP*, 12, 047.

[75] Iengo, R., Russo, J. G., & Serone, M. (2009). Renormalization group in Lifshitz-type theories. *JHEP*, 11, 20.

[76] Isachenkov, M., Liendo, P., Linke, Y., & Schomerus, V. (2018). Calogero-Sutherland Approach to Defect Blocks. *JHEP*, 10, 204.

[77] Itzykson, C. & Zuber, J. (2012). *Quantum Field Theory*. Dover Books on Physics. Dover Publications.

[78] Jack, I. & Osborn, H. (2014). Constraints on RG Flow for Four Dimensional Quantum Field Theories. *Nucl. Phys.*, B883, 425–500.

[79] Jackiw, R. & Pi, S. Y. (2011). Tutorial on Scale and Conformal Symmetries in Diverse Dimensions. *J. Phys.*, A44, 223001.

[80] Kapustin, A. (2006). Wilson-'t Hooft operators in four-dimensional gauge theories and S-duality. *Phys. Rev. D*, 74, 025005.

[81] Kar, A. & Rajeev, S. G. (2012). Non-Riemannian metric emergent from scalar quantum field theory. *Phys. Rev. D*, 86(6), 65022.

[82] Karch, A. & Sato, Y. (2018). Conformal Manifolds with Boundaries or Defects. *JHEP*, 07, 156.

[83] Klebanov, I. R. & Polyakov, A. M. (2002). AdS dual of the critical O(N) vector model. *Phys. Lett.*, B550, 213–219.

[84] Klebanov, I. R., Pufu, S. S., Sachdev, S., & Safdi, B. R. (2012). Renyi Entropies for Free Field Theories. *JHEP*, 04, 074.

[85] Koblitz, N. (1977). P-adic numbers. In *p-adic Numbers, p-adic Analysis, and Zeta-Functions*. Springer.

[86] Koffel, T., Lewenstein, M., & Tagliacozzo, L. (2012). Entanglement entropy for the long range Ising chain. *Phys. Rev. Lett.*, 109, 267203.

[87] Krivoruchenko, M. I. & Tursunov, A. A. (2019). Noether's theorem in non-local field theories. *Symmetry*, 12(1), 35.

[88] La Nave, G., Limtragool, K., & Phillips, P. W. (2019). Fractional Electromagnetism in Quantum Matter and High-Energy Physics. *Rev. Mod. Phys.*, 91(2), 021003.

[89] Lauria, E., Meineri, M., & Trevisani, E. (2018). Radial coordinates for defect CFTs. *JHEP*, 11, 148.

[90] Lauria, E., Meineri, M., & Trevisani, E. (2019). Spinning operators and defects in conformal field theory. *JHEP*, 08, 066.

[91] Lemos, M., Liendo, P., Meineri, M., & Sarkar, S. (2018). Universality at large transverse spin in defect CFT. *JHEP*, 09, 091.

[92] Lerner, E. b. Y. & Missarov, M. D. (1989). Scalar Models of p-adic Quantum Field Theory and Hierarchical Models. *Theor. Math. Phys.*, 78, 177–184.

[93] Lewkowycz, A. & Maldacena, J. (2014). Exact results for the entanglement entropy and the energy radiated by a quark. *JHEP*, 05, 025.

[94] Liendo, P., Linke, Y., & Schomerus, V. (2019). A Lorentzian inversion formula for defect CFT.

[95] Luijten, E. & Blöte, H. W. (2002). Boundary between long-range and short-range critical behavior in systems with algebraic interactions. *Physical review letters*, 89(2), 025703.

[96] Maldacena, J. M. (1999). The Large N limit of superconformal field theories and supergravity. *Int. J. Theor. Phys.*, 38, 1113–1133. [Adv. Theor. Math. Phys.2,231(1998)].

[97] Marino, E. C. (1993). Quantum electrodynamics of particles on a plane and the Chern-Simons theory. *Nucl. Phys.*, B408, 551–564.

[98] Marino, E. C., Nascimento, L. O., Alves, V. S., & Smith, C. M. (2014). Unitarity of theories containing fractional powers of the d'Alembertian operator. *Phys. Rev.*, D90(10), 105003.

[99] McAvity, D. M. & Osborn, H. (1995). Conformal field theories near a boundary in general dimensions. *Nucl. Phys.*, B455, 522–576.

[100] Metsaev, R. R. (1995). Massless mixed symmetry bosonic free fields in d-dimensional anti-de Sitter space-time. *Phys. Lett.*, B354, 78–84.

[101] Meurice, Y. (2007). Nonlinear aspects of the renormalization group flows of Dyson's hierarchical model. *Journal of Physics A: Mathematical and Theoretical*, 40(23), R39.

[102] Minwalla, S. (1998). Restrictions imposed by superconformal invariance on quantum field theories. *Adv. Theor. Math. Phys.*, 2, 783–851.

[103] Missarov, M. D. (2012). *p*-Adic Renormalization Group Solutions and the Euclidean Renormalization Group Conjectures. *P-Adic Numbers, Ultrametric Analysis, and Applications*, 4(2), 109–114.

[104] Monthus, C. (2015). Dyson hierarchical quantum ferromagnetic Ising chain with pure or random transverse fields. *Journal of Statistical Mechanics: Theory and Experiment*, 2015(5).

[105] Nishioka, T. & Sato, Y. (2021). Free energy and defect C-theorem in free scalar theory.

[106] Osborn, H. (1991). Weyl consistency conditions and a local renormalisation group equation for general renormalisable field theories. *Nuclear Physics B*, 363(2), 486 – 526.

[107] Osborn, H. & Petkou, A. C. (1994). Implications of conformal invariance in field theories for general dimensions. *Annals Phys.*, 231, 311–362.

[108] Paulos, M. F., Penedones, J., Toledo, J., van Rees, B. C., & Vieira, P. (2017). The S-matrix bootstrap. Part I: QFT in AdS. *JHEP*, 11, 133.

[109] Paulos, M. F., Rychkov, S., van Rees, B. C., & Zan, B. (2016). Conformal Invariance in the Long-Range Ising Model. *Nucl. Phys.*, B902, 246–291.

[110] Pelissetto, A. & Vicari, E. (2002). Critical phenomena and renormalization-group theory. *Physics Report*, 368(6), 549–727.

[111] Peskin, M. E. & Schroeder, D. V. (1995). *An Introduction to quantum field theory*. Reading, USA: Addison-Wesley.

[112] Polchinski, J. (1988). Scale and conformal invariance in quantum field theory. *Nuclear Physics B*, 303(2), 226 – 236.

[113] Rajabpour, M. A. (2011). Conformal symmetry in non-local field theories. *JHEP*, 06, 076.

[114] Rodriguez-Gomez, D. & Russo, J. G. (2017). Free energy and boundary anomalies on $\mathbb{S}^a \times \mathbb{H}^b$ spaces. *JHEP*, 10, 084.

[115] Sak, J. (1973). Recursion relations and fixed points for ferromagnets with long-range interactions. *Phys. Rev. B*, 8, 281–285.

[116] Sally, P. J. (1998). An Introduction to p-adic Fields, Harmonic Analysis and the Representation Theory of $SL(2)$. *Letters in Mathematical Physics*, 46(1), 1–47.

[117] Schwimmer, A. & Theisen, S. (2019). Osborn Equation and Irrelevant Operators. *J. Stat. Mech.*, 1908, 084011.

[118] Semenoff, G. W. (2012). Chiral Symmetry Breaking in Graphene. *Phys. Scripta*, T146, 014016.

[119] Söderberg, A. (2018). Anomalous Dimensions in the WF O(N) Model with a Monodromy Line Defect. *JHEP*, 03, 058.

[120] Suzuki, M., Yamazaki, Y., & Igarashi, G. (1972). Wilson-type expansions of critical exponents for long-range interactions. *Physics Letters A*, 42(4), 313–314.

[121] Teber, S. (2012). Electromagnetic current correlations in reduced quantum electrodynamics. *Phys. Rev.*, D86, 025005.

[122] Teber, S. & Kotikov, A. V. (2014). Interaction corrections to the minimal conductivity of graphene via dimensional regularization. *EPL*, 107(5), 57001.

[123] Vasiliev, M. A. (1990). Consistent equation for interacting gauge fields of all spins in (3+1)-dimensions. *Phys. Lett.*, B243, 378–382.

[124] Vladimirov, V. S., Volovich, I. V., & Zelenov, E. I. (1994). *p-adic Analysis and Mathematical Physics*. Series on Soviet and East European mathematics. World Scientific.

[125] Volovich, I. V. (1987). *Number theory as the ultimate physical theory*. Technical report.

[126] Weinberg, S. (1960). High-energy behavior in quantum field theory. *Phys. Rev.*, 118, 838–849.

[127] Wess, J. (1960). The conformal invariance in quantum field theory. *Il Nuovo Cimento (1955-1965)*, 18(6), 1086–1107.

[128] Wilson, K. G. & Fisher, M. E. (1972). Critical exponents in 3.99 dimensions. *Physical Review Letters*, 28(4), 240–243.

[129] Witten, E. (1998). Anti-de Sitter space and holography. *Adv. Theor. Math. Phys.*, 2, 253–291.

[130] Witten, E. (2003). SL(2,Z) action on three-dimensional conformal field theories with Abelian symmetry. (pp. 1173–1200).

[131] Yamaguchi, S. (2016). The ϵ-expansion of the codimension two twist defect from conformal field theory. *PTEP*, 2016(9), 091B01.

[132] Zamolodchikov, A. B. (1986). Irreversibility of the Flux of the Renormalization Group in a 2D Field Theory. *JETP Lett.*, 43, 730–732. [Pisma Zh. Eksp. Teor. Fiz.43,565(1986)].